PREDICTING THE STRENGTH OF NOTCHED WOOD BEAMS

by

Barry Louis Zalph

Dissertation submitted to the Faculty of the
Virginia Polytechnic Institute and State University
in partial fulfillment of the requirements for the degree of

DOCTOR OF PHILOSOPHY

in

Wood Science and Forest Products

APPROVED:

T. E. McLain, Chairman

T.D. Gerhardt

S.M. Holzer

G. Ifju

D.E. Kline

J.R. Loferski

June, 1989

Blacksburg, Virginia

PREDICTING THE STRENGTH OF NOTCHED WOOD BEAMS

by

Barry Louis Zalph

Committee Chairman: Thomas E. McLain
Wood Science and Forest Products

(ABSTRACT)

A simple expression using a critical fillet hoop stress (CFHS) model was derived to predict the capacity of a simply supported wood beam with a notch on the tension face between the supports. The derivation used the hypothesis that cracking initiates when the hoop stress tangent to the free surface of a round-cornered notch exceeds a critical value. This critical value is characteristic to the material. Finite element modeling was used to explore the effects of a broad range of notch geometries, notch locations, beam sizes, loading configurations, and material elastic properties on fillet hoop stress. The analyses assumed homogeneous, orthotropic, linear elastic behavior, and used a hybrid element to provide accurate results in the region of high stress gradients. Simplified, closed form expressions to predict maximum hoop stress were developed from the numerical results.

Notched beam tests included nine wood materials, encompassing hardwoods and softwoods in both green and kiln-dried conditions. A broad array of notch geometries was tested. A

theoretical framework related the experimental failure loads with the calculated maximum fillet hoop stress values. The dependence of failure loads on notch geometry, location, and loading condition was described well by the predictive expression derived from the finite element modeling. The CFHS model can be applied to sharp-cornered notches when an appropriate effective fillet radius is substituted into the strength equation. Preliminary test results showed the effective fillet radius to be material dependent; theoretical analysis suggested a beam depth dependence as well.

The notched beam strength equation utilizes a single material constant which can be experimentally determined from tests of beams with a single notch geometry. The notched beam strength parameter, κ, was found to be strongly related to specific gravity and cross-grain tensile strength. The regression equation from this work can be used to estimate κ for solid wood materials outside of this study.

CFHS results compared favorably with those of earlier models shown to be accurate over a more limited set of cases. In addition to its broad applicability, the CFHS method benefits from its reliance on only one, easily determined, material parameter and avoids the need for directional fracture toughness and elastic parameter data which are very difficult to obtain.

Acknowledgements

Numerous faculty, staff, and graduate students in the Department of Wood Science and Forest Products, and throughout Virginia Tech, gave me help and support during my studies. I thank them all for both the assistance and the warmth with which it was offered. I am most grateful for the friendly and astute guidance which Dr. Thomas McLain and Dr. Terry Gerhardt provided throughout this project. Thanks are due for his long hours of work on many aspects of the mechanical testing. I thank and Dr. Robert Rice for many helpful discussions on topics ranging from Forstner bits to FORTRAN. My special thanks go to for his tireless and good-natured assistance in sample preparation, testing, and keeping a clear head about technical problems which exhausted my own patience.

Many friends boosted my morale through graduate school. In particular, I thank and my mother, for their abiding love. Dr. Michael P. Wolcott was a source of mirth as well as inspiration with his passionate yet lighthearted approach to laboratory science and life in general. Finally, I offer my deepest thanks to my father, , who would have been proud.

List of Tables

List of Figures

1.0 Introduction

1.1 Uses of notched wood beams

A primary structural use of solid wood is in beams, i.e., bending elements. In many instances, the beam contains a notch or cutout. (In this work, the terms "notch" and "cut-out" refer to material removal from an edge of the beam, as opposed to a "hole", which refers to a void within the body of the beam.) Notches are quite common in wood pallets designed for fork-lift access from all four sides (Canadian Forestry Service 1976), and are also incorporated into roof rafters and floor joists used in building construction (Anderson 1975).

Notches on the tension side of wood beams are known to have a detrimental effect on beam load-carrying capacity (Scholten 1935). In addition to reducing the cross-section, cutouts introduce stress concentrations which cause stresses near the notch to be higher than would be predicted for a prismatic beam with a similar net section (Stieda 1966; Richards 1974; Gerhardt 1984a). Stieda (1966), for example, reported notched beam strengths for kiln-dried softwoods typically 40% below that predicted for unnotched beams of the same net section. This effect is well known for isotropic engineering elements. Analytically or experimentally

determined stress concentration factors are tabulated for many geometries and materials (Peterson 1974). The anisotropy of wood results in stress distributions around discontinuities which differ markedly from those experienced by isotropic materials with similar geometry and loading conditions. The complexities of the stress distributions around cutouts, combined with difficulties in defining and measuring material properties governing notched beam fracture, have hindered the development of an accurate, general method for estimating the load-bearing capacity of notched wood beams.

1.2 Objectives

The global objective of this research is to develop a practical technique for designing and evaluating wood beams with interior notches on the tension face. Several subobjectives are:

a) to develop closed-form equations which predict the strength of notched wood beams as a function of beam and notch geometry, loading conditions, and one or more material properties.

b) to develop means of estimating any material properties needed for the notched beam design technique.

c) to experimentally verify the analytically developed predictive equations.

d) to formulate a simplified design procedure for notched timber bending elements.

1.3 Overview

I employed finite element analysis and mechanical testing to derive and verify expressions which can predict the failure loads of notched wood beams. The underlying hypothesis is that a notched beam fails when the fillet hoop stress, i.e., the stress tangent to the free surface of a round-cornered (filleted) notch exceeds a critical value. The critical fillet hoop stress is characteristic of the material, and is related to other mechanical properties of the material. The equations arising from the model are also useful for sharp-cornered (unfilleted) notches with the use of appropriate empirical adjustments.

Notched beam strength equations were derived from numerical calculations over a wide range of notch and beam geometries. The effects of different notch locations and loading conditions (e.g., center-point, quarter-point, and uniformly distributed loading) were incorporated by means of a single term, the ratio of applied shear to applied moment (V/M) at the critical fillet. Extensive mechanical testing was conducted to verify, calibrate, and extend the theoretical predictions. Eight wood materials were tested, including green and dry softwoods and hardwoods of differing densities and anatomical structures. Notched and unnotched bending, block shear, and perpendicular-to-grain tensile tests were

performed on each material group, as well as measurements of moisture content and specific gravity. Relationships were derived between the notched beam strength parameter and standard wood properties. Predictions of the model were compared with the results of previous studies of beams with filleted and unfilleted notches.

2.0 Background and Previous Work

2.1 Predicting the notch effect on beam strength

At least three basic approaches have been used to estimate the reduced strength of notched timber beams. The first uses a "notch factor" to modify the wood bending strength (modulus of rupture, "MOR") and/or shear strength to account for the effect of the notch. This factor may come from analytical or experimental studies, but has historically been test-based.

A notch factor is applied to the allowable shear stress (F_v) in current U.S. and Canadian design practice for the case of shallow end notches, where shear strength governs beam failure (American Institute of Timber Construction 1985; National Forest Products Association 1986). Figure 1 shows the beam geometry to which this notch factor applies. This empirically-based adjustment covers only a small group of end-notched beams and makes no provisions for assessing the impact of notch length (i.e. distance from the support to the notch corner), notch angle or material properties on the severity of the notch effect.

For notches away from the supports, a factor applied to MOR would be difficult to generalize to a variety of notch configurations and species. This is because the MOR is primarily a measure of resistance to normal stresses

parallel-to-grain, whereas the failure of notched beams is always governed by shear stresses and perpendicular-to-grain tensile stresses (Stieda 1966; Gerhardt 1984; Bodig and Jayne 1982). In addition, MOR is a fictitious stress based on the assumptions of linear elastic behavior to failure and identical elastic properties in tension and compression (Bodig and Jayne 1982).

A second approach uses classical methods to calculate the stresses in the vicinity of the notch and compare them with a combined-stress failure criterion to predict failure. This calculation is cumbersome for wood due to its limited material symmetry (orthotropic at best). Numerical methods must be used in many practical cases for which closed-form solutions do not exist. Another difficulty is the lack of a proven combined-stress failure criterion for wood.

A third approach, allied to the second, is to treat the problem using linear elastic fracture mechanics (LEFM). This method calculates a force required to propagate a crack based on geometric and energy considerations. Although analogous in many ways to the classical technique, LEFM analysis assumes the preexistence of a stress singularity such as a crack. This simplifies the treatment of sharp-cornered notches which cannot be modeled explicitly by classical meth-

ods. Conversely, LEFM is not applicable to filleted notches without introducing a fictitious crack in the notch region.

2.1.1 Classical approaches

Numerous works have focused on stress fields around notches and other stress concentrations in wood by assuming plane elastic behavior with orthotropic material symmetry (Stieda 1966; Gerhardt 1984a, b; Green 1942; Green and Taylor 1945a,b; Abou-Ghaida and Gopu 1984; Masuda 1988). The accurate calculation of relative stresses or stress intensities in the vicinity of the notch does not, however, generally lead to a straightforward prediction of the critical load required to cause failure. This is because failure is typically due to the concurrent actions of normal and shear stresses (or, in the terms of LEFM, mixed Mode I and Mode II crack extension. See Section 2.1.2.) The means for assessing their combined effect on crack initiation and growth (i.e., a failure criterion) is uncertain and difficult to apply to the generally complicated stress distributions. In addition, necessary mechanical property information is difficult to obtain (Stieda 1966; Gerhardt 1984a; Masuda 1988; Mall, *et. al.* 1983; Hooley and Hibbert 1967). Much effort has gone towards addressing the problems of defining threshhold stresses and stress intensities which describe the fracture of wood in the presence of stress concentrations.

Many works include experimental studies to observe failure loads, as well as the location and direction of cracking. Both analytical and experimental results are covered in the following review.

2.1.1.1 Exact elasticity solutions

Green (1942) and Green and Taylor (1945) developed exact solutions for stresses around discontinuities in orthotropic materials. They solved for the stress distributions around circular holes in infinite planar sheets of a homogeneous orthotropic material subjected to pure tension or compression along each of the two axes of symmetry. Using elastic constants for spruce and oak, they calculated the locations of the stress maxima and the magnitudes of the externally applied loads required to exceed the uniaxial strengths of the wood in tension (parallel- and perpendicular-to-grain), compression (parallel- and perpendicular-to-grain), and shear (parallel-to-grain) near the hole. They noted that these failure predictions are only approximate, since "...the conditions of failure under complex stress have not been fully investigated...". In a later paper (1945), Green applied a similar classical elasticity method to solve for stresses around elliptical holes and square and triangular holes with rounded corners. No failure predictions were given in that report.

2.1.1.2 Experimental testing of classical models

Stieda (1964) published experimental results for stress concentrations around semicircular notches in hemlock and Douglas-fir based on photoelasticity measurements. He used the generalized form of Hankinson's interaction equation (Bodig and Jayne 1982) to predict the failure loads of the notched beams. The resulting load predictions underestimated the measured maximum loads by about 50%. The dependence of the stress concentration factors on notch radius followed the general form suggested by Green (1942) except for radii below about 0.5". For smaller radii, a limiting maximum stress concentration factor of about 2.5 was indicated.

Stieda (1966) showed distributions for shear and normal stresses around holes and notches of various shapes in orthotropic beams. His experimental work included unnotched and notched samples of three non-resinous softwoods. One semicircular and four rectangular notch geometries were tested. Third-point bending tests resulted in all samples appearing to fail in shear, although a number of cracking paths were observed. This indicates the deviation of wood from the simplifying assumptions of homogeneity and plane orthotropicity. Deep, narrow notches were seen to cause the greatest stress concentration, i.e. the lowest net section stresses at failure. Significant differences were found

between the strengths of beams with rectangular center notches having length-to-depth ratios (λ=L/D) of 0.16 and 16. (See Figure 2.) Small semicircular notches (D=0.125", R=0.04", L=0.08") reduced strength about as much as rectangular notches of the same length and depth. Stieda interpreted this as evidence of a limiting notch radius below which no further increase in stress concentration occurred. Notched beams tested in the green condition failed at a higher fraction of their unnotched ultimate strength (~57%-105% of unnotched strength, typically ~75%) than did kiln-dried notched beams (~35%-75% of unnotched strength, typically ~58%). This corresponded to the observation of characteristically rapid crack growth (i.e., brittle behavior) in the kiln-dried wood. In contrast, slow crack growth was commonly seen among the green samples. Stieda found that notched beam failure could be predicted approximately by:

$$\frac{6M}{t(h\text{-}D)^2} \geq 4\tau_{max} \qquad (2.1)$$

where:

M = applied moment at the inside corner of the notch;
τ_{max} = longitudinal shear strength;
t = beam thickness;
h = beam depth;
D = notch depth.

2.1.1.3 Numerical evaluation of stresses around notches

Gerhardt (1984a,b) and Abou-Ghaida and Gopu (1984) used the finite element method (FEM) to calculate stresses in notched beams. Gerhardt (1984b) gave a review of analytical and numerical techniques used to derive stress fields in notched media, and developed a new method to improve upon the accuracy, efficiency, and ease of use of earlier techniques. His hybrid finite element (1984b) models exactly the shape and stress-free condition of the free surface of a notch or hole. This obviates the need for a fine element grid in the region of the discontinuity. The element is applicable to a variety of geometries, including circular and elliptical voids and filleted notches. For regions away from the notch fillet(s), Gerhardt (1983,1984a) proposed an orthotropic cubic isoparametric finite element (FE) based on the work of Taylor (1977). Abou-Ghaida and Gopu (1984) used orthotropic isoparametric finite elements throughout their model, with an increasingly fine mesh towards the notch.

2.1.1.4 Critical fillet hoop stress model

Gerhardt (1984a) applied his hybrid FE (1984b) and isoparametric cubic element (1983) to model the stresses and deflections in notched and unnotched pallet stringers made from red oak in the green condition. An extensive program of mechanical tests of 510 notched and 90 unnotched stringers was

performed to verify the FE stiffness analysis and to establish relationships between measured failure loads and the stress distributions derived from the FE model. Both experimental and numerical results showed a strong relationship of beam strength to notch depth. Beams with unfilleted notches cracked at net section stresses about 24% below those carried by beams with filleted notches. However, no strength differences were attributed to fillet radius variations from 0.5" to 1.0". This deviated from the FEM prediction of 25% higher stresses for a fillet radius of 0.5" than for a 1.0" radius.

From his FEM results, Gerhardt derived closed-form equations for calculating the maximum hoop stress at the notch fillet. The functional relationship between maximum hoop stress and notch depth, which was independent of assumed elastic properties, was found to fit the experimental failure data very well. Thus, the observation of fracture initiating at a critical fillet hoop stress allowed failure predictions to be made without resorting to a combined stress failure criterion. The derived relationship (Gerhardt 1984a) for the moment capacity of a filleted, notched stringer under combined bending and shear is:

$$\frac{6M_{max}}{th^2} = \frac{K_{crit}}{\frac{1}{-1.26\phi + 1} + h(V/M)(1.13\phi + 0.30)} \qquad (2.2)$$

where :

M_{max} = applied moment at failure;

V/M = shear : bending ratio (function of loading geometry);

t = beam thickness;

h = beam height (depth);

K_{crit} = material constant;

ϕ = dimensionless notch depth = notch depth/beam depth.

Note: $0.267 \leq \phi \leq 0.667$.

The terms used to define the notch and loading geometries are shown in Figure 2. The constant, K_{crit}, is defined as $B\sigma_{max}$, where σ_{max} is the maximum fillet hoop stress at failure and B is a coefficient dependent on the wood's elastic constants. Although only one material was tested, the FE analysis was conducted for a variety of ratios of E_L/E_T and E_L/G_{LT} spanning the range of commercially important wood properties. (The subscripts L and T refer to longitudinal and transverse materials directions, respectively. "Transverse" properties are assumed independent of ring angle, i.e. radial and tangential properties are assumed equal.) Gerhardt hypothesized that K_{crit} is a material property of wood, independent of geometry and loading conditions. Thus, the strength prediction

equations could be applied to other species simply by determining K_{crit} at one notch depth for each species of interest. K_{crit} is presumably dependent on anatomical, environmental and other factors which influence the mechanical properties of wood.

Abou-Ghaida and Gopu (1984) found stresses which agreed well with Gerhardt's closed-form equations except for the case of end-notched beams. These were not treated by Gerhardt. They also examined the effect of notch length and did not find any influence on interior-notched beams with notch lengths from 1-3 times the notch depth. A significant notch length effect was shown for end-notched beams. No mechanical testing was reported by Abou-Ghaida and Gopu.

2.1.1.5 Finite small area failure theory:

A computational method has been proposed by Masuda (1988) to treat stresses around discontinuities in wood whether or not a stress singularity is present. He hypothesized that failure occurs when the average stresses within a "finite small area" around the discontinuity satisfy the von Mises criterion. Orthotropic linear elastic finite elements were used to calculate the stresses, but the method used to average the stresses was not stated. The appropriate size of the finite small area is said to be critical to the model, and is determined by calibration with experimental results. The

extent to which this critical size parameter varies between materials is not clear.

2.1.2 Fracture mechanics approaches

Fracture mechanical analyses recognize three distinct modes of crack propagation. The resistance of a material to crack growth is generally different in each mode. Mode I or "opening mode" fracture is crack growth perpendicular to an applied tensile stress (Figure 3). Mode II "forward shear" corresponds to crack propagation in response to in-plane shear stress (Figure 3). Mode III, out-of-plane (tearing) shear shear, is essentially absent in beams.

The usefulness of fracture mechanics to predict allowable loads for notched beams hinges on three basic requirements. The first is the knowledge of stress intensity fields around cutouts in wood. Second, reliable measurements of the critical stress intensity factors (fracture toughnesses), K_{Ic} and K_{IIc}, must be established for structural woods. Third, a means of describing failure due to mixed-mode loading is needed.

LEFM assumes linear, elastic material behavior to failure. Except in a small region surrounding the crack tip, a wood workpiece undergoes only elastic deformations. The total strain energy stored in the specimen is negligibly affected

by plasticity near the crack tip (Porter 1964; Gustafsson 1988). Thus, the assumption of linear elasticity gives acceptable results.

2.1.2.1 Calculation of stress intensities around notches

Many researchers have applied LEFM to notched wood beams (e.g.,Porter 1964; Sih, *et. al.* 1965; Leicester and Poynter 1979; Murphy 1979, 1986; Barrett 1981; Mall, *et. al.* 1983; Lum 1986; Gustafsson 1988). The calculation of stress intensity fields near notches in wood has been the subject of work by Sih, et. al. (1965), Wu (1967), Walsh (1972, 1974), Barrett and Foschi (1977), Murphy (1979), Lum (1986), and Gustafsson (1988), among others. As is true for stress concentrations, stress intensities in orthotropic media can be computed for only a few relatively simple cases without the aid of numerical techniques. Accordingly, finite element modeling has been applied by many workers to compute stress intensities around a wide range of discontinuities (e.g., Wu 1967; Foschi and Barrett 1976; Mall, *et. al.* 1983; Lum 1986). One limitation of the stress intensity approach to notched beam strength is the basic assumption of a sharp crack. Although sharp rectangular, triangular and slit notches in wood tend to behave in a manner similar to an ideal crack (Lum 1986; Murphy 1986), this has not been shown to be the case for filleted notches. Thus, any LEFM analysis of wood beams

with filleted notches would require the assumption of a crack (or other stress singularity) of known size in the fillet region. Masuda (1988) uses this approach for a cleavage test specimen with a rounded notch root. The calculated failure loads for four different sizes of cleavage specimen ranged from 65% to 77% of the mean experimentally determined failure loads. No such analysis for filleted notched beams has been published.

2.1.2.2 Fracture toughness measurements in wood

The determination of fundamental wood fracture parameters has been difficult and controversial. Of prime importance are the Mode I and Mode II fracture toughness values K_{Ic} and K_{IIc}, respectively. Since 1964, numerous publications have addressed these measurements on various woods (Porter 1964; Debaise, *et.al.* 1966; Wu 1967; Schniewind and Pozniak 1971; Woo and Chow 1979; Triboulot, *et. al.* 1981; Schniewind, *et. al.* 1982; Mall, *et. al.* 1983; Ashby, *et. al.* 1985). Unfortunately, measurements made in different laboratories on ostensibly similar materials have often differed by far more than the expected variance in mechanical properties from sample to sample of the given species (Schniewind and Pozniak 1971; Triboulot, *et. al.* 1981; Schniewind, *et. al.* 1982). In some cases, the differences appeared to have been attributable to the use of dissimilar specimen geometries, e.g. double-

cantilever beam versus single edge notch tensile (Schniewind, *et. al.* 1982; Blicblau and Cook 1986), but discrepancies have arisen despite the use of a common specimen type (Triboulot, *et. al.* 1981). To date, no standard exists for test methods nor workpieces for fracture toughness determinations in wood. This is reflected in the common research practice of including two or more specimen configurations in wood fracture toughness studies (e.g., Mall, *et. al.* 1983; Woo and Chow 1979; Ashby, *et. al.* 1985; Blicblau and Cook 1986). The foregoing difficulties have led to the current situation in which the database of fracture toughness for structural timbers is quite incomplete and uncertain, and the means for bringing it up to acceptable standards is not yet clear.

2.1.2.3 Mixed-mode failure criteria:

Another challenge in the application of LEFM to wood is the establishment of a mixed-mode failure criterion. The need to understand the interaction of opening and shear mode stress intensity factors in causing failure is particularly clear for notched beams, since the notch causes a combination of Mode I and Mode II loading for virtually any practical loading geometry (Leicester 1974; Murphy 1979; Lum 1986). An interaction equation derived from tests on balsa (assumed *Ochroma pyranidale*) was proposed by Wu (1967). In contrast, Williams and Birch (1976) found no influence of K_{IIc} on mixed

mode cracking of utile (*Entandrophragma utile*) and Scots pine (*Pinus sylvestris*). In tests of the Asian species kapur (*Dryobalanops spp.*) and gagil (*Hopea segal*), Woo and Chow (1979) found evidence of an interaction effect. However, they did not make measurements of K_{IIc} which would have allowed a direct comparison of their results with those of Wu. Mall, et. al.(1983) compared several failure criteria to their experimental data on mixed mode failure of red spruce (*Picea rubens*) and found that Wu's was the only one which fit the data. They point out that this agreement "...may be a fortuitous coincidence for these two species of wood, or possibly a trend for a wide range of species." Murphy (1986) also used Wu's failure criterion to successfully model the failure of four large Douglas-fir glued-laminated (glulam) beams with rectangular and slit notches.

Noting the absence of an accepted mixed-mode failure criterion, Masuda (1988) tested three expressions proposed previously by other researchers :

$$\left(\frac{K_I}{K_{I,c}}\right)^2 + \left(\frac{K_{II}}{K_{II,c}}\right)^2 \geq 1 \qquad (2.3)$$

$$\left(\frac{K_I}{K_{I,c}}\right) + \left(\frac{K_{II}}{K_{II,c}}\right) \geq 1 \qquad (2.4)$$

$$\left(\frac{K_I}{K_{I,c}}\right) + \left(\frac{K_{II}}{K_{II,c}}\right)^2 \geq 1 \quad \text{(Wu's criterion)} \qquad (2.5)$$

where :

K_I = mode I stress intensity
$K_{I,c}$ = critical mode I stress intensity (fracture toughness)
K_{II} = mode II stress intensity
$K_{II,c}$ = critical mode II stress intensity (fracture toughness)

For structural lumber beams of *Picea jezoensis* with central rectangular notches, equations (2.3), (2.4), and (2.5) had mean errors of +17% (overestimation), +11% and -11%, respectively for seven combinations of notch depth and beam depth. The usefulness of Wu's mixed-mode LEFM failure criterion has been shown in several studies, but further verification of its generality is needed.

2.1.2.4 LEFM applications to notched beam strength:

Leicester (1974) and Leicester and Poynter (1979) applied LEFM concepts to derive conservative design equations for beams with straight-sided notches of various angles and depths (e.g. Figure 4). Fracture mechanical analyses were used to obtain the general forms of the relationships of beam strength to notch depth, notch angle and root radius (Leicester 1974). In recognition of the difficulty of determining fracture toughnesses for the many species in use, Leicester (1974) used test data on mixed Australian species to derive regressions between the fracture toughnesses and

timber density. He also gave strength adjustment curves for the effects of slope of grain, moisture content and duration of load. A LEFM failure criterion, based on two species and two notch geometries, was proposed as a conservative design standard. In the later paper, the application of K_{Ic} and K_{IIc} as material parameters was eliminated in favor of block shear strength and bending strength. Their experimental findings, with *Pinus radiata*, showed minimal strength variation with notch depth, which contrasts with the strong notch-depth dependence noted by Gerhardt (1984) for filleted notches in red oak. Design equations for notched beam strength in pure bending and pure shear were given for three notch angles. The strength predictions are functions of beam depth and block shear strength or wood density. The dimensionless notch depth $\phi = D/h$ was assumed to be 0.5, giving conservative strength estimates over the range $0.2 \leq D/h \leq 0.8$. (Gerhardt's results (1984a) suggest that such a simplification is unjustifiable.) A combined stress failure criterion, expressed in terms of bending and shear strengths of the wood, was compared with data for two notch depths and one notch angle and found to be slightly conservative. No consideration was given to filleted notches.

Gustafsson (1988) presented a thorough LEFM derivation of the strength of a wood beam with a sharp-cornered notch or

sharp-tipped crack anywhere along its length. The result of the analysis was the failure criterion:

$$\tau\sqrt{8(\alpha-\alpha^2)/G_{xy}} + \sigma\sqrt{5(\alpha-\alpha^4)/E_x} \leq \sqrt{30G_c/h} \qquad (2.6)$$

where :

τ = nominal shear stress at the reduced section;
σ = nominal bending stress at the reduced section;
α = fractional net depth = $(1-\phi)$ = $(h-D)/h$;
G_{xy} = shear modulus;
E_x = longitudinal elastic modulus; and
G_c = critical strain energy release rate

This equation was further refined to account for the non-negligible size of the fracture region in smaller beams in which the notch corner (or crack tip) is a short distance from the support. The theoretical equation was compared with experimental results from 21 notched beams of *Pinus sylvestris* as well as with experimental results from nine other sources. For seven of the nine data sets, the theory gave good predictions of failure loads. The effects of beam depth, fractional notch depth and material properties were generally described well by the model. No method is given for estimating the strain energy release rate, G_c, or the shear modulus, G_{xy}, from more accessible test data. Thus, while elegant, Gustafsson's method has limited practical utility at present.

2.1.3 Environmental and loading factors

The mechanical properties of wood are well known to be functions of temperature, moisture content and rate of loading (Bodig and Jayne 1982). Notched wood beams can be exposed to various levels of each of these parameters depending upon their intended uses. Thus, it is important to determine whether each of these parameters affect the strength of notched and unnotched beams to the same extent or, rather, interact with the notch effect. If interactions occur, then they must be quantified to allow realistic assessments of notched beam strength to be made for practical situations.

Differences in the sensitivity of notched and unnotched beams to variations in these factors may be caused by differences in the stress distributions in the two cases. Shear and perpendicular-to-grain tensile stresses are critical near discontinuities, while longitudinal stresses at the outer fibers often give rise to failure in clear unnotched beams. (Note, however, that Gustafsson (1988) found that notched beam strength is essentially independent of tensile strength perpendicular to the grain.) Thus, an environmental or loading factor which influences longitudinal tensile and compressive strength more severely than shear and transverse tensile strength can be expected to impact unnotched beam strength

more than notched beam strength. The converse is expected to hold as well.

2.1.3.1 Moisture content effects:

In tests of three softwoods with five notch shapes, Stieda (1966) found significantly lower notch strength reductions for green samples than for kiln-dried samples. The cracking path and load-deflection curves were characteristically different between the two moisture content groups. The green specimens continued to bear load well after the inception of cracking, whereas the dry pieces tended to more rapid collapse after crack initiation. Leicester (1974) described the relative strength of end-notched messmate (*Eucalyptus obliqua*) beams at four moisture content (MC) levels. His data showed little effect of MC over the range 5%-20%, in contrast with the strengthening effect of reducing MC in prismatic beams. Schniewind, *et. al.* (1982) reported mode I fracture toughness tests of several species over a range of MC. Maximum toughness values were found to occur between 5% and 15% MC. Additional information on the moisture effects in mixed-mode loading conditions is needed before the findings of Schniewind, *et. al.* (1982) can be applied to predicting MC effects in notched beams. I surmise that the observed effect of seasoning on notched beam strength is related not only to the reduction of moisture content but also to the generation

of checks in the wood. For example, beams which are seasoned after notching are likely to fail at lower loads than those notched after seasoning, due to checking which will occur along the exposed surfaces of notches machined prior to drying. Thus, an investigation into the relationship of notched beam strength to moisture condition must provide control over both the MC at the time of testing and the density of seasoning-induced discontinuities.

2.1.3.2 Temperature effects:

Notched beam studies to date have focused on strength at room temperature. Climatic and usage conditions often require, however, that notched beams withstand their design loads during prolonged exposure to temperature extremes. Schniewind, *et. al.* (1982) calculated K_{Ic} values for several species over the temperature range 20°C-80°C, finding that increasing temperature decreased K_{Ic} and increased the effect of moisture content. The effects of temperature on K_{IIc} and mixed-mode failure are, as yet, unknown.

2.1.3.3 Effects of loading rate and duration:

Limited results to date indicate that notched beams may respond differently to long-term loading than do their unnotched counterparts. Blicblau and Cook (1986) performed perpendicular-to-grain tensile tests of radiata pine (*Pinus radiata*) and Douglas-fir at crosshead rates of 0.2 mm/min. to

50 mm/min. Unnotched, single-edge notch (SEN), and double-edge notch (DEN) specimens were tested. The notched specimens were used to determine K_{Ic}. Trends of K_{Ic} with loading rate were different for the two specimen geometries. The unnotched specimens showed approximately constant strength for all loading rates. Madsen (1975) loaded unnotched and center-notched Douglas-fir (*Pseudotsuga menziesii*) beams to achieve nominal times to failure of 1 minute and 1000 minutes. The notched beams showed much smaller strength reductions due to extended loading than did the unnotched controls. The stronger specimens in the notched group actually showed higher strengths in the 1000 minute tests than in the 1 minute tests. End-notched beams of messmate tested by Leicester (1974) also showed increases in strength with increasing time to failure from 1 minute to about 50 minutes, with a decline to roughly the 1-minute strength for a time to failure of about 200 minutes. Krebs, et. al. (1984) conducted long-term tests of spruce samples with sharp-cornered center notches at 66%, 72% and 78% of the predicted short-term breaking load. They found that the "Madison curve" (Wood 1951) relating prismatic beam strength to duration of load fit their notched beam data well. Thus, there is some disagreement in the literature regarding the relative effects of prolonged loading on notched and unnotched beams. It is not

apparent how notched beams respond to high rate loading, such as earthquake loads on a structure or impact loads on a pallet, nor to very long-duration loads, such as the dead load on a building.

2.1.4 Beam size effects

2.1.4.1 Probabilistic (weakest link) size effect

A statistical strength theory for unnotched wood beams was developed by Bohannan (1966) and refined by Liu (1981). The theory predicts that strength is inversely related to specimen volume for workpieces of similar geometry. As shown by Barrett (1974) and Barrett, *et. al.* (1975), there is a significant effect of specimen size and stress distribution on the transverse tensile strength of wood workpieces. These size effects were attributed to the stochastic nature of material strength, combined with a "weakest link" concept of the strength of a brittle material. Failure is said to occur when the local material strength at any point within the workpiece is exceeded by the local stresses; the remainder of the body fractures momentarily after the failure of the weakest link. The variability of strength within the body is considered by calculating the probability of failure as an integral of the probabilities of failure of differential volume elements. This formalizes the common-sense observation that failure will occur at the point where the ratio of

stresses to strength is the highest. Gustafsson (1988) stated that the volume of the critical region in a notched beam is not proportional to beam size; thus, the statistical size effect is minimal.

2.1.4.2 Linear elastic notched body size effect

Leicester (1969), Murphy (1986), Gustafsson (1988), and Masuda (1988) noted that notched wood workpieces show a size effect greater than that predicted from statistical strength theory. Their linear elasticity analyses, using constant material properties, predicted higher stresses in deeper beams with relative notch depth (ϕ) held constant. They each surmised that the high stress gradients associated with the notch give rise to this size effect. The expression derived by Leicester (1969) is:

$$\sigma_{f_2} = \left(\frac{L_1}{L_2}\right)^{\eta} \sigma_{f_1} \qquad (2.7)$$

where:

L_1 = characteristic size (e.g., beam depth) of specimen 1;
σ_{f_1} = fracture strength for specimen 1
L_2 = characteristic size of specimen 2;
σ_{f_2} = fracture strength for specimen 2
η = size effect exponent

This expression, with $\eta \cong 0.33\text{-}0.50$, was found by Leicester (1969) and Gustafsson (1988) to give good results. Thus, experimentally observed size effects were explained without resorting to a probabilistic strength theory.

2.2 Simplified prediction methods and design guidance

In the absence of a quantitative understanding of the weakening effect of notches in structural lumber, design codes recommend avoiding all notches or provide conservative estimates of notched beam strength for a limited set of cases. The Wood Handbook (USDA Forest Products Laboratory 1987) gives an equation, based on the LEFM analysis of Murphy (1979), which predicts crack initiation loads for sharp-cornered notches under combined shear and moment. The material parameters are fixed at values "...conservative for most species." To date, these are the only guidelines available for the engineer faced with evaluating a notched beam. All of the following procedures are specifically intended for notches on the tension side of bending members. It is recognized that notches on the compression side are less detrimental but may be significant (American Institute of Timber Construction 1985). Richards (1974) found that shallow curved notches between the supports on the compression side of

yellow-poplar beams reduced strength even less than predicted by net section theory.

2.2.1 North American design standards

The AITC Timber Construction Manual (TCM) (1985), the NFPA National Design Specification for Wood Construction (NDS) (1986), and the Canadian Standards Association Standard CAN3-086-M84 (reviewed by Lum 1986) include a method for designing beams notched on the tension side at the support. These references suggest avoiding such notches whenever possible. Stricter limits are imposed on notches located away from the supports. The NDS (NFPA 1986) states that:

> "Notches in sawn lumber bending members shall not exceed one-sixth the depth of the member and shall not be located in the middle third of the span. Where members are notched at the ends, the notch depth shall not exceed one-fourth the beam depth. The tension side of sawn lumber bending members of 4 inch or greater nominal thickness shall not be notched, except at ends of members"

The TCM, NDS, and CAN3-086-M84 suggest the following modified shear computation for end-notched beams:

$$f_v = \frac{3R_v}{2th_e} \cdot \frac{h}{h_e} \qquad (2.8)$$

where:

f_v = horizontal (longitudinal) shear stress (lb/in.^{2})

R_v = vertical reaction (lb);

t = width of beam (in.);

h = depth of beam (in.);

h_e = net depth of beam at notch (in.) (See Figure 1).

(The nomenclature varies among the three references.)

This shear correction factor for notched beams appeared in the 1935 Wood Handbook (USDA FPL 1935). The 1955 Wood Handbook (USDA FPL 1955) states that it was based on U.S. Forest Products Laboratory (FPL) work published in 1935 (i.e., Scholten 1935). It is interesting to note that both of those editions state that notches near the center of the tension face may be modeled conservatively using net section theory. (This has since been proven false, as described in Sections 2.1.1 and 2.1.2.) The TCM notes that "The equation... is an empirical equation developed for the condition of a square-cornered end notch, and the ratio of the depth of the notch to the depth of the beam should be limited to 1:10." None of the current North American standards provide equations for estimating the strength of interior-notched beams.

2.2.2 European design standards

Design guidance for beams with end notches is included in Eurocode No. 5: Common Unified Rules for Timber Structures (Crubile, *et. al.* 1988). This reference treats the case shown in Figure 4, i.e. straight-sided end notches with various notch angles. No consideration is given to interior notches. The equation, converted to the form and nomenclature of Equation 2.8, is:

$$f_v = \frac{3R_v}{2th_e} \cdot \frac{h}{6h_e - 5h + 2L}; \quad L < 3(h - h_e) \qquad (2.9)$$

where:

L = length of the tapered section (in.) (See Fig.4.)
(other terms defined as for Eq.(2.8))

For more gradually tapered notches ($L \geq 3(h - h_e)$), the net section stress is used. Equation (2.9) is a modification of the equation which appeared in the earlier version of Eurocode 5 (Crubile, et.al. 1985):

$$f_v = \frac{3R_v}{2th_e} \cdot \frac{h}{3h_e - 2h + L} \qquad (2.10)$$

with the same restriction on L. The reason for the changes is not given.

2.2.3 Australian design standards

In contrast with the North American standards, the equation adopted in Australian Timber Engineering Code

AS 1720.1-1988 of the Standards Association of Australia (SAA) allows the analysis of interior notches by including a bending moment term. The safety checking equation is:

$$f_b + 4f_s \leq g_{40}F_{sj} \qquad (2.11)$$

where:

f_b = nominal allowable bending stress = $6M/th_e^2$

f_s = nominal allowable shear stress = $1.5R_v/th_e$

F_{sj} = permissible shear stress for joint details

g_{40} = coefficient to account for notch taper, beam depth, and fractional notch depth.

The schematic drawing of Figure 4 also describes notches analyzed by this method. The allowable shear stress for joint details, F_{sj}, is calculated by multiplying the "basic working shear stress for joint details" by adjustment factors for duration of load, seasoning, temperature, and lateral stability. Table 1 gives the values of the coefficient g_{40} for various cases. Aside from its effect on net section stresses f_b and f_s, notch depth D enters the formula only for shallow notches ($\phi<0.1$). Even then, it appears (in g_{40}) with an exponent ≤ 0.45. This equation is derived from the fracture mechanics analysis of Leicester and Poynter (1979).

Table 1. *Coefficient g_{40} in S.A.A. Design Equation (Stds. Assoc. of Australia., 1988)*

Notch angle[1]		g_{40}	
L/D	α, degrees	$\phi > 0.1$	$\phi < 0.1$
0	90	$9.0/h^{0.45}$	$3.2/D^{0.45}$
2	27	$9.0/h^{0.33}$	$4.2/D^{0.33}$
4	14	$9.0/h^{0.24}$	$5.2/D^{0.24}$

[1] Refer to Figure 4 for notch geometric parameters.

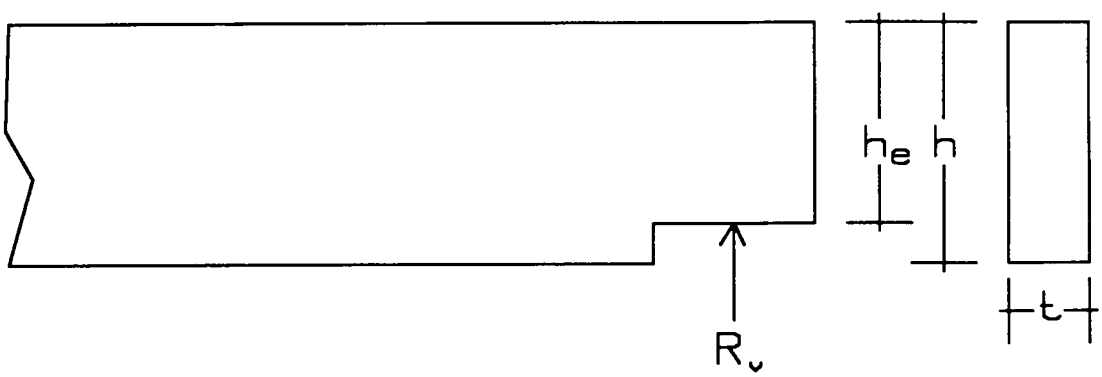

Figure 1. End notched beam geometry for North American design methods.

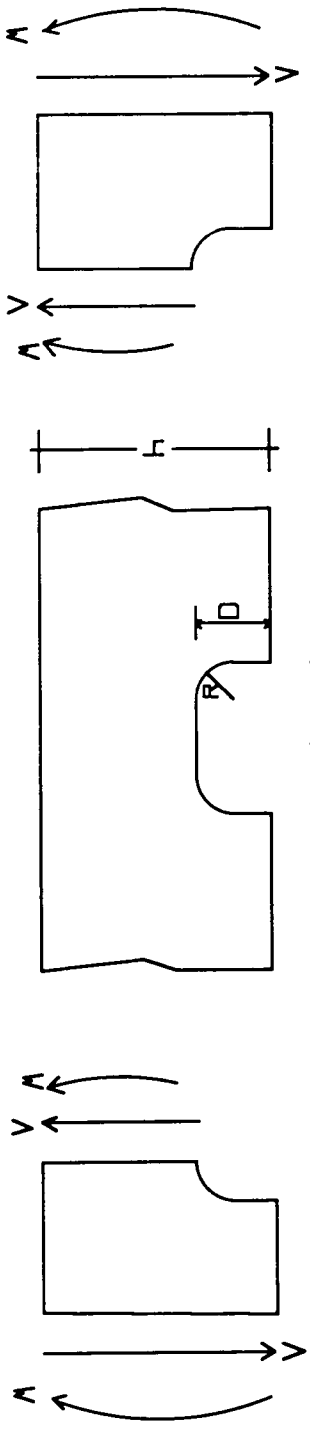

Figure 2. Interior-notched beam geometry. Arrows indicate the sign convention for positive V and M. Positive V and M generate tensile stresses along the notch fillet.

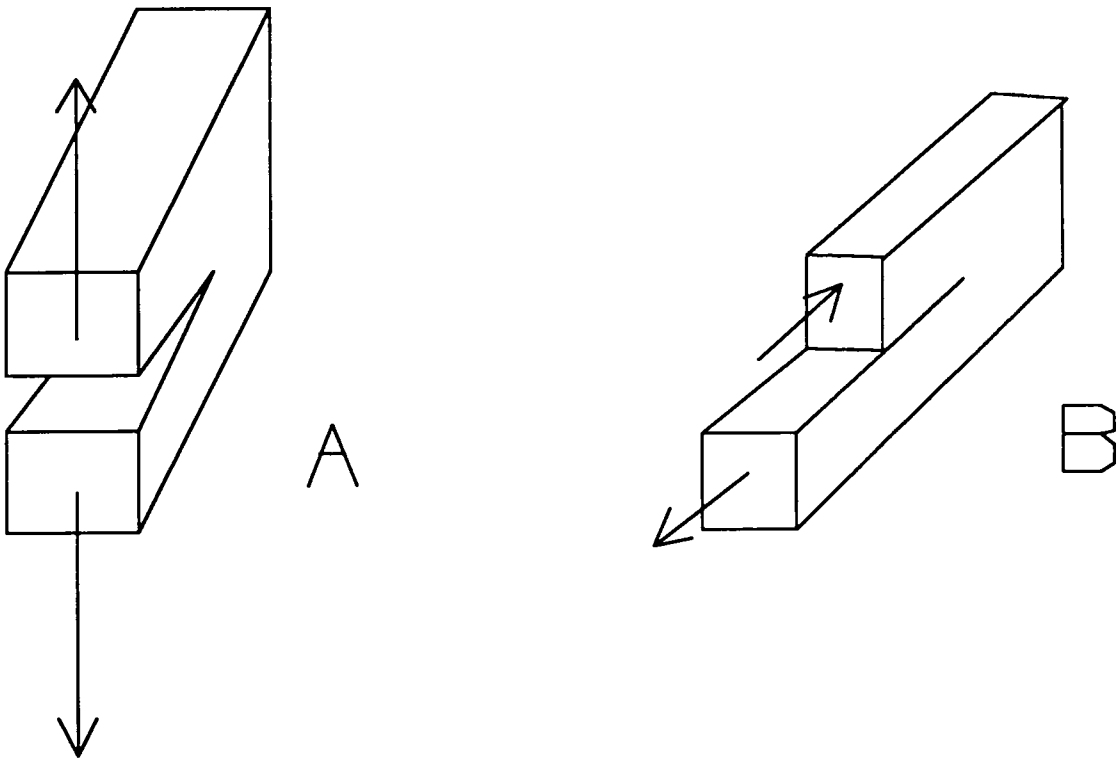

Fig. 3. Basic modes of crack surface displacement in beams. A. Opening (Mode I). B. Sliding shear (Mode II). Adapted from Murphy (1979).

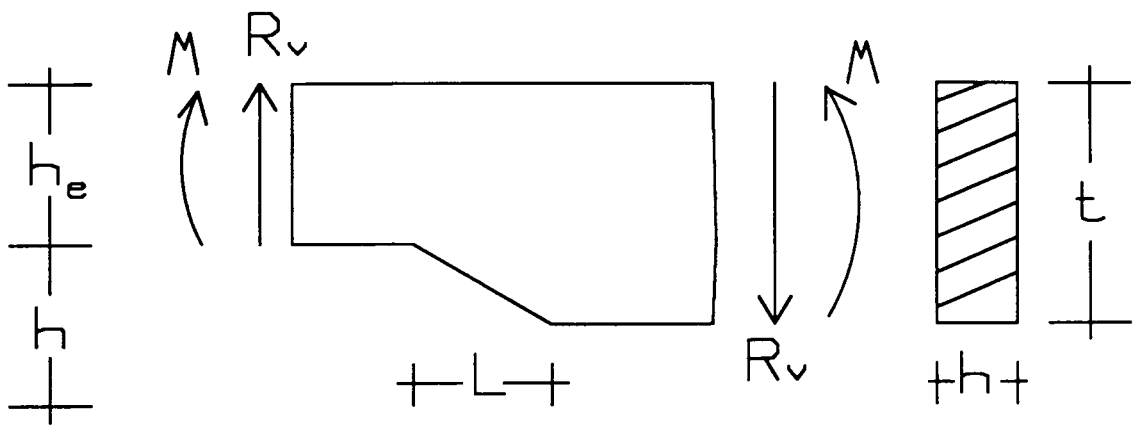

Figure 4. Notched beam geometry for Australian design methods. Adapted from Stds. Assoc. of Australia (1988).

3.0 Modeling

This study includes both theoretical modeling and mechanical testing of notched wood beams. Modeling serves three essential purposes. First, comparisons between theoretical and experimental results tests the validity of the underlying theory. Second, modeling facilitates the exploration of numerous cases throughout the sample space. An experimental program thoroughly covering similar ranges of the independent variables would be quite costly and time-consuming. Finally, theoretical findings are often easier to reduce to closed form, because their variability is insignificant or known *a priori*.

The model chosen for this study is the critical fillet hoop stress model of Gerhardt (1984a). It posits a relationship between the failure loads of notched beams and the maximum hoop stress at the critical fillet. Fillet hoop stress, $\sigma_{h,\theta}$, is defined as the non-zero principal stress acting on the free surface of a filleted notch corner at an angle θ from the horizontal, as shown in Figure 5. The critical fillet is defined as the one under the most severe loading, as determined by the applied moment and shear. In this work, $\sigma_{h,\theta}$ is calculated for a homogeneous orthotropic elastic body

under plane stress conditions. The material axes are coincident with the beam axes.

3.1 Finite Element Modeling

Finite element (FE) analysis was used to calculate $\sigma_{n,\theta}$ for 293 notched beams having different combinations of notch depth (D), fillet radius (R), notch length (L), beam depth (h), span (s), notch location, loading condition, and elastic parameters. Section 3.1.3 describes the experimental designs of the three substudies comprising the numerical modeling. The FE model calculated stresses, strains, and displacements with good computational efficiency while allowing nearly all cases of practical interest to be studied.

3.1.1 Finite element model

The FE program developed by Gerhardt (1983,1984a,b) was used for all stress computations. The program was modified slightly to run on an IBM 3090 using the VS FORTRAN Version 2 compiler. It is listed in Appendix 1.

3.1.1.1 Hybrid circular fillet element

Gerhardt's hybrid fillet element (subroutine ELMT02 in Appendix 1) satisfies all governing differential equations of anisotropic elasticity over the entire element. The fillet surface is an arc of a circle, i.e., not discretized into line segments. The condition of zero stress perpendicular to

the free surface of the fillet is inherent in the formulation. Compatibility with adjoining finite elements is enforced approximately at the nodes. The element may be used with various numbers of sides and nodes per side, and any fillet radius and arc length. (Appendix 2, a user's guide to the FE program, includes the options available when using the hybrid fillet element.) The configuration shown in Figure 6 was used throughout this study: four straight sides with four nodes per side, with all included angles equal to 90°, and a quarter-circular fillet (i.e., $0 \leq \theta \leq 90^{\circ}$).

3.1.1.2 Isoparametric cubic quadrilateral element

Outside of the fillet region(s), the beam was modeled using a 12-node isoparametric cubic quadrilateral element (subroutine ELMT01 in Appendix 1; Gerhardt 1983). It is a plane linear-elastic displacement-based element with no interior nodes (i.e., a serendipity element). Isotropic, orthotropic, or anisotropic material symmetry may be specified, as can plane stress or plane strain conditions. In this work, the orthotropic formulation is used, with the principal material axes aligned with the beam axes. Plane stress loading was assumed. The cubic element gives good results with a relatively coarse element mesh and over a wide range of aspect ratios (Gerhardt 1984a).

3.1.1.3 Requirements for accuracy

Several parameters were adjusted to achieve accurate results with the FE model. They include: 1) the order of Gauss quadrature used in evaluating the hybrid element stiffness matrix; 2) the number of terms in the Taylor series expansion of the stress function; 3) the shape and size of the hybrid fillet element; and 4) the shapes and sizes of isoparametric elements adjoining the fillet element.

Gauss quadrature is used to evaluate the stiffness matrix of the hybrid element. The order of quadrature is specified by the user for the best compromise between accuracy and computational economy. Numerous test cases involving disparate notch geometries and elastic parameters were run to establish the order of integration above which computed results were essentially invariant. Although twelve Gauss points along each element side proved sufficient in most cases, beams with high orthotropy ratios (e.g., $E_x/G_{xy} = 32$) required forty Gauss points for satisfactory accuracy. (Note that no integration is performed along the fillet surface.) All results given herein were computed using forty Gauss points per side.

Another user input is the number of terms included in the Taylor series expansion used to express the stress function in the hybrid element formulation (Gerhardt 1984b). The

number of series terms must exceed the number of element degrees of freedom (nodes per element times nodal degrees of freedom) minus three (the rigid body modes). In accord with Gerhardt (1984a,b), results were essentially unchanged by using more than the minimum allowable series terms, i.e. 12 for the 13-node, plane hybrid element.

The size and shape of the fillet element and the adjoining isoparametric elements are important in achieving an accurate solution. A test of the results of a given mesh is the comparison of the analytic displacement field calculated at the boundary of the fillet element and the nodal displacements calculated for the adjoining isoparametric element. Significant inconsistency of these displacements indicates an inappropriate mesh (assuming proper quadrature and series expansion). The following guidelines were established by trial and error.

The lengths of the fillet element sides adjacent to the fillet should be approximately equal to the fillet radius. This results in a nearly square element with non-fillet sides of length $\cong 2R$. Isoparametric elements which share a side with the fillet element should be approximately square. Non-rectangular elements or rectangular elements with aspect ratios (AR) much different from unity were problematic when placed in contact with the fillet element. FE analyses of

unnotched beams using the cubic isoparametric element gave good results with a variety of trapezoidal elements and rectangular elements with AR≤6. Only rectangular elements with 0.33<AR≤3 were used over the span of the beam for all cases reported herein. Higher aspect ratios were allowed for elements outside of the supports.

3.1.1.4 Input requirements

The user's guide in Appendix 2 describes all input data required for the FE program. The sizes and locations of notch fillets are specified in the definition of the hybrid element. All other notch and beam geometry is specified by the nodal coordinate mesh, to which boundary conditions and applied loads are applied. The element definitions, material properties, and program instructions (e.g., to treat multiple load cases) comprise the remainder of the input data file.

3.1.1.5 Program output

As used in this work, the FE program computes quantities which are written to several output files. These include: nodal displacements (u,v); stresses (σ_x, σ_y, τ_{xy}) and strains (ε_x, ε_y, γ_{xy}) at the Gauss points of each isoparametric element; displacements, stresses, and strains for 91 points at one-degree increments along the fillet surface; and $\sigma_{h,\theta}$ for 91 points at one-degree increments along the fillet surface. Additional stresses, strains, and displacements within the

hybrid element are readily output if needed (see Appendix 2). This feature was used diagnostically for testing different meshes and hybrid element quadratures.

3.1.2 Mesh generation

All input data, including nodal and element meshes, were generated using a microcomputer program written in the APL language (Gilman and Rose 1984; STSC, 1987). The APL functions and the overall program structure are shown in Appendix 3. The program was run on a personal computer based on an Intel 8088 processor (4.77 MHz clock speed) with an Intel 8087 floating-point coprocessor and 640 kilobytes of random-access memory, operating under the MS-DOS™ operating system. The data were written to a microcomputer disk ASCII file, which was uploaded to the IBM 3090 mainframe via modem. The STSC APL*PLUS interpreter allows code to be written and tested virtually line by line, if necessary, with no compilation or linking. It also provides for on-screen graphics, which were used to check the nodal locations and element connectivity. In addition to its interactive nature, APL offers numerous primitive array- and string-handling functions and branching structures which facilitate program development. Two meshes generated with this program are shown in Figure 7.

The mesh generator created data files which met all of the requirements for accuracy outlined in Section 3.1.1.3. To

The mesh generator created data files which met all of the requirements for accuracy outlined in Section 3.1.1.3. To test the mesh generator, I analyzed the notch geometries studied by Gerhardt (1984a) using the two extreme EP sets from his work. Since Gerhardt's computed $\sigma_{h,max}$ values were unavailable for comparison, I fit his closed-form equations to my results (Section 3.2.2). My best-fit coefficients were equal to his published values to three decimal places. This supports the validity of my mesh generation procedure.

3.1.2.1 End-notched beams

End-notched beams are being investigated in an ongoing study by other workers at this laboratory, and are not treated further here. The APL mesh generator was modified to generate FE input data files for end-notched beams with notches on the tension or compression face. The programs are diagramed, and the modified APL functions listed, in Appendix 4.

3.1.2.2 Interior-notched beams

Interior-notched beams, i.e., those with one or more notches within the supported span, were the focus of this work. Gerhardt (1984a) found minimal difference in stress results for single- and double-notched pallet stringers, in which notches were located symmetrically, 17 in. apart. As closer notch spacings are unusual (in pallets or elsewhere), only the single-notch case was treated in this study.

Single-notched beams were preferred for the experimental work as they require less machining time than do double-notched beams.

I performed two sets of FE calculations. The first set considered the effects of notch geometry, notch location, loading condition, and elastic parameters on maximum fillet hoop stress, $\sigma_{h,max}$, at a constant beam depth, h=3.5 in. The second focused on the effect of beam depth. Both series of numerical tests were designed to test the generality of Gerhardt's formulation (1984a), and to facilitate the derivation of algebraic equations to approximate the effects of the independent variables on $\sigma_{h,max}$.

Key to Gerhardt's method was the finding that $\sigma_{h,max}$ could be approximated as:

$$\sigma_{h,max} = f_1 \cdot \left(\frac{6M}{th^2}\right) + f_2 \cdot \left(\frac{6V}{th}\right) \qquad (3.1)$$

where:

f_1 = dimensionless apparent stress concentration factor for resultant moment;

f_2 = dimensionless apparent stress concentration factor for resultant shear;

M = resultant moment at the cross section containing the top of the critical fillet;

V = resultant shear at the cross section containing the top of the critical fillet.

It was helpful to rearrange equation (3.1) into the form:

$$MCF \equiv \frac{\sigma_{h,max}}{\left(\frac{6M}{th^2}\right)} = f_1 + f_2 \cdot \left(\frac{V}{M}\right) \cdot h \qquad (3.2)$$

MCF ("moment concentration factor") is the maximum hoop stress normalized by the gross section bending stress at the top of the fillet. For the shear-free case, equation (3.2) reduces to $MCF=f_1$. For center-point loaded beams, V/M is the reciprocal of the distance from the critical fillet to the nearest support. It is easily calculated from shear and moment diagrams (Figure 8; Byars and Snyder, 1975). The mesh generator calculates applied loads to give $6M/th^2=1$ at the critical fillet for each of three loading conditions: center-point, near-quarter-point, and uniformly distributed loading. Thus, each value of $\sigma_{h,max}$ (in units of lb_f/in^2) output by the FE program is numerically equal to the corresponding dimensionless MCF value. The mesh generator does not assure the presence of nodes at the quarter-span points, so the nearest nodes were chosen for the two-point loading condition. For the asymmetric offcenter-notched beams, these two "quarter points" were not, in general, exactly equidistant from the nearest support. Thus, there was no pure bending case for most of the offcenter-notched beams.

3.1.3 Experimental plan for FE modeling

The FE modeling was carried out in three studies. Each of these studies:

1) used MCF as the dependent variable;
2) included notch dimensions D, R, and L among the independent variables;
3) considered center-point (CP), quarter-point (QP), and uniformly distributed (UD) loading; and
4) used a central composite design (CCD), described below.

The CCD (Myers 1971) is an experimental design which allows a sample space with several independent variables to be probed efficiently when terms up to second order may be present and the levels of the independent variables can be precisely controlled by the experimenter. Five levels of each independent variable are used. Each level is at a predetermined fraction of the chosen range of the variable. A CCD is composed of a factorial portion, with 2^n runs (where n= number of independent variables), an axial portion, with 2n runs, and one or more center runs. The factorial portion matches the second and fourth levels of each independent variable to explore the outer-middle portions of the ranges. Each of the axial runs uses an extreme level of one variable with the central levels of the others. A center runs uses the central levels of all of the variables. The center run is generally

replicated more than the other runs. Since the FE model is deterministic, within-cell variance is zero, so no replication was needed. With three independent variables, for example, a CCD with one center run would involve $2^3+2(3)+1 = 15$ cells. By contrast, a full factorial design capable of discerning quadratic main effects would require $3^3=27$ cells. The full factorial design could, however, test for the three-way interaction which cannot be analyzed using the CCD.

3.1.3.1 Fixed beam depth study (h=3.5 inches)

The design of this study is shown in Table 2. For each of the five elastic parameter (EP) sets and three notch locations, it is a CCD with 3 independent variables (D, R, L) and 1 center run. The fifteen $(2^3+2(3)+1)$ notch geometries are shown in Table 3. Thus, a total of $5\times3\times15=225$ FE runs were conducted. Each included the three loading geometries, resulting in 675 computed values of MCF. For all beams, the overall length was 48in. and the span, s, was 44in..

Notch location was chosen to achieve desired values of V/M. The three notch positions were: 1) centered (V/M=0 for quarter-point bending); 2) near-center (V/M=0.05in.$^{-1}$ for center-point loading); and 3) far offcenter (V/M=0.10in.$^{-1}$ for center-point loading). Each center-notched beam was modeled using symmetry, i.e., only one half of the beam was explicitly modeled. The three notch locations and three loading

conditions give rise to nine levels of V/M for each notch geometry. Due to the finite number of possible loading points (nodes) in each mesh, only five of the nine V/M values were identical for each notch type. These were 0, 0.00833, 0.05, 0.07059, and 0.10in.$^{-1}$. The remaining three V/M ratios were between -0.056 and 0.0074in.$^{-1}$ for each beam.

The five EP sets are shown in Table 4. They were chosen to span the range of commercial wood properties. The orthotropy ratios E_x/G_{xy} and E_x/E_y influence $\sigma_{h,max}$ by affecting the ratios of longitudinal to transverse tensile stress and tensile to shear stress (Gerhardt 1984a). Poisson's ratio, ν_{xy}, was set to 0.40 in all cases as this parameter was found to exert minimal influence on the computed results (Gerhardt 1984a).

Notch depth ranged from 0.5-2.5in., or $\phi = D/h = 0.14\text{-}0.71$. This expands Gerhardt's range of $0.267 < \phi \leq 0.667$, and encompasses most practical cases in which the notch will govern beam capacity. Notch depth, D, was anticipated to be the overriding influence on stresses and failure loads (Stieda 1966; Gerhardt 1984a).

Preliminary tests confirmed Gerhardt's findings of minimal effect of fillet radius for $R \geq 0.5$in.. The main purpose of including R in this study was to quantify its effect in a way

which admitted extrapolation to R=0 (an unfilleted notch), which cannot be treated explicitly in a non-singular model. The range 0.2in.≤R≤0.5in. was selected. Below R=0.2in., FE modeling is cumbersome; above R=0.5in., dependence of beam strength on R is minimal (Gerhardt 1984a; Reeves 1973). The establishment of an effective fillet radius for unfilleted notches is discussed in Section 5.2.2.1.

Although Abou-Ghaida and Gopu (1984) found no significant notch length effect for D≤L≤3D, shorter notches are known to reduce strength (Stieda 1966; Murphy 1979). Longer notches are unexplored. I considered notches with 1in. ≤ L ≤ 9in..

3.1.3.2 Effect of beam size

The second FE study involved beam depth and span in addition to notch geometry, loading type, and material properties. It used the G32-E12 EP set with independent variables ϕ, R, L, h, and span, s. The third FE study used the G8-E12 EP set with independent variables ϕ, R, L, and h. (Span was dropped from the third study as it had no impact in the second. See Section 5.1.3.1.) Dimensionless notch depth, ϕ, was substituted for D to allow more straightforward interpretation of any beam depth effect. The second study included 43 runs ($2^5+2(5)+1$), and the third included 25 runs ($2^4+2(4)+1$).

For each study, a single offcenter notch geometry was used with the three loading conditions described above in Section 3.1.3.1. This resulted in three V/M ratios between 0 and 0.10in.$^{-1}$, and three MCF values, for each beam. The notch and beam geometries and resulting V/M ratios for each mesh are given in Tables 5 and 6.

Levels of R were 0.2-0.5in., as in the first FE study (Section 3.1.3.1). L ranged from 1.5-9.0in.. The range of ϕ, 0.2-0.7, was slightly smaller than that of the first study (0.14-0.71). Beam depths of 3.5-10.5in. were used in both substudies. The first substudy also included span over the range 44-88in.. A fixed span of 44in. was used in the second substudy, as in the *h*=3.5in. study.

3.2 Derivation of a Closed-Form Maximum Hoop Stress Model

The purpose of the closed-form expression is to estimate $\sigma_{h,max}$ without resorting to the FE model. The critical fillet hoop stress hypothesis is that notched beams crack in response to $\sigma_{h,max}$ exceeding a critical value. Thus, an accurate algebraic approximation of $\sigma_{h,max}$ facilitates prediction of failure loads of filleted notched beams.

3.2.1 Underlying assumptions

Several conditions must hold for the closed-form model to be useful. First, the cracking of notched beams must have some well-defined relationship to $\sigma_{h,max}$. Second, the fillet hoop stresses calculated under the assumptions of the FE analysis (plane stress, orthotropic elasticity, no slope-of-grain) must be closely analogous to the stresses along real notch fillets. Third, the expression used to approximate $\sigma_{h,max}$ must be sufficiently accurate over the range of practical cases. Fourth, any material parameters in the equation(s) must be readily obtainable by experiment or, preferably, through correlations with established material properties. Finally, the limitations of the model must be determined to prevent its misapplication.

3.2.2 Basic features of the model

Equation (3.1), restated below, is the basis of this work. It states that, upon determination of the stress concentration factors f_1 and f_2, $\sigma_{h,max}$ can be calculated directly from the resultant bending moment and shear force at the critical fillet. Different load placements which give rise to the same V and M are assumed to result in identical values of $\sigma_{h,max}$. No assumptions are made regarding any similarities between f_1 and f_2.

$$\sigma_{h,max} = f_1 \cdot \left(\frac{6M}{th^2}\right) + f_2 \cdot \left(\frac{6V}{th}\right) \qquad (3.1)$$

Gerhardt's FE results (1984a) were approximated well by f_1 and f_2 of the form:

$$f_1 = \frac{1}{(A\phi+B)} \tag{3.3}$$

$$f_2 = C\phi + D \tag{3.4}$$

with coefficients A, B, C, and D depending on elastic parameters. Equation (2.1) (Section 2.1.1.4) was derived from equations (3.1), (3.3) and (3.4) for cases in which the bending term dominates, as is typical in interior-notched beams. The simplification to a single material constant (K_{crit}) is very attractive for practical applications.

3.2.3 Theoretical relationship between maximum hoop stress and beam capacity

A notched beam strength equation was derived in three stages: 1) establishing the expression relating the FE-derived $\sigma_{h,max}$ to the independent variables (D, R, L, *h*, *s*, EP, and V/M); 2) rearranging the FE-based relationships to compare with the experimental results; and 3) determining any modifications to the FE-based equation needed to provide useful estimates of beam critical loads.

Ideally, elastic parameters should influence only one term in the closed-form expression, rather than appearing explicitly. The difficulty of obtaining reliable values of shear

modulus G_{LT} and transverse elastic modulus E_T dictate this goal. A simple approach is to assume a material dependence of the form:

$$f_1 = \mu_m \cdot F_1(D,R,L,h) \tag{3.5}$$

$$f_2 = \mu_v \cdot F_2(D,R,L,h) \tag{3.6}$$

where μ_m and μ_v depend on elastic properties and F_1 and F_2 are material-independent functions of notch and beam geometry. Under the assumption $\mu_m=\mu_v=\mu$, equation (3.2) may be rewritten:

$$\sigma_{h,max} = \frac{6M}{th^2} \cdot \mu \cdot \left(F_1 + F_2 \cdot h \cdot \frac{V}{M}\right) \tag{3.7}$$

$$\frac{6M}{th^2} = \frac{\sigma_{h,max}}{\mu} \cdot \frac{1}{F_1 + F_2 \cdot h \cdot \frac{V}{M}} \tag{3.8}$$

3.3 Application of the Closed-Form Expression to Experimental Results

The critical hoop stress hypothesis states that cracking occurs when $\sigma_{h,max} \geq \sigma_{h,i}$, where $\sigma_{h,i}$, the fillet hoop stress at crack initiation, is a material parameter Defining $\kappa_i \equiv \sigma_{h,i}/\mu$ allows equation (3.8) to be rewritten:

$$\frac{6M_i}{th^2} = \frac{\kappa_i}{F_1 + F_2 \cdot h \cdot \frac{V}{M}} \tag{3.9}$$

where:

M_i ≡ resultant moment at the critical fillet at crack initiation; and

κ_i ≡ notched beam strength parameter for crack initiation.

In equation (3.9), κ_i is the only material-dependent term. κ_i is formulated as a material parameter; as such, it should be independent of notch, beam, and loading geometry. Equation (3.9) is directly applicable to predicting notched beam capacity. Functions F_1 and F_2, once determined, reduce to known constants for a given notch geometry, κ_i is a material constant, and V/M is known for a given loading geometry. Derivations of the functions F_1 and F_2, and a discussion of the validity of equation (3.9), are given in Section 5.1.2.

Table 2. *Design of Main FE Study, h=3.5 in. (Parenthetical entries at right are numbers of levels of the given factor)*

Beam Dimensions:	*h*=3.5 in.; *s*=44 in.; *t*=1 in.	(1)
Notch Geometry:	15 combinations of D, R, L (Table 4)	(15)
Notch Location:	centered; critical fillet 10 in. from nearest support; critical fillet 20 in. from nearest support	(3)
Elastic Constants:	5 sets of E_x, E_y, G_{xy}, ν_{xy} (Table 3)	(5)
Loading Geometry:	center-point, two-point (nearly symmetric), uniformly distributed	(3)

Table 3. *Notch Geometries in h=3.5 in. FE Study*

D, in.	R, in.	L, in.
0.5000	0.35000	5.0000
0.9060	0.26091	7.3758
0.9060	0.26091	2.6242
0.9060	0.43909	7.3758
0.9060	0.43909	2.6242
1.5000	0.20000	5.0000
1.5000	0.35000	9.0000
1.5000	0.35000	5.0000
1.5000	0.35000	1.0000
1.5000	0.50000	5.0000
2.0940	0.26091	7.3758
2.0940	0.26091	2.6242
2.0940	0.43909	7.3758
2.0940	0.43909	2.6242
2.5000	0.35000	5.0000

Table 4. *Elastic Parameter Sets for FE Computations*

(E_x, E_y, G_{xy} in units of 10^6 $lb_f/in.^2$)

Designation	E_x	E_y	G_{xy}	ν_{xy}	E_x/E_y	E_x/G_{xy}
G8-E12	1.2	0.100	0.1500	0.40	12	8
G12-E12	1.2	0.100	0.1000	0.40	12	12
G17-E17	1.7	0.100	0.1000	0.40	17	17
G22-E22	1.1	0.050	0.0500	0.40	22	22
G32-E12	1.2	0.100	0.0375	0.40	12	32

Table 5. *FE Substudy, G32-E12 Elastic Properties*

Notch Geometry			Beam Geometry		V/M, in.$^{-1}$		
ϕ	R, in.	L, in.	*h*, in.	*s*, in.	CP[1]	QP[2]	UD[3]
0.55507	0.41304	6.681	8.4709	75.246	0.10	-0.00074	0.08467
			8.4709	56.754	0.10	0.00055	0.07861
			5.5291	75.246	0.10	-0.00074	0.08467
			5.5291	56.754	0.10	0.00055	0.07861
		3.319	8.4709	75.246	0.10	0.00032	0.08467
			8.4709	56.754	0.10	-0.00010	0.07861
			5.5291	75.246	0.10	0.00032	0.08467
			5.5291	56.754	0.10	-0.00010	0.07861
	0.28696	6.681	8.4709	75.246	0.10	0.00043	0.08467
			8.4709	56.754	0.10	0.00060	0.07861
			5.5291	75.246	0.10	0.00043	0.08467
			5.5291	56.754	0.10	0.00060	0.07861
		3.319	8.4709	75.246	0.10	0.00038	0.08467
			8.4709	56.754	0.10	0.00052	0.07861
			5.5291	75.246	0.10	0.00038	0.08467
			5.5291	56.754	0.10	0.00052	0.07861
0.34493	0.41304	6.681	8.4709	75.246	0.10	-0.00074	0.08467
			8.4709	56.754	0.10	-0.00029	0.07861
			5.5291	75.246	0.10	-0.00074	0.08467
			5.5291	56.754	0.10	0.00055	0.07861
		3.319	8.4709	75.246	0.10	0.00032	0.08467
			8.4709	56.754	0.10	-0.00010	0.07861
			5.5291	75.246	0.10	0.00032	0.08467
			5.5291	56.754	0.10	-0.00010	0.07861

[1] CP - center-point loading
[2] QP - quarter-point loading
[3] UD - uniformly distributed loading

Table 5, *continued. FE Substudy, G32-E12 Elastic Properties*

Notch Geometry			Beam Geometry		V/M, $in.^{-1}$		
ϕ	R, in.	L, in.	*h*, in.	*s*, in.	CP[1]	QP[2]	UD[3]
0.34493	0.28696	6.681	8.4709	75.246	0.10	0.00043	0.08467
			8.4709	56.754	0.10	0.00060	0.07861
			5.5291	75.246	0.10	0.00043	0.08467
			5.5291	56.754	0.10	0.00060	0.07861
		3.319	8.4709	75.246	0.10	0.00038	0.08467
			8.4709	56.754	0.10	0.00052	0.07861
			5.5291	75.246	0.10	0.00038	0.08467
			5.5291	56.754	0.10	0.00052	0.07861
0.20	0.35	5.0	7.0000	66.000	0.10	-0.00029	0.08214
0.70	0.35	5.0	7.0000	66.000	0.10	-0.00029	0.08214
0.45	0.20	5.0	7.0000	66.000	0.10	-0.00039	0.08214
	0.50	5.0	7.0000	66.000	0.10	0.00000	0.08214
	0.35	1.5	7.0000	66.000	0.10	0.00029	0.08214
		9.0	7.0000	66.000	0.10	-0.00065	0.08214
		5.0	3.5000	66.000	0.10	-0.00029	0.08214
			10.5000	66.000	0.10	-0.00029	0.08214
			7.0000	44.000	0.10	0.00086	0.07059
			7.0000	88.000	0.10	-0.00038	0.08718
			7.0000	66.000	0.10	-0.00029	0.08214

[1] CP - center-point loading
[2] QP - quarter-point loading
[3] UD - uniformly distributed loading

Table 6. *FE Substudy, G8-E12 Elastic Properties (s=44 in.)*

Notch Geometry				V/M, $in.^{-1}$		
ϕ	R, in.	L, in.	*h*, in.	CP[1]	QP[2]	UD[3]
0.32487	0.27492	3.3730	5.2481	0.10	0.01887	0.07059
			8.7519	0.10	0.01887	0.07059
		7.1270	5.2481	0.10	0.01868	0.07059
			8.7519	0.10	0.01868	0.07059
	0.42508	3.3730	5.2481	0.10	0.01912	0.07059
			8.7519	0.10	0.01912	0.07059
		7.1270	5.2481	0.10	0.01891	0.07059
			8.7519	0.10	0.01891	0.07059
0.57513	0.27492	3.3730	5.2481	0.10	0.01887	0.07059
			8.7519	0.10	0.01887	0.07059
		7.1270	5.2481	0.10	0.01868	0.07059
			8.7519	0.10	0.01868	0.07059
	0.42508	3.3730	5.2481	0.10	0.01912	0.07059
			8.7519	0.10	0.01912	0.07059
		7.1270	5.2481	0.10	0.01891	0.07059
			8.7519	0.10	0.01891	0.07059
0.20000	0.35000	5.2500	7.0000	0.10	0.01877	0.07059
0.70000	0.35000			0.10	0.01877	0.07059
0.45000	0.20000			0.10	0.01882	0.07059
	0.50000			0.10	0.01880	0.07059
	0.35000	1.5000		0.10	0.01903	0.07059
		9.0000		0.10	0.01869	0.07059
		5.2500	3.5000	0.10	0.01877	0.07059
			10.5000	0.10	0.01877	0.07059
			7.0000	0.10	0.01877	0.07059

[1] CP - center-point loading
[2] QP - quarter-point loading
[3] UD - uniformly distributed loading

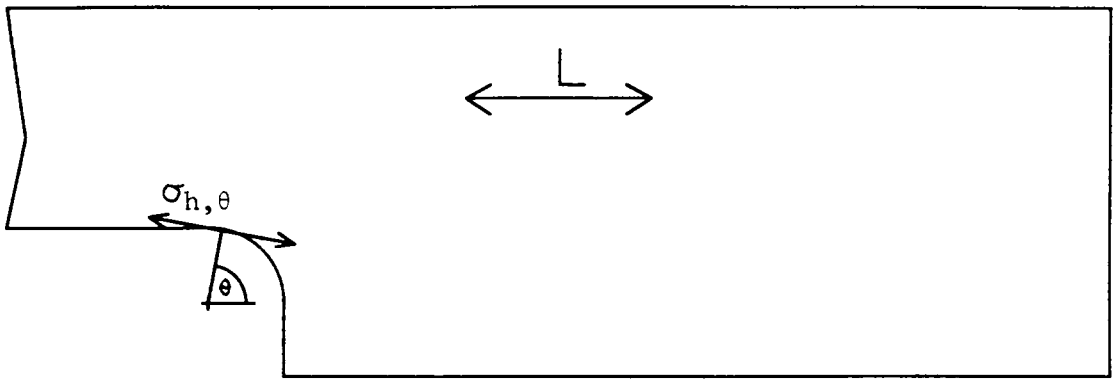

Figure 5. A. Fillet hoop stress $\sigma_{h,\theta}$ at θ = 80°. For θ approaching 90°, $\sigma_{h,\theta}$ acts nearly parallel-to-grain.

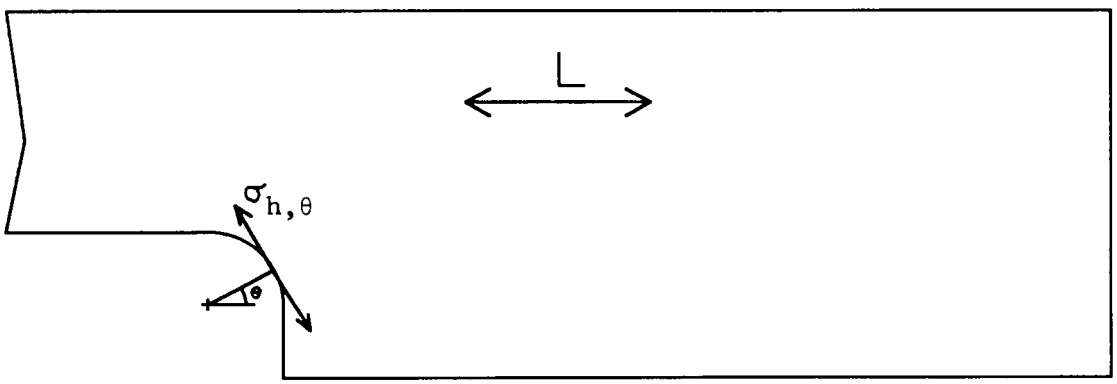

Figure 5. B. Fillet hoop stress $\sigma_{h,\theta}$ at θ = 30°. For small θ, $\sigma_{h,\theta}$ includes a large perpendicular-to-grain component.

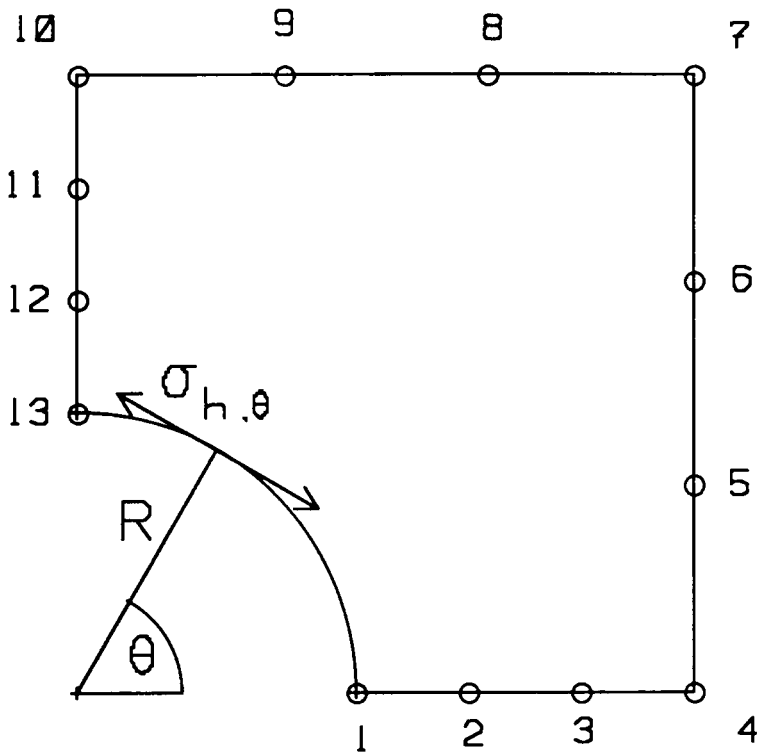

Figure 6. Hybrid fillet element of T.D. Gerhardt (1984a, b). R = fillet radius. $\sigma_{h,\theta}$ = fillet hoop stress at fillet angle θ.

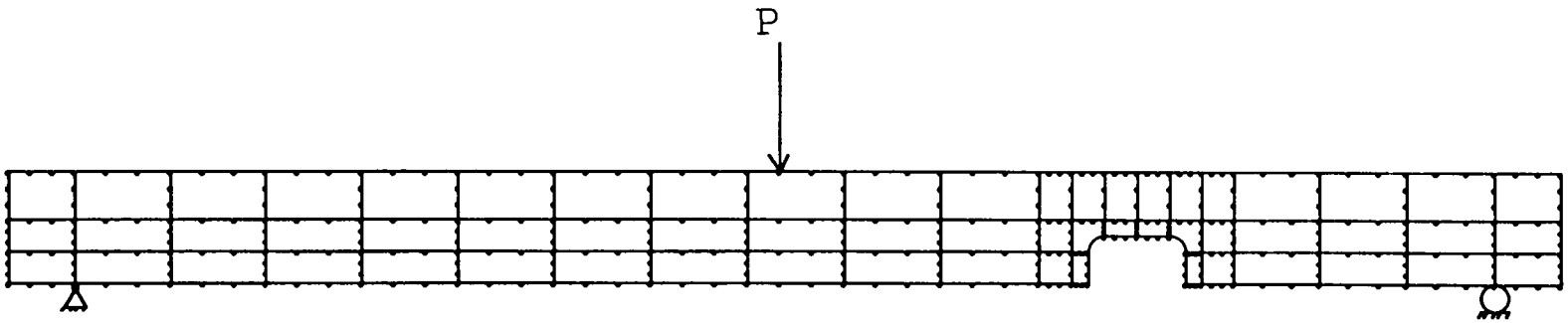

Figure 7a. FE mesh for offcenter-notched beam with center-point load. D=1.75in., R=0.75in., h=3.5in., s=48in. The supports are 2in. from each end.

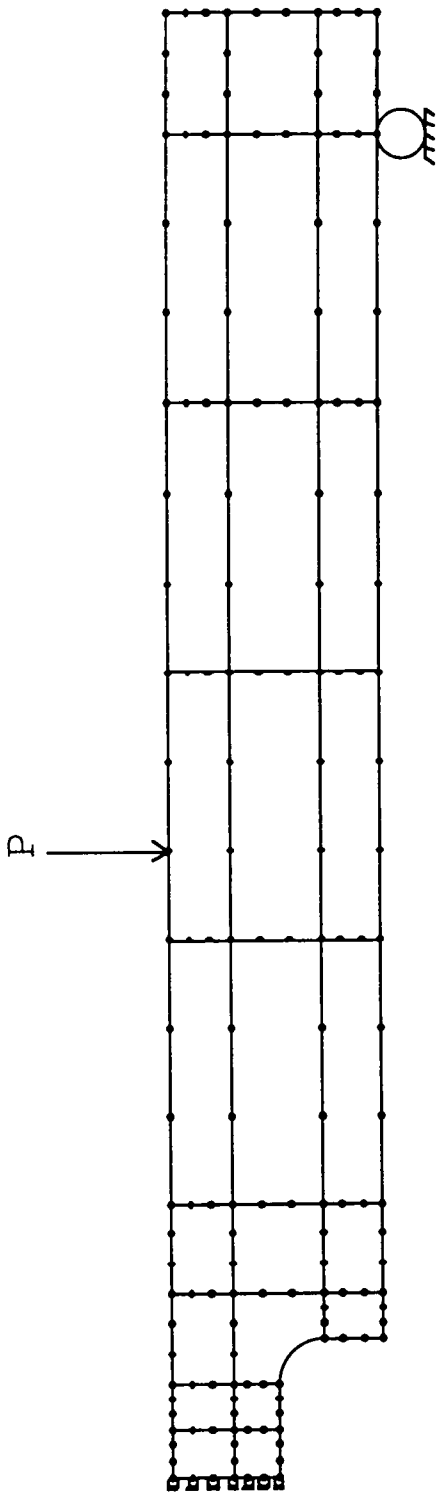

Figure 7b. FE mesh for center-notched beam with symmetrical point loads. Only the right half of the beam is explicitly modeled. D=1.75in., R=0.75in., h=3.5in., s=48in. The right support is 2in. from the right end.

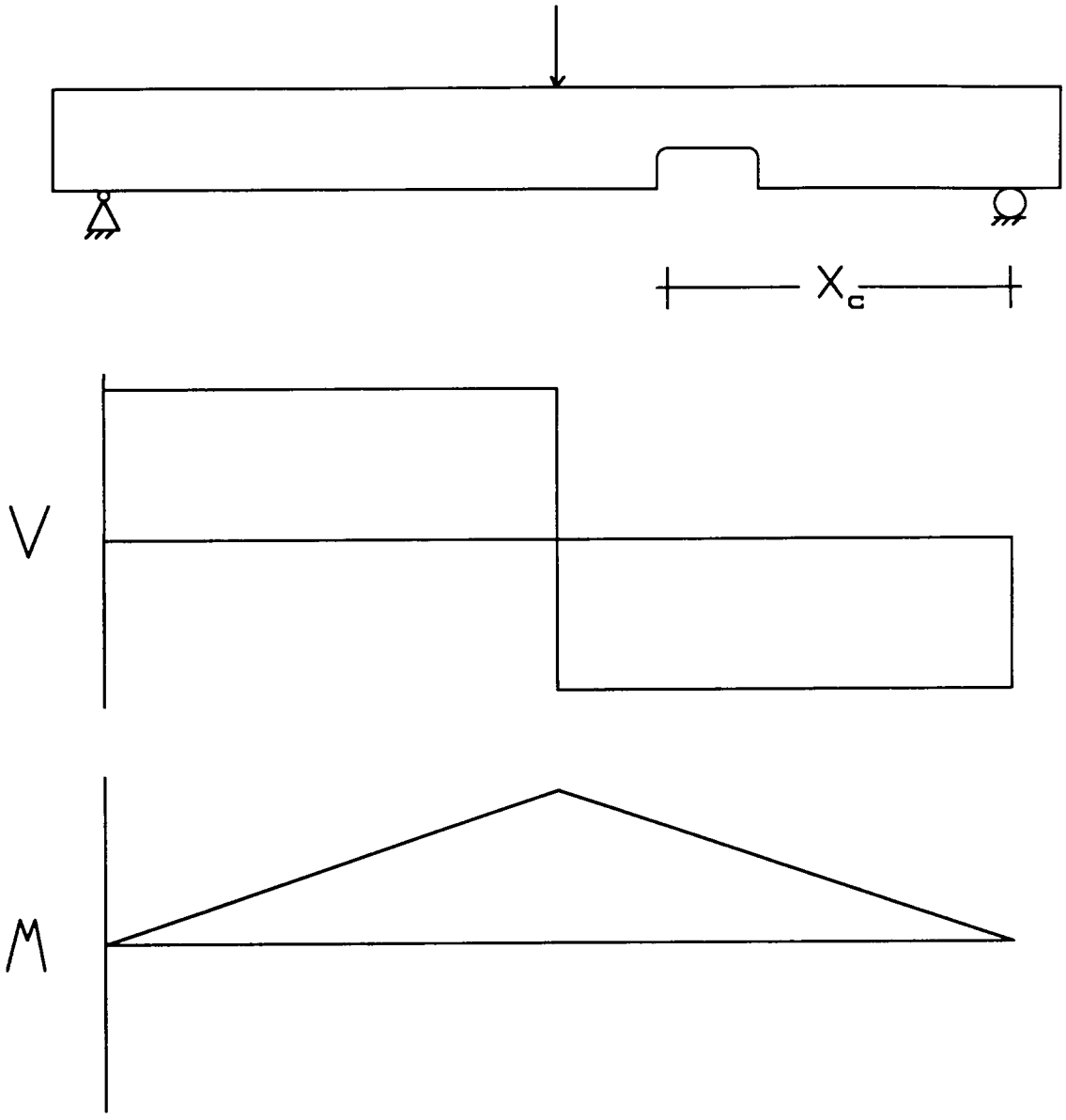

Figure 8. Shear and moment diagrams for an offcenter-notched beam under center-point loading. X_c = distance from the critical fillet to the nearest support. For this case, $V/M = 1/X_c$.

4.0 Mechanical and Physical Testing

4.1 Experimental Objectives

The experimental work served five primary purposes: 1) to test the validity of the critical fillet hoop stress model for a variety of notched beams; 2) to evaluate the material constant, κ, arising from the model; 3) to find a relationship between κ and other wood properties; 4) to elucidate the differences in strength between notched beams with and without fillets; and 5) to estimate the variability of notched beam strength. Satisfying these objectives involved tests of notched and unnotched beams and small, clear specimens of several wood materials.

4.2 Notched Beam Studies

The notched beam tests were performed in three studies, denoted A, B, and C in chronological order. Study A provided an initial assessment of the applicability of the theoretical model to materials other than green red oak, the only material tested by Gerhardt (1984a). It also provided information used to select the ranges of R and L explored in the subsequent studies. Study B was the principal effort (771 beams) to validate the theoretical model for eight wood materials. Study C was carried out to suggest extensions to the model to

handle sharp-cornered notches and very short notches (i.e., slit notches.)

4.2.1 Test variables

In all studies, three general classes of test parameters were varied: 1) notch geometry; 2) beam and loading geometry; and 3) material properties.

4.2.1.1 Notch geometry

As in the FE work, notch geometry was characterized by notch depth, D, fillet radius, R, and notch length, L, and by the corresponding nondimensional notch parameters ϕ, δ, ρ, and λ. Notch depth and length varied slightly due to manufacturing variation, but were typically within 0.020in. of target values. The actual dimensions, measured to the nearest 0.01in. and 0.001in. for L and D, respectively, were used in all computations.

Fillet radius was considered fixed by the radius of the cutting tool. All filleted notches had quarter-circular fillets, i.e., they extended from a vertical notch side to the horizontal notch top. (For L=2R, the two fillets meet at the notch top to form a semicircular fillet.) Thus, the choice of notch depth and length restricted fillet radius to $R \leq D$ and $R \leq L/2$. For this reason, radii greater than 0.75in. were incompatible with the minimum notch depth of 0.75in., and were

not used. A radius of zero was assigned to all sharp-cornered notches. The actual corner radii were no more than 0.030in. for the unfilleted notches, and were probably considerably less.

4.2.1.2 Beam and loading geometry

All test beams had the following approximate dimensions: thickness $t \cong 1.5$in.; depth $h \cong 3.5$in.; length $l \cong 48$in.; and span $s \cong 44$in. Under asymmetric loading, one of the two fillets is clearly more highly loaded, as shown by shear and moment diagrams (Figure 8, Chapter 3). This is termed the 'critical fillet'. Load and notch locations were varied to achieve V/M ratios of 0, 0.05in.$^{-1}$ and 0.10in.$^{-1}$ at the critical fillet. For V/M=0, the notch was located at center-span between quarter-point (QP) loads. An offcenter notch in center-point (CP) loading was used to achieve V/M>0. For an offcenter notch under CP loading, V/M = $1/x$, where x is the distance from the top of the critical fillet to the nearest support. Thus, for V/M=0.10in.$^{-1}$, the top of the critical (inside) fillet is 10in. from the support.

Implicit in the critical fillet hoop stress model is the assumption that cracking will initiate at the point of highest fillet hoop stress, which is always on the critical fillet. Of the 864 notched beams included in the data (Section 5.2.2), 53 (6.1%) cracked first at the outer fillet prior to

cracking at the inner (critical) fillet. Another 5 notches cracked only at the outer fillet. Eight other beams, not included in the results, failed with no cracking at either fillet. All eight were southern yellow pine (5 green, 3 dry) with notches far offcenter ($V/M=0.10 in.^{-1}$). Knots close to midspan, i.e., near the point of maximum moment, governed failure of these beams.

4.2.1.3 Materials

Eight materials were included in the tests: hard maple (*Acer* spp.), green; red oak (*Quercus* spp.), dry; yellow-poplar (*Liriodendron tulipifera*), dry and green; Douglas-fir (*Pseudotsuga menziesii*), dry; southern yellow pine (*Pinus* spp.), dry and green; and spruce (*Picea* spp.), dry. Each combination of species and moisture condition was considered as a separate material, that is, moisture content was not treated as an independent variable.

The six test species include three hardwoods (maple, oak, and yellow-poplar) and three softwoods (Douglas-fir, southern yellow pine, and spruce), which cover the major categories of anatomical structure of commercially important North American species. The range in dry-basis specific gravity for these materials brackets the specific gravities of most North American woods (Table 27, Chapter 5).

4.2.2 Design of experiments

In all three studies, all levels of ϕ and V/M were within the ranges of the FE work. Some tests included R or L below the lower limits of the FE work to investigate effects which were difficult or impossible to treat with the present FE model. Study B also included notches with R=0.75in., whereas the FE work included only R≤0.5in. The designs of studies A, B, and C are described below.

4.2.2.1 Preliminary study (A)

Study A was conducted to assess whether the critical fillet hoop stress model adequately described the general features of notched beam failure for cases outside of the range studied by Gerhardt (1984a). It also provided information for the selection of levels of R and L for the subsequent, larger experiments. In particular, study A was designed to help answer the questions:

1) What is the R effect for R<0.50in.?
2) Is there an L effect?
3) Are there any D-R, D-L, or R-L interactions?
4) Are there any interactions between notch geometry and material?

Study A was a full factorial experiment with two levels each of D and L and 3 levels of R, as shown in Table 7. Two levels of D were included to check for interactions between D

and R or L. The three levels of R (0, 0.25, and 0.375 inch) were repeatably machinable and covered the range expected to include R_{min}, the radius below which filleted and unfilleted notches behave identically. For a balanced experiment, the maximum radius of 0.375in. dictated that all notches have D≥0.375in. and L≥0.75in. (Section 4.2.1.1). I chose L≅0.75in. and L≅9.0in., and D≅0.6in. (ϕ≅0.17) and D≅2.0in. (ϕ≅0.57), as reasonable extremes.

Two materials, dry red oak and dry true fir (*Abies* spp.), were chosen to represent very different anatomical and mechanical properties. A single loading case, V/M=0 (pure bending throughout the notch region), was used to simplify testing and analysis of results. Test results at V/M=0 allowed the evaluation of κ and preliminary verification of the form of F_1 (Sections 3.2.3, 3.3, and 5.1.2). Two beams were tested per cell, with the following exceptions. The fir tests included third replications of geometries 2 and 9 (Table 7). The oak tests included three beams of geometries 6 and 10 and only one beam of geometries 3 and 12.

4.2.2.2 Main study (B)

The main study (B), provided a detailed test of the validity of the theoretically-derived model. All beam and loading geometries in study B coincided closely with those treated in the FE modeling. Target notch depths were from 14%-61% of

beam depth, i.e., $0.14 \leq \phi \leq 0.61$. This covered most practical cases while staying within the bounds of the model. The three experimental fillet radii, 0.25in., 0.5in., and 0.75in., were used to test the R-dependence predicted over the FE-modeled range (0.2in.-0.5in.), and to determine whether the FE-derived strength expression would be useful with larger radii.

The results of study A showed no influence of L, although the FE analysis suggested a small, but statistically significant, L effect. Thus, the 'SYP' substudy in study B (green and dry southern yellow pine) included L over the range 1.5in.-7.5in. to confirm the validity of dropping L from the experimental plan. It used a partial factorial design, with 21 cells incorporating five levels of D, three levels of R, and three levels of L (Table 8). The SYP substudy employed $V/M=0.10in.^{-1}$, so that an L effect in either the shear term (F_2) or the moment term (F_1) of equation (3.9) would be observable. These results showed essentially no L effect, leading to the choice of L=constant=1.5in. for the remainder of study B.

Study B was a full factorial design with five levels of D, three levels of R, and three V/M ratios. The fifteen notch geometries were tested at each of the three V/M ratios for each of the eight materials. Table 9 summarizes the

experimental design. As described in Table 9, study B included 771 notched beam tests.

4.2.2.3 Slit/sharp notch study (C)

Study C was a full factorial design employing two materials, two V/M ratios, and two levels each of D and L, with R=constant≅0. It used L=0.125in. and L=1.5in. to probe the magnitude of any slit notch effect. The two extreme V/M ratios, 0 and 0.10in.$^{-1}$, were used. Yellow-poplar, green, and southern yellow pine, dry, were tested. This choice was based on the results of study B, which showed variability to be lowest in green hardwoods and greatest in dry softwoods. The sharp notch study (C) employed $\phi \cong 0.21$ and $\phi \cong 0.51$. The notch geometries are given in Table 10. R=0 was used in all cases, to allow for the very short (L=0.125in.) notches. The R=0, L=1.5in. data from study C were also compared with R>0, L=1.5in. results from study B to help evaluate R_{min}.

4.2.3 Specimen selection and preparation

4.2.3.1 Material conditioning and selection

Materials for the tests were obtained from a variety of commercial sources. The maple and yellow-poplar were purchased from log yards within 100 miles of Blacksburg, and sawn, jointed, and planed in the Department of Wood Science and Forest Products. Rough-sawn, green southern yellow pine

was purchased from a local sawmill. For dry tests, the yellow-poplar and southern yellow pine were kiln-dried in-house to average moisture contents (MC) of about 10%, using standard drying schedules to minimize checking (Lamb, 1988). The red oak for study B was supplied with MC of 5-6% by a regional supplier of wood to the furniture industry. The red oak used in study A was purchased green from a local mill and kiln-dried to about 10% MC in-house. The Douglas-fir and spruce for study B, and the fir for study A, were purchased in the kiln-dried condition from local building supply distributors. The spruce (study B) and fir (study A) were selected from commercial SPF (spruce-pine-fir) lumber; they may have contained small amounts of the other species within that marketing class (Amer. Soc. for Testing and Matls., 1986a). The green specimens all had average MC above 29%, although some surface drying occurred during storage.

It was necessary to store the green materials for extended periods (several weeks to several months) prior to testing. During storage, all green lumber was wrapped in polyethylene sheeting. Blue stain developed on the yellow-poplar during covered outdoor storage (in October and November) prior to putting the dressed material under refrigeration. Blue stain was inhibited, but not entirely prevented, on the pine by dipping the green boards into a dilute solution of chlorine

bleach (sodium hypochlorite). Blue stain was not problematic for the maple, as it was acquired much closer to the time of testing, and was stored at a lower average termperature. Several months elapsed between the V/M=0 tests and the other tests. During that time, blue stain grew on both the pine and the yellow-poplar, despite their refrigeration. Although blue stain is not generally considered a strength-reducing defect, some researchers have disputed this view (Bodig and Jayne 1982; Panshin and de Zeeuw 1980). Blue stain is commonly associated with significant reductions in wood toughness under impact loading. Consequently, the test results for the green materials may not be typical for those species. While blue stain growth is often concurrent with the growth of wood-decaying fungi, I doubt that such decay proceeded to a serious extent, because the average temperature of the boards was probably below 50°F throughout the storage period, and was typically below 40°F.

Beams were selected for notching on the basis of freedom from knots in the prospective notch region, and lack of visible slope of grain. Notched beams with visible cracks or deviation from the desired notch shape were discarded. Twisted boards were culled due to difficulties that they caused during mechanical testing (Section 4.2.4).

4.2.3.2 Notch machining techniques

All notches in studies A and B were machined with a 1.5 horsepower router using a two-flute carbide bit (Figure 9). For the R=0 notches in study A, the router bit was aligned with the depth dimension of the beam and moved along the thickness dimension, acting as an end mill. Thus, the fillet radius approximated the radius of the carbide cutting tip. A template was built from plywood and tempered hardboard to confine the router bit to a straight path through the board. For notches over 0.75in. long, the bulk of the material was removed with a chisel after cutting slits in the board at about 0.75in. intervals with a radial arm saw. The slit depth was slightly less than the notch depth. The router provided the finish pass to final dimensions.

The process for machining the filleted notches of studies A and B is shown in the photographs in Figures 10-13. Thirteen templates (e.g., Figure 10) were made, each defining a particular combination of notch length and fillet radius. The upper edges of the clamps visible in Figure 10 rested along the bottom edge of the board and determined the notch depth. The template was clamped to the face of the board to define the size, shape, and location of the notch (Figure 11). The clamps also held the board firmly to the workbench. The rough outline of the notch was then sketched on the beam.

For notches deeper than 1in., the notch was roughed out using a 1.125in.-diameter carbide-tipped Forstner bit in a hand-held drill (Figure 12). This type of edge-guided bit allows holes to be drilled overhanging an edge or overlapping another hole. Thus, a series of drilled holes can be used to rough out a longer notch. The router and drill were industrial tools which used 0.5in.-shank bits.

Figure 13-15 show the steps of the machining process. In Figure 13, the beam of Figure 11 has been pre-notched with the Forstner bit. Figure 14 shows the placement of the router on the pre-notched beam to complete the notch. In the final machining pass, the router base rides along the inner edge of the template. Figure 15 shows the finished notch. The right edge of the notch shows some chipping out, which is typical of the method. This was not of concern, as this portion of the notch is nearly stress-free. Figure 16 is a close-up view of the notch. The notch surface is quite smooth, especially around the critical (left) fillet. The clockwise rotation of the router bit always resulted in a smooth left fillet and some chipping along the right edge. In center-notch tests, in which both fillets were equally critical, there was no indication that one fillet was systematically weaker than the other.

A different machining technique was used for the sharp-cornered notches of study C. Slit notches were formed with a radial arm saw in several passes to progressively greater depths. The resulting notch lengths varied from 0.128in. to 0.136in. For the 1.5in. long notches, radial arm saw cuts were made at the notch ends and at two intermediate points. A chisel was then used to remove the bulk of the material from the notch. The radial arm saw was then adjusted to the desired notch depth, and the blade was passed over the notch region several times to remove excess material. Finally, the beam was placed under the blade and moved slowly perpendicular to the plane of the blade to smooth the top of the notch. (The great care required in this method may preclude its use when large numbers of notches must be made.) Figure 17 shows a notch (after testing) made with this method. Note that the small asperities in the notch top do not appear to have influenced the cracking.

4.2.4 Bending test methods

Bending tests were carried out on two testing machines using two loading configurations. In all cases, the span was 44in. In studies A and B, the V/M=0 tests were performed on a Tinius Olsen screw-type universal testing machine using quarter-point bending. A 10,000-pound capacity compression load cell was bolted to the crosshead to allow load to be

recorded using an x-y plotter. A steel I-beam bolted to the load cell transmitted the load to two hardwood loading blocks (contact radius=8in.) which contacted the beam under test. Any misalignment of the load assembly (e.g., due to a twisted beam) gave rise to transverse loads which introduced errors into the load cell readings. For this reason, critical loads were read from the Tinius Olsen dial gauge whenever possible. The dial gauge readings, particularly at ultimate load, were used to confirm the load cell readings for each specimen. Center-span deflections were measured using a linear variable-differential transformer (LVDT) mounted on a deflection yoke, as described in ASTM Standard D143 (Amer. Soc. for Testing and Matls. 1986b). The LVDT drove the x-axis of the x-y plotter and the load cell drove the y-axis, giving a P-δ curve for each beam.

The V/M>0 tests in study B and all of study C were carried out using a servohydraulic universal testing machine made by MTS. Figures 18a and 18b show an offcenter-notched beam being prepared for a center-point loading test on this machine. Visible behind the technician in Figure 18a is the x-y recorder used for the P-δ traces. The beam rested on aluminum bearing blocks which sat on tubular steel supports, one of which was free to roll. Thus, compression at the supports was minimized, free rotation was allowed at both ends, and

axial constraint was minimized. The deflection yoke rested on nails driven into the workpiece at mid-depth immediately above each support. The LVDT core was connected by a steel ring to a third nail in the beam. This nail was placed at mid-span and mid-depth for offcenter-notched beams. For center-notched beams, this nail was located at the center of the net depth. This gave deflection measurements which were essentially independent of any compression effects at the supports or loading point(s).

All tests were conducted at a free-running crosshead rate of 0.10 in./min. The servohydraulic system maintained a set speed throughout the test. Since the crosshead rate of the screw-type machine may be slightly dependent on specimen compliance, there may have been slight differences in actual testing rate between the two test setups. Any such difference is presumed to be minor in its effect, as accepted testing practice specifies the same apparent crosshead speed for both screw-type and servohydraulic testing machines (Amer. Soc. for Testing and Matls. 1986b).

4.3 Small, Clear Specimen Tests

4.3.1 Selection of specimens

After testing to destruction, a moisture content (MC)-specific gravity (SG) specimen was cut from each notched beam

from studies B and C. Samples were taken from an area 1-6in. from the notch, while avoiding large knots, included bark, pitch pockets, and other anatomical deviations. At least 93 SG and MC determinations were made on each of the eight materials.

Block shear (S) and cross-grain tension ($T_{\perp}$) specimens were cut from each beam in the V/M=0.10in.$^{-1}$ series in study B. At least 30 S and $T_{\perp}$ values were obtained for each material. Samples were cut from an uncracked area of each beam and knots and sloping grain were avoided.

4.3.2 Test methods

4.3.2.1 Specific gravity and moisture content

Specific gravity on an oven-dry volume and weight basis was measured on a single specimen from each beam using method B of ASTM D2395-83 (Amer. Soc. for Testing and Matls. 1986c).

4.3.2.2 Block shear strength

Block shear strength was determined in accordance with the methods of ASTM D143 (Amer. Soc. for Testing and Matls. 1986b) except for the following points. Ring angle was not measured and varied by beam. The specimen thickness, 1.5in., was equal to the beam thickness, which is less than the standard 2.0in. However, Bendtsen and Porter (1978) found no significant differences between shear test results obtained

using 1.5in. versus 2.0in. specimen thickness. Consequently, the data were not adjusted for specimen thickness.

4.3.2.3 Perpendicular-to-grain tensile strength

As with the block shear tests, the specimen, apparatus, and test method used for the $T_{\perp}$ measurements followed ASTM D143 with minor exceptions. Again, the origin of the work-pieces from 1.5in. x 3.5in. beams limited specimen thickness to 1.5in. and precluded any control of ring angle. Although wood displays a strength-size relationship for $T_{\perp}$ (Barrett 1974; Barrett, *et. al.* 1975), the ratio of strengths for 1.5in. versus 2.0in. (ASTM standard) specimen thickness is unlikely to exceed $(2.0/1.5)^{0.25} = 1.075$ (Barrett 1974). Since the strength-size relationship for $T_{\perp}$ has not been quantified for species other than Douglas-fir, I did not apply any size adjustment to the $T_{\perp}$ results.

4.4 Unnotched Bending Tests

Quarter-point bending tests were performed on 30 unnotched control beams of each material tested in study B. Unnotched beams were selected from the same material stock as the notched beams. No knots were allowed on the tension face between the loading points, and severely twisted boards were rejected. The same loading geometry and test procedures were used for the unnotched beams as for the V/M=0 notched beams

(Section 4.2.4). Unnotched beams had nominal dimensions similar to those of the notched beams: t = 1.5in.; h = 3.5in.; l = 48in.; and s = 44in.

TABLE 7. *Target Experimental Notch Dimensions*
Study A
(D, R, L in units of inches)

Geometry[1]	D	R	L	$\phi \equiv D/h$	$\delta \equiv R/D$	$\rho \equiv R/h$	$\lambda \equiv L/h$
1	0.6	0.	0.75	0.17	0.	0.	0.21
2			9.0				2.57
3		0.25	0.75		0.42	0.071	0.21
4			9.0				2.57
5		0.375	0.75		0.63	0.11	0.21
6			9.0				2.57
7	2.0	0.	0.75	0.57	0.	0.	0.21
8			9.0				2.57
9		0.25	0.75		0.13	0.071	0.21
10			9.0				2.57
11		0.375	0.75		0.19	0.11	0.21
12			9.0				2.57

[1] arbitrary geometry index number.

TABLE 8. *Target Experimental Notch Dimensions*
Study B
(D, R, L in units of inches)

Geometry[1]	D	R	L	$\phi \equiv D/h$	$\delta \equiv R/D$	$\rho \equiv R/h$	$\lambda \equiv L/h$
13 S	0.75	0.25	2.5	0.21	0.33	0.071	0.71
14 S,B		0.5	1.5		0.67	0.14	0.43
15 S		0.5	7.5		0.67	0.14	2.14
16 S		0.75	2.5		1.00	0.21	0.71
17 S	1.1	0.25	2.5	0.31	0.23	0.071	0.71
18 S,B		0.5	1.5		0.46	0.14	0.43
19 S		0.5	7.5		0.46	0.14	2.14
20 S		0.75	2.5		0.68	0.21	0.71
21 S,B	1.45	0.25	1.5	0.41	0.17	0.071	0.43
22 S		0.25	7.5		0.17	0.071	2.14
23 S		0.5	2.5		0.35	0.14	0.71
24 S,B		0.75	1.5		0.52	0.21	0.43
25 S		0.75	7.5		0.52	0.21	2.14
26 S	1.8	0.25	2.5	0.51	0.14	0.071	0.71
27 S,B		0.5	1.5		0.28	0.14	0.43
28 S		0.5	7.5		0.28	0.14	2.14
29 S		0.75	2.5	1	0.42	0.21	0.71
30 S	2.15	0.25	2.5	0.61	0.12	0.071	0.71
31 S,B		0.5	1.5		0.23	0.14	0.43
32 S		0.5	7.5		0.23	0.14	2.14
33 S		0.75	2.5		0.35	0.21	0.71
34 B	0.75	0.25	1.5	0.21	0.33	0.071	0.43
35 B		0.75	1.5		1.0	0.21	0.43
36 B	1.1	0.25	1.5	0.31	0.23	0.071	0.43
37 B		0.75	1.5		0.68	0.21	0.43
38 B	1.45	0.5	1.5	0.41	0.35	0.14	0.43
39 B	1.8	0.25	1.5	0.51	0.14	0.071	0.43
40 B		0.75	1.5		0.42	0.21	0.43
41 B	2.15	0.25	1.5	0.61	0.12	0.071	0.43
42 B		0.75	1.5		0.35	0.21	0.43

[1] arbitrary geometry index number. S = SYP substudy. B = study B.

Table 9. *Experimental Design - Main Notched Beam Study (B)*

		Levels[1]
Beam Dimensions, in.:	$h \cong 3.5$, $t \cong 1.5$, $s \cong 44$, $l \cong 48$	(1)
Notch Dimensions:	15 combinations of D, R; L≅1.5in.	(15)
V/M, $in.^{-1}$:	0, 0.05, 0.10	(3)
Material:	Douglas-fir, dry; southern yellow pine, dry and green; spruce, dry; hard maple, green; red oak, dry; yellow-poplar, dry and green	(8)
Replications:	2 per cell, plus a third "center run" (D≅1.45in., R≅0.5in.), i.e. 31 tests per level of V/M for each material	
Total Tests:	31x3x8 = 744, + 24 additional for SYP sub-study, + 3 extra replications = 771.	

[1] number of levels of the given factor

TABLE 10. *Target Experimental Notch Dimensions*
Study C
(D, R, L in units of inches)

Geometry[1]	D	R	L	$\phi \equiv D/h$	$\delta \equiv R/D$	$\rho \equiv R/h$	$\lambda \equiv L/h$
43	0.75	0.	0.13	0.21	0.	0.	0.037
44		0.	1.5		0.	0.	0.43
45	1.80	0.	0.13	0.51	0.	0.	0.037
46		0.	1.5		0.	0.	0.43

[1] arbitrary geometry index number.

Figure 9. The router and carbide double-fluted straight bit used to machine notches for studies A and B. The circular router base, from which the bit protrudes, rests on the workpiece during machining.

Figure 10. A template used to guide the router base for machining notches. The radius and length of the template cutout and the radii of the router bit and router base determine the radius of the notch fillet. The metal clamps set the notch depth.

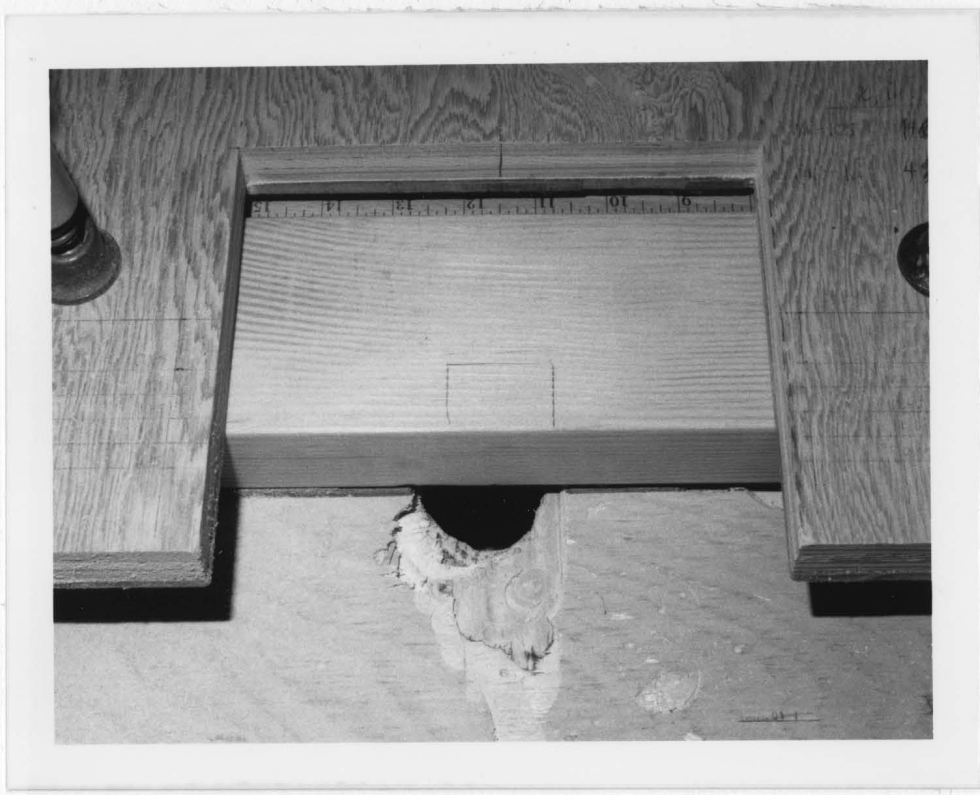

Figure 11. A notching template clamped to a beam to be notched. The notch outline has been sketched on the workpiece.

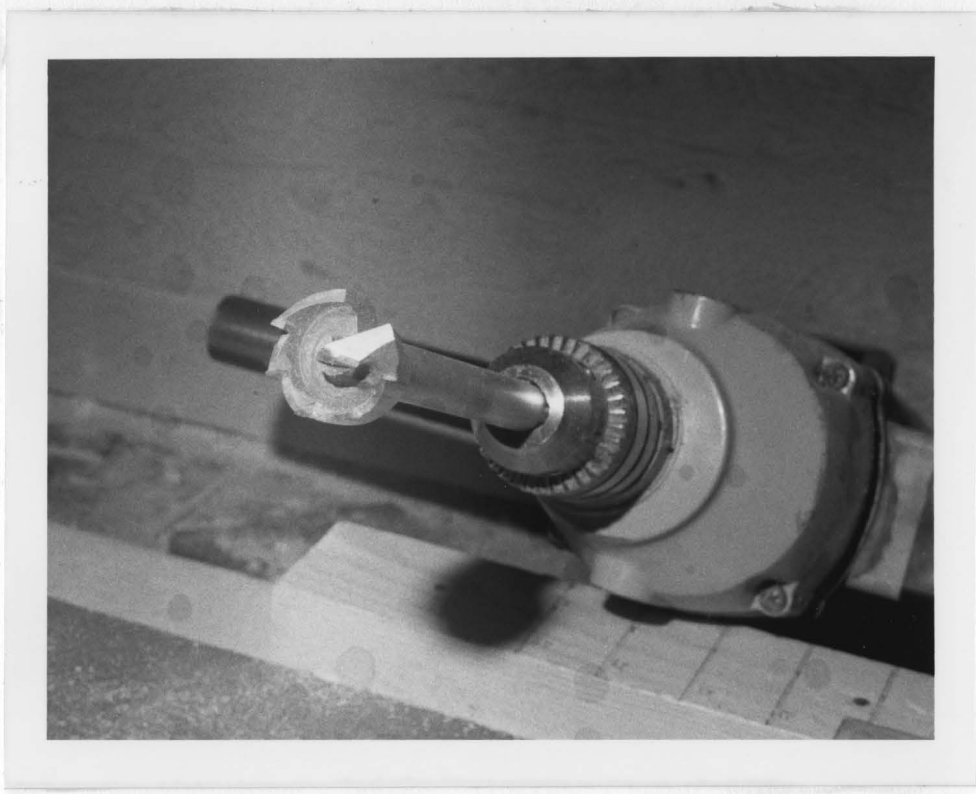

Figure 12. The power drill and carbide-tipped Forstner bit used for rough-machining notches with D>0.75in.

Figure 13. The beam of Figure 11 after rough machining a notch using the drill and bit shown in Figure 12.

Figure 14. The router in position for finish machining of a pre-notched beam.

Figure 15. The beam of Figure 13, after finish machining. The chipping-out of the lower right (outer) notch corner is inconsequential due to low stress in that area.

Figure 16. Magnified view of the notch of Figure 15. Note the smooth machined surface, particularly in the fillet regions which govern failure.

Figure 17. Unfilleted notch, after testing. This notch was machined with a radial arm saw using the method described in Section 4.2.3.2, page 80. Imperfections in notch shape away from the corners had no effect on crack initiation or propagation.

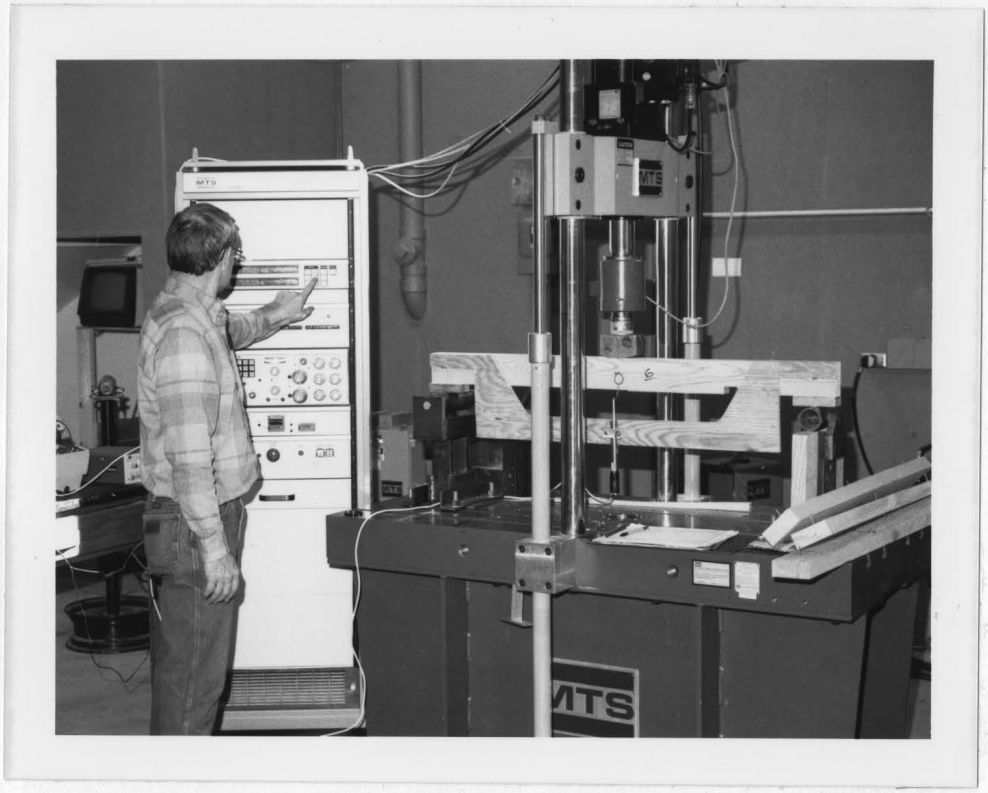

Figure 18a. Test rig for bending tests using servohydraulic universal testing machine. Overall view, including control console and chart recorder.

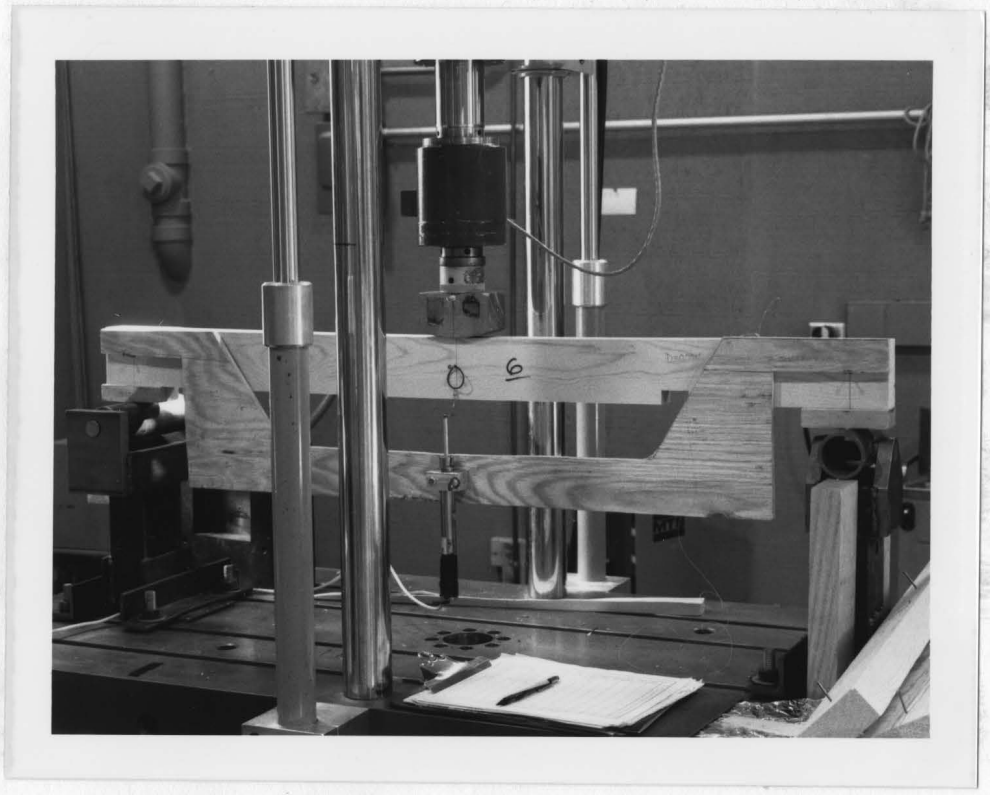

Figure 18b. Test rig for bending tests using servohydraulic universal testing machine. Close-up view of workpiece, load head, supports, and deflection yoke.

5.0 Results

5.1 FE Modeling Results

The FE results are examined in terms of MCF, defined in Section 3.1.3 as:

$$MCF \equiv \frac{\sigma_{h,max}}{\left(\frac{6M}{th^2}\right)} = f_1 + f_2 \cdot \left(\frac{V}{M}\right) \cdot h \qquad (3.2)$$

As noted in Section 3.1.3, $6M/th^2 = 1$ for all of the FE work, so any statements regarding MCF are directly applicable to $\sigma_{h,max}$. The results of the individual FE studies are given in the sections describing their use in developing the model.

5.1.1 Linearity of MCF with V/M

Equation (3.2) predicts a linear relationship between MCF and V/M. This is a restatement of Gerhardt's premise that $\sigma_{h,max}$ is a linear combination of an applied moment term and an applied shear term (Equation 3.1). To describe the MCF from individual FE runs, equation (3.2) is rewritten:

$$MCF_{ijk} = f_{1,ik} + f_{2,ik} \cdot \left(\frac{V}{M}\right)_{ij} \cdot h_i \qquad (5.1)$$

where:

- i denotes notch and beam geometry;
- j denotes loading condition; and
- k denotes elastic parameter (EP) set.

(Note: The comma in the subscript does not indicate differentiation.)

The main study includes 15 notch geometries (i=1-15), nine loading conditions (j=1-9), and five EP sets (k=1-5). Appendix 5, Numerical Results, gives the 675 (15×9×5) values of MCF computed in the main FE study. The notch geometries and EP sets are given in Tables 3 and 4, Chapter 3. The nine loading conditions result from the three notch locations (centered, slightly offcenter, and far offcenter) and three load geometries (center-point, quarter-point, and uniformly-distributed) described in Section 3.1.3.1. Ideally, V/M should be a function of only loading condition. However, the FE mesh generator does not invariably place nodes at the quarter points of a beam; nodes may not be symmetric along the length of an offcenter-notched beam. Thus, the "quarter-point" loadings were approximate, and only 5 of the 9 V/M ratios were exactly equal for all 15 notch geometries. For this reason, the V/M term in equation (5.1) requires both i and j subscripts.

Linearity of MCF with V/M was tested for each of the 5 EP sets and 15 notch geometries of the main study by linear regression using the model:

$$\mathbf{MCF = A + B \cdot (V/M)} \qquad (5.2)$$

Comparison of equations (5.1) and (5.2) show that $f_{1,ik} = A$ and $f_{2,ik} = B/h$. The 75 values of f_1 and f_2 (i=1-15 and k=1-5)

derived from equations (5.1) and (5.2) are given in Appendix 5. Each regression analysis included nine levels of V/M. All 75 of these regressions were significant at the α=0.0001 level. The worst fit yielded a coefficient of determination r^2=0.93; in 75% (56/75) of the cases, $r^2 \geq 0.98$. Thus, the effects of notch location and loading conditions on MCF are accurately described by the single parameter V/M. This is in keeping with the findings of Gerhardt (1984a).

5.1.2 Elastic parameter effects

The influence of elastic parameters on MCF was evaluated from the results of the main study. The goal was to derive an equation to approximate the FE results with the fewest material-dependent parameters. A method involving a single material constant, μ, is outlined in equations (3.5)-(3.7) in Section 3.2.3, as a simplification of a two-constant model:

$$f_1 = \mu_M \cdot F_1 (D,R,L,h) \qquad (3.5)$$

$$f_2 = \mu_V \cdot F_2 (D,R,L,h) \qquad (3.6)$$

where :

- μ_M ≡ material parameter for resultant moment;
- μ_V ≡ material parameter for resultant shear;
- F_1 ≡ material-independent apparent stress concentration factor for resultant moment; and
- F_2 ≡ material-independent apparent stress concentration factor for resultant shear.

Thus:

$$\sigma_{h,max} = \frac{6M}{th^2}\cdot\left(\mu_M\cdot F_1 + \mu_V\cdot F_2\cdot h\cdot\frac{V}{M}\right) \qquad (5.3)$$

In terms of MCF:

$$MCF = \mu_M\cdot F_1 + \mu_V\cdot F_2\cdot h\cdot\frac{V}{M} \qquad (5.4)$$

F_1 and F_2 are hypothesized to be material-invariant functions of notch and beam geometry, and the material parameters μ_M and μ_V should be independent of geometry. I set $\mu_M=\mu_V=1$ for the G17-E17 EP set (subscript k=3; see Table 3, Chapter 3), making this the baseline against which the EP effect was calibrated. F_1 and F_2 are then equivalent to f_1 and f_2 derived from the G17-E17 results. No subscript is used on h in the above equations as it was fixed at 3.5in. throughout the main study.

For $\mu_M = \mu_V$, equation (5.4) may be written:

$$MCF = \mu\cdot\left(F_1 + F_2\cdot h\cdot\frac{V}{M}\right) \qquad (5.5)$$

where:

μ = material parameter for arbitrary loading.

From the regressions described in Section 5.1.1, f_1 and f_2 were calculated for each of the 75 combinations of notch geometry and elastic parameters. The estimates of the proposed material parameters μ, μ_M, and μ_V were derived for each EP set

using two separate linear regressions; one allowed a non-zero intercept and the other did not:

$$MCF_{ijk} = a + b \cdot MCF_{ij3} \tag{5.6a}$$

$$MCF_{ijk} = \mu_k \cdot MCF_{ij3} \tag{5.6b}$$

$$f_{1,ik} = a + b \cdot f_{1,i3} \tag{5.7a}$$

$$f_{1,ik} = \mu_{M,k} \cdot f_{1,i3} \tag{5.7b}$$

$$f_{2,ik} = a + b \cdot f_{2,i3} \tag{5.8a}$$

$$f_{2,ik} = \mu_{V,k} \cdot f_{2,i3} \tag{5.8b}$$

where a and b are regression coefficients, and the subscript k refers to the k^{th} EP set. The subscript k=3 corresponds to the baseline G17-E17 EP set, for which $\mu_M=\mu_V=1$.

The second regression (equation b) of each pair gave the desired material parameter as the slope of a line through the origin, i.e., the y-intercept term was suppressed in the calculation. The first regression (equation a) of each pair provided a statistical test of the assumption of a non-significant intercept, that is, a=0.

All of the regressions were unquestionably significant ($p<<0.0001$) and, as desired, the intercept terms were all

non-significant ($p>0.1$). The resulting values of μ, μ_M, and μ_V are given in Table 11. Several features are noteworthy. The low standard error of μ, across levels of V/M and notch geometry, is striking. This supports the validity of the one-constant formulation of equation (5.5). However, the values of μ_M and μ_V are not equal for a given EP set. (The exception is, by definition, at the baseline EP set). This apparent contradiction is due to the relatively small contribution of the shear term ($F_2 \cdot V/M \cdot h$) to MCF in comparison with that of the moment term (F_1). Over the 75 cases, the moment term (F_1) is always at least 8.7 times larger than the shear term ($F_2 \cdot V/M \cdot h$); ratios ≥ 20 are typical. Thus, any error in the prediction of MCF from assuming $\mu_V=\mu_M=\mu$ is negligible, since $\mu \approx \mu_M$. Table 11 also shows that μ_V is more variable than μ_M, and has a greater dependence on EPs. Plots of the regression residuals versus D, R, and L show clear relationships between each of the "material constants" and L, with an apparent L-EP interaction. The magnitude of this effect is small, as is suggested by the low variation shown in Table 11.

These discrepancies, while of little consequence in the present work, must be addressed further before extending this model to cases outside of the ranges from which it was derived. One such application is to notched beams under shear-

dominated loading, e.g., end-notched beams. Gerhardt's closed-form expression (equation (2.2), Section 2.1.1.4) was also derived from equation (3.1) using a single material parameter based primarily on the EP-dependence of the moment term. Equation (2.2) was found by Abou-Ghaida and Gopu (1984) to severely underestimate $\sigma_{h,max}$ for end-notched beams.

Gerhardt (1984a) used a different procedure to formulate his simplified model (equation (2.2), Section 2.1.1.4). He decomposed equation (3.1) into a notch depth dependence and a material dependence by identifying relationships between the coefficients of his closed-form f_1 and f_2 functions (equations (3.3) and (3.4), Section 3.2.2) which were essentially constant across EP sets. These relationships were used to recast the notch depth dependence in a material-invariant form. As noted in Section 5.1.4.2 below, similar relationships exist between the coefficients of the f_1 and f_2 functions which I derived. Thus Gerhardt's method is probably applicable to my work, although its application would be complicated by the additional terms which I used to account for fillet radius and beam depth as well as notch depth.

5.1.3 Notch and beam geometry effects

Linear and nonlinear regression models were used to derive appropriate algebraic expressions to account for the effects of notch and beam dimensions on MCF. Results obtained by

fitting equations to the material-dependent geometry functions (f_1 and f_2) were equivalent to those obtained by considering the material-independent functions F_1 and F_2. The following development is based on f_1 and f_2. The closed-form representations of F_1 and F_2 are identical to those of f_1 and f_2, respectively, derived from the baseline G17-E17 EP set (Section 5.1.2).

5.1.3.1 Effects of beam depth and span

The two FE substudies described in Section 3.1.3.2 included variable beam depth and span, as well as variable notch geometry. The G32-E12 substudy (Table 5, Chapter 3) was conducted first. As only one EP set was involved, no calculation of EP-dependence was possible. The three levels of V/M for each notch geometry were used to derive f_1 and f_2 values according to equation (5.1). Values of MCF, f_1, and f_2 for both substudies are included in Appendix 5. Linearity of MCF with V/M was excellent, with $r^2 \geq 0.96$ in all cases and $r^2 \geq 0.99$ in 36 of the 43 cases.

Nineteen pairs of observations were available in which all parameters were identical except for beam span. The span:depth ratio in these runs ranged from 6.7-12.6. These represent short, deep beams for which any span:depth effect should be evident. The largest difference between values of f_1 at these different span:depth ratios was <0.44%; the largest

such difference between values of f_2 was <3% (for a 2:1 difference in span:depth ratio). Typical differences were much smaller. Based on these results, I fixed span at 44in. for the G8-E32 substudy, and did not include span in any of the predictive equations.

The set of 19 pairs of geometries differing only in beam depth, *h*, showed a clear dependence of MCF, f_1, and f_2 on *h*. Three expressions of the form of equation (2.7) were used to determine depth effect exponents, η:

$$\frac{MCF_a}{MCF_b} = \left(\frac{h_a}{h_b}\right)^{\eta} \tag{5.9}$$

$$\frac{f_{1,a}}{f_{1,b}} = \left(\frac{h_a}{h_b}\right)^{\eta} \tag{5.10}$$

$$\frac{f_{2,a}}{f_{2,b}} = \left(\frac{h_a}{h_b}\right)^{\eta} \tag{5.11}$$

where subscripts a and b refer to different levels of *h*.

Values of exponent η were obtained by taking logarithms of both sides of equations (5.9)-(5.11) and performing the linear regression (with no intercept term), for example:

$$\ln\left(\frac{f_{2,a}}{f_{2,b}}\right) = \eta \cdot \ln\left(\frac{h_a}{h_b}\right) \tag{5.12}$$

was analyzed as:

$$Y = bX \tag{5.13}$$

For the G32-E12 substudy, this gave η=0.50 for MCF, η=0.45 for f_1 and η=0.18 for f_2. The G8-E12 substudy yielded η=0.47 for MCF, η=0.36 for f_1 and η=0.54 for f_2. All of these regressions were highly significant ($p \leq 0.01$). Another method of accounting for the beam depth effect is described in Section 5.1.4.1 below.

5.1.4 Formulating a simplified model

5.1.4.1 Describing geometry effects using dimensionless parameters

To facilitate the application of a strength equation to diverse sizes of notched beams, it is convenient to express notch geometry in terms of dimensionless variables. Several such nondimensional notch geometry parameters were investigated in this work, including:

$\phi \equiv D/h$
$\delta \equiv R/D$
$\rho \equiv R/h$
$\lambda \equiv L/h$
$\alpha \equiv L/D$
$\zeta \equiv 2R/L$

Any main effect or interaction term involving notch dimensions can be expressed using the dimensionless parameters and h. The only dimensionless parameter with a clear physical meaning, *a priori*, was ϕ, the relative notch depth. The FE substudies were therefore designed around levels of ϕ, R, and

L, rather than assuming any particular nondimensional forms for the radius and length effects.

5.1.4.2 Closed-form approximations of geometry functions

Numerous linear and nonlinear functions of the notch dimensions (or nondimensional geometry parameters) and h were fit to the 43 values of f_1 and f_2 resulting from the G32-E12 substudy. I investigated functional forms including:

$$f = h^{C_4}(C_0 + C_1D + C_2R + C_3L) \tag{5.14}$$

$$f = \frac{h^{C_4}}{C_0 + C_1D + C_2R + C_3L} \tag{5.15}$$

$$\Psi \equiv \frac{1}{f} = h^{-C_4}(C_0 + C_1D + C_2R + C_3L) \tag{5.16}$$

$$f = C_0 D^{C_1} R^{C_2} L^{C_3} h^{C_4} \tag{5.17}$$

$$f = C_0 \exp(C_1D + C_2R + C_3L + C_4 h) \tag{5.18}$$

where f denotes f_1 or f_2. For the main study, in which h=3.5in., equations (5.14) and (5.16) reduced to linear models.

Nonlinear model coefficients were estimated using the iterative Marquardt algorithm of the NLIN procedure in SAS® (SAS® Institute 1985). Regressions were also performed using various combinations of the dimensionless parameters in equations similar to equations (5.14)-(5.18). Equations (5.15)

and (5.16) appear identical, but result in different parameter estimates and predictive accuracy. This is because the reciprocal transformation causes the distribution of the residuals to change (Draper and Smith 1981; Box, et. al. 1978). Only one (if any) of the two models is likely to meet the assumptions of the regression analysis for a given data set, i.e., normally distributed residuals with a mean of zero and constant variance.

The relative performance of the various models was essentially constant across data sets. That is, the best models for f_1 and f_2 in the G8-E12 substudy were also those most appropriate for the G32-E12 substudy and the 5 EP sets of the main study. The best model found for f_1 was:

$$f_1 = \frac{1}{\psi_1} \tag{5.19}$$

where

$$\psi_1 = C_0 + C_1\phi + C_2\delta \tag{5.20}$$

The best model found for f_2 was:

$$f_2 = C_3\phi^{C_4}\rho^{C_5}\lambda^{C_6}h^{C_7} \tag{5.21}$$

For nonlinear models, significance was judged on the basis of the ratio of the residual mean square to the regression mean square. Although some other models were comparable to equations (5.20) or (5.21) in terms of their high significance

and small maximum residuals, none besides (5.20) and (5.21) had satisfactorily homogeneous variance of residuals. Equation (5.21) was recast to simplify comparisons between the substudies and the main study in which h = 3.5in.:

$$f_2 = C_3 \phi^{C_4} \rho^{C_5} \lambda^{C_6} \left(\frac{h}{3.5\text{in.}} \right)^{C_7} \qquad (5.22)$$

The best-fit coefficients for equations (5.20) and (5.22) are given in Tables 12 and 13a, along with the maximum and minimum (most negative) percent differences between predicted and actual values for each data set. Histograms of the residuals, $f - f_{predicted}$, did not contradict the assumption of normality. Plots of the residuals versus the predicted values, and versus the independent variables, showed neither a systematic lack of fit nor a significant inhomogeneity of variance (Draper and Smith 1981). One or more of these three conditions was violated by each of the rejected models.

Equations (5.19) and (5.20) for f_1 do not contain L or h terms, as the coefficients of L, λ, or ζ were non-significant in all analyzed cases. The h effect is implicit in the (ϕ,δ) formulation; no separate h term is necessary to account for the observed variation of f_1 with h (Section 5.1.3.1). Regression equations involving other combinations of independent variables often gave a significant beam depth exponent, C_4. Eliminating h from the expression greatly simplifies the

analysis, as equation (5.20) is linear, whereas the more general form, equation (5.16), in nonlinear.

Regression analysis for f_2 using equation (5.22) yielded a significant depth-effect exponent, C_7, for the G8-E12 EP set, but not for the G32-E12 set. Although the term λ^{C_6} is statistically justifiable, it very slightly detracts from the accuracy of the overall MCF model (Section 5.1.5). This is because increasing λ increases f_2 ($C_6>0$), whereas MCF drops with increasing λ. This apparent contradiction is due to a mild inverse relationship between f_1 and λ which is not described well by any of the regression equations (5.14)-(5.22). That is, the coefficient of λ was non-significant in all of the f_1 analyses despite a discernible λ main effect in the data. Because of the relatively large influence of the moment term on MCF in comparison with that of the shear term (Section 5.1.2), the statistically non-significant λ effect on f_1 has a larger impact on MCF than does the statistically significant λ effect on f_2.

Table 13b gives the best-fit coefficients for equation (5.22), omitting λ (i.e., $C_6=0$). The error of prediction increased due to the omission of the λ term, and the large errors ($|e|\geq 11\%$) were generally associated with the notch geometry with the smallest L (L=1in.). The other fourteen notch geometries typically gave much lower errors. Deleting

the L=1in. geometry from the regression calculation results in somewhat smaller errors. I chose to use the results of all 15 notch geometries to maintain applicability over a wider range of L.

As noted in Section 5.1.2, certain combinations of the coefficients in f_1 and f_2 yield material-invariant constants. The quantity $(C_0+C_2)/C_1$ =1.426±1% for the five EP sets of the main series (Table 12). Similarly, $C_4 \cdot C_5$=-0.363±3.6% for those five EP sets (Table 13b). I did not attempt to use these constants, following the method of Gerhardt (1984a), to derive a simplified model. Instead, I used the method of Section 5.1.2, in which the effects of material and geometry on fillet hoop stress are explicitly separated *a priori*. The results of this analysis are given below in Section 5.1.4.3.

5.1.4.3 Delineating material and geometry effects

The "material-invariant" geometry functions F_1 and F_2 were defined by equations (5.20) and (5.22), using the coefficients for the baseline (G17-E17) EP set:

$$F_1 = \frac{1}{0.165 - 0.217\phi + 0.145\delta} \tag{5.23}$$

$$F_2 = 1.23\,\phi^{0.67}\rho^{-0.55}\left(\frac{h}{3.5\text{in.}}\right)^{0.164} \tag{5.24}$$

Since the beam depth exponent has not been evaluated for the baseline EP set, I used the exponent 0.164 derived from

the G8-E12 substudy data. Based on the negligible beam depth effect calculated from the G32-E12 data ($C_7 \cong 0$), I expect $C_7 \leq 0.164$ for all intermediate EP sets. Setting $C_7=0.164$ will give conservative results (high values of F_2 and MCF) for beams with $h \geq 3.5$in. for all EP sets in this work.

Substituting equations (5.23) and (5.24) into equation (5.5) gives:

$$MCF = \mu \left[\frac{1}{0.165 - 0.217\phi + 0.145\delta} + \frac{V}{M} \cdot h \cdot 1.23\, \phi^{0.67} \rho^{-0.55} \left(\frac{h}{3.5\text{in.}} \right)^{0.164} \right] \qquad (5.25)$$

The value of μ for each EP set is given in Table 11.

5.1.5 Goodness of fit of the simplified model

Values of MCF calculated from equation (5.25) were compared with the 879 actual MCF results from the three FE studies. Error statistics are shown in Table 14. The residuals (MCF_{actual}-$MCF_{predicted}$) were examined for systematic biases. Equation (5.25) tends to overpredict MCF for deep notches with small radii and underpredict MCF for short notches (low levels of L). The latter result is a direct consequence of eliminating L from the model (Section 5.1.3.2). The indication of a notch geometry-material property interaction effect on MCF (Section 5.1.2) is of particular concern for application of equation (5.25) to notch geometries or elastic parameters outside the range of this work. Nonetheless, the simplified model does remarkably well in describing the

variations in MCF with notch depth, notch length, fillet radius, beam depth, and elastic property ratios.

Figure 19 is a plot of predicted MCF, calculated from equation (5.25), versus actual FE-derived MCF, for the G32-E12 EP set. This gives a visual indication of the goodness of fit of equation (5.25). The algebraic expression represents MCF well over the entire range of notch geometries. The cluster of points at MCF≈35, for which the errors are greatest, all represent the greatest notch depth (ϕ=0.71). For this very deep notch, equation (5.25) overpredicts MCF (i.e., is conservative) by about 13%. The cluster of points at MCF≈13, for which predicted MCF is below actual MCF, represents notches with L=1in., the smallest notch length. In these cases, the predictions are about 13% low (unconservative). Aside from these two extreme geometries, the simplified model provides estimates nearly indistinguishable from the actual MCF.

5.2 Mechanical Test Results

5.2.1 Evaluating the notched beam strength parameter κ

Equation (3.9) gives the proposed correspondence between the FE-derived model and mechanical test results:

$$\frac{6M_i}{th^2} = \frac{\kappa_i}{F_1 + F_2 \cdot h \cdot \frac{V}{M}} \qquad (3.9)$$

where $\kappa_i \equiv \sigma_{h,i}/\mu$ and $\sigma_{h,i}$ is the maximum fillet hoop stress at crack initiation. (Equation (3.9) can be applied to describe events other than crack initiation, as detailed below.) To predict crack initiation moments from equation (3.9) does not require knowledge of $\sigma_{h,i}$ or μ. The single material parameter κ_i is determined from mechanical test results, in a manner similar to that for determining MOR. Inserting the expressions for F_1 and F_2 gives:

$$\frac{6M_i}{th^2} = \frac{\kappa_i}{\left[\frac{1}{0.165 - 0.217\phi + 0.145\delta} + \frac{V}{M}\cdot h \cdot 1.23\,\phi^{0.67}\rho^{-0.55}\left(\frac{h}{3.5\text{in.}}\right)^{0.164}\right]} \qquad (5.26)$$

Solving for κ_i:

$$\kappa_i = \frac{6M_i}{th^2}\left[\frac{1}{0.165 - 0.217\phi + 0.145\delta} + \frac{V}{M}\cdot h \cdot 1.23\,\phi^{0.67}\rho^{-0.55}\left(\frac{h}{3.5\text{in.}}\right)^{0.164}\right] \qquad (5.27)$$

Equation (5.27) is used to evaluate κ_i from notched beam test data, where M_i and V/M are known. Conversely, upon determining κ_i for a given material, equation (5.26) can be used to predict moment capacity. Other critical values of κ are defined to correspond with other critical levels of M.

For each test beam described in Sections 4.2.2.1-4.2.2.3, four separate critical test loads were measured, from which critical values of M were calculated. These were: load at crack initiation, P_i; load at the proportional limit, P_{pl}; load just prior to the first major drop in load, $P_{2\%}$; and

ultimate (maximum) load, P_u. P_{pl}, $P_{2\%}$, and P_u were measured from the recorded load-displacement (P-δ) curve (Figure 20); P_i was read from the testing machine when the first visible crack was observed. After examining the P-δ curves from several materials, a 2% drop in load was chosen as the first major drop, because: 1) it often coincided with, but rarely preceded, the first visible cracking; and 2) any electronic noise in the test setup was below 2% of the reading. (This noise, visible on the x-y recorder trace but not on the testing machine load gauge, was eliminated after about the first quarter of the tests were completed.)

Best-fit values of κ were determined for each material and critical point as follows. Equation (3.9) was rearranged to show κ as the proportionality constant in the linear relationship:

$$\frac{6M_{crit}}{th^2} = \kappa_{crit}\,\mathbf{g} \qquad (5.28)$$

where $\mathbf{g} \equiv 1/(F_1+F_2 \cdot h \cdot V/M)$ and the subscript "crit" refers to a given critical point on the beam's P-δ curve. Using equations (5.23) and (5.24) to evaluate F_1 and F_2 gives a value of $\mathbf{g}$ for each beam. A linear regression, with no intercept term, was performed to find the best value of κ for each material at each critical point. This technique also provided a measure of the significance of the predictive model.

Figures 21-24 show the dependence of the theoretical geometry factor **g** on ϕ at various levels of V/M, δ, and R (or ρ at h=constant). Examination of equations (5.26) and (5.28) shows that **g** is equivalent to normalized failure moment, $6M_i/th^2$, for $\kappa_{crit}=1$. Predicted failure moment for a given material is thus directly proportional to **g**. The dashed vertical lines in the figures represent the limits within which ϕ was varied in the FE modeling. The curves show that predicted failure loads drop to ≤ 0 for notches with ϕ above ~0.75. This is clearly unrealistic, and demonstrates a limitation of the empirical fits used to approximate the FE results. For ϕ below the lower limit of 0.14, the equation predicts rapid strength increase with decreasing notch depth. This extrapolation should also be viewed with suspicion in the absence of experimental verification. Discontinuities in slope of the curves of Figures 23 and 24 occur at $R=\phi\delta h=0.50$in., as I assumed that increasing R above 0.50in. would have no effect on **g**. This assumption was based on experimental results given in Section 5.2.2.2.

5.2.2 Notched beam results

5.2.2.1 Study A: preliminary tests

Study A (Sections 4.2.1.1 and 4.2.1.4) was conducted primarily to determine the ranges over which R and L should be varied in the later studies. Proportional limit loads were

not identified in this study. Normalized bending moments, i.e.,

$$M^* \equiv \frac{6M}{th^2} \tag{5.29}$$

calculated for crack initiation (M^*_i), first major drop in load ($M^*_{2\%}$), and ultimate load (M^*_u), are given in Table 15.

Study A was analyzed first using M^* instead of κ, because $\delta=\rho=0$ and $\lambda=0.21$ are not within the range of the simplified model and equation (5.27) may not be valid. Analyses of variance (ANOVA) provided insight into the relative sizes of the main effects and potential interactions. Tables 16 and 17 give the results of two families of ANOVA models: 1) using all data for a given material, classifying the data by D, R, and L; and 2) using the data for a given material at approximately constant D, classifying the data by R and L. When D is fixed, variations in R are equivalent to variations in δ, whereas a δ effect would be a (R/D) interaction term in a model including D. The ANOVA results show that notch depth accounted for most of the variability in M^* (Tables 16 and 17). M^*_i for notches with R=0.375in. were higher than those with R=0 (Table 15), but the differences were not statistically significant for these small sample sizes. The ANOVAs showed no statistically significant R or L effects. A material effect (dry red oak versus dry fir) was not tested statistically, but is evident from Table 15.

For beams loaded in pure bending (V/M=0), equation (3.9) simplifies to:

$$\frac{6M_{crit}}{th^2} = \frac{\kappa_{crit}}{F_1} \tag{5.30}$$

or

$$\frac{6M_{crit}}{th^2} = \kappa_{crit} \cdot g \,, \tag{5.28}$$

where

$$g = \frac{1}{F_1} = 0.165 - 0.217\phi + 0.145\delta \tag{5.31}$$

Although equation (5.31) does not give a singularity at R=0 (δ=0), its application below δ=0.125 (the minimum value in the main FE study) would be an unverified extrapolation. Thus, I used equations (5.28) and (5.31) with the R>0 data from study A to evaluate κ_i, $\kappa_{2\%}$, and κ_u for the test materials. In addition to regressions of the form of equation (5.28), I performed regressions including a constant term:

$$\frac{6M_{crit}}{th^2} = A + Bg \tag{5.32}$$

to test the hypothesis of a non-zero intercept. In all cases, the intercept term A was non-significant (p>0.10), and the model with no intercept was more highly significant. Results of equation (5.28) for fir and oak at the three critical moments are given in Table 18. All regressions were very highly significant (p<0.0001). Results of the R=0 tests are interpreted in Section 5.2.2.4.

Based on the lack of difference between R=0 and R=0.25in. results and the difficulty of notching beams with 0<R<0.25in. I chose not to include radii <0.25in. in the later experimental work. FE meshes for R<0.25in. required very large numbers of nodes and elements (over 240 elements and 1300 nodes), complicating mesh generation and the archiving of results. Since no R effect was apparent below R=0.25in., I chose R=0.20in. as the smallest FE radius. Additional tests (the SYP substudy) were performed prior to dropping L as an independent variable.

5.2.2.2 Study B, SYP substudy

Study B, including the SYP substudy, constituted the bulk of the mechanical testing. The SYP substudy was conducted to test the necessity of including L as an independent variable in the remaining tests. Regression models and cell-by-cell comparisons of critical moments failed to show any significant L effects. On that basis, I dropped L from the remainder of study B. The results of the SYP substudy are included in the analyses of study B presented below.

Two sets of κ_i, κ_{pl}, $\kappa_{2\%}$, and κ_u values were calculated from equation (5.28). Set 1 is based on the R values given in Table 8 (Chapter 4); in set 2, R=0.5in. was substituted for each R=0.75in. value in the table. Set 2 was included because R=0.5in. (ρ=0.143) was the upper limit of the FE

studies, and it was not clear that the radius effect predicted by equations (5.26) and (5.27) would be valid for larger radii. In terms of δ=R/D, the largest value in the FE work was 0.70, while the experimental work included δ=1.0 (R=D=0.75in.). Based on previous work (Gerhardt 1984a, Reeves 1973), I expected to find a maximum radius, R_{max}, above which changes in R would not affect critical loads. Using δ and ρ corresponding to R=0.5in. in equation (5.27) for notches with R=0.75in. is equivalent to hypothesizing R_{max}=0.5in. The results of these regressions are given in Table 19. I found that κ estimates had lower standard errors and the regression models slightly higher F statistics when I calculated κ using R_{max}=0.5in. (Table 19).

The regression results presented in Table 19 show the simplified model to be useful in predicting notched beam critical loads. Highly significant relationships ($p \leq 0.0001$) exist between each of the normalized bending moments and the FE-derived geometry term **g**. The standard errors are generally lowest for κ_i and κ_{pl}. As described in Section 5.3, two additional methods were applied to the notched beam data to check the validity of the predictive model. The first method involved testing κ for (undesired) relationships with notch and loading geometry. These results are described in Section 5.3.1. The second method examined the relationships between

κ and established material properties. Results of that investigation are given in Section 5.3.2.

Several trends in κ are apparent from Table 19. κ_i, $\kappa_{2\%}$, and κ_u are considerably less variable in the hardwoods than in the softwoods. For green materials, $\kappa_{2\%}$ and κ_u values are similar, whereas dry materials show $\kappa_u > \kappa_{2\%}$. The standard errors of κ_u are much higher than those of κ_i, κ_{pl}, or $\kappa_{2\%}$. This reflects the fact that ultimate beam capacity is often governed by material characteristics distant from the notch, e.g., slope of grain. The green materials showed lower variability in κ_u because failure of the green beams often occurred coincident with initial cracking, while the dry beams more often exhibited extended crack growth after crack initiation. This contrasts with the behavior observed by Steida (1966): green notched beams of western hemlock (*Tsuga heterophylla*) and balsam fir (*Abies grandis*) commonly continued to bear load after crack initiation, whereas the kiln-dried beams did not.

I chose to consider only κ_i and $\kappa_{2\%}$ in the remaining analyses. A basic assumption of the model is that notched beams fail in response to fillet hoop stress exceeding a critical value. The FE computations hold only prior to crack initiation; the local geometry and stress distribution are altered greatly by the presence of a crack. Thus, the model cannot be expected to predict beam capacity after cracking has

begun. For crack extension some small distance from the critical fillet, the applied loading and notch depth (or net section) are about the same as for the uncracked fillet. It is reasonable to expect that the crack extension load in this region is roughly proportional to the crack initiation load. This is why the model can predict the first major (≥2%) drop in load, as demonstrated by the relatively low standard errors of $\kappa_{2\%}$. The proportional limit was not observed to have any consistent relationship to crack initiation, so it was not analyzed further. As expected, the ultimate load was the most variable and least clearly related to the load at crack initiation. It, too, was dropped from subsequent analyses.

5.2.2.3 Study C: unfilleted and slit notches

Study C involved sharp-cornered notches, half of which had L≤0.14in. The two materials, green yellow-poplar and dry southern yellow pine (SYP) were different than those used in the other tests of unfilleted notches (fir and red oak in study A). Two yellow-poplar beams were tested per cell. Due to the higher variability found previously in the SYP, I tested three SYP beams per cell. Cell means for the four D-L cells are given in Tables 20 and 21 for the dry SYP and green yellow-poplar, respectively. No consistent L effect is evident. For each material and V/M (0 and 0.10in.$^{-1}$), an ANOVA was conducted to determine any differences in M_i^* due to D, L,

or a D-L interaction. These results are summarized in Table 22. The D term was highly significant in all cases. Although there was a significant D-L interaction for yellow-poplar with V/M=0, the L term was never significant. Thus, no slit-notch effect is evident.

The results of study C (R=0) were compared to the results of study B (R>0) to further establish the differences between sharp and filleted notch behavior. These calculations, and similar ones for study A, are shown in Section 5.2.2.4 below.

5.2.2.4 Effective fillet radii for unfilleted notches

Two methods were used to estimate the effective fillet radius, R_{min}, below which filleted notches are equal in strength to sharp-cornered notches. The first method was applied to pure bending (V/M=0) test results which included notches with R=0 and R>0 in specimens which were otherwise comparable. This method allowed the direct calculation of R_{min} from equations 5.28-5.31. For tests of beams where V/M≠0, R_{min} was estimated by comparing normalized crack initiation moments (M_i^*) for filleted versus unfilleted notches.

Test results from beams with V/M=0 and R>0 were used to evaluate κ_i with equations (5.28) and (5.31). This κ_i was then substituted into equation (5.28) with the M_i from the unfilleted notched beam tests to determine the effective **g**:

$$g = \frac{\left(\frac{6M_i}{th^2}\right)}{\kappa_i} \tag{5.33}$$

Rearranging equation (5.31), values of δ_{min} and R_{min} were calculated for the unfilleted notches:

$$\delta_{min} = \frac{g - 0.165 + 0.217\phi}{0.145} \tag{5.34}$$

$$R_{min} = \phi h \frac{g - 0.165 + 0.217\phi}{0.145} \tag{5.35}$$

These calculations were made for the fir and oak of study A, which included both filleted and unfilleted notches. They were also applied to the V/M=0 tests of study C (R=0, dry SYP and green yellow-poplar) combined with the R>0, V/M=0 results for the same materials in study B. Group mean values of δ_{min} and R_{min} for the four species are given in Table 23, with their standard deviations and standard errors. The table includes three calculations for each material. The first is based on all of the specimens, while the second and third segregated the data on the basis of notch depth. (Studies A and C each used two target levels of D.)

Both δ_{min} and R_{min} are quite variable, although less so for the green yellow-poplar. Since κ_i is assumed constant for all specimens of a given material, equations (5.33)-(5.35) result in all material variability, modeling error, and testing error being lumped together into the apparent variability of

δ_{min} and R_{min}. Mean values of δ_{min} and R_{min} appear to vary with notch depth, and δ_{min} shows a greater D-dependence than does R_{min}. For practical use, notch depth-independence would be helpful. Thus, I consider only R_{min} in the following remarks.

For the green yellow-poplar, R_{min} had a mean value of 0.20in. which was representative of both notch depths ($\phi \approx 0.21$ and $\phi \approx 0.51$). Dry fir (study A) and dry SYP (studies B and C) were nearly identical to one another for both deep notches ($R_{min} \approx 0.11$in.) and shallow notches ($R_{min} \approx 0.32$in.). The levels of notch depth were not the same for the two studies, however; study A used $\phi \approx 0.17$ and $\phi \approx 0.57$, whereas study C used $\phi \approx 0.21$ and $\phi \approx 0.51$. The similarity between the fir and SYP results may be fortuitous or may indicate a two-regime R_{min} behavior typical of a wider group of softwoods. Dry red oak (study A) showed the most extreme D-dependence, with $R_{min} \approx 0$ for $\phi \approx 0.17$ and $R_{min} \approx 0.35$ for $\phi \approx 0.57$.

I also calculated R_{min} for the V/M=0 tests by replacing M_i and κ_i in equation (5.33) with $M_{2\%}$ and $\kappa_{2\%}$, respectively. R_{min} and δ_{min} results were similar with those reported above, except in the case of the green yellow-poplar. For that material, R_{min} and δ_{min} values calculated from $M_{2\%}$ are 1.7-2.1 times higher than those calculated from M_i. I have no explanation for this apparent anomaly. All other trends and statistical inferences were the same for both sets of calculations.

For notches loaded under combined shear and moment, equations (5.26) and (5.27) cannot be solved directly for R_{min}, δ_{min}, or ρ_{min}, so the following iterative method was used. κ_i was determined as before from the R>0 specimens for which equations (5.26) and (5.27) are defined:

$$M_i^* \equiv \frac{6M_i}{th^2} = \kappa_i g \tag{5.36}$$

I assumed that this value of κ_i was applicable also to the unfilleted specimens of the same material, and compared mean values for the R=0 and R=0.25in. groups (for each level of D):

$$\frac{\overline{(M_i^*)}_{R=0}}{\overline{(M_i^*)}_{R=0.25in.}} = \frac{g_{(R=R_{min})}}{g_{(R=0.25in.)}} \tag{5.37}$$

Then,

$$g_{(R=R_{min})} = g_{(R=0.25in.)} \frac{\overline{(M_i^*)}_{R=0}}{\overline{(M_i^*)}_{R=0.25in.}} \tag{5.38}$$

All terms on the right-hand side of equation (5.38) are known: the two group mean M_i^* are experimental quantities, while $g_{(R=0.25in.)}$ is calculated from the definition of g and equations (5.23) and (5.24), using the dimensions (ϕ, δ, ρ, and h) of the notches with R=0.25in.:

$$g \equiv \frac{1}{F_1 + F_2 \cdot \frac{V}{M} \cdot h} = \frac{1}{\frac{1}{C_0 + C_1\phi + C_2\delta} + C_3 \phi^{C_4} \rho^{C_5} \frac{V}{M} h} \tag{5.39}$$

(As $h \approx 3.5$in. for all of the beams, I have omitted the small h dependence in the shear term.) Fillet radius R appears in both δ and ρ, so equation (5.39) cannot be solved directly for R_{min} for a given value of $\mathbf{g}_{(R=Rmin)}$. Solving iteratively, I obtained the values of R_{min} listed in Table 24. The results are separated by levels of D for each of the 2 materials. For the dry pine, there was a fairly small difference in R_{min} due to notch depth: $R_{min} \cong 0.15$in. at $\phi \cong 0.21$ versus $R_{min} \cong 0.18$in. at $\phi \cong 0.51$. For the green yellow-poplar, however, the difference was drastic: $R_{min} \cong 0.17$in. at $\phi \cong 0.21$ versus $R_{min} \cong 0.004$in. at $\phi \cong 0.51$. (For $V/M \neq 0$, equation (5.39) always gives $R_{min} > 0$, since the shear term becomes infinite at R=0.)

Although this method did not lend itself to a straightforward test of statistical significance of the values of R_{min}, another calculation indicated that larger sample sizes are needed to establish R_{min} more reliably. Two-sided T-tests were conducted to determine the significance of differences in values of M_i^* for R=0 (study C) versus R=0.25in. (study B) notches with $V/M = 0.10\text{in.}^{-1}$. These results are given in Table 25. The T-tests showed no significant difference between R=0 and R=0.25in. crack initiation moments in three of the four cases. This implies $R_{min} > 0.25$in. for those cases, in contrast with the above estimates of $0 < R_{min} < 0.25$in. for all four groups. Only for deep notches in green yellow-poplar could

the hypothesis of equal means be rejected ($p=0.0053 << \alpha=0.05$). Thus, the present experiments had insufficient power to discern the small differences between filleted (R=0.25in.) and unfilleted beam strength for the more variable materials, and the reported values of R_{min} must be regarded as preliminary findings.

5.2.3 Unnotched beam results

MOR results from the unnotched beam tests are given in Table 26. As noted for κ (Section 5.2.2.2), the softwoods were more variable than the hardwoods. The MOR values are comparable with published values for each material (Bodig and Jayne 1982). Table 26 includes the ratio of mean $\kappa_{2\%}$ to mean MOR for each material. This ratio varies by more than 2:1 from material to material, with the green materials showing the highest ratios. This implies that drying causes a greater strength increase in unnotched than in notched beams. The relationship between κ and MOR is explored further in Section 5.3.2.

5.2.4 Small, clear specimen test results

Results of the specific gravity (SG), moisture content (MC), perpendicular-to-grain tension ($T_\perp$), and block shear (S) tests are given in Table 27. The MC and SG results are from tests on nearly every notched beam in the main study (B). The $T_\perp$ and S results came from roughly 1/3 of the study

B beams. Table 27 includes mean MOR, κ_i, and $\kappa_{2\%}$ for each material for comparison.

5.3 Compatibility of the theoretical model with the experimental findings

Three methods were used to assess the validity of equations (5.26)-(5.28). The first method was a graphical comparison of the critical loads predicted by the model with the actual measured loads. Figure 25 shows the predicted versus actual crack initiation loads (P_i) for the eight species tested in the main series (study B); Figure 26 shows the corresponding $P_{2\%}$ values. Both plots demonstrate the goodness of fit indicated by the very high F-statistics and low standard errors of the equation (5.28) regression results (Table 19). As expected from the regression results, the P_i predictions are generally more accurate than the $P_{2\%}$ predictions.

Next, the residuals of equation (5.28) were examined for relationships with V/M and notch dimensions. If κ is purely material-dependent, then it should be independent of geometry. The assumptions used in deriving the simplified model, with its single material constant and no notch length term, were expected to result in some geometry-dependence of κ. The usefulness of the model hinges on the magnitude of the geometry-dependent residuals. If there is any significant geometry dependence of κ for cases of practical interest, then a method of adjustment for geometry effect(s) is needed.

Results of this examination of regression residuals are given in Section 5.3.1.

The third method tested the relationship of κ to other material constants. Equations (5.26)-(5.28) state that critical bending moments can be computed from a material term (κ) and a geometry term ($\mathbf{g}$) which are independent of one another. Theoretically, then, any beam-to-beam or material-to-material variations in κ should be due to differences in material properties. In practice, this should be reflected in strong correlations of κ with one or more standard wood properties. Results of these correlation analyses are given in Section 5.3.2.

5.3.1 Relationships between κ and geometry

Residuals from the regression equation (5.28) were examined to determine whether κ was geometry-dependent. This analysis was done for each of the eight materials at the κ_i and $\kappa_{2\%}$ critical points. Typical residual plots are shown in Figures 27-31, for spruce at crack initiation. These plots show results obtained by substituting R_{max}=0.5in. for all input values of R=0.75in. (Sections 5.2.1, 5.2.2.2).

These plots show that κ is not systematically related to any of the geometric variables from the mechanical tests (ϕ, δ, ρ, and V/M). I concluded that the theoretically-derived term, $\mathbf{g}$, closely approximates the geometry-dependence of

notched beam failure loads. This is a key validation of the model.

Nonetheless, the plots of residuals versus predicted values (e.g., Figure 27) show non-homogeneity of variance, i.e., the values of M_i are more variable at high levels of **g** than at low levels of **g**. The variance of the residuals is also clearly a function of ϕ. This indicates that better estimates of κ may be obtained using a weighted regression technique (Draper and Smith 1981; Neter and Wasserman 1974). The present estimates are unbiased, but their standard errors are not as low as could be obtained, in theory, with an appropriate weighted regression. Initial efforts at a weighted regression did not yield a significant improvement in the behavior of the residuals or the variance of the estimates.

5.3.2 Relationships between κ and other material parameters

Two approaches were taken to finding the relationships between κ, S, $T_\perp$, MOR, and SG. First, linear models were constructed relating group mean κ_i and $\kappa_{2\%}$ to the group means of S, $T_\perp$, MOR, and SG. Since eight materials were tested, each regression model had eight total degrees of freedom. The results of the best simple and multiple regressions are given in Table 28. For both κ_i and $\kappa_{2\%}$, the best model is:

$$\kappa = C_1 T_\perp + C_2 SG \qquad (5.40)$$

with no intercept term. This model was highly significant ($p \leq 0.0001$) for both κ_i and $\kappa_{2\%}$. $T_\perp$ and SG were found to be essentially independent, with $r^2=0.33$ and no discernible non-linear relationship on an x-y plot. Collinearity diagnostics from the SAS REG procedure (SAS Institute, 1985) give a maximum condition number = 7.7, far below the range which would indicate a problem with collinearity.

The second method involved performing similar regressions relating κ_i and $\kappa_{2\%}$ for individual specimens to the values of S, $T_\perp$, and SG for the identical specimens. Results of these regressions are shown in Table 29. Again, equation (5.40) was found to describe the variance of κ values well, giving highly significant regressions ($p \leq 0.0001$) for both κ_i and $\kappa_{2\%}$. The collinearity diagnostics again showed no problem with collinearity of $T_\perp$ and SG (maximum condition number=5.3). I interpret the strong relationship between κ and the material properties $T_\perp$ and SG as clear evidence that κ is essentially a material constant.

5.4 Summary of Key Findings

The simplified model of notched beam strength, equations (5.26)-(5.27), was shown to give good predictions of critical loads. Crack initiation load is predicted particularly well. Ultimate load was found to be the most variable, and least

well-described by the model. For engineering purposes, ultimate failure may be considered coincident with the first major drop in load (i.e., $P_{2\%}$), which is much more predictable than ultimate capacity.

The decomposition of notched beam failure loads into a geometry factor and a material factor was validated. This formulation is applicable to hardwoods and softwoods over a wide range of specific gravity and properties. The material parameter, κ, used in the model, can be estimated well by a linear combination of perpendicular-to-grain tensile strength and specific gravity. This allows failure predictions to be made for species for which κ has not been determined directly.

Notch fillet radius affects beam strength over a fairly small range of radii, $R_{min} \leq R \leq R_{max}$, where $R_{max} \approx 0.5$in. R_{min} varied from 0.004in.-0.35in., depending on material, notch depth, and V/M. In most cases, R_{min} was smaller for deeper notches. Most of the reported values of R_{min} are speculative, as the experiments to date have been insufficiently powerful to assure statistical significance.

Table 11. *FE material constants μ, μ_M, and μ_V defined in equations (5.4) and (5.5)*

	μ (n=135)[1]		μ_M (n=15)[2]		μ_V (n=15)[2]	
EP Set[3]	Estimate	SE[4]	Estimate	SE[4]	Estimate	SE[4]
G8-E12	0.860	.0010	0.862	.0027	0.688	.0080
G12-E12	0.911	.0005	0.913	.0013	0.785	.0035
G17-E17	1.000	0	1.000	0	1.000	0
G22-E22	1.078	.0006	1.076	.0013	1.220	.0083
G32-E12	1.154	.0016	1.150	.0045	1.442	.0200

[1] n = number of observations in the regression = (15 notch geometries)·(3 notch locations)·(3 loading conditions)

[2] n = number of observations in the regression = 15 notch geometries

[3] elastic property set (Table 4, Section 3.1.3.1)

[4] standard error of the estimate

Table 12. *Coefficients of FE-derived geometry function f_1 from equations (5.19) and (5.20)*

EP Set[1]	n[2]	C_0	C_1	C_2	R^2	ε_{max}[3], %	ε_{min}, %
G8-E12	15	0.1921	-0.2535	0.1705	.998	4.6	-11.8
G12-E12	15	0.1822	-0.2400	0.1582	.998	5.9	-11.9
G17-E17	15	0.1649	-0.2170	0.1452	.997	7.8	-11.6
G22-E22	15	0.1518	-0.1997	0.1364	.996	9.2	-11.4
G32-E12	15	0.1440	-0.1888	0.1224	.993	12.9	-12.2
.....							
G8-E12	40	0.1710	-0.2257	0.2032	.994	10.0	-22.7
G32-E12	58	0.1132	-0.1475	0.1670	.984	12.0	-16.3

[1] elastic property set (Table 4, Section 3.1.3.1)

[2] number of observations of f_1

[3] $\varepsilon \equiv 100\% \cdot (f_1 - f_{1,predicted}) / f_1$.

Table 13a. *Coefficients of FE-derived geometry function f_2 equation (5.22)*

EP [2]	n[3]	C_3	C_4	C_5	C_6	ε, %[1] mean	max.	min.
G8-E12	15	0.9093	0.6729	-0.5144	0.0452	2.2	4.0	-11.6
G12-E12	15	0.9634	0.6446	-0.5313	0.0892	2.3	4.0	-11.4
G17-E17	15	1.2130	0.6639	-0.5390	0.1137	2.7	5.1	-11.0
G22-E22	15	1.6760	0.7060	-0.4987	0.1245	3.0	4.5	-8.4
G32-E12	15	1.8818	0.7112	-0.5140	0.1846	3.7	7.5	-8.5
.....								
G8-E12	40	0.9151	0.7086	-0.5378	0.0439	3.4	13.5	-10.6
G32-E12	58	1.8382	0.8117	-0.5381	0.2955	4.5	11.9	-18.7

[1] $\varepsilon \equiv 100\% \cdot (f_2 - f_{2,predicted}) / f_2$.

[2] elastic property set (Table 4, Section 3.1.3.1)

[3] number of observations of f_2

Results below the dotted line are for the main FE study plus the variable beam depth substudy of the given EP set. These also include the beam depth exponent η: η=0.1639 for G8-E12, and η=-0.0351 for G32-E12.

Table 13b. *Coefficients of FE-derived geometry function f_2 equation (5.22), omitting λ*

EP [2]	n[3]	C_3	C_4	C_5	ε, %[1] mean	max.	min.
G8-E12	15	0.9123	0.6749	-0.5180	3.2	5.4	-10.7
G12-E12	15	0.9702	0.6494	-0.5388	5.7	7.7	-12.4
G17-E17	15	1.2257	0.6708	-0.5483	7.1	9.1	-17.6
G22-E22	15	1.7024	0.7146	-0.5075	7.4	9.1	-20.1
G32-E12	15	1.9208	0.7266	-0.5296	10.4	16.8	-40.5

[1] $\varepsilon \equiv 100\% \cdot (f_2 - f_{2,predicted})/f_2$.

[2] elastic property set (Table 4, Section 3.1.3.1)

[3] number of observations of f_2

Table 14. *Comparison of FE-computed MCF with MCF from algebraic equation (5.25)*

EP Set	Mean $\|\varepsilon\|$[1], %	ε_{max}, %	ε_{min}, %
G8-E12	2.3	6.1	-11.3
G12-E12	2.5	6.8	-11.3
G17-E17	2.7	8.5	-11.8
G22-E22	2.9	9.8	-12.4
G32-E12	3.5	13.6	-12.9

[1] $\varepsilon = 100\% \cdot (MCF - MCF_{predicted})/MCF$.

Table 15. *Preliminary study (A) notched beam test results*

D	R	L	Fir			Oak		
(inches)			M_i^* [1]	$M_{2\%}^*$	M_u^*	M_i^*	$M_{2\%}^*$	M_u^*
				(lb_f/in^2)			(lb_f/in^2)	
0.61	0	.72	2525	3185	4215	5881	5881	7210
			(479) [2]	(268)	(1476)	(749)	(749)	(2163)
0.61	0	9.0	2936	2936	5658	5619	6344	7189
			(1160)	(1160)	(1197)	(600)	(1312)	(1532)
0.56	.25	.71	2593	2895	2895	6792	6816	8373
			(141)	(222)	(222)	(NA) [3]	(NA)	(NA)
0.57	.25	9.0	2927	3195	4736	6416	6438	10303
			(246)	(133)	(681)	(2270)	(2239)	(251)
0.56	.375	.78	2464	2827	3511	6302	6302	6980
			(607)	(489)	(1456)	(962)	(962)	(2103)
0.58	.375	8.9	3545	3545	6287	4883	5955	6810
			(217)	(217)	(2249)	(967)	(1296)	(2469)
2.00	0	.72	677	677	821	1191	1209	1447
			(164)	(164)	(39)	(50)	(25)	(363)
2.00	0	9.0	631	646	959	947	1114	1479
			(117)	(95)	(150)	(74)	(33)	(22)
1.96	.25	.70	668	755	917	813	884	1519
			(61)	(144)	(156)	(736)	(725)	(26)
1.98	.25	8.9	658	708	1515	1092	1101	1858
			(63)	(7.2)	(67)	(706)	(715)	(946)
1.95	.375	.76	745	745	849	1457	1660	1785
			(185)	(185)	(332)	(803)	(514)	(338)
1.94	.375	8.9	1037	1037	1669	1829	1853	2476
			(108)	(108)	(912)	(NA)	(NA)	(NA)

[1] $M^* \equiv 6M/th^2$. Subscripts: i - crack initiation
2% - 1st 2% drop in load
u - ultimate capacity

[2] Parenthetical quantities are cell standard deviations.

[3] NA - not available (only one observation in the cell)

Table 16. *ANOVA results for geometry effects, study A, fir*

Variables[1] Dep.	Indep.	n[2]	Levels of D	Significant Terms[3]	p(model)[4]	R^2
M_i	D,R,L	26	all	D (≤0.0001)	≤0.0001	0.90
M_i	R,L	13	2.0"	R (0.04)	0.0723	0.71
M_i	R,L	13	0.6"	none	0.66	0.32
$M_{2\%}$	D,R,L	26	all	D (≤0.0001)	≤0.0001	0.92
$M_{2\%}$	R,L	13	2.0"	none	0.0723	0.62
$M_{2\%}$	R,L	13	0.6"	none	0.66	0.19
M_u	D,R,L	26	all	D (≤0.0001), L (0.0061)	≤0.0001	0.88
M_u	R,L	13	2.0"	L (0.04)	0.21	0.58
M_u	R,L	13	0.6"	L (0.04)	0.21	0.58

[1] Dep.- dependent variable; Indep. - independent variables

[2] n - number of observations

[3] terms meeting the significance criterion $p \leq \alpha = 0.05$. The significance level, p, of each significant term is given in parentheses

[4] significance of the model

Table 17. *ANOVA results for geometry effects, study A, oak*

Variables[1]			Levels	Significant		
Dep.	Indep.	n[2]	of D	Terms[3]	p(model)[4]	R^2
M_i	D,R,L	24	all	D (≤0.0001)	≤0.0001	0.93
M_i	R,L	12	2.0"	none	0.75	0.31
M_i	R,L	12	0.6"	none	0.74	0.31
$M_{2\%}$	D,R,L	24	all	D (≤0.0001)	≤0.0001	0.92
$M_{2\%}$	R,L	12	2.0"	none	0.64	0.37
$M_{2\%}$	R,L	12	0.6"	none	0.99	0.07
M_u	D,R,L	24	all	D (≤0.0001),	≤0.0001	0.91
M_u	R,L	12	2.0"	none	0.72	0.33
M_u	R,L	12	0.6"	none	0.49	0.45

[1] Dep.- dependent variable; Indep. - independent variables

[2] n - number of observations

[3] terms meeting the significance criterion $p \leq \alpha = 0.05$. The significance level, p, of each significant term is given in parentheses.

[4] significancé of the model

Table 18. *Regression results of equation (5.28) for study A, R>0.*

Material	Critical Point[1]	n[2]	κ	SE[3]	F_{model}[4]
Red oak, dry	i	16	27160	1860	213
	2%	16	28480	1710	278
	u	16	35850	2840	160
True fir, dry	i	17	13570	616	485
	2%	17	14620	527	770
	u	17	20684	1880	121

[1] i = crack initiation; 2% = first major (≥2%) drop in load: u = ultimate (maximum)

[2] number of observations

[3] standard error of the mean

[4] F-statistic for (1, n-1) degrees of freedom

Table 19. *Regression results of equation (5.28) for study B*

		R_{max} = 0.50in.[1]			R_{max} = 0.75in.[1]		
Material	Load[2]	κ	S.E.[3]	F[4]	κ	S.E.[3]	F[4]
Douglas-Fir	i	14570	381	1466	13310	395	1137
(n=93)[5]	pl	13990	391	1280	12810	391	1072
	2%	17450	810	465	15780	811	378
	u	26170	1269	425	23580	1282	338
Spruce	i	12950	343	1422	11820	356	1100
(n=93)	pl	11670	369	998	10640	375	805
	2%	13310	393	1145	12120	406	892
	u	18280	915	399	16600	890	348
Southern	i	13620	341	1595	12530	349	1288
Yellow	pl	13000	321	1644	11970	324	1368
Pine, dry	2%	14330	388	1363	13180	392	1133
(n=107)	u	18680	875	456	17190	835	424
Southern	i	13160	342	1478	12120	341	1266
Yellow	pl	10010	271	1361	9230	268	1184
Pine, green	2%	14160	437	1049	13030	430	918
(n=106)	u	15420	512	906	14170	506	784

[1] computed using $R=R_{max}$ for any observations in which $R>R_{max}$

[2] i = crack initiation; pl = proportional limit ; 2% = first drop in load ≥2%; u = ultimate

[3] S.E.: standard error of the parameter estimate

[4] F: F-statistic for (1,n-1) degrees of freedom

[5] number of specimens

Table 19, continued. *Regression results of equation (5.28), study B*

Material	Load[2]	R_{max} = 0.50in.[1] κ	S.E.[3]	F[4]	R_{max} = 0.75in.[1] κ	S.E.[3]	F[4]
Hard Maple	i	21360	373	3276	19560	416	2209
(n=93)	pl	15460	433	1274	14080	460	935
	2%	21350	376	3219	19540	424	2124
	u	22300	460	2350	20380	508	1610
Red Oak	i	18800	392	2304	17260	392	1941
(n=93)	pl	18130	421	1858	16644	417	1595
	2%	19380	411	2219	17770	421	1784
	u	24880	876	807	22800	846	727
Yellow-	i	17970	311	3330	16490	333	2458
Poplar,	pl	17870	315	3221	16420	332	2448
dry	2%	18400	366	2532	16930	356	2268
(n=94)	u	25750	1048	603	23560	1021	532
Yellow-	i	15130	224	4568	13830	245	3174
Poplar,	pl	11580	338	1177	10580	329	1035
green	2%	15390	217	5024	14060	242	3388
(n=93)	u	16040	256	3920	14650	279	2766

[1] computed using $R=R_{max}$ for any observations in which $R>R_{max}$

[2] i = crack initiation; pl = proportional limit ; 2% = first drop in load ≥2%; u = ultimate

[3] S.E.: standard error of the parameter estimate

[4] F: F-statistic for (1,n-1) degrees of freedom

[5] number of specimens

Table 20. *Mechanical test results, study C - southern yellow pine, dry, R=0*

D	L	V/M	M_i^* [1]	M_{pl}^*	$M_{2\%}^*$	M_u^*
0.755	0.125	0.00	2328	2328	2328	3814
			(476) [2]	(279)	(476)	(993)
0.768	1.500	0.00	2553	2111	3064	3495
			(449)	(250)	(375)	(575)
1.808	0.125	0.00	855	712	887	1188
			(49)	(37)	(26)	(518)
1.800	1.517	0.00	794	684	842	954
			(303)	(249)	(319)	(246)
0.782	0.138	0.10	1995	1625	2528	2873
			(512)	(269)	(882)	(1399)
0.768	1.507	0.10	2544	2135	3276	4759
			(400)	(340)	(530)	(833)
1.813	.138	0.10	786	732	848	848
			(92)	(28)	(76)	(76)
1.807	1.503	0.10	523	439	656	665
			(185)	(102)	(242)	(246)

[1] $M^* \equiv 6M/th^2$ at crack initiation (i), proportional limit (pl), first ≥2% drop in load (2%), or ultimate (u).

[2] Parenthetical quantities are cell standard deviations.

Table 21. *Mechanical test results, study C - Yellow-poplar, green, R=0*

D	L	V/M	M_i^*[1]	M_{pl}^*	$M_{2\%}^*$	M_u^*
0.756	0.129	0.00	2310	2169	2881	3459
			(67)	(125)	(584)	(234)
0.776	1.496	0.00	2460	2195	3237	3237
			(62)	(213)	(102)	(102)
1.816	0.134	0.00	1097	869	1218	1304
			(9)	(77)	(28)	(149)
1.813	1.490	0.00	923	816	1203	1315
			(35)	(7)	(61)	(176)
0.756	0.132	0.10	2465	1490	2678	2678
			(63)	(106)	(139)	(139)
0.750	1.497	0.10	2146	1402	2442	2442
			(336)	(84)	(420)	(420)
1.809	0.130	0.10	683	681	735	745
			(96)	(99)	(107)	(93)
1.808	1.509	0.10	479	504	569	569
			(35)	(19)	(88)	(88)

[1] $M^* \equiv 6M/th^2$ at crack initiation (i), proportional limit (pl), first ≥2% drop in load (2%), or ultimate (u).

[2] Parenthetical quantities are cell standard deviations.

Table 22. *ANOVA results, study C (R=0)*

Material	V/M, $in.^{-1}$	$p(F>F_{obs})$ [1]				
		D	L	D*L	Model	R^2
SYP[2], dry	0	≤.0001	.70	.51	.0004	.88
SYP[2], dry	0.10	≤.0001	.93	.23	≤.0001	.90
Y-P[3], green	0	≤.0001	.75	.01	≤.0001	>.99
Y-P[3], green	0.10	.0002	.11	.67	.0008	.98

[1] for the null hypothesis that the coefficient of the given term is zero.
[2] southern yellow pine
[3] yellow-poplar

Table 23. *R_{min}, δ_{min} for studies A and C (V/M=0), calculated from crack initiation moments (M_i)*

Material	D, in.	R_{min}, in.			δ_{min}, in.		
		Mean	SD[1]	SE[2]	Mean	SD[1]	SE[2]
Fir, dry	all	0.23	0.23	0.077	0.32	0.41	0.135
Fir, dry	2.0	0.11	0.12	0.062	0.06	0.06	0.031
Fir, dry	0.6	0.32	0.27	0.119	0.53	0.45	0.200
Oak, dry	all	0.18	0.20	0.071	0.29	0.33	0.115
Oak, dry	2.0	0.006	0.07	0.037	0.003	0.037	0.018
Oak, dry	0.6	0.35	0.08	0.044	0.58	0.15	0.073
SYP[3], dry	all	0.22	0.20	0.057	0.25	0.25	0.072
SYP[3], dry	1.8	0.12	0.18	0.074	0.065	0.10	0.041
SYP[3], dry	0.75	0.33	0.17	0.068	0.43	0.22	0.090
Y-P[4], green	all	0.20	0.064	0.023	0.19	0.10	0.037
Y-P[4], green	1.8	0.19	0.086	0.043	0.10	0.047	0.024
Y-P[4], green	0.75	0.21	0.040	0.020	0.28	0.050	0.025

[1] standard deviation

[2] standard error of the mean

[3] southern yellow pine, study C

[4] yellow-poplar, study C

Table 24. *R_{min} for study C, V/M=0.10in.$^{-1}$, from equations (5.37) - (5.39)*

Data Set	$(\overline{M_i^*})_{R=0}$ (psi)	$(\overline{M_i^*})_{R=0.25in.}$ (psi)	$g_{(R=0.25in.)}$	$g_{(R=R_{min})}$	R_{min} (in.)
SYPd[1], D≅0.75in.	2429	2815	0.1505	0.1299	0.145
SYPd[1], D≅1.8in.	655	721	0.0677	0.0615	0.175
Y-Pg[2], D≅0.75in.	2305	2589	0.1505	0.1340	0.165
Y-Pg[2], D≅1.8in.	581	1169	0.0677	0.0336	0.004

[1] southern yellow pine, dry

[2] yellow-poplar, green

Table 25. *T-test results, normalized crack initiation bending moments (M_i^*), R=0 versus R=0.25in., V/M=0.10$^{in.-1}$*

Material	D (in.)	R (in.)	n[1]	Mean	SD[2]	SE[3]	T[4]	p[5]
SYPd[6]	0.75	0	6	2430	347	142	-0.98	0.37
		0.25	2	2810	895	634		
SYPd[6]	1.8	0	6	654	194	79	-0.38	0.71
		0.25	3	721	346	200		
Y-Pg[7]	0.75	0	4	2310	270	135	-1.01	0.37
		0.25	2	2590	446	316		
Y-Pg[7]	1.8	0	4	581	132	66	-5.51	<.01
		0.25	2	1170	93	66		

[1] number of observations

[2] standard deviation

[3] standard error of the mean

[4] T-statistic for H_0: $(M_i^*)_{R=0} = (M_i^*)_{R=0.25in.}$

[5] probability of $|T| > |T_{obs}|$ for the above null hypothesis, i.e., probability that the R=0 and R=0.25in. results are from random samples from the same parent distribution.

[6] southern yellow pine, dry

[7] yellow-poplar, green

Table 26. *Unnotched bending strength (MOR)*

Material	n[1]	Mean (psi)	COV[2]	$\frac{\kappa_{2\%}}{MOR}$ [3]
Douglas-fir, dry	30	12780	0.27	1.37
Spruce, dry	30	7670	0.27	1.74
Southern Pine, dry	30	7960	0.32	1.80
Southern Pine, green	31	6300	0.18	2.25
Hard Maple, green	30	7420	0.20	2.88
Red Oak, dry	30	12810	0.17	1.51
Yellow-poplar, dry	30	10630	0.15	1.73
Yellow-poplar, green	13	6230	0.09	2.47

[1] number of observations

[2] coefficient of variation

[3] $\kappa_{2\%}$ calculated using R_{max}=0.50in. (Table 19)

Table 27. *Results of unnotched bending and small, clear specimen tests*

Material	Shear (psi)	$T_{\perp}$[1] (psi)	SG[2]	MOR[3] (psi)	κ_i[4] (psi)	$\kappa_{2\%}$[4] (psi)
Douglas-fir, dry	1755	360	0.55	12780	14570	17450
no. of specimens:	(30)	(30)	(93)	(30)	(93)	(93)
Spruce, dry	990	301	0.44	7670	12950	13310
no. of specimens:	(31)	(31)	(93)	(30)	(93)	(93)
SYP, dry	1255	358	0.50	7960	13620	14330
no. of specimens:	(44)	(45)	(107)	(30)	(107)	(107)
SYP, green	835	287	0.51	6300	13160	14160
no. of specimens:	(44)	(44)	(106)	(30)	(106)	(106)
Maple, green	1440	575	0.63	7420	21360	21350
no. of specimens:	(31)	(31)	(93)	(30)	(93)	(93)
Red Oak, dry	2260	673	0.63	12810	18800	19380
no. of specimens:	(31)	(32)	(93)	(30)	(93)	(93)
Yellow-poplar, dry	1780	655	0.49	10630	17970	18400
no. of specimens:	(31)	(31)	(94)	(30)	(94)	(94)
Yellow-poplar, green	890	472	0.47	6230	15130	15390
no. of specimens:	(31)	(31)	(94)	(30)	(94)	(94)

[1] perpendicular-to-grain tensile strength

[2] specific gravity

[3] modulus of rupture

[4] κ_i and $\kappa_{2\%}$ calculated using R_{max}=0.50in. (Table 19)

Table 28. *Regressions of κ versus unnotched wood properties, using group mean values*

Variables[1]		C_0[2]		C_1		C_2		Model[3]	
Dep.	Indep.	Est.	S.E.	Est.	S.E.	Est.	S.E.	R^2	p
κ_i	$T_\perp$	8080	1890	17.09	3.91			.76	.0047
κ_i	SG	-1560*	6050	33190	11380			.59	.027
κ_i	S	10820	2950	3.66	2.00			.36	.12
κ_i	MOR	13060	4130	0.32	0.44			.08	.50
κ_i	$T_\perp$, SG	1050*	3840	12.7	3.89	17210	8610	.87	.0064
κ_i	$T_\perp$, SG	NA[4]	NA	12.4	3.50	19370	3180	NA	.0001
$\kappa_{2\%}$	$T_\perp$	9880	2080	14.9	4.32			.66	.014
$\kappa_{2\%}$	SG	-1170*	4760	33920	8960			.71	.0091
$\kappa_{2\%}$	S	11020	2400	4.07	1.62			.51	.046
$\kappa_{2\%}$	MOR	12200	3530	0.50	0.38			.23	.23
$\kappa_{2\%}$	$T_\perp$, SG	713*	3510	9.09	3.56	22430	7870	.87	.0059
$\kappa_{2\%}$	$T_\perp$, SG	NA	NA	8.94	3.19	23890	2900	NA	.0001

[1] Dep.: dependent variable; Indep.: independent variable(s)

[2] Est.: parameter estimate; S.E.: standard error of estimate

[3] R^2: coefficient of determination

p: probability that the observed F-statistic would result if the "dependent" variable were not, in fact, correlated with the "independent" variable(s).

[4] NA: not applicable for models with no intercept term

* This coefficient is not significant at α=0.05.

Table 29. *Regressions of κ versus small, clear specimen properties, using individual specimen values*

Variables[1]		C_0[2]		C_1		C_2		Model[3]	
Dep.	Indep.	Est.	S.E.	Est.	S.E.	Est.	S.E.	R^2	p
κ_i	$T_\perp$	8890	612	13.5	1.26			.30	≤.0001
κ_i	SG	-1760*	1480	31500	2770			.32	≤.0001
κ_i	S	9710	737	3.83	0.51			.18	≤.0001
κ_i	$T_\perp$,SG	-1740*	1340	9.56	1.20	23390	2700	.45	≤.0001
κ_i	$T_\perp$,SG	NA[4]	NA	9.56	1.20	20200	1090	NA	≤.0001
κ_2	$T_\perp$	9300	657	13.7	1.35			.28	≤.0001
κ_2	SG	-1678*	1590	32330	2960			.31	≤.0001
κ_2	S	9840	776	4.12	0.53			.18	≤.0001
κ_2	$T_\perp$,SG	-1660*	1450	9.66	1.31	24140	2920	.42	≤.0001
κ_2	$T_\perp$,SG	NA[4]	NA	9.66	1.31	21090	1190	NA	≤.0001

[1] Dep.: dependent variable; Indep.: independent variable(s)

[2] Est.: parameter estimate; S.E.: standard error of estimate

[3] R^2: coefficient of determination;
p: probability that the observed F-statistic would result if the "dependent" variable were not, in fact, correlated with the "independent" variable(s).

[4] NA: not applicable for models with no intercept term

* This coefficient is not significant at α=0.05.

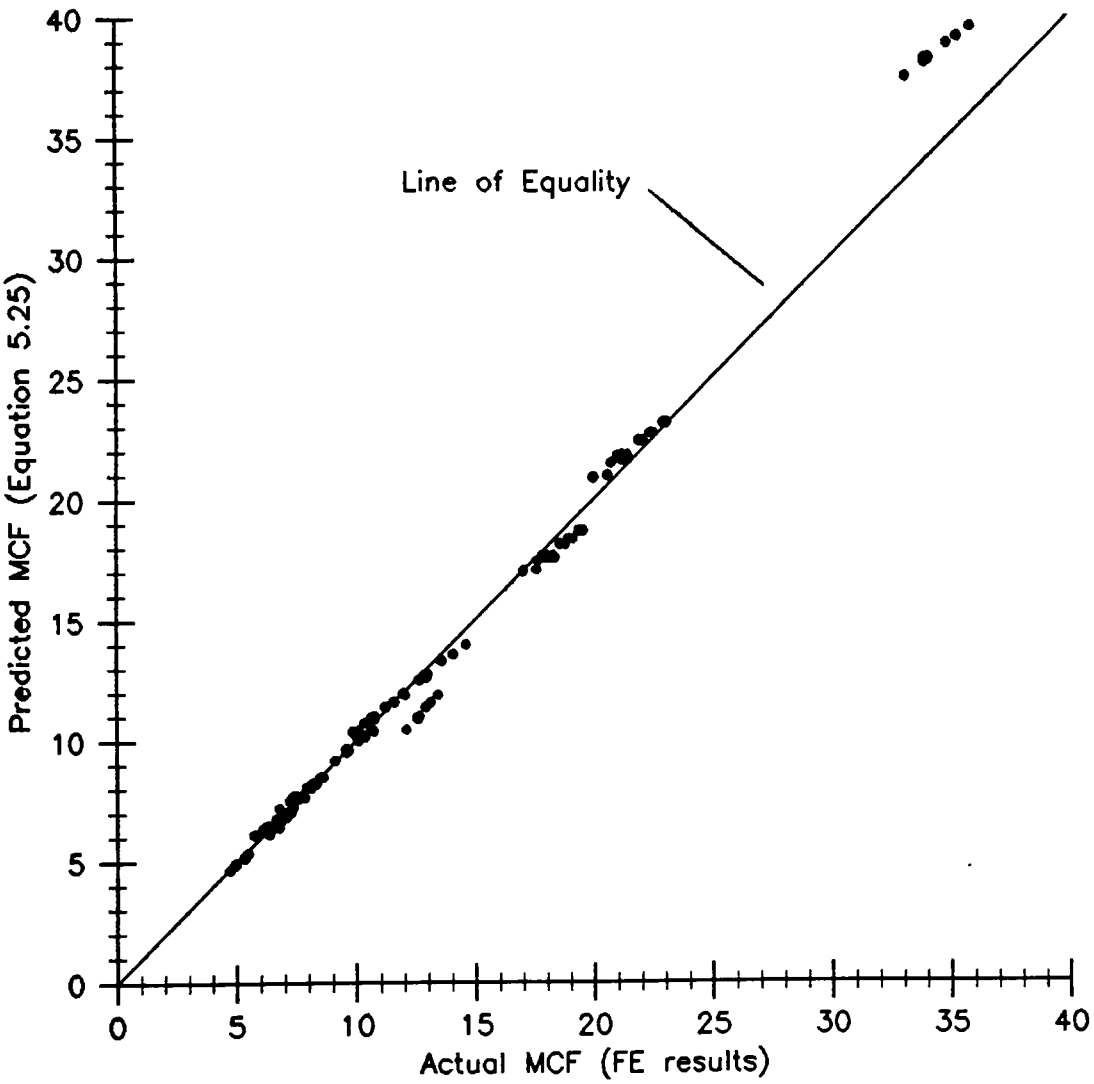

Figure 19. Predicted versus FE-computed MCF for the G32-E12 elastic property set.

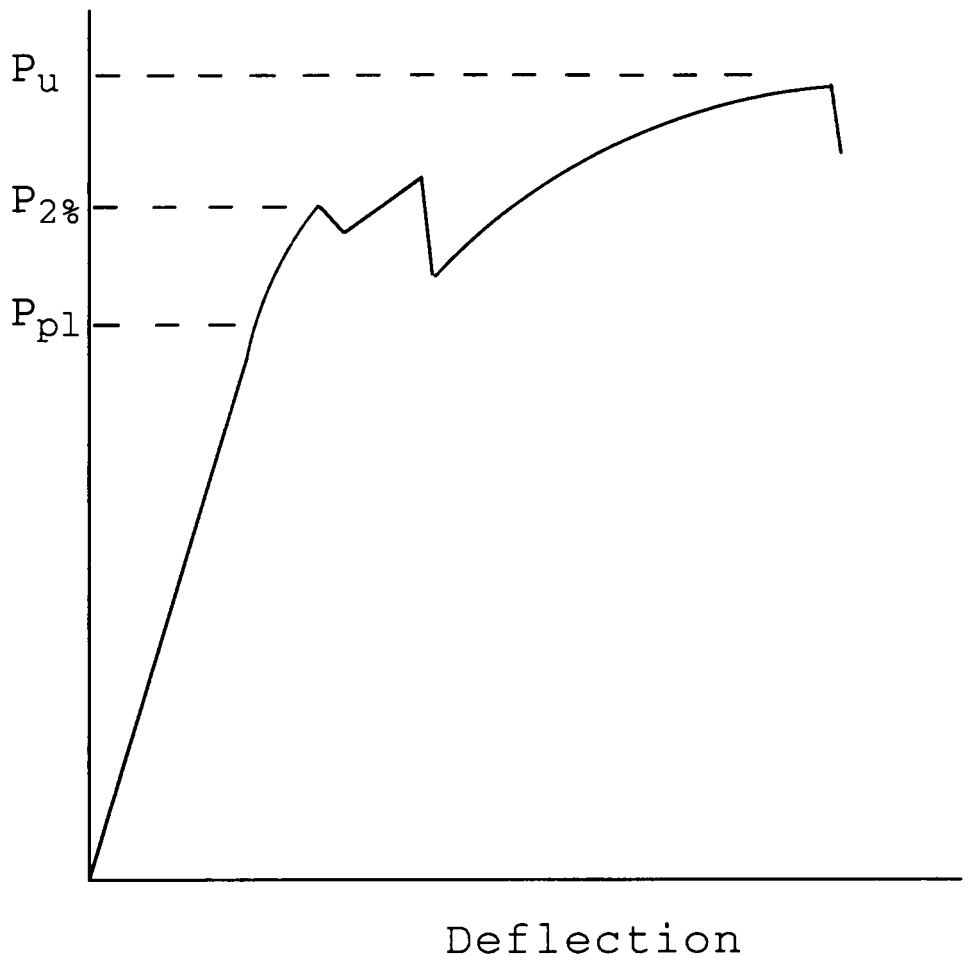

Figure 20. Schematic load-displacement curve for a notched wood beam.

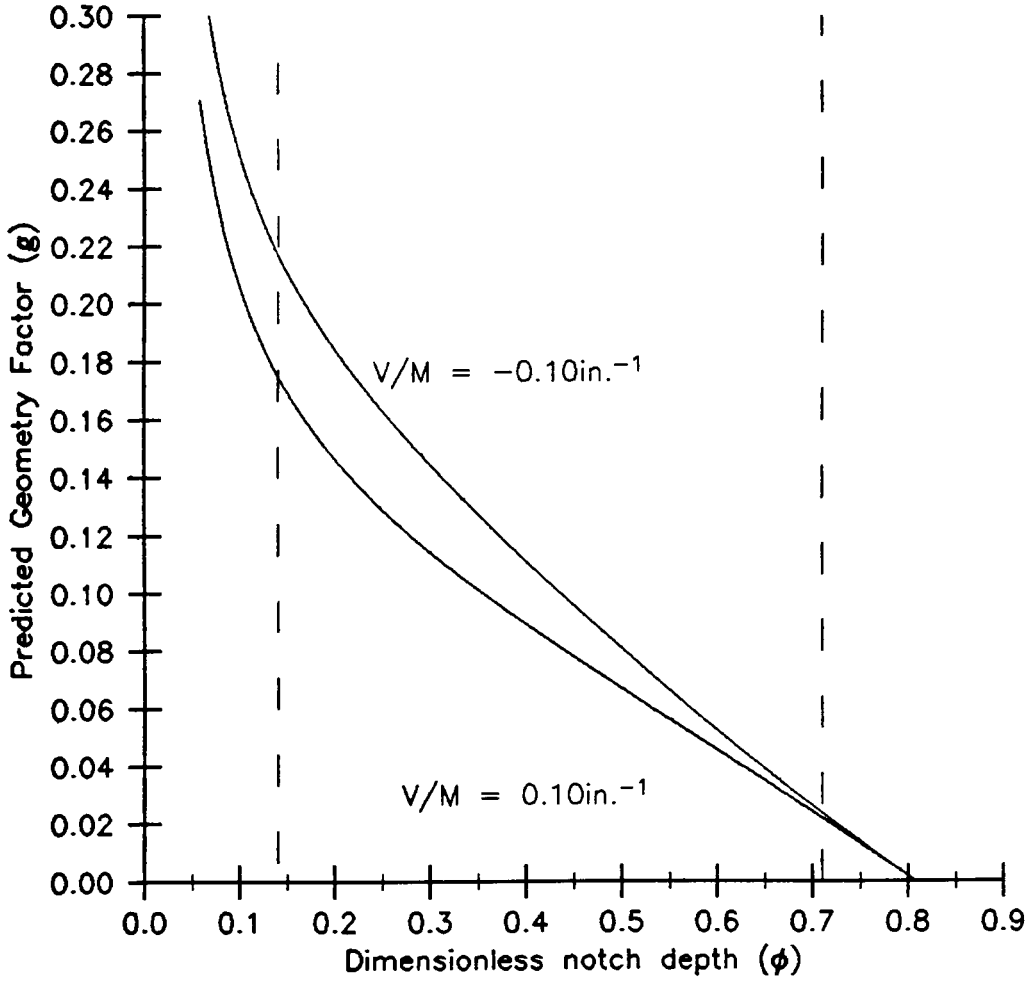

Figure 21. Theoretical geometry factor g versus notch depth, for R = 0.20in. and h = 3.5in.

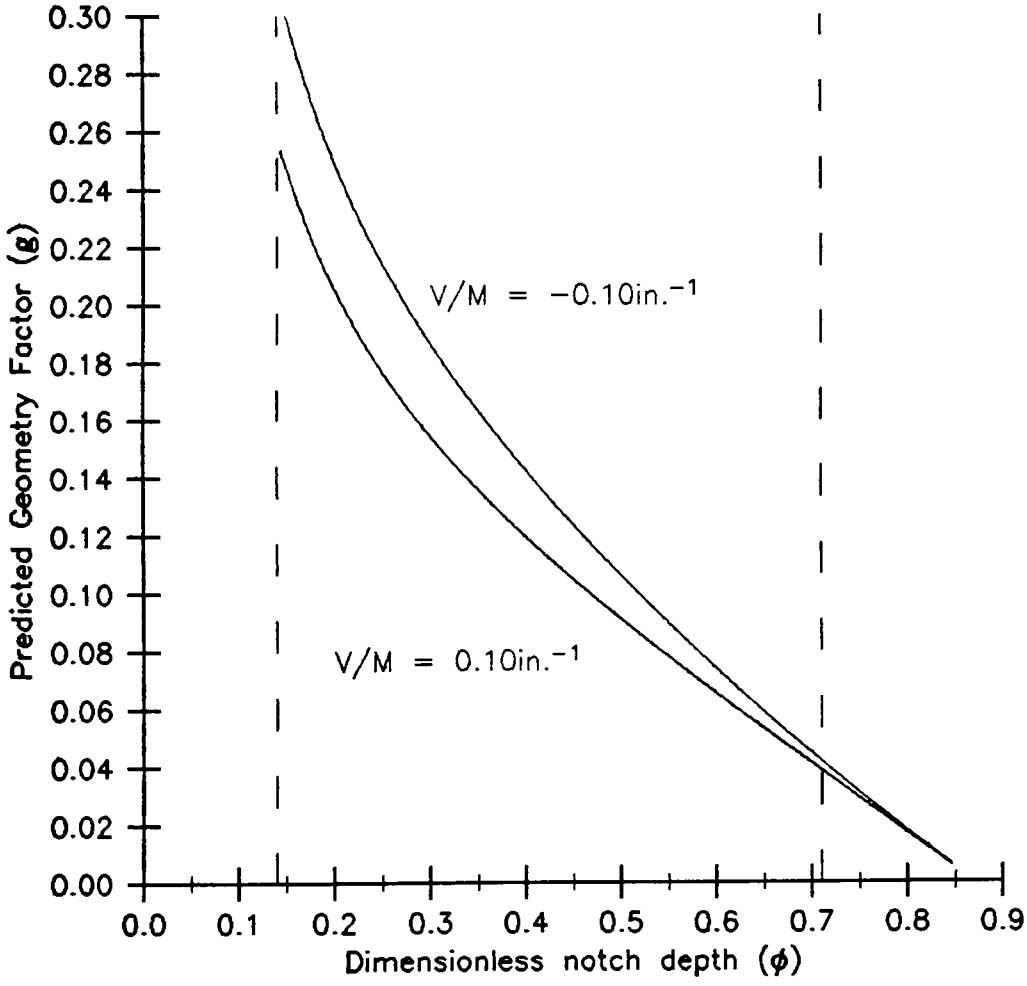

Figure 22. Theoretical geometry factor g versus notch depth, for R = 0.50in. and h = 3.5in.

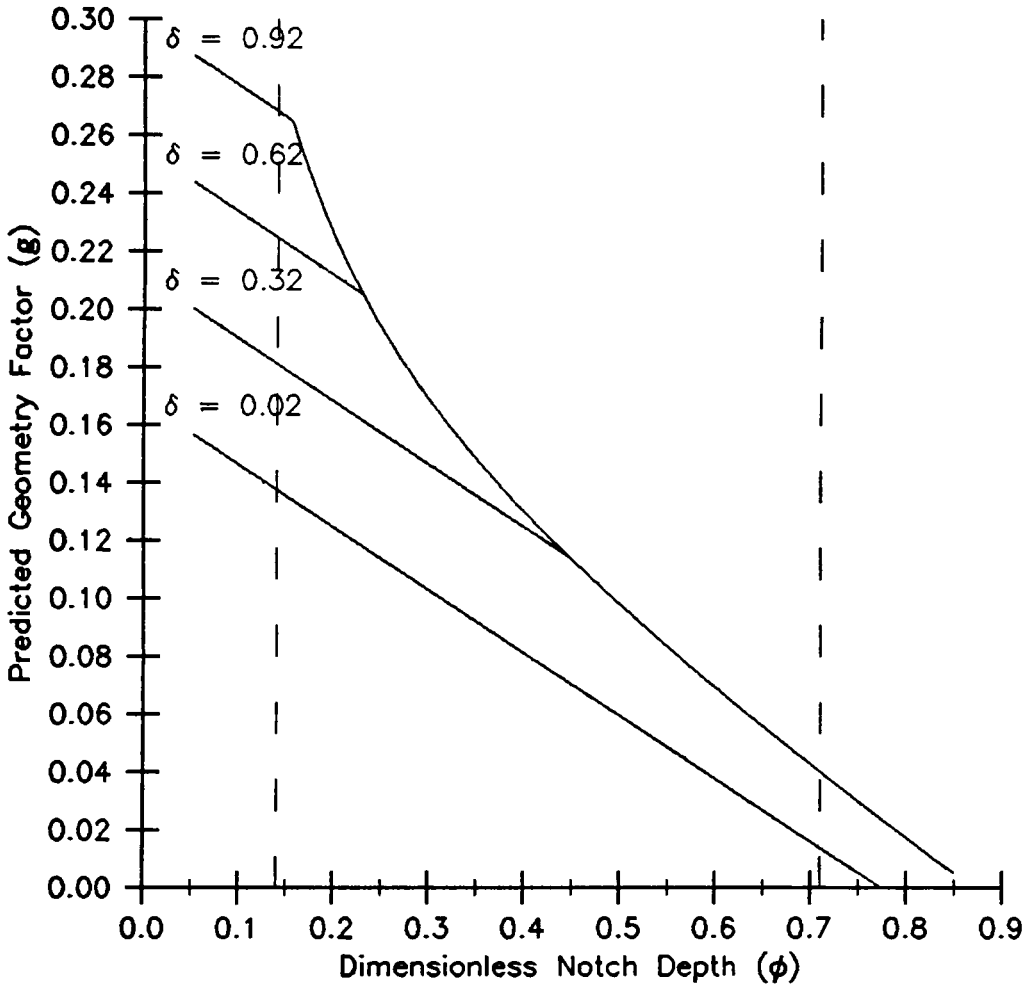

Figure 23. Theoretical geometry factor **g** versus notch depth, for V/M = 0 and h = 3.5in.

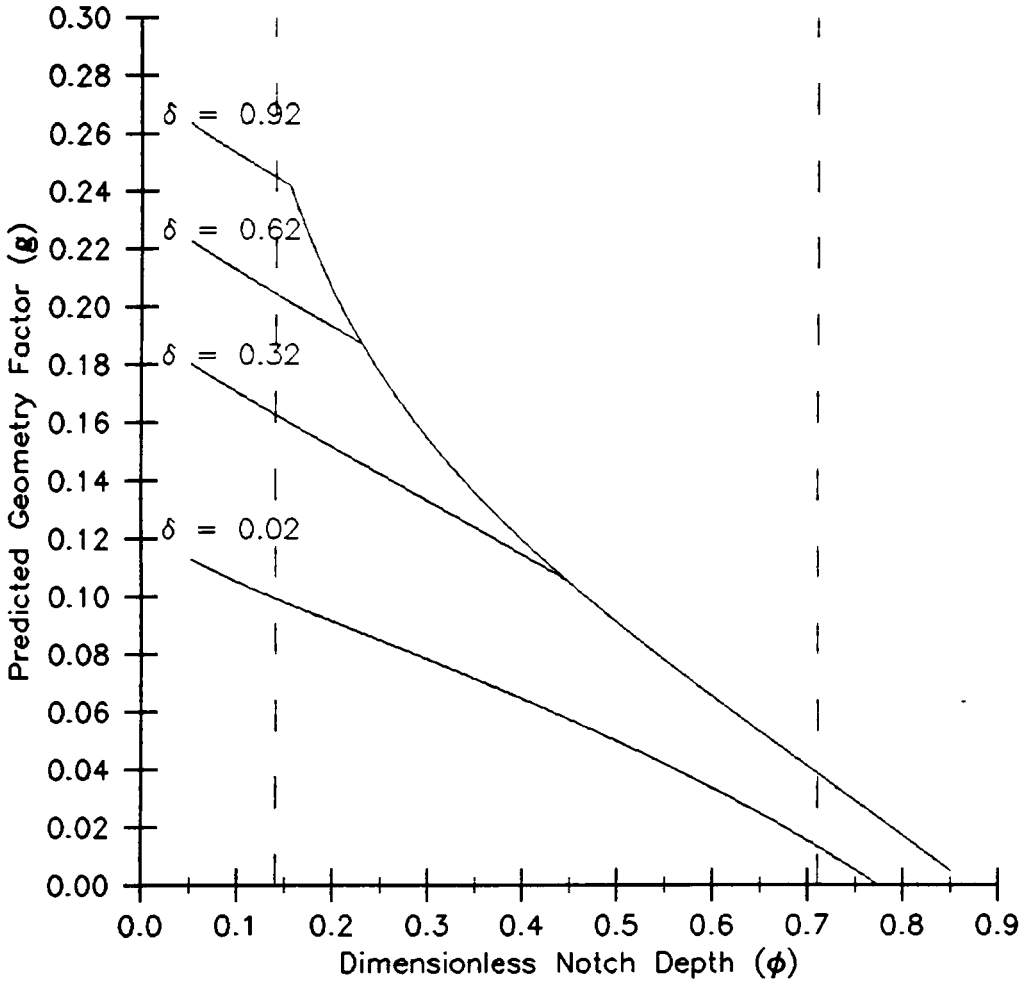

Figure 24. Theoretical geometry factor g versus notch depth, for V/M = 0.10in.$^{-1}$ and h = 3.5in.

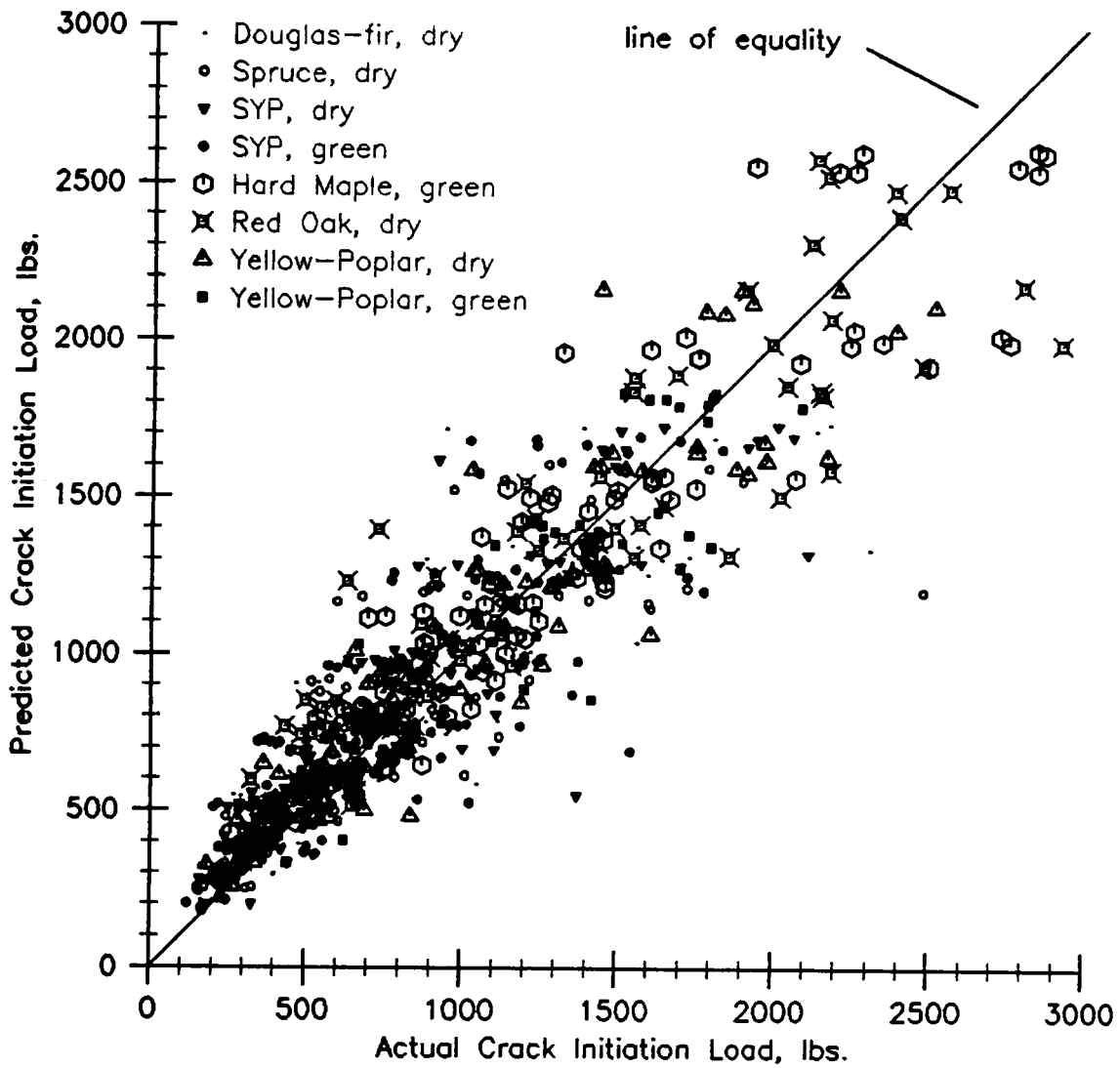

Figure 25. Predicted versus actual crack initiation loads, Study B. Eight species. R_{max}=0.5in.

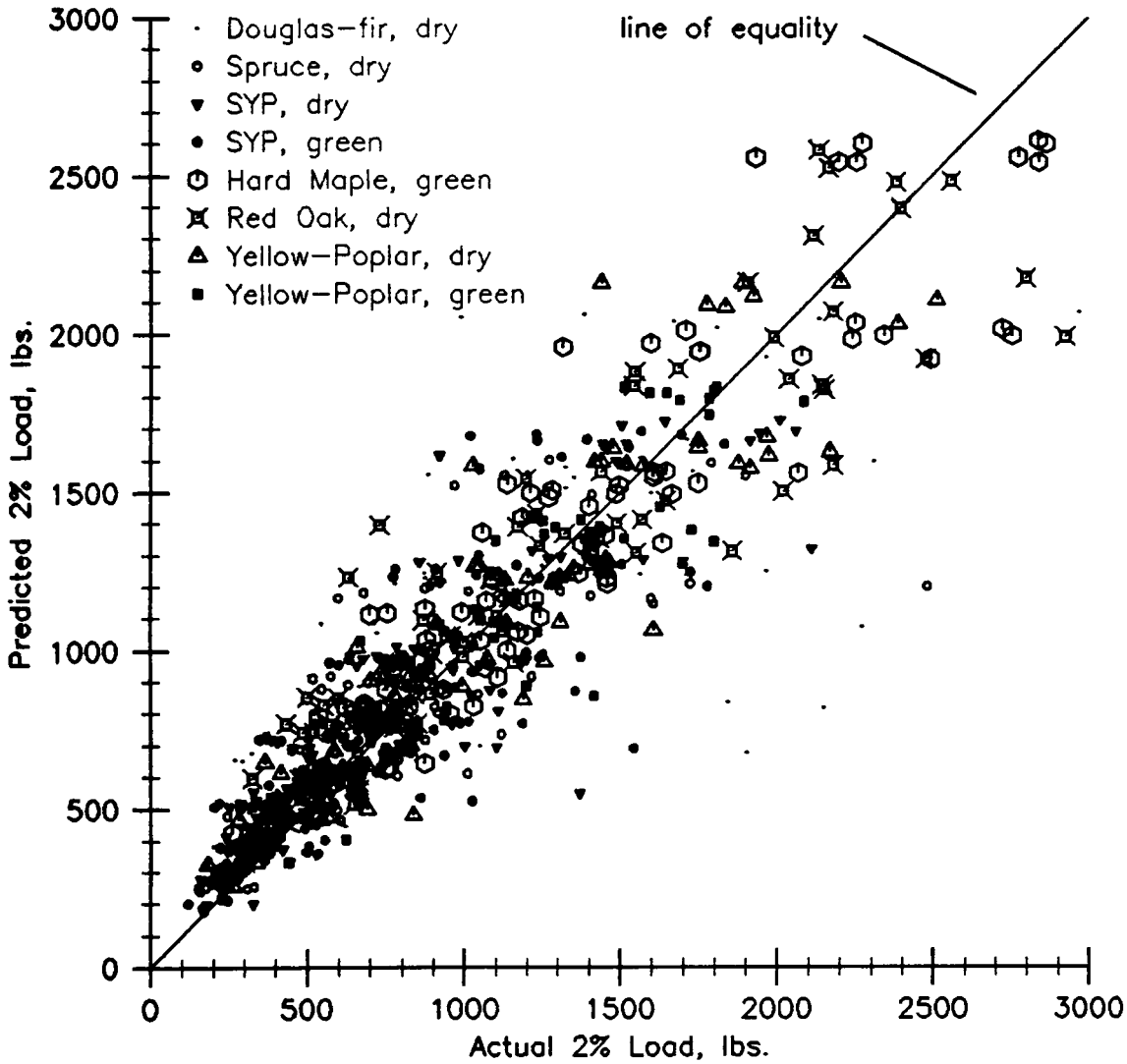

Figure 26. Predicted versus actual load at first >2% drop in load. Study B. Eight species. R_{max}=0.5in.

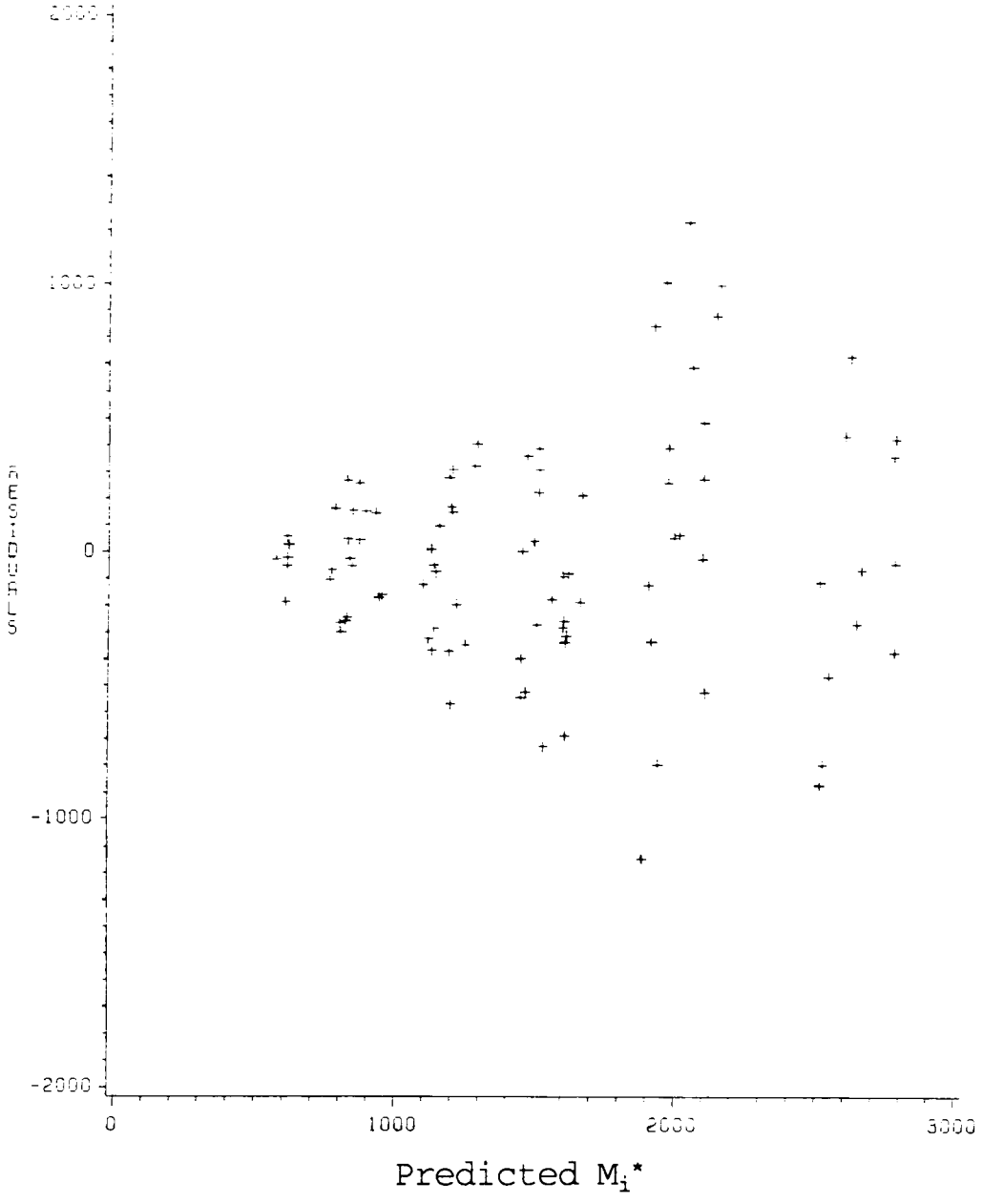

Figure 27. Residuals of equation (5.28) versus predicted values. Spruce, study B, at crack initiation.

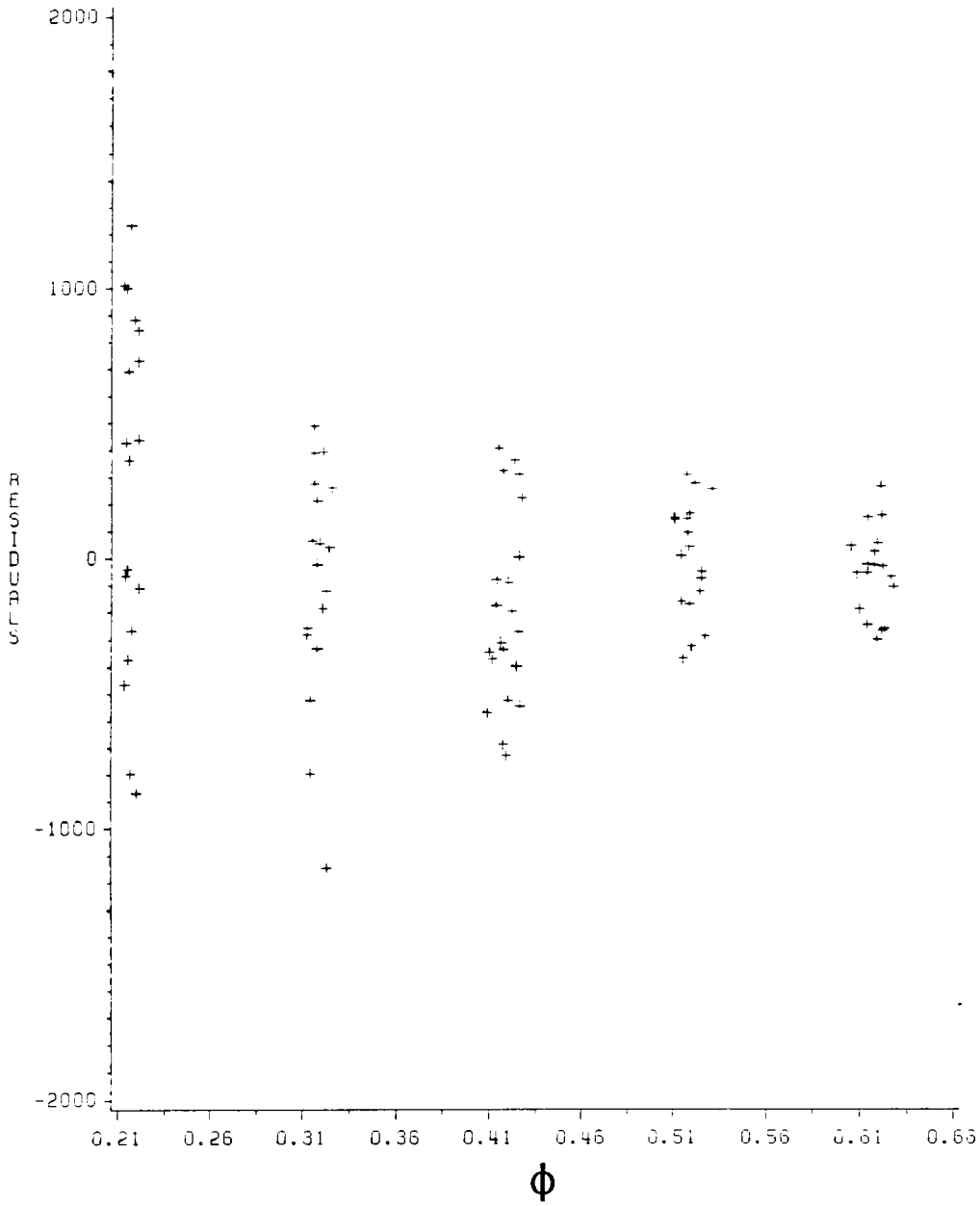

Figure 28. Residuals of equation (5.28) versus dimensionless notch depth, ϕ. Spruce, study B, at crack initiation.

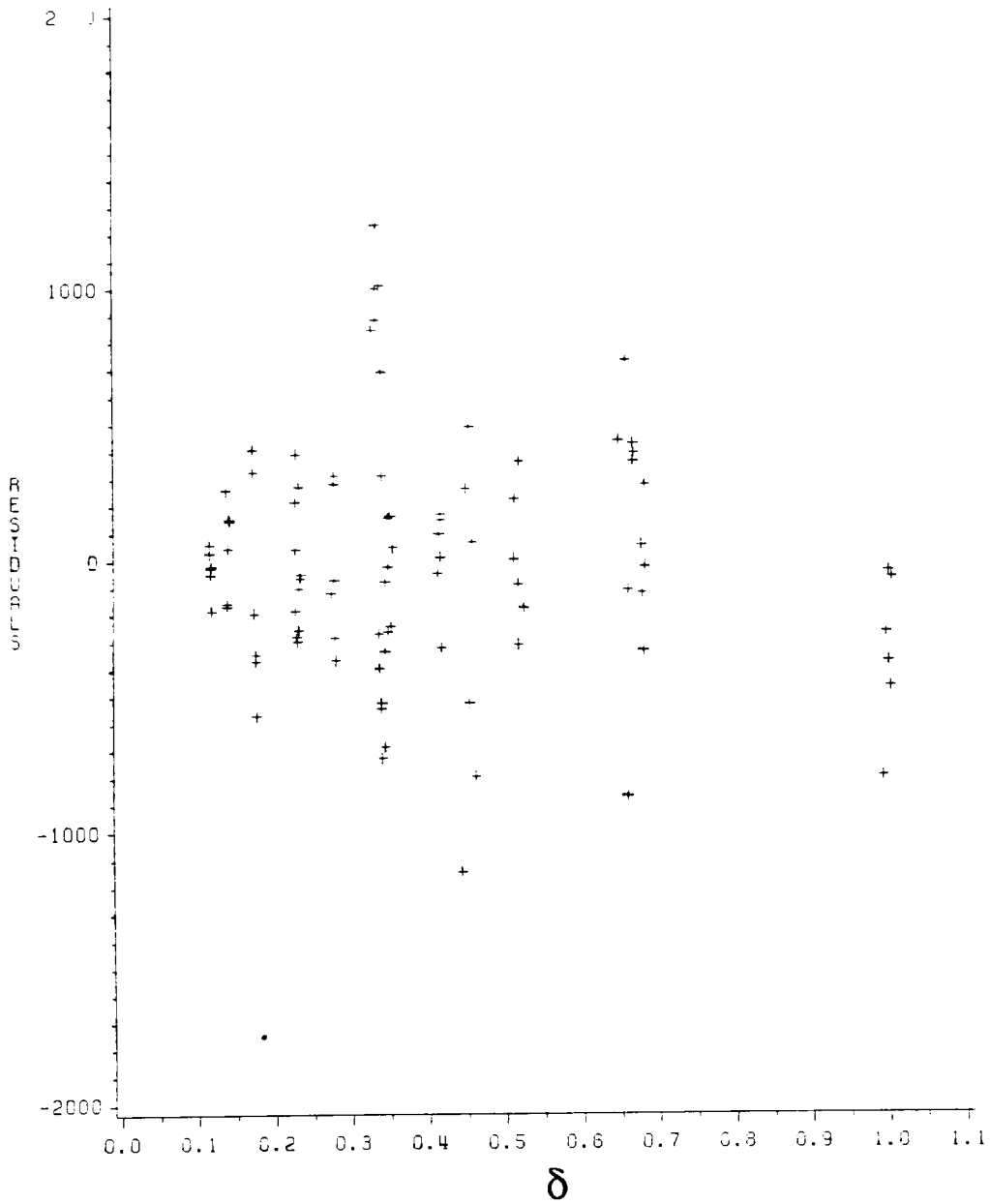

Figure 29. Residuals of equation (5.28) versus $\delta \equiv R/D$. Spruce, study B, at crack initiation.

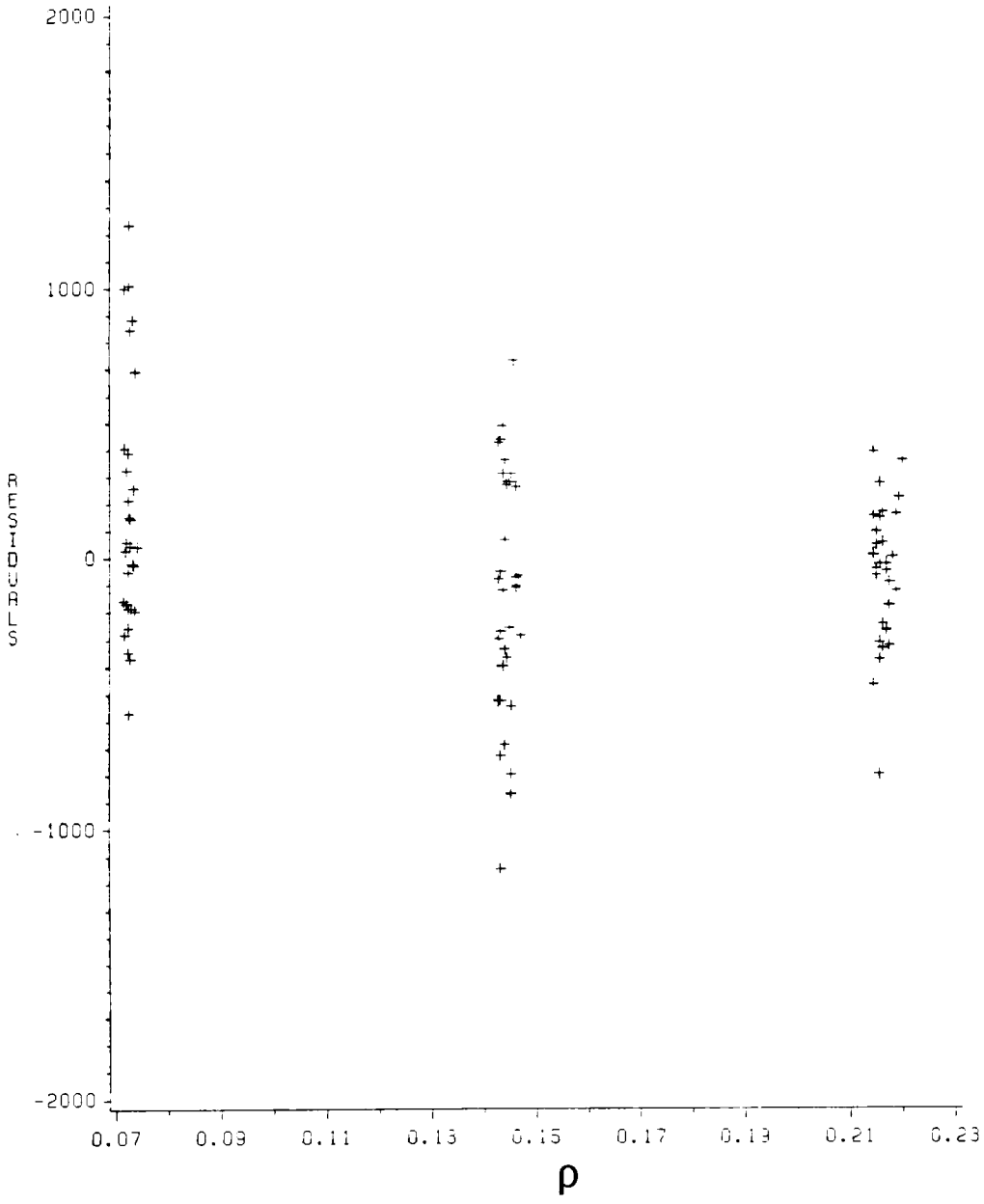

Figure 30. Residuals of equation (5.28) versus $\rho \equiv R/h$. Spruce, study B, at crack initiation.

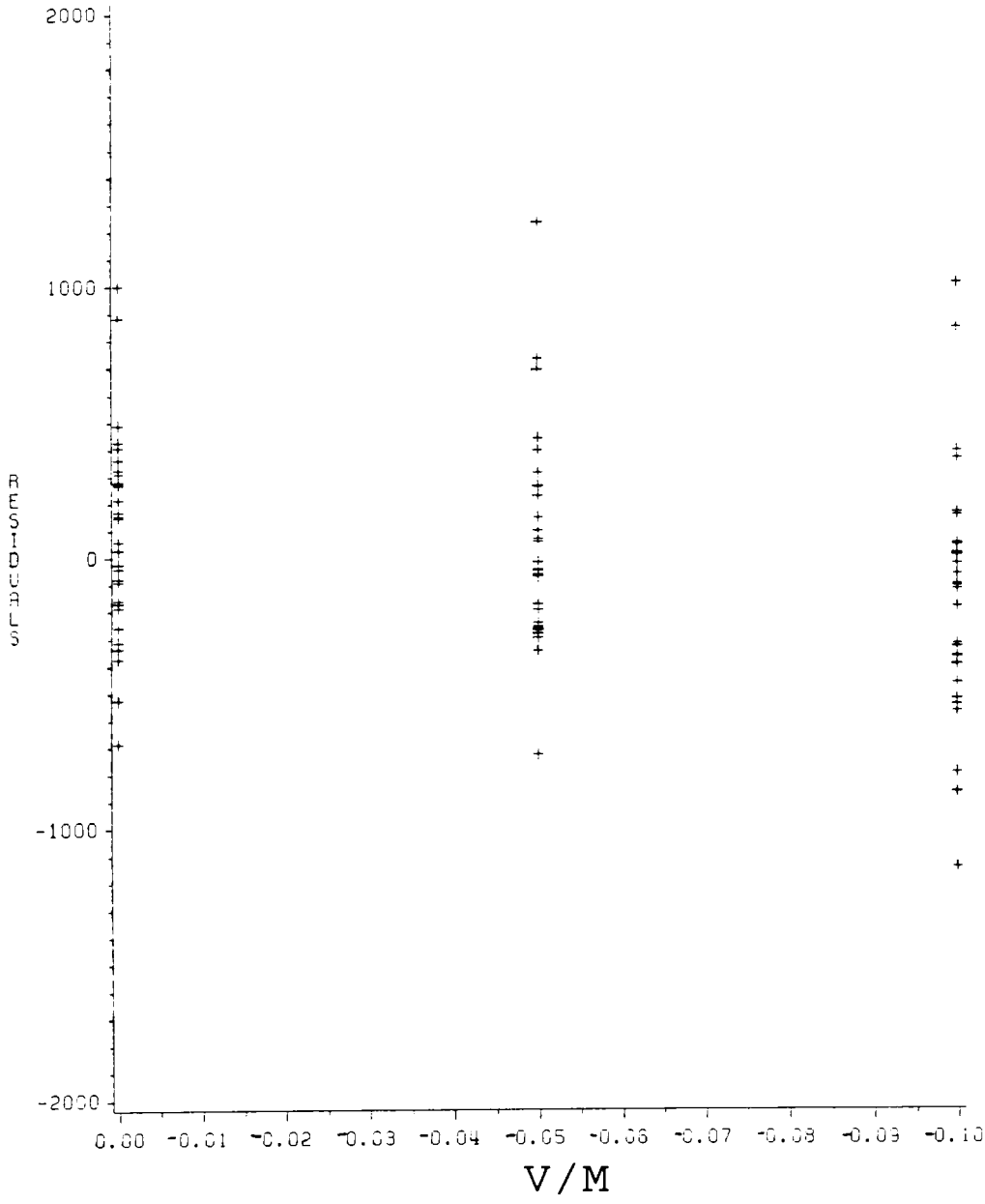

Figure 31. Residuals of equation (5.28) versus V/M. Spruce, study B, at crack initiation.

6.0 Discussion

6.1 Satisfying the Objectives of the Project

The primary objective of this work was to develop a closed form expression to estimate notched beam strength with accuracy and generality. In addition, the model was to be easy to use, and rely on readily obtainable material properties. I based the model on the following hypotheses:

1) Fillet hoop stress governs notched beam failure over wide ranges of geometries and material properties.
2) Sharp-cornered notches can be modeled as filleted notches with small, finite radii.
3) The notched beam strength parameter, κ, is a material parameter which can be approximated as a function of recognized clear-wood properties.

The accuracy and applicability of the critical fillet hoop stress (CFHS) model, equations (5.26) and (5.27), depends on the correctness of these hypotheses.

6.2 Comparisons with Other Models

The success of the CFHS model in meeting the above objectives can be assessed, in part, by comparing it with other notched beam models. The accuracy, generality, and ease of use of the CFHS model are discussed below in connection with its similarities with, and deviations from, previous methods of approximating notched beam strength.

6.2.1 Comparison with Gerhardt's model

Equation (5.26) can be compared readily with Gerhardt's (1984a) closed form strength expression, equation (2.2). Both expressions take the form of equation (3.9):

$$\frac{6M_i}{th^2} = \frac{\kappa_i}{F_1 + F_2 \cdot h \cdot \frac{V}{M}} \qquad (3.9)$$

Agreement of equations (5.26) and (2.2) requires that the geometry-dependent denominators in their right-hand sides differ only by a constant factor, independent of ϕ or V/M. In that case, the material constants K_{crit} and κ_{crit} would be related by the same factor. The term in equation (2.2) corresponding to F_1 is:

$$F_1' = \frac{1}{-1.26\phi + 1} \qquad (6.1)$$

and for shear:

$$F_2' = 1.13\phi + 0.30 \qquad (6.2)$$

The shear term, however, has coefficients chosen to correspond to the most anisotropic EP set (G32-E24) in Gerhardt's work. Although he did not include the G17-E17 EP set which I used as my baseline, he did analyze beams with G16-E24 and G16-E12 EPs. Estimating G17-E17 coefficients as the average of Gerhardt's G16-E24 and G16-E12 coefficients gives:

$$F_2' = 0.84\phi + 0.23 \qquad (6.3)$$

To make equation (5.26) directly comparable to equation (2.2), I set R=0.5in. and h=3.75in., as used by Gerhardt, and simplified F_1 and F_2 (equations 5.23 and 5.24) to:

$$F_1 = \frac{1}{0.165-0.217\phi+\frac{0.0193}{\phi}} \tag{6.4}$$

$$F_2 = 3.77\phi^{0.67} \tag{6.5}$$

Table 30 gives the ratios F_1/F_1' and F_2/F_2' for the 7 levels of ϕ analyzed by Gerhardt. The average ratio of the moment terms is 3.73, with a coefficient of variation (COV) of 5.8%; the shear terms have an average ratio of 3.59, with a COV of 0.7%. Thus, the ratio of the right-hand side denominators of the two predictive equations is constant at ~3.7, independent of ϕ and V/M. When F_2' is calculated with equation (6.2) instead of equation (6.3), F_2/F_2' averages 2.70, with COV=2.2%. Due to the predominance of the moment term (Section 5.1.2), however, the ratio of the denominators is determined primarily by the ratio F_1/F_1', and will remain close to 3.7 for all geometries and loadings investigated in the two studies. Only for a deep beam with a notch close to a support (i.e., for a large value of h·V/M) will there be a significant difference between the predictions of the two models. Thus, I conclude that my model is consistent with Gerhardt's, with the additional flexibility to accomodate fillet radii below

0.5in. and various beam depths. Although the original data were not available for me to evaluate the regression equation (5.28) for Gerhardt's test beams, the above analysis indicates that the present model would essentially duplicate the very good predictive accuracy reported by Gerhardt.

6.2.2 Comparison with Gustafsson's LEFM model

Equation (2.6), Section 2.1.2.4, is Gustafsson's (1988) expression to describe fracture of unfilleted notched beams. McLain (1989) showed that equation (2.6) can be rewritten as:

$$\frac{6M}{th^2}\sqrt{\left(\frac{1}{(1-\phi)^3}-1\right)}+\frac{6V}{th}\sqrt{0.1\frac{E_x}{G_{xy}}\frac{\phi}{1-\phi}}\le\sqrt{\frac{6G_cE_x}{h}} \qquad (6.6)$$

where G_c = critical strain energy release rate (with units of psi-in. or MPa-m). This has the same form as Gerhardt's expression, on which the CFHS model is based:

$$\frac{6M}{th^2}f_1+\frac{6V}{th}f_2=\sigma_{h,max} \qquad (3.1)$$

where f_1 and f_2 are functions of notch geometry and elastic parameters. The right-hand side of each expression is a material constant, with units of force per unit area, involving both strength and elastic properties. The factors multiplying the normalized moment and shear are dimensionless functions of geometry and elastic properties in both cases.

Introducing $F_1=f_1/\mu$ and $F_2=f_2/\mu$ (Section 5.1.2) and the criterion $\sigma_{h,max}\leq\sigma_{h,i}$, equation (3.1) can be rewritten:

$$\frac{6M}{th^2}F_1 + \frac{6V}{th}F_2 \leq \frac{\sigma_{h,i}}{\mu} \equiv \kappa_i \qquad (6.7)$$

where F_1 and F_2 are material-independent geometry functions. Equation (6.7) is a restatement of the CFHS model. The appearance of E_x/G_{xy} in the shear term of equation (6.6) prevents the two models from being equivalent in general. They may yield similar results over a range of practical cases, however.

To compare the two models, I rearranged them into the form of equation (3.9):

$$\frac{6M_i}{th^2} = \frac{\kappa_i}{F_1 + h\cdot\frac{V}{M}\cdot F_2} \qquad (6.8)$$

$$\frac{6M_i}{th^2} = \frac{\sqrt{\frac{6G_cE_x}{h}}}{F_1^* + h\cdot\frac{V}{M}\cdot F_2^*}, \qquad (6.9)$$

where

$$F_1^* \equiv \sqrt{\left(\frac{1}{(1-\phi)^3 - 1}\right)} \qquad (6.10)$$

and

$$F_2^* \equiv \sqrt{0.10\,\frac{E_x}{G_{xy}}\,\frac{\phi}{1-\phi}} \qquad (6.11)$$

Comparison of equations (6.8) and (6.9) shows that the condition for equivalence of the two models is:

$$\frac{\kappa_i}{F_1 + h \cdot \frac{V}{M} \cdot F_2} = \frac{\sqrt{\frac{6G_cE_x}{h}}}{F_1^* + h \cdot \frac{V}{M} \cdot F_2^*} \qquad (6.12)$$

Thus:

$$\frac{\sqrt{\frac{6G_cE_x}{h}}}{\kappa_i} = \frac{F_1^* + h \cdot \frac{V}{M} \cdot F_2^*}{F_1 + h \cdot \frac{V}{M} \cdot F_2} = \text{constant} \equiv C_c \qquad (6.13)$$

independent of material or geometry. Since F_2^* involves E_x/G_{xy}, whereas F_1, F_2, and F_1^* are material-independent, equation (6.13) can hold strictly only for a given level of E_x/G_{xy}. There are presently no data sets for which G_c, E_x, and κ_i are all known, so the left-hand side of equation (6.13) is difficult to estimate with any certainty. The geometric terms can be evaluated, however, at various levels of E_x/G_{xy}, ϕ, and V/M.

Table 31 summarizes several such comparisons of the two models. The comparison constant, C_c, has been calculated at six levels of ϕ (0.15, 0.25, 0.35, 0.45, 0.55, 0.65) for each level of h, E_x/G_{xy}, and V/M in the table. The mean and COV of C_c over the six levels of ϕ are tabulated. Since Gustafsson's model is formulated only for sharp-cornered notches, a value of R_{min} was needed for each calculation of F_1 and F_2. The R_{min} values in Table 31 were chosen by trial and error to minimize the variability of C_c with ϕ and V/M. The low coefficients of variation (0.06-0.14) indicate that C_c is reasonably constant with ϕ. That is, the two models predict similar effects of ϕ

over the range $0.15 \leq \phi \leq 0.65$. As expected, C_c is somewhat sensitive to E_x/G_{xy}, due to the changing influence of the shear term F_2^* as E_x/G_{xy} is varied. Neither h nor V/M appears to exert a significant effect on C_c. Thus, the simplified fillet hoop stress model predicts geometry effects consistent with those predicted by Gustafsson's fracture mechanics approach for unfilleted notches. The success of this comparison depends on the proper choice of R_{min}, which is dependent on E_x/G_{xy} and h. The estimates of R_{min} given in Table 31 suggest a linear dependence on h, i.e., a constant value of $\rho_{min} \equiv R_{min}/h$ for each ratio E_x/G_{xy}. (As only one beam depth was included in my mechanical tests, this hypothesis could not be tested against my experimental data.)

Gustafsson presented considerable experimental verification of his LEFM model. Its agreement with the present model is a key validation of the second and third basic hypotheses stated in Section 6.1. Equation (6.13) suggests a correspondence between κ_i and fundamental material parameters:

$$\kappa_i = \frac{\sqrt{\frac{6G_c E_x}{h}}}{C_c} = C_e \sqrt{\frac{G_c E_x}{h}} \qquad (6.14)$$

where $C_e = \frac{\sqrt{6}}{C_c} \cong 17.5$. The compatability of the CFHS model with Gustafsson's work supports the applicability of the CFHS model to unfilleted notches, given a suitable choice of R_{min}

(or ρ_{min}, as described above). This choice is discussed further in Section 6.3.2. It is encouraging that the two models, developed by entirely different methods (albeit from the common assumptions of a homogeneous, orthotropic, linear-elastic material) yield such similar geometry dependencies over the wide range of cases depicted in Table 31. The close correspondence between the models further justifies the simplifying assumptions used in Section 5.1.2 to derive the CFHS model.

6.2.3 Comparison with net section theory

This work was predicated on the inadequacy of existing methods for estimating notched beam strength. The simplest means for computing the failure load of a notched beam is to compare the nominal net section bending and shear stresses in the beam with the corresponding clear wood strength values:

$$\frac{6M}{t(h\text{-}D)^2} \leq MOR \qquad (6.15)$$

and

$$\frac{3V}{2t(h\text{-}D)} \leq S_{max} \qquad (6.16)$$

where MOR and S_{max} are the modulus of rupture and shear strength, respectively. This method is known to give unconservative results (unrealistically high allowable M and V) in many practical situations (Section 1.1). Thus, I expected the CFHS failure load predictions to be lower than those of

net section (NS) theory. For the interior-notched beams of interest, nominal NS bending stress is always ≥13 times greater than nominal NS shear stress, whereas the ratio $MOR/S_{max}<8$ for all materials tested (Table 27, Chapter 5). Thus, bending (equation 6.15) always governs failure. Due to the lack of design guidance for interior-notched beams, it has been common practice to apply the method intended for end-notched beams, equation (2.8). That method provides only a check of the shear capacity of the beam, and therefore will not give useful predictions of the capacity of interior-notched beams.

In Figures 32 and 33, I have plotted normalized maximum bending moment, $6M_{max}/th^2$, versus notch depth, for the NS and CFHS beam strength models. For Figure 32, I used R=0.2in., while Figure 33 was based on R=0.5in.. In both cases, I set h=3.5in. and V/M=0.10in.$^{-1}$. Each graph includes predictions for dry Douglas-fir and green hard maple, based on the values of MOR and $\kappa_{2\%}$ which I measured. These materials gave the highest and lowest values, respectively, of the ratio $MOR/\kappa_{2\%}$ (Table 26, Chapter 5). Since MOR governs the NS strength prediction while $\kappa_{2\%}$ controls the CFHS prediction, these materials show relatively high and low deviations between the two models.

For R=0.2in. (Figure 32), the CFHS model is considerably more conservative for both materials for all levels of ϕ. The maximum ratio between the two predicted failure moments is over 3:1, for Douglas-fir at the lowest modeled notch depth (ϕ=0.14). For R=0.5in. (Figure 33), the CFHS prediction for maple slightly exceeds the NS prediction for $\phi \geq 0.59$. Again, the greatest disparities are at low levels of ϕ. In light of the accuracy shown by the CFHS method (Sections 5.2, 6.2.1, and 6.2.2), the figures are clear evidence of the overestimation of failure loads by NS bending theory.

6.3 Recommendations for Application of the CFHS Model

The CFHS model was developed to predict static strength of wood beams with filleted or unfilleted rectangular or semi-circular notches on the tension face between simple supports. The following are some guidelines for the practical application of the model.

6.3.1 Determination of κ for engineering use

As with MOR, the direct determination of κ_i and $\kappa_{2\%}$ for a given beam requires a destructive test. In general, however, one is concerned with the mean or n^{th} percentile of the distribution of κ for a population of beams of a given material. (κ is used here to denote κ_i or $\kappa_{2\%}$.) For this purpose, two methods are available. The first consists of destructive

testing of a random sample of notched beams from the target population. The beams can have fixed D, R, notch location, loading geometry, t, and h. The values of κ derived from these tests will be applicable to any notch, beam, and loading geometry. With this method, all appropriate statistical moments of the κ distributions can be determined to the desired degree of accuracy, dependent upon sample size.

For materials for which specific gravity (SG) and cross-grain tensile strength ($T_\perp$) data are available, a second approach can be used. The regression equation (5.40) can be used to estimate mean κ values from mean values of SG and $T_\perp$. This method, although less exact than the first, obviates further notched beam testing.

6.3.2 Strength estimation for unfilleted notches

Equation (5.26) can be used to estimate the critical loads of unfilleted notched beams. This requires an appropriate value of ρ_{min}. For most commercial North American woods, ρ_{min}=0.0086 (i.e., R_{min}=0.030in. for h=3.5in.) should be conservative, based on $E_x/G_{xy} \leq 24$ (Table 31). Tables 23 and 24 give experimentally-derived values of R_{min} which are much larger (less conservative) than this recommendation, except in two cases which I believe to be anomalously low. Prior to extensive use of this model for unfilleted notches, I suggest

further work to establish reliable values of R_{min} (Section 6.4.5).

6.3.3 Geometric limitations of the model

Although applicable over a wide range of notch, beam, and loading geometries, the CFHS formulation is likely to give inaccurate results outside of the domain for which it was derived. The current limits include:

$-0.07\text{in.}^{-1} \leq V/M \leq 0.10\text{in.}^{-1}$

$0.14 \leq \phi \leq 0.71$

$R \geq 0.20\text{in.}$ for filleted notches

$0.057 \leq \rho \leq 0.143$

$0.125 \leq \delta \leq 0.70$

The lower limits on ρ and δ apply only for filleted notches. For $R>0.5\text{in.}$, ρ and δ corresponding to $R=0.5\text{in.}$ should be used in equations (5.26) and (5.27).

The above range of V/M should include nearly all interior notches of practical interest. Notch depths $\phi<0.14$ may be encountered in some deep beams. It would be conservative to assume $\phi=0.14$ in such cases, although this may be overconservative for ϕ below about 0.10. The use of equations (5.26) or (5.27) with $\phi<0.14$ is likely to lead to overestimation of notched beam strength. Conversely, the introduction of $R<0.20\text{in.}$ into these equations is likely to result in an underestimation of strength, except when $R=R_{min}<0.2\text{in.}$ is being used to describe an unfilleted notch.

6.3.4 Material property limitations of the model

The range of elastic parameters spanned by the five EP sets (Table 4, Chapter 3) includes virtually all wood materials found in North American construction and most woods worldwide. I am not aware of any reason that the CFHS approach would be limited to any particular range of wood strength properties.

6.4 Extensions to the Model

Two general areas are open for additional development and refinement of the CFHS model. The first considers topics which have been addressed, but not fully resolved, by the present work. The second explores parameters which are expected to affect notched beam strength but which have not been included in studies to date.

6.4.1 End-notched beams

End-notched beams comprise a large class of commercially important notched beams not covered by this work. The CFHS model was formulated for cases in which moment dominates, i.e., low V/M ratios. End-notched beams often deviate from this assumption. In addition, when the notch fillet is located near the support, the stress field due to bending and shear at the fillet may interact with the stress field due to compression over the support. Thus, the dependencies of $\sigma_{h,max}$

on notch and beam geometry may be significantly different for end-notched beams than for interior-notched beams.

6.4.2 Effects of rate and duration of loading

High-rate and long-duration loads may influence notched beam strength differently than they influence clear wood strength (Section 2.1.3.3). The loading rates for notched beams can differ vastly from application to application. Understanding the time-dependence of notched beam strength will require experimental data and a theoretical framework for loading rate effects under combined stresses, such as occur in the fillet region.

6.4.3 Effects of combined flexural and axial loading

The CFHS model was derived for simply supported beams. Beams in structures typically experience some degree of end restraint, resulting in axial loading in addition to the applied transverse loading. Finite element modeling can be used to assess the degree to which this changes the stress distributions around notch fillets. Any changes in the angular location, θ_{max}, of $\sigma_{h,max}$ due to axial loading could alter the failure mechanism and capacity of the notched beams.

6.4.4 Effects of cracks and notch surface irregularities

Cracks, saw cuts, and other small-radius voids extending into a beam from the fillet surface are expected to reduce

beam strength. The degree of strength loss will probably depend on the shape, size, and location of the flaw. The most common sources of these flaws are seasoning checks and poorly controlled machining. Checks will result when a beam is notched in the green condition and then allowed to dry. The CFHS model may be usable to estimate the strength of these notches by treating them as unfilleted notches with an appropriate equivalent geometry. Any CFHS formulation should be compared with a LEFM model such as Gustafsson's, as this problem includes a stress singularity and falls naturally within the realm of LEFM.

6.4.5 Verification of unfilleted and slit notch effects

The mechanical test results reported here for slit notches and unfilleted notches are equivocal due to small sample sizes and high variability. Additional tests should be conducted to verify the values of R_{min} inferred from the comparisons of Section 6.2.2, and to substantiate the slit notch effect noted by Stieda (1966) and Murphy (1979). Based on the new tests, the CFHS model should be supplemented with more authoritative values of R_{min} and, if necessary, a correction to account for very short notches.

6.4.6 Beam depth effect

A beam depth effect was predicted by the FE modeling (Section 5.1.3.1), but no mechanical testing was done to verify

that prediction. I am unaware of any work on filleted interior-notched beams which included variable beam depth. On the basis of the comparison of the CFHS model with Gustafsson's model (Section 6.2.2), I hypothesized that the effective fillet radius, R_{min} is also a function of beam depth, *h*. Validation and quantification of these effects are important to the general utility of the CFHS method.

6.4.7 Tools for notched beam design and evaluation

In addition to the guidelines given in Section 6.3, data and procedures for the engineering use of the CFHS model should be prepared. That work should include:

1) establishment and tabulation of allowable values of $\kappa_{2\%}$ for wood materials in commercial use;
2) development of graphical, tabular, or computational aids for evaluating the terms of equation (5.26);
3) formulation of simple methods of adjusting predicted strength for load duration, seasoning conditions (e.g., notched green, allowed to dry in service), service environment, and partial end fixity.

With the advent of these extensions, the CFHS model will provide a highly versatile tool for estimating the critical loads of beams with tension-side notches.

Table 30. *Comparison of the notch depth dependencies given by Gerhardt (1984a) and the present model.*

		F_2/F_2' [1]	
ϕ	F_1/F_1' [2]	G17-E17 [3]	G32-E24 [4]
0.267	3.70	3.42	2.58
0.333	3.85	3.54	2.67
0.4	3.92	3.60	2.71
0.467	3.92	3.64	2.73
0.533	3.84	3.65	2.74
0.6	3.64	3.65	2.74
0.667	3.24	3.63	2.73
Mean:	3.73	3.59	2.70
COV [5], %:	6.5	2.4	2.2

[1] F_2 = shear-based "stress concentration" in present model
F_2' = shear-based "stress concentration" in Gerhardt's model

[2] F_1 = moment-based "stress concentration" in present model
F_1' = moment-based "stress concentration" in Gerhardt's model

[3] F_2' calculated using coefficients estimated for the G17-E17 EP set by averaging the coefficients for the G16-E12 and G16-E24 EP sets.

[4] F_2' calculated using coefficients for the G32-E24 EP set, as used by Gerhardt in formulating equation (2.2).

[5] coefficient of variation

Table 31. *Comparison constant, C_c, relating the geometry dependencies predicted by the present model and Gustafsson's (1988) LEFM model for unfilleted notches.*

h, in.	E_x/G_{xy}	R_{min}[2], in.	C_c[1], V/M=0 mean	C_c, V/M=0 COV	C_c, V/M=0.10in.$^{-1}$ mean	C_c, V/M=0.10in.$^{-1}$ COV
3.5	8	0.1	0.153	0.11	0.154	0.10
	17	0.04	0.140	0.13	0.140	0.10
	32	0.02	0.136	0.14	0.134	0.11
20	8	0.5	0.151	0.11	0.150	0.07
	17	0.2	0.139	0.13	0.134	0.07
	32	0.13	0.136	0.13	0.139	0.06

[1] C_c was calculated from equation (6.13) for 6 levels of ϕ (0.15, 0.25, 0.35, 0.45, 0.55, 0.65) at each level of h, E_x/G_{xy}, and V/M. The mean and COV (coefficient of variation) were calculated over the 6 levels of ϕ.

[2] Each value of R_{min} was chosen approximately to minimize the variability of C_c with ϕ and V/M at the given levels of h and E_x/G_{xy}.

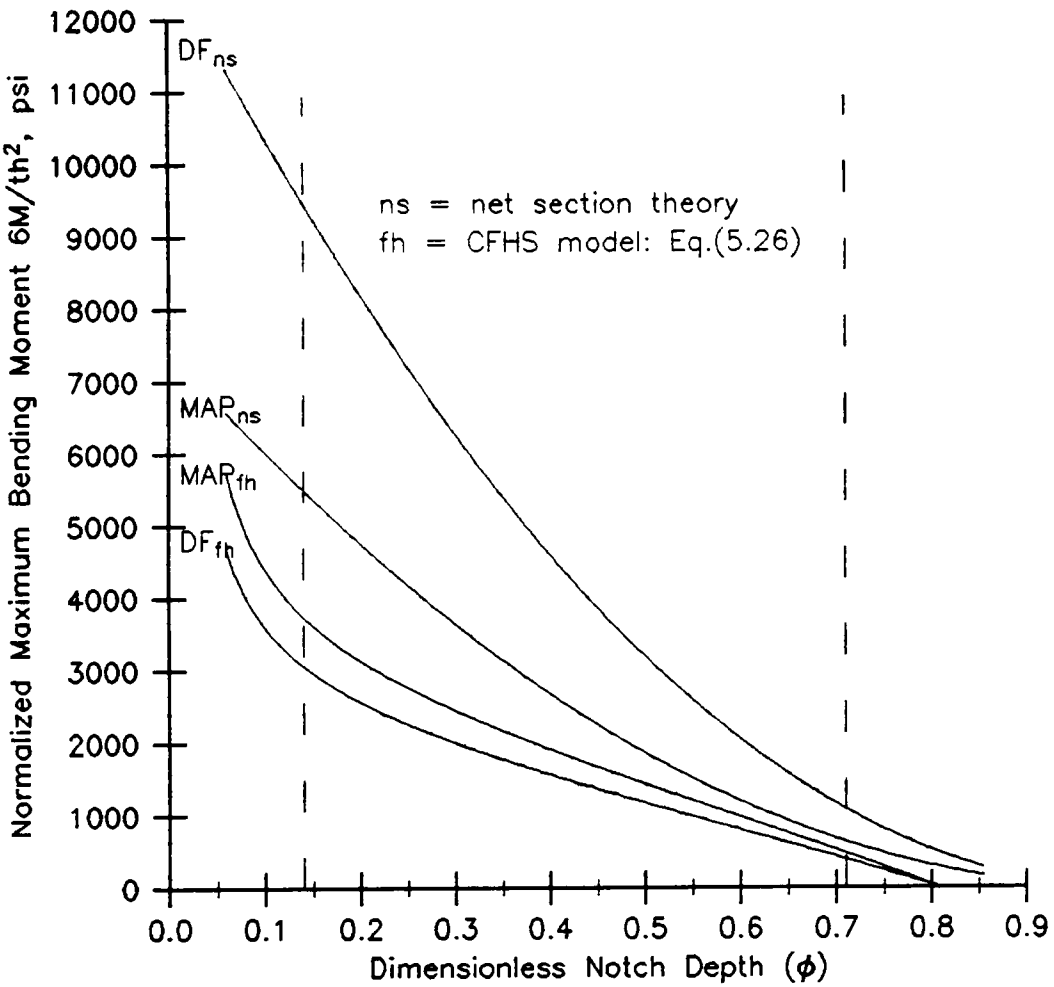

Figure 32. Comparison of CFHS Model with Net Section theory. R = 0.20in., h = 3.5in., V/M = 0.10in.$^{-1}$.

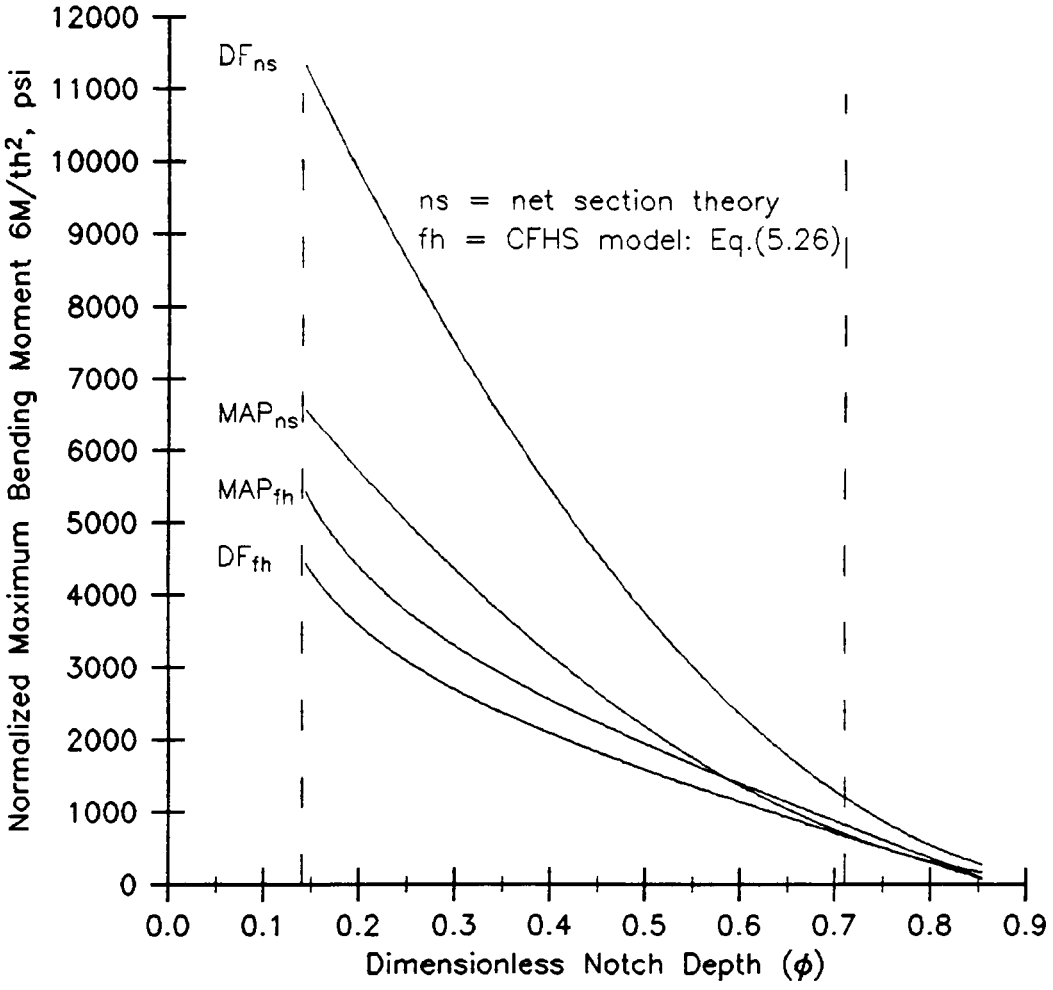

Figure 33. Comparison of CFHS model with net section theory. R = 0.50in., h = 3.5in., V/M = 0.10in.$^{-1}$.

7.0 Summary and Conclusions

A critical fillet hoop stress (CFHS) model, based on the work of Gerhardt (1984a,b) has been used to develop an expression for predicting the failure loads of beams with filleted notches on the tension side between the supports. The effects of notch location and loading condition are described well by a single parameter, V/M, the ratio of resultant shear to resultant moment at the section containing the critical notch fillet. Effects of notch depth, D, and fillet radius, R, are treated explicitly in the model. Computer modeling and mechanical testing showed the effect of notch length to be negligible for L≥1.5in. (at h=3.5in.). A beam depth effect was found in the FE analysis and incorporated into the model, but was not tested.

The model has been verified with notched beam tests of eight wood materials, three notch locations and twenty-one filleted notch geometries. The closed form strength equation, with a single material parameter, κ, accurately described the trends in notched beam critical loads with notch geometry, notch location, and loading geometry. Load at crack initiation was most reliably predicted; useful predictions of the load preceding the first major (≥2%) drop in load were also obtained. κ evaluated at the first major

drop in load ($\kappa_{2\%}$) can be used to compute a conservative estimate of notched beam ultimate load. The geometry-dependencies predicted by the CFHS model agreed well with those predicted by Gerhardt's model (1984a) for filleted notches.

The applicability of the CFHS approach to sharp-cornered notches hinges on the identification of an effective fillet radius ,R_{min}, to be substituted into the equation for beams with R=0. Comparison of the CFHS model with the LEFM-derived formula of Gustafsson (1988) suggests that ρ_{min}=R_{min}/h is constant for a given elastic parameter ratio E_x/G_{xy}. The value of ρ_{min} characterizing a material can be used in the CFHS expression to estimate the strength of unfilleted notched beams of that material. With appropriate values of R_{min}, the CFHS model gave predictions similar to Gustafsson's for the effects of notch depth and V/M. Comparison of the two models also suggested a relationship between κ and the material parameters G_c (critical strain energy release rate) and E_x (longitudinal elastic modulus).

Four materials, two notch locations and eight unfilleted notch geometries were tested to evaluate R_{min}. Experimentally derived values of R_{min} were too variable, given the small sample sizes, to verify the theoretical predictions. Pending

further testing, I believe that ρ_{min}=0.0086 can be used conservatively for most commercial species.

A highly significant relationship was found between κ and perpendicular-to-grain tensile strength and specific gravity. This relationship can be used to estimate κ for wood materials for which notched beam tests have not been performed. This is an important attribute of this method, in contrast with methods relying on material properties such as orthotropic moduli and fracture toughness, which are difficult to obtain. κ was related only weakly to block shear strength.

The CFHS approach is uniquely general in its applicability. It is the only closed form method available for treating the effect of fillet radius, including R≈0, and it treats the beam depth effect which.was not studied by Gerhardt (1984a). In its current form, the predictive equation is not applicable to end-notched beams or other cases in which bending is not predominant. The separation of material and geometry terms in the expression, and the use of a single material parameter, need to be validated for shear-dominated cases. For interior-notched beams, however, the CFHS model allows accurate strength approximations to be made for nearly all practical notch geometries using readily obtained material property data and a simple algebraic expression.

8.0 Literature Cited

Abou-Ghaida, S., and V.K.A. Gopu. 1984. Shear strength of notched timber beams. Proc. Pacific Timber Engin. Conf., Auckland, NZ, May 21-25, 1984.

American Institute of Timber Construction. 1985. Timber Construction Manual. 3rd Ed.. 825pp. John Wiley & Sons, New York.

American Society for Testing and Materials. 1986a. Standard nomenclature of domestic hardwoods and softwoods. ASTM D1165-80. Philadelphia, PA.

American Society for Testing and Materials. 1986b. Standard methods of testing small clear specimens of timber. ASTM D143-83. Philadelphia, PA.

American Society for Testing and Materials. 1986c. Specific gravity of wood and wood-base materials. ASTM D2395-83. Philadelphia, PA.

Anderson, L.O. 1975. Wood Frame House Construction. Agriculture Handbook No. 73, U.S.D.A. Forest Service.

Ashby, M.F., K.E. Easterling, R. Harrysson, and S.K. Maiti. 1985. The fracture and toughness of woods. Proc. R. Soc. London A398: 261-280.

Barrett, J.D. 1974. Effect of size on tension perpendicular-to-grain strength of Douglas-fir. Wood and Fiber 6(2):126-143.

Barrett, J.D. 1981. Fracture mechanics and the design of wood structures. Phil. Trans. R. Soc. London A 299:217-226.

Barrett, J.D., and R.O. Foschi. 1977. Mode II stress-intensity factors for cracked wood beams. Engin. Fracture Mechanics 2:223-233.

Barrett, J.D., R.O. Foschi, and S.P. Fox. 1975. Perpendicular-to-grain strength of Douglas-fir. Can. J. Civ. Eng. 2(1):50-57.

Beery, W.H., G. Ifju, and T.E. McLain. 1983. Quantitative wood anatomy - relating anatomy to transverse tensile strength. Wood and Fiber Sci. 15(4):395-407.

Bendtsen, B.A., and S. Porter. 1978. Comparison of results from standard 2-inch with 1-1/2-inch shear block tests. Forest Prod. J. 28(7):54-56.

Blicblau, A.S., and D.J. Cook. 1986. Aspects of wood fracture toughness at various testing speeds. Civil Eng. Trans. 28(2):153-157.

Bodig, J., and B.A. Jayne. 1982. Mechanics of Wood and Wood Composites. 697pp. Van Nostrand Reinhold, New York.

Bohannan, B. 1966. Effect of size on bending strength of wood members. USDA For. Serv. Res. Paper FPL 56. For. Prod. Lab., Madison, WI.

Box, G.E.P., W.G. Hunter, and J.S. Hunter. 1978. Statistics for experimenters. 644pp. John Wiley and Sons, New York. pp.232-241.

Byars, E.F., and R.D. Snyder. 1975. Engineering Mechanics of Deformable Bodies. 3rd Ed. 499 pp. Intext Educational Publishers, New York. pp.216-224.

Canadian Forestry Service. 1976. Reusable Wood Pallets: Selection and Proper Design. Forestry Technical Rept. 11. Can. For. Svc. Eastern For. Prod. Lab., Ottawa, Ontario.

Crubile, P., J. Ehlbeck, H. Bruninghoff, H.J. Larsen and J. Sunley. 1985. Eurocode 5: Common Unified Rules for Timber Structures. Drafting Panel EC5. Commission of the European Communities, Paris, France.

Crubile, P., J. Ehlbeck, H. Bruninghoff, H.J. Larsen and J. Sunley. 1988. Eurocode No. 5: Common Unified Rules for Timber Structures. Directorate-General, Telecommunications, Information Industries and Innovation. Commission of the European Communities, Luxembourg, Belgium.

Debaise, G.R., A.W. Porter, and R.E. Pentoney. 1966. Morphology and mechanics of wood fracture. Mater. Res. and Stand. 6(10):493-499.

Draper, N.R., and H. Smith. 1981. Applied regression analysis. 2nd ed. 699pp. John Wiley and Sons, New York. pp.141-149, 221-225.

Easterling, K.E., R.Harrysson, L.J. Gibson, and M.F. Ashby. 1982. On the mechanics of balsa and other woods. Proc. R. Soc. London A383:31-41.

Gerhardt, T.D. 1983. Plane Stress Analysis of Wood Members Using Isoparametric Finite Elements. USDA For. Serv. Gen. Tech. Rept. FPL 35. For. Prod. Lab., Madison, WI.

Gerhardt, T.D. 1984a. Strength and stiffness analysis of notched, green oak pallet stringers. Res. Paper FPL 452. USDA For. Svc. For. Prod. Lab. Madison, WI.

Gerhardt, T.D. 1984b. A hybrid/finite element approach for stress analysis of notched anisotropic materials. ASME J. Applied Mechanics 51:804-810.

Gilman, L., and A.J. Rose. 1984. APL: An Interactive Approach. 3rd Ed. 357 pp. John Wiley & Sons, New York.

Green, A.E. 1942. Stress systems in aeolotropic plates, IV. Proc. R. Soc. London A 180:173-208.

Green, A.E. 1945. Stress systems in isotropic and aeolotropic plates, V. Proc. R. Soc. London A 184:231-252.

Green, A.E., and G.I. Taylor. 1945. Stress systems in aeolotropic plates, III. Proc. R. Soc. London A 184:181-195.

Gustafsson, P.J. 1988. A study of strength of notched beams. Paper CIB-W18A/21-10-1. Intl. Council for Bldg. Rsch. Studies and Documentation, Vancouver, B.C., Canada.

Hooley, R.F., and P.D. Hibbert. 1967. Stress concentrations in timber beams. J. Structural Div., Proc. of ASCE. 93(ST2):127-139.

Krebs, H.J., P. Hoffmeyer, and L.G. Nielsen. 1984. Duration of load tests with notched spruce beams at two moisture levels. Proc. IUFRO Timber Engineering Meeting, 1984, Xalapa, Mexico. IUFRO, Vienna, Austria.

Lamb, F.M. 1988. Personal communication regarding dry kiln operating schedules. Assoc. Prof., Dept. of Wood Sci. and Forest Prods., VPI&SU.

Leicester, R.H. 1969. The size effect of notches. Proc. 2nd Australasian Conf. on Mech. of structures and materials. V4:1-20.

Leicester, R.H. 1974. Fracture strength of wood. Proc. First Autralian Conf. on Engin. Materials, Sydney, 1974. Univ. of New South Wales, Sch. of Civil Engin., Kensington, Australia.

Leicester, R.H., and W.G. Poynter. 1979. On the design strength of notched beams. In Proc. of the 19th Forest Products Research Conference. Melbourne, Australia.

Liu, J.Y. 1981. A Weibull analysis of wood member bending strength. Pages 57-64 in Failure prevention and reliability - 1981. F.T.C. Loo, ed. Am. Soc. Mech. Eng., Fairfield, NJ.

Lum, C. 1986. Stress-Intensity Factors for V-Notches in Orthotropic Plates Using Singular Finite Elements. M.S. Thesis. Dept. of Civil Engineering, Univ. of British Columbia, Vancouver, B.C., Canada.

Madsen, B. 1975. Duration of load tests for wood in tension perpendicular to grain. For. Prods. Jour. 25(8): 48-53.

Mall, S., J.F. Murphy, and J.E. Shottafer. 1983. Criterion for mixed mode fracture in wood. ASCE J. Engin. Mechanics 109(3):680-690.

Masuda, M. 1988. Theoretical consideration on fracture criteria of wood - proposal of finite small area theory. Pages 584-595 in Proc. of the 1988 Intl. Conf. on Timber Engineering, Seattle, WA, 1988. For. Prods. Res. Soc. Madison, WI.

McLain, T.E. 1989. Summary - comparison of Gerhardt and Gustafsson. Personal communication. Assoc. Prof., Dept. of Wood Sci. and Forest Prods., VPI&SU.

Murphy, J.F. 1979. Using fracture mechanics to predict failure in notched wood beams. Pages 159-173 in Proc. of the 1st Intl. Conf. on Wood Fracture. Banff, Alberta, 1979. Forintek Canada Corp. Vancouver, B.C., Canada.

Murphy, J.F. 1986. Strength and stiffness reduction of large notched beams. J. Struct. Engin. 112(9):1989-2000.

Myers, R.H. 1971. Response Surface Methodology. 246 pp. Allyn and Bacon, Boston.

National Forest Products Association. 1986. National Design Specification for Wood Construction. Natl. For. Prods. Assoc.. Washington, DC. 87pp.

Neter, J., and W. Wasserman. 1974. Applied Linear Statistical Models. 834pp. Richard D. Irwin, Inc., Homewood, IL. pp.131-136.

Panshin, A.J., and C. de Zeeuw. 1980. Textbook of Wood Technology. Fourth Ed.. 687pp. McGraw-Hill, New York.

Peterson, R.E. 1974. Stress Concentration Factors. 314pp. John Wiley and Sons, New York.

Porter, A.W. 1964. On the mechanics of fracture in wood. For. Prods. Jour. 14(8):325-331.

Reeves, J.R. 1973. The effect of stringer design and leading-edge design on the strength characteristics of wooden pallets. M.Arch. thesis, VPI&SU. pp.13-16,66-67.

Richards, D.B. 1974. Strength of wood beams with shallow curved notches. Wood Science 7(1):77-84.

SAS Institute, Inc. 1985. SAS user's guide: statistics. Version 5 edition. SAS Institute, Inc., Cary, NC. 956pp.

Schniewind, A.P., T. Ohgama, T. Aoki, and T. Yamada. 1982. Effect of specific gravity, moisture content, and temperature on fracture toughness of wood. For. Prods. Jour. 15(2):101-109.

Schniewind, A.P., and R.A. Pozniak. 1971. On the fracture toughness of Douglas fir wood. Engin. Fracture Mechanics 2:223-233.

Scholten, J.A. 1935. Rounding notches makes stronger joists. American Lumberman. No. 3039. Jan. 19, 1935.

Sih, G.C., P.C. Paris, and G.R. Irwin. 1965. On cracks in rectilinearly anisotropic bodies. Intl. J. Fracture Mech. 1:189-203.

Standards Assoc. of Australia. 1988. SAA Timber Structures Code. Part 1 - Design Methods. AS 1720.1-1988. SAA, North Sydney, N.S.W..

Stieda, C.K.A. 1964. Stress concentrations in notched timber beams. Trans. Engin. Inst. of Canada. Vol.7, No.A-5. Paper No. EIC-64-BR & STR 5. 6pp.

Stieda, C.K.A. 1966. Stress concentrations around holes and notches and their effect on the strength of wood beams. J. of Materials 1(3):560-582.

STSC, Inc. 1987. APL*PLUS System for the PC: Programmer's Manual. STSC, Rockville, MD.

Taylor, R.L. 1977. Computer procedures for finite element analysis. Ch. 24, Pages 677-757 in The Finite Element Method. 3rd Ed. O.C. Zienkiewicz, editor. McGraw-Hill, London. 757pp.

Triboulot, P., P. Jodin, and G. Pluvinage. 1981. Application of fracture mechanics to wood. Pages 907-917 in Analytical and Experimental Fracture Mechanics. G.C. Sih and M. Mirabile, eds. Sijthoff & Noordhoff, Rockville, MD.

USDA Forest Products Laboratory. 1935. Wood Handbook. USDA For. Prod. Lab., Madison, WI.

USDA Forest Products Laboratory. 1955. Wood Handbook, 1955 edition. Hdbk. No. 72, USDA For. Prod. Lab., Madison, WI.

USDA Forest Products Laboratory. 1987. Wood Handbook: Wood as an Engineering Material. Hdbk. No. 72, USDA For. Prod. Lab., Madison, WI.

Walsh, P.F. 1972. Linear fracture mechanics in orthotropic materials. Engin. Fracture Mechanics 4:533-541.

Walsh, P.F. 1974. Linear fracture mechanics solutions for zero and right angle notches. Div. of Building Research, Technol. Paper (second series). No. 2:1-16. CSIRO Australia Division of Building, Construction, and Engineering, Highett, Victoria, Australia.

Williams, J.G., and M.W. Birch. 1976. Mixed mode fracture in anisotropic media. Pages 125-137 in Cracks and Fracture: STP601. ASTM, Philadelphia.

Woo, C.W., and C.L. Chow. 1979. Mixed mode fracture in orthotropic media. Pages 387-396 in Proc. of an Intl. Conf. on Fracture Mechanics in Engineering Application, Bangalore, India,1979. Sijthoff & Noordhoff, Germantown, MD.

Wood, L.W. 1951. Relation of Strength of Wood to Duration of Load. Rept. No. R1916, USDA For. Prod. Lab., Madison, WI.

Wu, E.M. 1967. Application of fracture mechanics to anisotropic plates. ASME J. Applied Mechanics 34:967-974.

```
C  THIS IS THE PLANE STRESS/ PLANE STRAIN FINITE ELEMENT ANALYSIS
C  PROGRAM WRITTEN BY DR. T.D. GERHARDT (SEE FPL GEN. TECH. REPT. 35
C  AND J. APPL. MECH., V.51 (1984)).  IT IS BASED ON THE PROGRAM OF
C  R.L. TAYLOR IN ZIENKIEWICZ, "THE FINITE ELEMENT METHOD",
C  (3RD ED.,1977).
C
C*************************************************************************
C                                                                        *
C                            MAIN PROGRAM                                *
C                                                                        *
C*************************************************************************
C.... SET PROGRAM CAPACITY * MAX MUST AGREE WITH DIMENSION OF M
      COMMON M(1000000)
      COMMON /PSIZE/ MAX
      MAX = 1000000
C
C....ERRSET IS A SYSTEM SUBROUTINE (IBM VS FORTRAN, V2) TO ADJUST SYSTEM
C....BEHAVIOR UPON ENCOUNTERING ERRORS.  THE 1ST ERRSET CALL SUPPRESSES
C....ALL BUT THE FIRST ERROR MESSAGE FOR FLOATING POINT UNDERFLOW AND
C....ALLOWS AN UNLIMITED NUMBER OF SUCH "ERRORS".  ANY FP UNDERFLOW
C....VALUE IS SET TO 0.  THE SECOND ERRSET CALL TERMINATES EXECUTION
C....UPON THE FIRST OCCURENCE OF "FORMATTED I/O END OF FILE", ERROR 212.
C
      CALL ERRSET (208, 256, 1, 1, 1)
      CALL ERRSET (212, 1, 1, 1, 0)
      CALL PCONTR
      END
C*************************************************************************
C                                                                        *
C                              PCONTR                                    *
C                                                                        *
C*************************************************************************
      SUBROUTINE PCONTR
      IMPLICIT DOUBLE PRECISION (A-H,O-Z)
      LOGICAL PCOMP
      COMMON /CDATA/ O,HEAD(20),NUMNP,NUMEL,NUMMAT,NEN,NEQ,IPR
      COMMON /LABEL/ PDIS(6),A(6),BC(2),DI(6),CD(3),TE(3),FD(3)
      COMMON M(30000)
      COMMON /ZEROB/ N13
      DIMENSION TITL(20),WD(3)
      DATA WD/4HFEAP,4HMACR,4HSTOP/
C.... READ A CARD AND COMPARE FIRST 4 COLUMNS WITH MACRO CONTROL LIST.
1     READ(5,1000) TITL
      IF(PCOMP(TITL(1),WD(1)))  GO TO 100
      IF(PCOMP(TITL(1),WD(2)))  GO TO 200
      IF(PCOMP(TITL(1),WD(3)))  RETURN
      GO TO 1
C.... READ AND PRINT CONTROL INFORMATION.
100   DO 101 I = 1,20
101   HEAD(I) = TITL(I)
      READ (5,1001) NUMNP,NUMEL,NUMMAT,NDM,NDF,NEN,NAD
      WRITE (6,2000) HEAD,NUMNP,NUMEL,NUMMAT,NDM,NDF,NEN,NAD
      PDIS(2) = A(NDM)
      NEN1 = NEN + 1
C.... NST = D.O.F./ELEMENT.
      NST = NEN*NDF + NAD
```

```
      NST = NEN*NDF + NAD
C....
C.... SET POINTERS FOR ALLOCATION OF DATA ARRAYS.
C.... N0-1=STORAGE NEEDED FOR UL (LOCAL NODAL DISP'S AND VELOCITIES)
C.... N1-N0=STORAGE NEEDED FOR XL (LOCAL NODAL COORODINATES)
C.... N2-N1=STORAGE NEEDED FOR TL (LOCAL NODAL TEMPERATURES)
C.... N3-N2=STORAGE NEEDED FOR LD (LOCAL EQUATION NUMBERS)
C....
      N0 = 1 + NST*2*IPR
      N1 = N0 + NEN*NDM*IPR
      N2 = N1 + NEN*IPR
      N3 = N2 + NST
C....
C.... N4-N3=STORAGE NEEDED FOR P  (ELEMENT LOAD VECTOR)
C.... N5-N4=STORAGE NEEDED FOR S (ELEMENT STIFFNESS MATRIX)
C.... N6-N5=STORAGE NEEDED FOR IE.  N7-N6=STORAGE NEEDED FOR  D.
      N4 = N3 + NST*IPR
      N5 = N4 + NST*NST*IPR
      N6 = N5 + NUMMAT
      N7 = N6 + 50*NUMMAT*IPR
C....
C.... N8-N7=STORAGE NEEDED FOR ID.  N9-N8=STORAGE NEEDED FOR  X.
C.... N10-N9=STORAGE NEEDED FOR IX. N11-N10=STORAGE NEEDED FOR  F.
C.... N12-N11=STORAGE NEEDED FOR  T. N13-N12=INITIAL ESTIMATE OF
C.... THE NUMBER OF EQUATIONS (NEQ) - STORAGE NEEDED FOR JDIAG.
      N8 = N7 + NDF*NUMNP
      N9 = N8 + NDM*NUMNP*IPR
      N10 = N9 + NEN1*NUMEL
      N11 = N10 + NDF*NUMNP*IPR
      N12 = N11 + NUMNP*IPR
      N13 = N12 + NDF*NUMNP
C....
C.... CHECK THAT SUFFICIENT MEMORY EXISTS
      CALL SETMEM(N13)
C.... ZERO M.
      CALL PZERO(M,N12)
C.... SET FLAG III=0 TO ZERO ID,F,T IN PMESH. ? ISN'T THIS REDUNDANT?
      III = 0
C.... CALL MESH INPUT SUBROUTINE TO READ AND PRINT ALL MESH DATA
      CALL PMESH(M(N2),M(N5),M(N6),M(N7),M(N8),M(N9),M(N10),M(N11),NDF,
     1    NDM,NEN1,III)
C....
C...  ESTABLISH PROFILE OF RESULTING EQUATIONS FOR STIFFNESS,MASS,ECT.
C.... PROFILE COMPUTES THE NUMBER OF EQUATIONS NEEDED TO SOLVE
C.... THE PROBLEM, NEQ.
      CALL PROFIL(M(N12),M(N7),M(N9),NDF,NEN1,NAD)
C.... NOTE THAT NAD NOW HAS THE VALUE JDIAG(NEQ) WHICH IS THE STORAGE
C.... NEEDED FOR THE STRUCTURE MATRIX K IN COLUMN FORM.
C....
C.... N13-N12=STORAGE NEEDED FOR JDIAG
C.... N14-N13=STORAGE NEEDED IN B  (GLOBAL DISPLACEMENTS)
C.... NE-N14=STORGE NEEDED IN DR (GLOBAL FORCES AND ITERATIVE DISP'S)
C.... ARRAY M(NE) WILL STORE MACRO CONTROLS IN ARRAY CT
      N13 = N12 + NEQ
      N14 = N13 + NEQ*IPR
      NE  = N14 + NUMNP*NDF*IPR
C....
C.... CHECK THAT SUFFICIENT MEMORY EXISTS AND ZERO B
      CALL SETMEM(NE)
      CALL PZERO(M(N13),NEQ*IPR)
      GO TO 1
C.... CALL MACRO SOLUTION MODULE FOR ESTABLISHING SOLUTION ALGOTIHM
200   CALL PMACR(M,M(N0),M(N1),M(N2),M(N3),M(N4),M(N5),M(N6),M(N7),
     1M(N8),M(N9),M(N10),M(N11),M(N12),M(N13),M(N14),M(NE),NDF,NDM,
     2NEN1,NST,NE)
      GO TO 1
C.... INPUT/OUTPUT FORMATS
```

```
1000  FORMAT(20A4)
1001  FORMAT(1615)
2000  FORMAT(1H1,20A4//5X,30HNUMBER OF NODAL POINTS       =,I6/5X,30HNUM
     1BER OF ELEMENTS          =,I6/5X,30HNUMBER OF MATERIAL SETS
     2=,I6/5X,30HDIMENSION OF COORDINATE SPACE=,I6/5X,30HDEGREE OF FREED
     3OMS/NODE      =,I6/5X,30HNODES PER ELEMENT (MAXIMUM)  =,I6/5X,30HE
     4XTRA D.O.F. TO ELEMENT      =,I6)
      END
C*********************************************************************
C                                                                     *
C                              PMACR                                  *
C                                                                     *
C*********************************************************************
      SUBROUTINE PMACR (UL,XL,TL,LD,P,S,IE,D,ID,X,IX,F,T,JDIAG,B,DR,CT
     1,NDF,NDM,NEN1,NST,NEND)
C
C.... MACRO INSTRUCTION SUBPROGRAM
C
C.... CONTROLS PROBLEM SOLUTION AND OUTPUT ALGORITHMS BY
C.... ORDER OF SPECIFYING MACRO COMMANDS IN ARRAY WD.
C
      IMPLICIT DOUBLE PRECISION (A-H,O-Z)
      LOGICAL AFR,BFR,CFR,AFL,BFL,CFL,DFL,EFL,FFL,GFL,PCOMP,ZDL
      COMMON M(30000)
      COMMON /CDATA/ O,HEAD(20),NUMNP,NUMEL,NUMMAT,NEN,NEQ,IPR
      COMMON /LABEL/ PDIS(6),Z(6),BC(2),DI(6),CD(3),TE(3),FD(3)
      COMMON /PRLOD/PROP
      COMMON/TDATA/ TIME,DT,C1,C2,C3,C4,C5
      COMMON /ZEROB/ N13
      DIMENSION WD(23),CT(4,*),CTL(4),LVS(9),LVE(9),JDIAG(*),
     1   UL(*),XL(*),TL(*),LD(*),P(*),S(*),IE(*),D(*),ID(*),X(*),
     2   IX(*),F(*),T(*),B(*),DR(*)
      DATA WD/4HTOL  ,4HDT   ,4HSTRE,4HDISP,4HTANG,4HFORM,4HLOOP,4HNEXT,
     1         4HPROP,4HDATA,4HTIME,4HCONV,4HSOLV,4HLMAS,4HCMAS,4HMESH,
     2         4HEIGE,4HEXCD,4HUTAN,4HREAC,4HCHEC,4HLNZD,4HOTMH/
      DATA NWD/23/,ENDM/4HEND /,NV,NC/1,1/
C.... SET INITIAL VALUES OF PARAMETERS
      DT = 0.0
      PROP = 1.0
      NPLD = 0
      RNMAX = 0.0
      TIME = 0.0
      TOL = 1.0D-09
      UN = 0.0
C.... INITIALIZE LOGICAL VARIABLES
      AFL = .TRUE.
      AFR = .FALSE.
      BFL = .TRUE.
      BFR = .FALSE.
      CFL = .TRUE.
      CFR = .FALSE.
      DFL = .TRUE.
      EFL = .TRUE.
      FFL = .FALSE.
      GFL = .TRUE.
      ZDL = .FALSE.
C.... SET NE = STORAGE REQUIRED TO THIS POINT AND
C.... NNEQ = TOTAL DOF WHEN DELETED ONES ARE INCLUDED.
      NE = NEND
      NNEQ = NDF*NUMNP
C....
      WRITE(6,2001) O,HEAD
C.... READ MACRO CARDS
      LL = 1
      LMAX = 16
C.... CHECK STORAGE REQUIREMENTS FOR CT - 1ST APPROXIMATION.
```

```
      CALL SETMEM(NE+LMAX*4*IPR)
C.... INITIALIZE - CT(1,1) = 'LOOP' , CT(3,1) = 1.0
      CT(1,1) = WD(7)
      CT(3,1) = 1.0
C....
100   LL = LL + 1
      IF(LL.LT.LMAX) GO TO 110
         LMAX = LMAX + 16
         CALL SETMEM(NE+LMAX*4*IPR)
C.... READ MACRO INSTRUCTION AND STORE IN CT(1,LL). NOTE
C.... THAT LL = 2 FOR FIRST ONE.
110   READ(5,1000)  (CT(J,LL),J=1,4)
      WRITE(6,2000) (CT(J,LL),J=1,4)
      IF(.NOT.PCOMP(CT(1,LL),ENDM)) GO TO 100
C.... CHANGE LAST MACRO STATEMENT 'END ' TO 'NEXT'
C.... UPDATE NE TO INCLUDE STORAGE NEEDED FOR CT.
      CT(1,LL) = WD(8)
      NE = NE + LL*4*IPR
C....
C.... SET LOOP MARKERS
C.... LX = NUMBER OF MACRO COMMANDS SPECIFIED
      LX = LL - 1
         DO 230 L = 1,LX
C....    CHECK FOR 'LOOP' STATEMENTS. NOTE THAT
C....    CT(1,1) = 'LOOP' AND CT(LL,1) = 'NEXT'.
C....    IF CT(1,L) = 'LOOP' PROCEED
         IF(.NOT.PCOMP(CT(1,L),WD(7))) GO TO 230
C....
         J = 1
         K = L + 1
C....       FIND CONCLUSION OF CURRENT 'LOOP', I.E. WHEN J = 0.
C....       I WILL DROP OUT TO LABEL THIS 'NEXT' STATEMENT
C....       THIS IS THE MOTIVATION FOR CHANGING 'END ' TO 'NEXT'.
C....       ALSO, CHECK TO SEE IF LOOPS ARE NESTED DEEPER THAN
C....       EIGHT TIMES OR IF AN UNEQUAL NUMBER OF LOOP/NEST
C....       STATEMENTS ARE PRESENT INSIDE THE LOOPS.
            DO 210 I = K,LL
            IF(PCOMP(CT(1,I),WD(7))) J = J + 1
            IF(J.GT.9) GO TO 401
            IF(PCOMP(CT(1,I),WD(8))) J = J - 1
210         IF(J.EQ.0) GO TO 220
            GO TO 400
C**** ************
C....          STORE POSITION OF 'LOOP' IN 'NEXT' STATEMENT
C....          STORE POSITION OF 'NEXT' IN 'LOOP' STATEMENT
220            CT(4,I) = L
               CT(4,L) = I
C**** ************
230      CONTINUE
C.... CHECK LOOP/NEXT BALENCE FOR ENTIRE PROGRAM
      J = 0
      DO 240 L = 1,LL
      IF(PCOMP(CT(1,L),WD(7))) J = J + 1
240   IF(PCOMP(CT(1,L),WD(8))) J = J - 1
      IF (J.NE.0) GO TO 400
C#### ##################################
C.... EXECUTE MACRO INSTRUCTION PROGRAM
C#### ##################################
C.... INITIALIZE L AND LV. L IS A COUNTER FOR THE MACRO CONTROL
C.... STATEMENTS WHILE LV DETERMINES THE 'NESTEDNESS' OF
C.... EACH LOOP-NEXT DO LOOP.
      LV = 0
      L = 1
C.... CHECK ALL (NWD=23) MACRO INSTRUCTIONS.TO ADD MORE, ADD
C.... TO WD ARRAY IN DATA STATEMENT, INCREASE DIMENSION OF WD,
C.... AND CHANGE NWD IN DATA STATEMENT.ALSO, ADD TO GO TO STATEMENT
```

```
299    DO 300 J = 1,NWD
300    IF(PCOMP(CT(1,L),WD(J))) GO TO 310
       GO TO 330
310    I = L - 1
C.... DO NOT WRITE ADDED 'LOOP' AND 'NEXT' STATEMENTS
       IF(L.NE.1.AND.L.NE.LL)
      1WRITE(6,2010) I,(CT(K,L),K = 1,4)
C.... FIND APPROPRIATE MACRO CONTROL CODE
C**** ************************************************************
       GO TO (1,2,3,4,5,6,7,8,9,10,11,12,13,14,15,16,17,18,19,20,
      1         21,22,23),J
C**** ************************************************************
C.... SET SOLUTION TOLERANCE
1      TOL = CT(3,L)
       GO TO 330
C.... SET TIME INCREMENT
2      DT = CT(3,L)
       GO TO 330
C.... PRINT STRESS VALUES
3      LX = LVE(LV)
C      WRITE (6,*) 'PMACR DIAGNOSTIC: JUST AFTER LINE LABEL 3.'
       IF(DMOD(CT(3,LX),DMAX1(CT(3,L),1.0D00)).EQ.0.0D00)
      1 CALL PFORM(UL,XL,TL,LD,P,S,IE,D,ID,X,IX,F,T,JDIAG,DR,DR,DR,
      2    NDF,NDM,NEN1,NST,4,B,M(NV),.FALSE.,.FALSE.,.FALSE.,.FALSE.)
       GO TO 330
C.... PRINT DISPLACEMENTS
4      LX = LVE(LV)
       IF(DMOD(CT(3,LX),DMAX1(CT(3,L),1.0D00)).NE.0.0D00) GO TO 330
       WRITE(6,2003) O,HEAD,TIME,PROP
       CALL PRTDIS(ID,X,B,F,NDM,NDF)
       GO TO 330
C.... FORM TANGENT STIFFNESS
19     IF(CFL) CALL PSETM(NC,NE,JDIAG(NEQ)*IPR,CFL)
       CALL PZERO(M(NC),JDIAG(NEQ)*IPR)
       CFR = .TRUE.
5      IF(J.EQ.5) CFR = .FALSE.
       IF(GFL) CALL PSETM(NA,NE,JDIAG(NEQ)*IPR,GFL)
       IF(NPLD.GT.0) PROP = PROPLD(TIME,0)
       CALL PZERO(M(NA),JDIAG(NEQ)*IPR)
       CALL PFORM(UL,XL,TL,LD,P,S,IE,D,ID,X,IX,F,T,JDIAG,DR,M(NA),M(NC),
      2    NDF,NDM,NEN1,NST,3,B,M(NV),.TRUE.,.FALSE.,CFR,.FALSE.)
       AFR = .TRUE.
       GO TO 330
C.... FORM OUT OF BALANCE FORCE FOR TIME STEP/ITERATION
C.... FIRST PUT SPECIFIED FORCES IN THE APPROPRIATE POSITIONS OF
C.... DR. THEN DETERMINE OUT OF BALANCE INTERNAL FORCES FOR
C.... NON-LINEAR ANALYSIS. THEN CHECK CONVERGENCE.
6      IF(NPLD.GT.0) PROP = PROPLD(TIME,0)
       CALL PLOAD(ID,F,DR,NNEQ,PROP)
       BFR = .TRUE.
       IF(ZDL) GO TO 330
       CALL PFORM(UL,XL,TL,LD,P,S,IE,D,ID,X,IX,F,T,JDIAG,DR,DR,DR,
      2    NDF,NDM,NEN1,NST,6,B,M(NV),.FALSE.,.TRUE.,.FALSE.,.FALSE.)
       RN1 = 0.
       DO 61 N = 1,NEQ
61     RN1 = RN1 + DR(N)**2
       RN1 = DSQRT(RN1)
       RNMAX = DMAX1(RNMAX,RN1)
       WRITE(6,2005) RNMAX,RN1,TOL
       IF(RN1.GE.RNMAX*TOL) GO TO 330
C.... CONVERGENCE HAS BEEN OBTAINED. SET 'NEXT' COUNTER TO THAT
C.... IN 'LOOP'. SET L = END LOOP - 1
       LX = LVE(LV)
       LO = LVS(LV)
       CT(3,LX) = CT(3,LO)
       L = LX - 1
```

```
      GO TO 330
C.... SET LOOP START INDICATORS
C.... ARRAYS LVS(LV) AND LVE(LV) (OF DIMENSION 9) ARE SET EQUAL TO
C.... THE INITIAL (L) AND FINAL (LX=CT(4,L)) MACRO STATEMENT POSITIONS
C.... FOR THE CURRENT LOOP WHICH IS NESTED LV + 1 TIMES.
7     LV = LV + 1
      LX = CT(4,L)
      LVS(LV) = L
      LVE(LV) = LX
C.... INITIALIZE 'NEXT'  COUNTER .
      CT(3,LX) = 1.
      GO TO 330
C....
C.... LOOP TERMINATOR CONTROL
C.... THIS ROUTINE DETERMINES WHETHER THE CURRENT LOOP HAS
C.... BEEN COMPLETED (SET LV = LV - 1) OR WHETHER TO RETURN TO THE
C.... THE APPROPRIATE 'LOOP' STATEMENT (SET L = N = CT(4,L)).
8     N = CT(4,L)
C.... INCREMENT 'NEXT' COUNTER
      CT(3,L) = CT(3,L) + 1.0
C**** COMPARE 'NEXT' COUNTER CT(3,L) WITH THE NUMBER OF LOOPS SPECIFIED IN
C**** THE 'LOOP' STATEMENT CT(3,N). NOTE IF NOTHING IS SPECIFIED FOR
C**** CT(3,N), THE LOOP IS EXECUTED ONCE.
      IF(CT(3,L).GT.CT(3,N)) LV = LV - 1
      IF(CT(3,L).LE.CT(3,N)) L = N
C****
      GO TO 330
C....
C.... INPUT PROPORTIONAL LOAD TABLE
9     NPLD = CT(3,L)
      PROP = PROPLD(0.,NPLD)
      GO TO 330
C.... READ COMMAND
10    READ(5,1000) (CTL(I),I=1,4)
      IF(.NOT.PCOMP(CT(2,L),CTL(1))) GO TO 402
      IF(PCOMP(CTL(1),WD(1))) TOL = CTL(3)
      IF(PCOMP(CTL(1),WD(2))) DT=CTL(3)
      GO TO 330
C.... INCREMENT TIME
11    TIME = TIME + DT
      RNMAX = 0.0
      UN = 0.0
      GO TO 330
C.... COMPUTE CONVERGENCE TEST
12    RN2 = 0.0
      DO 121 N = 1,NEQ
      UN = UN + B(N)**2
121   RN2 = RN2 + DR(N)**2
      UN = DMAX1(UN,RN2)
      CN = DSQRT(UN)
      RN2 = DSQRT(RN2)
      WRITE(6,2002) CN,RN2,TOL
      LX = LVE(LV)
      LO = LVS(LV)
      IF(RN2.LT.CN*TOL) CT(3,LX) = CT(3,LO)
      GO TO 330
C.... SOLVE THE EQUATIONS
13    IF(CFR) GO TO 131
      CALL ACTCOL(M(NA),DR,JDIAG,NEQ,AFR,BFR)
      GO TO 132
131   CALL UACTCL(M(NA),M(NC),DR,JDAIG,NEQ,AFR,BFR)
132   AFR = .FALSE.
      IF(.NOT.BFR) GO TO 330
      BFR = .FALSE.
      DO 133 N = 1,NEQ
133   B(N) = B(N) + DR(N)
```

```
      GO TO 330
C.... FORM A LUMPED MASS APPROXIMATION
14    AFL = .FALSE.
      BFL = .TRUE.
      IF(EFL) CALL PSETM(NN,NE,NEQ*IPR,EFL)
      CALL PZERO(M(NN),NEQ*IPR)
      GO TO 140
C.... FORM A CONSISTENT MASS APPROXIMATION
15    AFL = .TRUE.
      BFL = .FALSE.
      IF(DFL) CALL PSETM(NM,NE,JDIAG(NEQ)*IPR,DFL)
      CALL PZERO (M(NM),JDIAG(NEQ)*IPR)
140   CALL PFORM(UL,XL,TL,LD,P,S,IE,D,ID,X,IX,F,T,JDIAG,M(NN),M(NM),
     1   M(NM),NDF,NDM,NEN1,NST,5,B,M(NV),AFL,BFL,.FALSE.,.FALSE.)
      GO TO 330
C.... INPUT MESH CHANGES CAN BE MADE EXCEPT FOR
C.... BOUNDARY RESTRAINTS (I IS SET TO 1 IN PMESH)
C.... SINCE PROFIL IS NOT CALLED.
C.... I IS SET TO -1 SO ID,F,T ARE NOT RE-ZEROED IN PMESH.
C.... NOTE B IS RE-ZEROED !!!
16    I = -1
      CALL PMESH(LD,IE,D,ID,X,IX,F,T,NDF,NDM,NEN1,I)
      IF(I.GT.0) GO TO 404
      CALL PZERO(M(N13),NEQ*IPR)
      GO TO 330
17    J = NM
      IF(DFL) J = NN
      CALL PEIGS(M(NA),M(J),F,X,B,DR,ID,IX,JDAIG,NDF,NDM,NEN1,DFL)
      GO TO 330
C.... MACRO *EXCD* EXPLICIT INTEGRATION OF EQUATIONS OF MOTION
C.... FIRST CALL SETS MEMORY ONLY.
18    IF(FFL) GO TO 181
      NQ = NE
      NV = NQ + NEQ*IPR
      NR = NV + NDF*NUMNP*IPR
      NE = NR + NEQ*IPR
      CALL SETMEM(NE+1)
      CALL PZERO(M(NQ),NE-NQ)
      FFL = .TRUE.
      GO TO 330
181   IF(.NOT.BFR.OR.EFL) GO TO 403
      CALL EUPDAT(DR,B,M(NQ),M(NR),M(NN),DT,NEQ)
      GO TO 330
C.... COMPUTE REACTIONS AND PRINT
20    CALL PZERO(DR,NNEQ*IPR)
      CALL PFORM(UL,XL,TL,LD,P,S,IE,D,ID,X,IX,F,T,JDAIG,DR,DR,DR,
     1   NDF,NDM,NEN1,NST,6,B,M(NV),.FALSE.,.TRUE.,.FALSE.,.TRUE.)
      CALL PRTREA(DR,NDF)
      GO TO 330
21    CALL PFORM(UL,XL,TL,LD,P,S,IE,D,ID,X,IX,F,T,JDAIG,DR,DR,DR,
     1   NDF,NDM,NEN1,NST,2,B,F,.FALSE.,.FALSE.,.FALSE.,.FALSE.)
      GO TO 330
C.... SET ZDL = .TRUE. FOR LINEAR PROBLEMS WITH NO SPECIFIED
C.... NON-ZERO DISPLACEMENTS.
22    ZDL = .TRUE.
      GO TO 330
23    CALL OUTMSH(X,IX,NDM,NEN1)
C.... INCREMENT THE COUNTER L AND CHECK FOR COMPLETION.
330   L = L + 1
      IF(L.GT.LL) RETURN
      GO TO 299
C....
400   WRITE(6,4000)
      RETURN
401   WRITE(6,4001)
      RETURN
402   WRITE(6,4002)
```

```
      RETURN
403   WRITE(6,4003)
      RETURN
404   WRITE(6,4004)
      RETURN
1000  FORMAT(A4,1X,A4,1X,2F5.0)
2000  FORMAT(10X,A4,1X,A4,1X,2G15.5)
2001  FORMAT(A1,20A4//5X,18HMACRO INSTRUCTIONS//5X,15HMACRO STATEMENT,5X
     1,10HVARIABLE 1,5X,10HVARIABLE 2)
2002  FORMAT(5X,29HDISPLACEMENT CONVERGENCE TEST/10X,7HUNMAX =,G15.5,5X,
     1   7HUN    =,G15.5,5X,7HTOL   =,G15.5)
2003  FORMAT(A1,20A4,10X,4HTIME,G13.5//5X,17HPROPORTIONAL LOAD,G13.5)
2004  FORMAT(5X,4HCN =,G12.5,5X,4HDN =,G12.5,5X,4HUN =,G12.5,5X,4HAG =
     1   ,G12.5,5X,4HAC =,G12.5)
2005  FORMAT(5X,22HFORCE CONVERGENCE TEST/10X,7HRNMAX =,G15.5,5X,
     1   7HRN    =,G15.5,5X,7HTOL   =,G15.5)
2010  FORMAT(2X,19H**MACRO INSTRUCTION,I4,13H EXECUTED**  ,2(A4,2X), 6H
     1V1 = ,G13.4, 8H , V2 = ,G13.4)
4000  FORMAT(5X,46H**FATAL ERROR 10** UNBALANCED LOOP/NEXT MACROS )
4001  FORMAT(5X,45H**FATAL ERROR 11** LOOPS NESTED DEEPER THAN 8)
4002  FORMAT(5X,57H**FATAL ERROR 12** MACRO LABEL MISMATCH ON A READ COM
     1MAND)
4003  FORMAT(5X,63H**FATAL ERROR 13** MACRO EXCD MUST BE PRECEDED BY LMA
     1S AND FORM)
4004  FORMAT(5X,84H**FATAL ERROR 14** ATTEMPT TO CHANGE BOUNDARY RESTRAI
     1NT CODES DURING MACRO EXECUTION )
      END
C*********************************************************************
C                                                                    *
C                            PMESH                                   *
C                                                                    *
C*********************************************************************
      SUBROUTINE PMESH(IDL,IE,D,ID,X,IX,F,T,NDF,NDM,NEN1,III)
C
C.... DATA INPUT SUBROUTINE
C
      IMPLICIT DOUBLE PRECISION (A-H,O-Z)
      LOGICAL PRT,ERR,PCOMP
      COMMON /CDATA/ O,HEAD(20),NUMNP,NUMEL,NUMMAT,NEN,NEQ,IPR
      COMMON/ELDATA/ DM,N,MA,MCT,IEL,NEL
      COMMON /LABEL/ PDIS(6),A(6),BC(2),DI(6),CD(3),TE(3),FD(3)
      COMMON /WRITE/ PRT
*     CHARACTER*4 WD(10), VA(2), BL, X(NDM,*)
      DIMENSION IE(*),D(50,*),ID(NDF,*),IX(NEN1,*),XHED(17)
     1  ,F(NDF,*),T(*),IDL(*), X(NDM,*), VA(2), WD(10)
      DATA WD/4HCOOR,4HELEM,4HMATE,4HBOUN,4HFORC,4HTEMP,4HEND ,4HPRIN,
     1  4HNOPR,4HPAGE/,BL/4HBLAN/,VA/4H VAL,2HUE/,LIST/10/
      ERR = .FALSE.
C.... WHEN PMESH IS CALLED FROM PMACR, III = -1 . THUS,
C.... ID,F,AND T ARE NOT RE-ZEROED.
      IF (III.LT.0) GO TO 10
C....    INITIALIZE ARRAYS
         DO 101 N = 1,NUMNP
         DO 100 I = 1,NDF
         ID(I,N) = 0
100      F(I,N) = 0.0
101      T(N) = 0.0
10    READ(5,1000) CC
      DO 20 I = 1,LIST
20    IF(PCOMP(CC,WD(I))) GO TO 30
      GO TO 10
30    GO TO (1,2,3,4,5,6,7,8,9,11),I
C.... NODAL COORDATE DATA INPUT
1     DO 102 N = 1,NUMNP
102   X(1,N) = BL
      CALL GENVEC (NDM,X,CD,PRT,ERR)
```

```
      GO TO 10
C.... ELEMENT DATA INPUT
2     CALL ELNODE(IX,NEN1,PRT,ERR,IDL)
      GO TO 10
C.... MATERIAL PROPERTY INPUT.
3     IF(PRT)  WRITE(6,2004)  O,HEAD
      DO 300  N=1,NUMMAT
      READ  (5,1002)  MA,IEL,XHED
      IF (PRT)  WRITE (6,2003)  MA,IEL,XHED
      IE(MA) = IEL
C.... BY SETTING NST TO 1, S AND P ARE TAKEN AS SCALARS IN THE
C.... CALL TO ELMLIB, ALSO, MAPPING DUM TO U FORCES U TO BE
C.... TREATED AS A SCALAR. IN THIS WAY, U,S,P NEED NOT BE DIMENSIONED
C.... IN THIS SUBROUTINE
      CALL  ELMLIB(D(1,MA),DUM,X,IX,T,S,P,NDF,NDM,1,1)
300   CONTINUE
      GO TO 10
C.... READ IN RESTRAINT CONDITIONS FOR EACH NODE.
4     CALL RESTRT(ID,BC,NDF,PRT,III,IDL)
      GO TO 10
C.... FORCE/DISPL DATA INPUT
5     CALL GENVEC(NDF,F,FD,PRT,ERR)
      GO TO 10
C.... TEMPERATURE DATA INPUT
6     CALL GENVEC(1,T,TE,PRT,ERR)
      GO TO 10
7     IF(ERR) STOP
      RETURN
8     PRT = .TRUE.
      GO TO 10
9     PRT = .FALSE.
      GO TO 10
11    READ(5,1001) O
      GO TO 10
1000  FORMAT(A4)
1001  FORMAT(79X,A1)
1002  FORMAT (I5,4X,I1,17A4)
2003  FORMAT(//5X,12HMATERIAL SET,I3,17H FOR ELEMENT TYPE,I2,5X,17A4)
2004  FORMAT  (A1,20A4////5X,19HMATERIAL PROPERTIES,/)
      END
C*******************************************************************************
C                                                                              *
C                          BLOCK DATA                                          *
C                                                                              *
C*******************************************************************************
      BLOCK DATA
      IMPLICIT DOUBLE PRECISION (A-H,O-Z)
      LOGICAL PRT
      COMMON /CDATA/ O,HEAD(20),NUMNP,NUMEL,NUMMAT,NEN,NEQ,IPR
      COMMON /LABEL/ PDIS(6),A(6),BC(2),DI(6),CD(3),TE(3),FD(3)
      COMMON /WRITE/ PRT
      DATA A/2H,1,2H,2,2H,3,2H,4,2H,5,2H,6/,CD/4H COO,4HRDIN,4HATES/
      DATA TE/4H TEM,4HPERA,4HTURE/,FD/4H FOR,4HCE/D,4HISPL/
      DATA PDIS/4H(I10,2H, ,4HF13.,4H4,  ,4H6E13,4H.4) /
      DATA BC/4H B.C,2H. /,DI/4H DIS,2HPL,4H VEL,2HDC,4H ACC,2HEL/
      DATA O/1HO/,IPR/2/
      DATA PRT/.TRUE./
      END
C*******************************************************************************
C                                                                              *
C                            SETMEM                                            *
C                                                                              *
C*******************************************************************************
      SUBROUTINE SETMEM(J)
C
C.... MONITOR AVAILBLE MEMORY IN BLANK COMMON
C
```

```
      COMMON M(30000)
      COMMON/PSIZE/ MAX
      K = J
      IF(K.LE.MAX) RETURN
      WRITE(6,1000)  K,MAX
      STOP
1000  FORMAT(5X,49H**ERROR 01** INSUFFICIENT STORAGE IN BLANK COMMON/
     1   17X,11HREQUIRED  =,I8/17X,11HAVAILABLE =,I8/)
      END
C*********************************************************************
C                                                                     *
C                        FUNCTION PCOMP                               *
C                                                                     *
*********************************************************************
      LOGICAL FUNCTION PCOMP(A,B)
      IMPLICIT DOUBLE PRECISION (A-H,O-Z)
C...  IT MAY BE NECESSARY TO REPLACE THE FOLLOWING ALPHANUMERIC
C...  COMPARISON STATEMENT IF COMPUTER PRODUCES AN OVERFLOW
      PCOMP =.FALSE.
      IF (A.EQ.B) PCOMP = .TRUE.
      RETURN
      END
C*********************************************************************
C                                                                     *
C                             TRANSF                                  *
C                                                                     *
*********************************************************************
      SUBROUTINE TRANSF(BETA,T,ITYPE)
      IMPLICIT DOUBLE PRECISION (A-H,O-Z)
      DIMENSION T(3,3)
      DATA PI/3.14159265358979238D00/
C.... THIS SUBROUTINE CONSTRUCTS THE PLANE TRANSFORMATION MATRIX FOR
C.... AN ANGLE OF BETA DEGREES. WHEN ITYPE = 0, T-EPS IS FORMED.
C.... WHEN ITYPE = 1,T-SIG IS FORMED (SEE CONCEPTS AND APPLICATIONS
C.... OF FINITE ELEMENT ANALYSIS , R. D. COOK,1974, PG.212)
      BETA = BETA*PI/180.
      T(1,1) = DCOS(BETA)**2
      T(1,2) = DSIN(BETA)**2
      T(2,1) = T(1,2)
      T(2,2) = T(1,1)
      T(3,3) = T(1,1) - T(1,2)
      IF (ITYPE.EQ.0)  THEN
         DUM12 = 1.0D00
         DUM21 = 2.0D00
      ELSE
         DUM12 = 2.0D00
         DUM21 = 1.0D00
      END IF
      T(1,3) = DUM12*DCOS(BETA)*DSIN(BETA)
      T(2,3) = -T(1,3)
      T(3,2) = DUM21*DCOS(BETA)*DSIN(BETA)
      T(3,1) = -T(3,2)
      RETURN
      END
C*********************************************************************
C                                                                     *
C                             BTREB                                   *
C                                                                     *
C*********************************************************************
      SUBROUTINE BTREB (B,IBCOLS,E11,E12,E22,E33,PROD)
      IMPLICIT DOUBLE PRECISION (A-H,O-Z)
      DIMENSION  B(3,3),PROD(3,3)
C.... THIS SUBROUTINE COMPUTES THE MATRIX MULTIPLICATION BT*E*B = PROD
C.... E IS A 3 BY 3 SYMMETRIC MATRIX WITH NON ZERO COMPONENTS E(1,1),
C.... E(1,2),E(2,1),E(2,2),E(3,3).   B IS A 3 BY 3 MATRIX.
C.... PROD IS A SYMMETRIC MATRIX. ONLY THE UPPER HALF IS COMPUTED.
      DO 1 I=1,3
```

```
      B1I = B(1,I)
      B2I = B(2,I)
      DUM1 = E11*B1I + E12*B2I
      DUM2 = E12*B1I + E22*B2I
      DUM3 = E33*B(3,I)
      DO 1 J=I,3
1     PROD(I,J) = B(1,J)*DUM1 + B(2,J)*DUM2 + B(3,J)*DUM3
      RETURN
      END
C*********************************************************************
C                                                                    *
C                            PROFIL                                  *
C                                                                    *
C*********************************************************************
      SUBROUTINE PROFIL (JDIAG,ID,IX,NDF,NEN1,NAD)
C....
C.... THIS ROUTINE DETERMINES THE PROFILE OF THE GLOBAL STIFFNESS
C.... MATRIX, K. THE COLUMNS OF THIS MATRIX ARE STORED IN A ONE DIMEN-
C.... -SIONAL ARRAY WITH THE CORRESPONDING LOCATION OF THE DIAGONAL TERM
C.... FOR COLUMN III STORED IN JDIAG(III). THE NUMBER OF EQUATIONS, NEQ,
C.... AND TOTAL STORAGE NEEDED FOR THE COLUMNS OF K, JDIAG(NEQ) (=NAD)
C.... ARE DETERMINED.
C???? THE METHODOLOGY NECESSARY WHEN A NON-ZERO DISPLACEMENT
C???? IS SPECIFIED OR WHEN TWO DOF ARE REQUIRED TO BE EQUAL IS NOT CLEAR.
C
      IMPLICIT DOUBLE PRECISION (A-H,O-Z)
      COMMON /CDATA/ O,HEAD(20),NUMNP,NUMEL,NUMMAT,NEN,NEQ,IPR
      DIMENSION JDIAG(*),ID(NDF,*),IX(NEN1,*)
C.... DETERMINE THE EQUATION NUMBERS
      NEQ = 0
      DO 50 N = 1,NUMNP
         DO 40 I = 1,NDF
C....    ID.NE.0 WHEN THE NODAL DISPLACEMENT COMPONENT I IS FIXED.
C....    THE ASSOCIATED EQUATION IS ELIMINATED.
         J = ID(I,N)
         IF(J) 30,20,30
20             NEQ = NEQ + 1
C....          SET ID EQUAL TO THE EQUATION NUMBER FOR UNRESTRAINED DOF.
               ID(I,N) = NEQ
C....          INITIALIZE THE ARRAY JDIAG
               JDIAG(NEQ) = 0
               GO TO 40
C....             SET ID EQUAL TO 0 FOR FIXED DOF.
30             ID(I,N) = 0
40       CONTINUE
50    CONTINUE
C.... COMPUTE COLUMN HEIGHTS
C**** LOOP OVER THE ELEMENTS.
      DO 500 N = 1,NUMEL
C******** LOOP OVER THE NODES IN EACH ELEMENT.
         DO 400 I = 1,NEN
C....    IX(I,N) = 0 WHEN NODE I DOES NOT EXIST IN ELEMENT N.
         II = IX(I,N)
         IF(II.EQ.0) GO TO 400
C********** NODE II EXISTS IN ELEMENT N. LOOP OVER THE DOF FOR NODE II.
            DO 300 K = 1,NDF
            KK = ID(K,II)
C....       KK = EQUATION NUMBER.
            IF(KK.EQ.0) GO TO 300
C************** DOF K OF NODE II IS NOT FIXED AND IT IS ASSOCIATED WITH
C************** EQUATON NUMBER KK. LOOP OVER THE REMAINING NODES IN
C************** ELEMENT N STARTING WITH I. IN THIS WAY, PREVIOUSLY MADE
C************** COMPARISIONS ARE NOT REPEATED.
               DO 200 J = I,NEN
               JJ = IX(J,N)
```

```
                IF(JJ.EQ.0) GO TO 200
C*************** NODE JJ EXISTS IN ELEMENT N. LOOP OVER THE DOF FOR
C*************** NODE JJ.
                DO 100 L = 1,NDF
                LL = ID(L,JJ)
                IF(LL.EQ.0) GO TO 100
C****************** DOF L OF NODE JJ IS NOT FIXED AND IT IS
C****************** ASSOCIATED WITH EQUATION NUMBER LL.
C###################
C################### CHOOSE THE LARGEST EQUATION NUMBER OF THE TWO,
C################### SINCE LOCATIONS ABOVE, NOT BELOW, THE DIAGONAL
C################### ARE REQUIRED.
                M = MAXO(KK,LL)
C###################
C################### THE COLUMN HEIGHT ABOVE THE DIAGONAL FOR ANY
C################### DOF IS EQUAL TO THE MAXIMUM DIFFERENCE IN EQUATION
C################### NUMBERS OF THAT DOF WITH ALL OTHERS IN THE ELEMENT.
C################### THIS RESULT MUST BE COMPARED WITH RESULTS FROM
C################### OTHER ELEMENTS THE DOF IS CONNECTED TO.
                JDIAG(M) = MAXO(JDIAG(M),IABS(KK-LL))
C###################
100             CONTINUE
200           CONTINUE
300         CONTINUE
400       CONTINUE
500     CONTINUE
C.... COMPUTE DIAGONAL POINTERS FOR PROFILE
      NAD = 1
      JDIAG(1) = 1
      IF (NEQ.EQ.1) RETURN
C.... JDIAG(N) = LOCATION OF DIAGONAL TERMS IN STIFFNESS MATRIX.
      DO 600 N = 2,NEQ
600      JDIAG(N) = JDIAG(N) + JDIAG(N-1) + 1
      NAD = JDIAG(NEQ)
      RETURN
      END
C*****************************************************************************
C                                                                             *
C                              RESTRT                                         *
C                                                                             *
C*****************************************************************************
      SUBROUTINE RESTRT(ID,BC,NDF,PRT,III,IDL)
C
C.... THIS SUBROUTINE INPUTS NODAL BOUNDRY CONDITIONS.
C
      IMPLICIT DOUBLE PRECISION (A-H,O-Z)
      LOGICAL PRT
      COMMON /CDATA/ O,HEAD(20),NUMNP,NUMEL,NUMMAT,NEN,NEQ,IPR
      DIMENSION BC(2),IDL(NDF),ID(NDF,*)
      IF(PRT) WRITE(6,2000) O,HEAD,(I,BC,I=1,NDF)
C.... SET FLAG III = 1 UPON ENTERING THE SUBROUTINE.
C.... IF PMESH IS CALLED FROM PMACR, THE RESTRAINTS
C.... CAN NOT BE CHANGED. THIS SERVES AS A CHECK IN PMACR.
      III = 1
      N = 0
      NG = 0
402   L = N
      LG = NG
C.... N = NODE NUMBER.  NG = NODE INCREMENT FOR GENERATION.
C.... IDL(I),I=1,NDF  IS NON-ZERO FOR SPECIFIED DISPLACEMENT AND ZERO
C.... OTHERWISE.
      READ(5,1001) N,NG,IDL
C.... CHECK FOR A BLANK CARD TO TERMINATE INPUT AND WRITE B. C.'S
C.... WHEN INPUT IS COMPLETE.
      IF (N.LE.O.OR.N.GT.NUMNP) GO TO 60
      DO 51 I = 1,NDF
```

```
      ID(I,N) = IDL(I)
C.... IF LG.NE.0 (GENERATION WILL OCCUR ) .AND. IF IDL OF PREVIOUSLY
C.... INPUT NODE IDL(I).LT.0 .AND. IF THE CURRENTLY INPUT NODE IDL(I)
C.... .EQ. 0  THEN SET  ID(I,N) = -1
C.... THUS THE RESTRAINT CONDITIONS FOR THE SECOND NODE OF THE
C.... GENERATION PAIR DO NOT HAVE TO BE SPECIFIED.
51    IF(LG.NE.0.AND.IDL(I).EQ.0.AND.ID(I,L).LT.0) ID(I,N) = -1
      LG = ISIGN(LG,N-L)
C.... GENERATE RESTRAINT CONDITIONS.
52    L = L + LG
      IF((N - L)*LG.LE.0) GO TO 402
C.... SINCE ID(I,J) IS INITIALLY ZERO, A POSITIVE VALUE ON THE FIRST
C.... GENERATION CARD WILL RESULT IN ZEROS FOR THE SUBSEQUENTLY
C.... GENERATED NODES.
      DO 53 I = 1,NDF
53    IF(ID(I,L-LG).LT.0) ID(I,L) = -1
      GO TO 52
C....
C.... PRINT THE NON ZERO COMPONENTS IN THE ARRAY ID.
60    DO 58 N = 1,NUMNP
      DO 56 I = 1,NDF
56    IF(ID(I,N).NE.0) GO TO 57
      GO TO 58
57    IF(PRT) WRITE(6,2007) N,(ID(I,N),I=1,NDF)
58    CONTINUE
      RETURN
1001  FORMAT(1615)
2000  FORMAT(A1,20A4//5X,17HNODAL B.C.        //6X,4HNODE,9(I7,A4,A2)/1X)
2007  FORMAT(I10,9I13)
      END
C*******************************************************************************
C                                                                              *
C                              PZERO                                           *
C                                                                              *
C*******************************************************************************
      SUBROUTINE PZERO(PP,NN)
      DIMENSION PP(NN)
C
C.... ZERO REAL ARRAY
C.... PP SHOULD NOT BE DOUBLE PRECISION SINCE THE STORAGE
C.... REQUIREMENTS ARE AUTOMATICALLY DETERMINED BY NN.
C
      DO 100 N = 1,NN
100   PP(N) = 0.0
      RETURN
      END
C*******************************************************************************
C                                                                              *
C                                ELMLIB                                        *
C                                                                              *
C*******************************************************************************
      SUBROUTINE ELMLIB(D,U,X,IX,T,S,P,NDF,NDM,NST,ISW)
C
C.... ELEMENT LIBRARY
C
      IMPLICIT DOUBLE PRECISION (A-H,O-Z)
      COMMON/ELDATA/ DM,N,MA,MCT,IEL,NEL
      DIMENSION  P(NST),S(NST,NST),D(*),U(*),X(*),IX(*),T(*)
      IF (IEL.LT.1.OR.IEL.GT.3)  GO TO 400
      IF(ISW.LT.3) GO TO 30
      DO 20 L = 1,NST
      P(L) = 0.0
      DO 20 M = 1,NST
20    S(L,M) = 0.0
30    GO TO (1,2,2),IEL
1     CALL ELMT01(D,U,X,IX,T,S,P,NDF,NDM,NST,ISW)
```

```
      GO TO 10
2     CALL ELMT02(D,U,X,IX,T,S,P,NDF,NDM,NST,ISW)
10    RETURN
400   WRITE (6,4000)  IEL
      STOP
4000  FORMAT  (5X,40H** FATAL ERROR 04** ELEMENT CLASS NUMBER ,I3,6H INP
     1UT)
      END
C*********************************************************************
C                                                                     *
C                            ADDSTF                                   *
C                                                                     *
C*********************************************************************
      SUBROUTINE ADDSTF(A,B,C,S,P,JDIAG,LD,NST,NEL,AFL,BFL,CFL)
C
C.... ASSEMBLE GLOBAL ARRAYS
C
      IMPLICIT DOUBLE PRECISION (A-H,O-Z)
      LOGICAL AFL,BFL,CFL
      DIMENSION A(*),B(*),JDIAG(*),P(*),S(NST,*),LD(*) ,C(*)
         DO 200 J = 1,NEL
         K = LD(J)
         IF(K.EQ.0) GO TO 200
         IF(BFL) B(K) = B(K) + P(J)
         IF(.NOT.AFL.AND..NOT.CFL) GO TO 200
         L = JDIAG(K) - K
            DO 100 I = 1,NEL
            M =LD(I)
            IF(M.GT.K.OR.M.EQ.0) GO TO 100
            M = L + M
            IF(AFL) A(M) = A(M) + S(I,J)
            IF(CFL) C(M) = C(M) + S(J,I)
100         CONTINUE
200      CONTINUE
      RETURN
      END
C*********************************************************************
C                                                                     *
C                            PSETM                                    *
C                                                                     *
C*********************************************************************
      SUBROUTINE PSETM(NA,NE,NJ,AFL)
C
C.... SET NA = NE AND INCREMENT NE BY NJ. CHECK IF STORAGE IS
C.... AVAILABLE FOR NE LOCATIONS AND SET AFL = .FALSE.  .
C
      IMPLICIT DOUBLE PRECISION (A-H,O-Z)
      LOGICAL AFL
      NA = NE
      NE = NE + NJ
      AFL = .FALSE.
      CALL SETMEM(NE)
      RETURN
      END
C*********************************************************************
C                                                                     *
C                            PLOAD                                    *
C                                                                     *
C*********************************************************************
      SUBROUTINE PLOAD(ID,F,DR,NNEQ,PROP)
C
C.... FORM LOAD VECTOR IN COMPACT FORM
C
      IMPLICIT DOUBLE PRECISION (A-H,O-Z)
      DIMENSION ID(*),F(*),DR(*)
      DO 100 N = 1,NNEQ
```

```
      J = ID(N)
100   IF(J.GT.0) DR(J) = F(N)*PROP
      RETURN
      END
C*********************************************************************
C                                                                     *
C                            PGAUSS                                   *
C                                                                     *
C*********************************************************************
      SUBROUTINE PGAUSS(L,LINT,XI,ETA,WT)
C
C.... GAUSS POINTS AND WEIGHTS FOR TWO DIMENSIONS
C
      IMPLICIT DOUBLE PRECISION (A-H,O-Z)
      DIMENSION LR(9),LZ(9),LW(9),XI(*),ETA(*),WT(*)
      DATA LR/-1,1,1,-1,0,1,0,-1,0/,LZ/-1,-1,1,1,-1,0,1,0,0/
      DATA LW/4*25,4*40,64/
      LINT = L*L
      GO TO (1,2,3),L
C.... 1X1 INTEGRATION
1     XI(1) = 0.
      ETA(1) = 0.
      WT(1) = 4.
      RETURN
C.... 2X2 INTEGRATION
2     G = 1./DSQRT(3.D00)
      DO 21 I =1,4
      XI(I) = G*LR(I)
      ETA(I) = G*LZ(I)
21    WT(I) = 1.
      RETURN
C.... 3X3 INTEGRATION
3     G = DSQRT(0.6D00)
      H = 1./81.
      DO 31 I = 1,9
      XI(I) = G*LR(I)
      ETA(I) = G*LZ(I)
31    WT(I) = H*LW(I)
      RETURN
      END
C*********************************************************************
C                                                                     *
C                            PSTRES                                   *
C                                                                     *
C*********************************************************************
      SUBROUTINE PSTRES(SIG,P1,P2,P3)
C
C.... COMPUTE PRINCIPAL STRESSES (2 DIMENSIONS)
C
      IMPLICIT DOUBLE PRECISION (A-H,O-Z)
      DIMENSION SIG(3)
C.... STRESSES MUST BE STORED IN ARRAY SIG(3) IN THE ORDER
C          TAU-XX,TAU-XY,TAU-YY
      XI1 = (SIG(1) + SIG(3))/2.
      XI2 = (SIG(1) - SIG(3))/2.
      RHO = DSQRT(XI2*XI2 + SIG(2)*SIG(2))
      P1 = XI1 + RHO
      P2 = XI1 - RHO
      P3 = 45.0
      IF(XI2.NE.0.0) P3 = 22.5*ATAN2(SIG(2),XI2)/ATAN(1.0)
      RETURN
      END
C*********************************************************************
C                                                                     *
C                            ELNODE                                   *
C                                                                     *
C*********************************************************************
```

```
      SUBROUTINE ELNODE(IX,NEN1,PRT,ERR,IDL)
C
C.... THIS SUBROUTINE READS THE NODAL CONNECTIONS OF EACH ELEMENT.
C
      IMPLICIT DOUBLE PRECISION (A-H,O-Z)
      LOGICAL PRT,ERR
      COMMON /CDATA/ O,HEAD(20),NUMNP,NUMEL,NUMMAT,NEN,NEQ,IPR
      DIMENSION IDL(NEN1),IX(NEN1,*)
      L = 0
      DO 206 I =1,NUMEL,50
      IF(PRT) WRITE(6,2001) O,HEAD,(K,K=1,NEN)
      J = MINO(NUMEL,I+49)
      DO 206 N =I,J
      IF (L-N) 200,202,203
200   READ(5,1001) L,LK,(IDL(K),K=1,NEN),LX
C.... CHECK FOR A BLANK CARD. THIS ROUTINE WILL GENERATE ELEMENT DATA
C.... FOR THE REMAINDER OF THE ELEMENTS WHEN L = 0.
      IF(L.EQ.0) L = NUMEL + 1
      IF(LX.EQ.0) LX = 1
C.... ELEMENTS MUST BE IN ORDER.  L = ELEMENT NUMBER. LK = ELEMENT
C.... MATERIAL SET NUMBER.  IDL(K) GIVES SEQUENCE OF INTERNAL NODES.
C.... LX = INCREMENT NECESSARY TO GENERATE REMAINING ELEMENTS.
      IF(L-N) 201,202,203
C.... THIS IMPLIES THAT THE ELEMENTS ARE OUT OF ORDER.
201   WRITE(6,3001) L,N
      ERR = .TRUE.
      GO TO 206
202   NX = LX
      DO 207 K = 1,NEN
207   IX(K,L) = IDL(K)
      IX(NEN1,L) = LK
      GO TO 205
C.... THESE STATEMENTS GENERATE THE ELEMENTS WHEN DESIRED.
203   IX(NEN1,N) = IX(NEN1,N-1)
      DO 204 K =1,NEN
      IX(K,N) = IX(K,N-1) + NX
C.... THIS ENSURES IX = 0 FOR ELEMENTS WITH LESS NODES THAN NEN.
204   IF(IX(K,N-1).EQ.0) IX(K,N) = 0
205   IF(PRT) WRITE(6,2002) N,IX(NEN1,N),(IX(K,N),K=1,NEN)
206   CONTINUE
      RETURN
1001  FORMAT(1615)
2001  FORMAT(A1,20A4//5X,8HELEMENTS//3X,7HELEMENT,2X,8HMATERIAL,
     1   14(I3,5H NODE)/(20X,14(I3,5H NODE)))
2002  FORMAT(2I10,14I8/(20X,14I8))
3001  FORMAT(5X,20H**ERROR 03** ELEMENT,I5,22H APPEARS AFTER ELEMENT,I5)
      END
C*********************************************************************
C                                                                    *
C                              GENVEC                                *
C                                                                    *
C*********************************************************************
      SUBROUTINE GENVEC(NDM,X,CD,PRT,ERR)
C
C.... READ NODAL COORDINATES AND GENERATE NODAL COORDINATES ON STRAIGHT
C.... BOUNDARIES WHEN DESIRED
C
      IMPLICIT DOUBLE PRECISION (A-H,O-Z)
      LOGICAL PRT,ERR,PCOMP
      COMMON /CDATA/ O,HEAD(20),NUMNP,NUMEL,NUMMAT,NEN,NEQ,IPR
      DIMENSION X(NDM,*),XL(7),CD(3)
      DATA BL/4HBLAN/
      N = 0
      NG = 0
102   L = N
      LG = NG
```

```
      READ (5,1000) N,NG,XL
C.... CHECK FOR BLANK CARD TO END INPUT STRING
      IF(N.LE.0.OR.N.GT.NUMNP) GO TO 108
      DO 103 I = 1,NDM
103   X(I,N) = XL(I)
C.... TEST FOR INTERPOLATION
      IF(LG) 104,102,104
C.... GIVE THE NODE NUMBER INCREMENT (LG) THE CORRECT SIGN
104   LG = ISIGN(LG,N-L)
C.... COMPUTE NUMBER OF INTERVALS LINE IS BROKEN INTO (LI)
      LI = (IABS(N-L+LG)-1)/IABS(LG)
      ZLI = LI
C.... COMPUTE COORDINATE INCREMENTS ALONG THE LINE
      DO 105 I = 1,NDM
105   XL(I) = (X(I,N)-X(I,L))/ZLI
106   L = L + LG
C.... DETERMINE IF GENERATION IS COMPLETE
      IF((N-L)*LG.LE.0) GO TO 102
      IF(L.LE.0.OR.L.GT.NUMNP) GO TO 110
      DO 107 I = 1,NDM
107   X(I,L) = X(I,L-LG) + XL(I)
      GO TO 106
110   WRITE(6,3000) L,(CD(I),I=1,3)
      ERR = .TRUE.
      GO TO 102
108   DO 109 I = 1,NUMNP,50
      IF(PRT) WRITE(6,2000) O,HEAD,(CD(L),L=1,3),(L,CD(1),CD(2),L=1,NDM)
      N = MINO (NUMNP,I+49)
C.... CHECK IF COORDINATES ARE STORED FOR ALL NODES
      DO 109 J = I,N
      IF(PCOMP(X(1,J),BL)) WRITE(6,2008) J
109   IF(.NOT.PCOMP(X(1,J),BL).AND.PRT) WRITE(6,2009) J,(X(L,J),L=1,NDM)
      RETURN
1000  FORMAT(2I5,7F10.0)
2000  FORMAT(A1,20A4//5X, 5HNODAL,3A4//6X,4HNODE,9(I7,A4,A2))
2008  FORMAT(I10,38H NODE HAS NOT BEEN INPUT OR GENERATED )
2009  FORMAT(I10,9F13.4)
3000  FORMAT(5X,43H**FATAL ERROR 02** ATTEMPT TO GENERATE NODE,I5,3H IN
     1   ,3A4)
      END
C*********************************************************************
C                                                                    *
C                            PRTREA                                  *
C                                                                    *
C*********************************************************************
      SUBROUTINE PRTREA(R,NDF)
C
C.... PRINT NODAL REACTIONS
C
      IMPLICIT DOUBLE PRECISION (A-H,O-Z)
      DIMENSION R(NDF,*),RSUM(6),ASUM(6)
      COMMON /CDATA/ O,HEAD(20),NUMNP,NUMEL,NUMMAT,NEN,NEQ,IPR
      DO 50 K = 1,NDF
      RSUM(K) = 0.
50    ASUM(K) = 0.
      DO 100 N = 1,NUMNP,50
      J = MINO(NUMNP,N+49)
      WRITE(6,2000) O,HEAD,(K,K=1,NDF)
      DO 100 I = N,J
      DO 75 K = 1,NDF
      R(K,I) = -R(K,I)
      RSUM(K) = RSUM(K) + R(K,I)
75    ASUM(K) = ASUM(K) + DABS(R(K,I))
100   WRITE(6,2001) I,(R(K,I),K=1,NDF)
C.... PRINT STATICS CHECK
      WRITE(6,2002) (RSUM(K),K=1,NDF)
      WRITE(6,2003) (ASUM(K),K=1,NDF)
```

```
      RETURN
2000  FORMAT(A1,20A4//5X,15HNODAL REACTIONS//6X,4HNODE,
     1  6(I9,4H DOF))
2001  FORMAT(I10,6E13.4)
2002  FORMAT(/7X,3HSUM,6E13.4)
2003  FORMAT(/3X,7HABS SUM,6E13.4)
      END
C*********************************************************************
C                                                                    *
C                            PROPLD                                  *
C                                                                    *
C*********************************************************************
      FUNCTION PROPLD(T,J)
C
C.... PROPORTIONAL LOAD TABLE (ONE LOAD CARD ONLY)
C
      IMPLICIT DOUBLE PRECISION (A-H,O-Z)
      DIMENSION A(5)
      IF(J.GT.0) GO TO 200
C.... COMPUTE VALUE AT TIME T
      PROPLD = 0.0
      IF(T.LT.TMIN.OR.T.GT.TMAX) RETURN
      L = MAXO(L,1)
      PROPLD = A(1) + A(2)*T + A(3)*(DSIN(A(4)*T+A(5)))**L
      RETURN
C.... INPUT TABLE OF PROPORTIONAL LOADS
200   I = 1
      READ(5,1000)    K,L,TMIN,TMAX,A
      WRITE(6,2000) I,K,L,TMIN,TMAX,A
      RETURN
1000  FORMAT(2I5,7F10.0)
2000  FORMAT(5X,23HPROPORTIONAL LOAD TABLE//24H  NUMBER    TYPE    EXP.,
     1 14H  MINIMUM TIME,15H   MAXIMUM TIME, 5X,2HA1,13X,2HA2,13X,2HA3,
     2   13X,2HA4,13X,2HA5/(3I8,7G15.5))
      END
C*********************************************************************
C                                                                    *
C                              PFORM                                 *
C                                                                    *
C*********************************************************************
      SUBROUTINE PFORM(UL,XL,TL,LD,P,S,IE,D,ID,X,IX,F,T,JDIAG,B,A,C,NDF,
     1   NDM,NEN1,NST,ISW,U,UD,AFL,BFL,CFL,DFL)
C
C.... COMPUTE ELEMENT ARRAYS AND ASSEMBLE GLOBAL ARRAYS
C
      IMPLICIT DOUBLE PRECISION (A-H,O-Z)
      LOGICAL AFL,BFL,CFL,DFL
      COMMON /CDATA/ O,HEAD(20),NUMNP,NUMEL,NUMMAT,NEN,NEQ,IPR
      COMMON /ELDATA/ DM,N,MA,MCT,IEL,NEL
      COMMON/PRLOD/ PROP
      DIMENSION XL(NDM,*),LD(NDF,*),P(*),S(NST,*),IE(*),D(50,*),ID(NDF,*
     1),X(NDM,*),IX(NEN1,*),F(NDF,*),JDIAG(*),B(*),A(*),C(*),UL(NDF,*)
     2   ,TL(*),T(*),U(*),UD(NDF,*)
C.... LOOP ON ELEMENTS
*     WRITE (6,*) 'PFORM DIAGNOSTIC: AT BEGINNING, ISW = ', ISW
      IEL = 0
      DO 110 N = 1,NUMEL
C.... SET UP LOCAL ARRAYS
         DO 108 I = 1,NEN
         II = IX(I,N)
         IF(II.NE.0) GO TO 105
            TL(I) = 0.
            DO 103 J = 1,NDM
103         XL(J,I) = 0.
            DO 104 J = 1,NDF
            UL(J,I) = 0.
```

```
            UL(J,I+NEN) = 0.
104         LD(J,I) = 0
            GO TO 108
105            IID = II*NDF - NDF
               NEL = I
               TL(I) = T(II)
               DO 106 J = 1,NDM
106            XL(J,I) = X(J,II)
               DO 107 J = 1,NDF
               K = IABS(ID(J,II))
               UL(J,I+NEN) = UD(J,II)
               UL(J,I) = F(J,II)*PROP
               IF(K.GT.0) UL(J,I) = U(K)
               IF(DFL) K = IID + J
107            LD(J,I) = K
108      CONTINUE
C.... FORM ELEMENT ARRAY
      MA = IX(NEN1,N)
      IF(IE(MA).NE.IEL) MCT = 0
      IEL = IE(MA)
      CALL ELMLIB(D(1,MA),UL,XL,IX(1,N),TL,S,P,NDF,NDM,NST,ISW)
C.... ADD TO TOTAL ARRAY
      IF(AFL.OR.BFL.OR.CFL) CALL ADDSTF(A,B,C,S,P,JDIAG,LD,NST,NEL*NDF,
     1   AFL,BFL,CFL)
110   CONTINUE
      RETURN
      END
C*********************************************************************
C                                                                    *
C                              ELPROP                                *
C                                                                    *
C*********************************************************************
      SUBROUTINE ELPROP(D)
C...  THIS SUBROUTINE DETERMINES THE ELEMENT PROPERTY MATRIX FOR
C.... ISOTROPIC OR ORTHOTROPIC MATERIALS UNDER PLANE STRESS/STRAIN
C.... LOADING CONDITIONS FROM THE APPRPRIATE MATERIAL CONSTANTS.
C....
C.... DEPENDING ON THE VALUE OF ITYPE, EITHER THE MODULI OF ELASTICITY
C.... (A(I,J)) OR THE COEFFICIENTS OF DEFORMATION (a(I,J)) ARE DETERMINED
C.... WHERE, {SIG} = [A]*{EPS}  AND  {EPS} = [a]*{SIG}
C....
C.... FOR ANISOTROPIC MATERIALS, THE MATRIX COEFFIENTS MUST BE INPUT.
      IMPLICIT DOUBLE PRECISION (A-H,O-Y)
      IMPLICIT COMPLEX*16  (Z)
      LOGICAL PRT
      COMMON /CDATA/ O,HEAD(20),NUMNP,NUMEL,NUMMAT,NEN,NEQ,IPR
      COMMON/ELDATA/ DM,N,MA,MCT,IEL,NEL
      COMMON /ROOTS/ ZS(2),ZB,ZC
      COMMON /CHECKR / ZO(2)
      COMMON /WRITE/ PRT
      DIMENSION  D(*),WD(2),T(3,3),DXY(3,3)
      DATA  WD/4HRESS,4HRAIN/
      READ (5,1000) MATYPE,I,L,K,ANGLE
      READ (5,1001)  D(4),E1,RNU12,E2,G,E3,RNU13,RNU23
C.... DETERMINE WHETHER THE PROBLEM IS PLANE STRESS OR PLANE STRAIN.
      IF (I.NE.0)  I=1
      IF (I.EQ.0)  I=2
C.... DETERMINE WHETHER ELASTIC CONSTANTS OR COEFFICIENTS OF DEFORMATION
C.... ARE TO BE DETERMINED
      IF (IEL.EQ.1)  ITYPE = 0
      IF (IEL.EQ.2.OR.IEL.EQ.3)  ITYPE = 1
C.... STORE CONSTANTS NEEDED FOR CALCULATION OF STIFFNESS MATRIX
      D(1)  = MATYPE
      D(2)  = L
      D(3)  = K
      IF (IEL.EQ.2.OR.IEL.EQ.3)   THEN
         READ  (5,1010) NUMNOD,NODSID,NUMSID,LO,LF,ISYM,NSTRPT,NUMINT,
```

```
     1                                    NUMOUT,IFIX2,IFIX1
         READ  (5,1001) (D(KKK),KKK=16,21)
         IF (PRT.AND.IEL.EQ.2) WRITE(6,2002) WD(I),MATYPE,D(16),D(17),
     1                                       D(20),D(21)
         IF (PRT.AND.IEL.EQ.3) WRITE(6,2003) WD(I),MATYPE,D(16),D(20),
     1                                       D(21)
         IF (PRT) WRITE(6,2005) NUMNOD,NODSID,NUMSID,IFIX2,IFIX1,LO,LF
         IF (PRT.AND.ISYM.EQ.1)  WRITE(6,2006)
         IF (PRT.AND.ISYM.EQ.-1) WRITE(6,2007)
         IF (PRT.AND.ISYM.EQ.2)  WRITE(6,2008)
         IF (PRT) WRITE(6,2013) NSTRPT,D(18),D(19)
         IF (NUMOUT.NE.0) THEN
            ISUM = NUMOUT*4 + 30
            READ  (5,1001) (D(KKK),KKK=31,ISUM)
            IF (PRT) WRITE(6,2014) NUMOUT,(D(KKK),KKK=31,ISUM)
         END IF
         D(11) = NUMNOD
         D(12) = NODSID
         D(13) = NUMSID
         D(14) = LO
         D(15) = LF
         D(23) = ISYM
         D(24) = NUMINT
         D(25) = NSTRPT
         D(26) = IFIX2
         D(27) = IFIX1
         D(30) = NUMOUT
      ELSE
         IF (PRT) WRITE(6,2000) WD(I),MATYPE
      END IF
      GO TO (1,2,2,4),MATYPE
C.... ISOTROPIC MATERIAL
1     IF (ITYPE.EQ.0)  THEN
         D(5) = E1*(1. + (1-I)*RNU12)/(1. + RNU12)/(1. - I*RNU12)
         D(6) = RNU12*D(5)/(1. + (1 - I)*RNU12)
         D(8) = E1/2./(1. + RNU12)
         D(7) = D(5)
      ELSE
         IF (I.EQ.1) THEN
            D(5) = 1.0D00/E1
            D(6) = -RNU12*D(5)
         ELSE
            D(5) = (1.0D00 - RNU12**2)/E1
            D(6) = -(1.0D00 + RNU12)*RNU12/E1
         END IF
         D(7) = D(5)
         D(8) = 2.0D00*(1.0D00 + RNU12)/E1
         IF (IEL.EQ.2.OR.IEL.EQ.3)   THEN
            WRITE (6,2101)
            STOP
         END IF
      END IF
      IF (PRT) WRITE(6,2102)  E1,RNU12
      GO TO 20
C.... ORTHOTROPIC MATERIAL
2     IF (MATYPE.EQ.2.AND.PRT)  WRITE (6,2202)
      IF (MATYPE.EQ.3.AND.PRT)  WRITE (6,2302)  ANGLE
      IF (PRT)  WRITE (6,2203)  E1,E2,RNU12,G
      RNU21 = RNU12*E2/E1
      IF (I.EQ.1)  THEN
C.... PLANE STRESS
         IF (ITYPE.EQ.0)  THEN
            DUM = 1.0 - RNU12*RNU21
            D(5) = E1/DUM
            D(7) = E2/DUM
            D(6) = RNU12*D(7)
            D(8) = G
```

```
         ELSE
            D(5) = 1.0D00/E1
            D(6) = -RNU12*D(5)
            D(7) = 1.0D00/E2
            D(8) = 1.0D00/G
         END IF
      ELSE
C.... PLANE STRAIN
         RNU31 = RNU13*E3/E1
         RNU32 = RNU23*E3/E2
         IF (ITYPE.EQ.0)  THEN
            DUM = 1. - RNU12*RNU21 - RNU13*RNU31 - RNU23*RNU32 -
     1       RNU21*RNU32*RNU13 - RNU12*RNU31*RNU23
            D(5) = E1*(1. - RNU23*RNU32)/DUM
            D(6) = E2*(RNU12 + RNU32*RNU13)/DUM
            D(7) = E2*(1. - RNU13*RNU31)/DUM
            D(8) = G
         ELSE
            D(5) = (1.0D00 - RNU13*RNU31)/E1
            D(7) = (1.0D00 - RNU32*RNU23)/E2
            D(6) = -(RNU12 + RNU32*RNU13)/E1
            D(8) = 1.0D00/G
         END IF
         IF (PRT)  WRITE (6,2204)  E3,RNU13,RNU23
      END IF
20    IF (IEL.EQ.1)  THEN
         IF (PRT) WRITE (6,2001) D(4),L,L,K,K
      ELSE
         IF (PRT) WRITE (6,2009) D(4),NUMINT,L,K
      END IF
      IF (MATYPE.EQ.3) GO TO 3
21    IF (IEL.NE.1)  THEN
         CALL CLPXCT(D,MATYPE,IEL)
         IF (PRT)  WRITE (6,2410)  ZS(1),ZS(2),ZO(1),ZO(2)
      END IF
      RETURN
C.... TRANSFORM PROPERTIES MATRIX TO GLOBAL (X,Y) COORDINATES.
3     CALL TRANSF (ANGLE,T,ITYPE)
      CALL BTREB (T,3,D(5),D(6),D(7),D(8),DXY)
      KK=5
      DO 31 II=1,3
      DO 31 JJ=II,3
      D(KK) = DXY(II,JJ)
      KK = KK + 1
31    CONTINUE
      GO TO 21
C.... ANISOTROPIC MATERIAL
4     IF (PRT)  WRITE (6,2402)  E1,RNU12,E2,G,E3,RNU13
      D(5) = E1
      D(6) = RNU12
      D(7) = E2
      D(8) = G
      D(9) = E3
      D(10) = RNU13
      GO TO 20
1000  FORMAT (4I5,F10.0)
1001  FORMAT (8F10.0)
1010  FORMAT(16I5)
2000  FORMAT(//,5X,8HPLANE ST,A4,23H LINEAR ELASTIC ELEMENT,10X,'MATYPE
     1= ',I2,/)
2001  FORMAT(/20X,7HDENSITY,10X,E18.5,//20X,44HGAUSS PTS IN XI, ETA DIRE
     1CTIONS RESPECTIVELY,/,30X,'(1). FOR STIFFNESS COMPUTATION',5X,I1,
     2  ',',I1,/,30X,'(2). FOR STRESS COMPUTATION',8X,I1,',',I1)
2002  FORMAT (//,5X,8HPLANE ST,A4,' LINEAR HYBRID ELEMENT ',10X,
     1'MATYPE = ',I2,///10X,'ELLIPTICAL MAPPING FUNCTION',//15X,
     2'A    = ',E18.5,/,15X,'B    = ',E18.5,/,15X,'X0   = ',E18.5,
```

```
     3/,15X,'Y0   = ',E18.5)
2003  FORMAT (//,5X,8HPLANE ST,A4,' LINEAR HYBRID ELEMENT ',10X,
     1'MATYPE = ',I2,///10X,'FILLET MAPPING FUNCTION',//15X,
     2'RHO  = ',E18.5,/,15X,'X0   = ',E18.5,/,15X,'Y0   = ',E18.5)
2005  FORMAT (/15X,'NUMBER OF NODES          = ',I2,/15X,'NUMBER OF NODES
     1/ SIDE = ',I2,/15X,'NUMBER OF SIDES          = ',I2,//15X,'U & V ',
     2'FIXED AT NODE ',I2,/15X,'U     FIXED AT NODE ',I2,//15X,
     3'THE LAURENT SERIES EXPANSION IS SUMMED FROM M =',I3,' TO N =',I3,
     4//)
2006  FORMAT (15X,'****** SYMMETRY IMPOSED ABOUT THE X AXIS ******',//)
2007  FORMAT (15X,'****** SYMMETRY IMPOSED ABOUT THE Y AXIS ******',
     1      10X,'M AND N MUST BE ODD ******',//)
2008  FORMAT (15X,'****** SYMMETRY IMPOSED ABOUT THE X AND Y AXES ',
     1      '******',10X,'M AND N MUST BE ODD ******',//)
2013  FORMAT (15X,'STRESSES WILL BE EVALUATED AT ',I3,' POINTS ',
     1    'BETWEEN THETA = ',F6.2,' AND ',F6.2,'  DEGREES'//)
2014  FORMAT (15X,'DISPLACEMENTS,STRAINS, AND STRESSES WILL BE ',
     1    'CALCULATED (AND WRITTEN ON FILE 26) ON ',I2,' LINES',
     2    /,15X,'WITH THE FOLLOWING INITIAL (X(I),Y(I)) AND END ',
     3    '(X(E),Y(E)) POINTS',/,32X,'X(I)',16X,'Y(I)',16X,'X(E)',
     4    16X,'Y(E)',4(/,20X,4E20.4),//)
2009  FORMAT (/20X,7HDENSITY,10X,E18.5,//15X,'NUMBER OF GAUSS INTERVALS
     1/ SIDE = ',I3,/20X,'GAUSS PTS ALONG INTEGRATION',
     2' INTERVAL',/,30X,'(1). FOR STIFFNESS COMPUTATION',5X,I2,
     3   /,30X,'(2). FOR STRESS COMPUTATION',8X,I2)
2101  FORMAT (10X,'***** ERROR --- ISOTROPIC MATERIAL SPECIFIED FOR ',
     1            'ORTHOTROPIC NOTCH ROOT ELEMENT *****')
2102  FORMAT (10X,'ISOTROPIC MATERIAL',//,15X,18HYOUNG'S MODULUS = , 4X,
     1E18.5,/,15X,18HPOISSON'S RATIO = ,10X,F8.5)
2202  FORMAT (10X,'ORTHOTROPIC MATERIAL, PRINCIPAL DIRECTIONS (1,2) COIN
     1CIDE WITH GLOBAL (X,Y) AXES RESPECTIVELY')
2203  FORMAT (1X,//,15X, 7HE1   = ,  E18.5,/,15X,7HE2   = ,  E18.5,/,15X
     1,7HNU12 = , 6X,F8.5,/,15X,7HG12  = ,E18.5)
2204  FORMAT (15X,7HE3   = , E18.5,/,15X,7HNU13 = , 6X,F8.5,/,15X,7HNU23
     1 = ,6X,F8.5)
2302  FORMAT (10X,'ORTHOTROPIC MATERIAL, PRINCIPAL DIRECTION 1 ORIENTED
     1AT A CCW ANGLE OF ',F9.4,' DEGREES FROM THE GLOBAL X AXIS.')
2402  FORMAT  (10X,'ANISOTROPIC MATERIAL',//,15X,'E(1,1) = ',E18.5,/,15X
     1,'E(1,2) = ',E18.5/,15X,'E(1,3) = ',E18.5,/,15X,'E(2,2) = ',E18.5,
     2/,15X,'E(2,3) = ',E18.5,/,15X,'E(3,3) = ',E18.5)
2410  FORMAT  (//,20X,'ROOTS OF CHARACTERISTIC EQUATION',/,30X,
     1   'S(1) = ',2D30.15,/,30X,'S(2) = ',2D30.15,//,20X,
     2    'CHECK OF CHARACTERISTIC EQUATIONS',/,30X,'Z0(1) = ',2D30.15,
     3    /,30X,'Z0(2) = ',2D30.15,/)
      END
C*************************************************************************
C                                                                        *
C                            PRTDIS                                      *
C                                                                        *
C*************************************************************************
      SUBROUTINE PRTDIS(ID,X,B,F,NDM,NDF)
C
C.... OUTPUT NODAL VALUES
C
      IMPLICIT DOUBLE PRECISION (A-H,O-Z)
      LOGICAL PCOMP
      COMMON/PRLOD/ PROP
      COMMON /CDATA/ O,HEAD(20),NUMNP,NUMEL,NUMMAT,NEN,NEQ,IPR
      COMMON /LABEL/ PDIS(6),A(6),BC(2),DI(6),CD(3),TE(3),FD(3)
      COMMON /TDATA/ TIME,DT,C1,C2,C3,C4,C5
      COMMON/ENGYS/ AENGY
      DIMENSION X(NDM,*),B(*),UL(6),ID(NDF,*),F(NDF,*)
      DATA BL/4HBLAN/
      DO 102 II = 1,NUMNP,50
      WRITE(6,2000) O,HEAD,TIME,(I,CD(1),CD(2),I=1,NDM),(I,DI(1)
     1   ,DI(2),I=1,NDF)
      JJ = MINO(NUMNP,II+49)
```

```
      DO 102 N = II,JJ
      IF (PCOMP(X(1,N),BL)) GO TO 101
      DO 100 I = 1,NDF
      UL(I) = F(I,N)*PROP
      K = IABS(ID(I,N))
100   IF(K.GT.0) UL(I) = B(K)
*     WRITE(6,PDIS) N,(X(I,N),I=1,NDM),(UL(I),I=1,NDF)
      WRITE(6,500) N,(X(I,N),I=1,NDM),(UL(I),I=1,NDF)
      WRITE(23,500) N,(X(I,N),I=1,NDM),(UL(I),I=1,NDF)
101   CONTINUE
102   CONTINUE
      WRITE (6,999) AENGY
      RETURN
500   FORMAT (I10, 2F13.4, 6E13.4)
999   FORMAT (//,20X,'STRUCTURE POTENTIAL =',D15.5,/)
2000  FORMAT(A1,20A4//5X,19HNODAL DISPLACEMENTS,5X,4HTIME,E13.5//
     1   6X,4HNODE,9(I7,A4,A2))
      END
C*******************************************************************************
C                                                                              *
C                                  ACTCOL                                      *
C                                                                              *
C*******************************************************************************
      SUBROUTINE ACTCOL(A,B,JDIAG,NEQ,AFAC,BACK)
      IMPLICIT DOUBLE PRECISION (A-H,O-Z)
      LOGICAL AFAC,BACK
      COMMON/ENGYS/ AENGY
      DIMENSION A(*),B(*),JDIAG(*)
C
C.... ACTIVE COLUMN PROFILE SYMMETRIC EQUATION SOLVER
C
C.... REPLACE K(I,J) BY L(J,I) IF I DOESN'T EQUAL J
C.... AND BY U(I,I) IF I=J . REPLACE B(J) BY Y(J) .
      AENGY = 0.0
      JM1DGL = 0
C        IS IS THE ROW NUMBER OF THE SECOND NON-ZERO
C        TERM IN COLUMN J OF THE STIFFNESS MATRIX.
         DO 600 J = 1,NEQ
         JDGL = JDIAG(J)
         JCOLHT = JDGL - JM1DGL
         IS = J - JCOLHT + 2
         IF(JCOLHT-2) 600,300,100
100         IF(.NOT.AFAC) GO TO 500
C           K IS THE ARRAY POSITION OF THE SECOND NON-
C           ZERO ENTRY IN STIFFNESS COLUMN J
            IE = J - 1
            K = JM1DGL + 2
            ID = JDIAG(IS - 1)
C              REPLACE A(K), I.E. K(I,J), BY U(I,J) EXCEPT
C              WHEN I=J , WHEN K(I,J) IS THE FIRST NON-
C              ZERO TERM IN COLUMN J, U(I,J) = K(I,J)
               DO 200 I = IS,IE
               IR = ID
               ID = JDIAG(I)
               IH = MINO(ID-IR-1,I-IS+1)
               IF(IH.GT.0) A(K) = A(K) - DOT(A(K-IH),A(ID-IH),IH)
200            K = K + 1
C           WHEN I=J, REPLACE A(K), I.E. K(I,I), BY
C           U(I,I).  WHEN I NOT = J, REPLACE A(K), I.E. U(I,J),
C           BY L(J,I)
300         IF(.NOT.AFAC) GO TO 500
            IR = JM1DGL + 1
            IE = JDGL - 1
            K = J - JDGL
               DO 400 I = IR,IE
               ID = JDIAG(K+I)
               IF(A(ID).EQ.0.0) GO TO 400
```

```
                D = A(I)
                A(I) = A(I)/A(ID)
                A(JDGL) = A(JDGL) - D*A(I)
400             CONTINUE
C....         REDUCE RHS
500           IF(BACK) B(J) = B(J) - DOT(A(JM1DGL+1),B(IS-1),JCOLHT-1)
600         JM1DGL = JDGL
        IF(.NOT.BACK) RETURN
C.... DIVIDE BY DIAGONAL PIVOTS
            DO 700 I = 1,NEQ
            ID = JDIAG(I)
            IF(A(ID).NE.0.0) B(I) = B(I)/A(ID)
700         AENGY = AENGY + B(I)*B(I)*A(ID)
        AENGY = -AENGY/2.0
C.... BACKSUBSTITUTE
        J = NEQ
        JDGL = JDIAG(J)
800     D = B(J)
        J = J - 1
        IF(J.LE.0) RETURN
        JM1DGL = JDIAG(J)
        IF(JDGL-JM1DGL.LE.1) GO TO 1000
        IS = J - JDGL + JM1DGL + 2
        K = JM1DGL - IS + 1
            DO 900 I = IS,J
900         B(I) = B(I) - A(I+K)*D
1000    JDGL = JM1DGL
        GO TO 800
        END
C*************************************************************************
C                                                                        *
C                              ELMT01                                    *
C                                                                        *
C*************************************************************************
        SUBROUTINE ELMT01(D,UL,XL,IX,TL,S,P,NDF,NDM,NST,ISW)
C
C.... PLANE STRESS/STRAIN ELASTIC LINEAR ELEMENT ROUTINE.
C
        IMPLICIT DOUBLE PRECISION (A-H,O-Z)
        COMMON /CDATA/ O,HEAD(20),NUMNP,NUMEL,NUMMAT,NEN,NEQ,IPR
        COMMON/ELDATA/ DM,N,MA,MCT,IEL,NEL
        DIMENSION D(*),UL(NDF,*),XL(NDM,*),IX(*),TL(*),S(NST,*),P(*)
       1  ,SHP(3,12),XI(9),ETA(9),WT(9),SIG(6),EPS(3)
C.... GO TO CORRECT ARRAY PROCESSOR.
*       WRITE (6,*) 'SUBROUTINE ELMT01 IS BEING CALLED.'
        GO TO (1,2,3,4,5,4), ISW
C.... INPUT MATERIAL PROPERTIES.
1       CALL ELPROP(D)
        LINT = 0
        RETURN
2       RETURN
3       L = D(2)
        IF(L*L.NE.LINT) CALL PGAUSS(L,LINT,XI,ETA,WT)
        MATYPE = D(1)
C.... FOR EACH INTEGRATION POINT COMPUTE STIFFNESS CONTRIBUTION
        DO 320 L = 1,LINT
        CALL SHAPE(XI(L),ETA(L),XL,SHP,DETJAC,NDM,NEL,IX,.FALSE.)
        DV = DETJAC*WT(L)
        D11 = D(5)*DV
        D12 = D(6)*DV
        IF (MATYPE.LE.2) THEN
            D22 = D(7)*DV
            D33 = D(8)*DV
        ELSE
            D13 = D(7)*DV
            D22 = D(8)*DV
            D23 = D(9)*DV
```

```
            D33 = D(10)*DV
         END IF
C....
C....       FOR EACH NODE J COMPUTE DB = D*B
C....
            DO 320 J = 1,NEL
            IF (MATYPE.LE.2) THEN
               DB11 = D11*SHP(1,J)
               DB12 = D12*SHP(2,J)
               DB21 = D12*SHP(1,J)
               DB22 = D22*SHP(2,J)
               DB31 = D33*SHP(2,J)
               DB32 = D33*SHP(1,J)
            ELSE
               DB11 = D11*SHP(1,J) + D13*SHP(2,J)
               DB12 = D12*SHP(2,J) + D13*SHP(1,J)
               DB21 = D12*SHP(1,J) + D23*SHP(2,J)
               DB22 = D22*SHP(2,J) + D23*SHP(1,J)
               DB31 = D33*SHP(2,J) + D13*SHP(1,J)
               DB32 = D33*SHP(1,J) + D23*SHP(2,J)
            END IF
C....
C....          FOR EACH NODE I COMPUTE S = BT*DB
C....
               DO 320 I = 1,J
               S(I+I-1,J+J-1)=S(I+I-1,J+J-1)+SHP(1,I)*DB11+SHP(2,I)*DB31
               S(I+I-1,J+J)=S(I+I-1,J+J)+SHP(1,I)*DB12+SHP(2,I)*DB32
               S(I+I,J+J-1)=S(I+I,J+J-1)+SHP(1,I)*DB31+SHP(2,I)*DB21
               S(I+I,J+J)=S(I+I,J+J)+SHP(1,I)*DB32+SHP(2,I)*DB22
320            CONTINUE
C....
C.... COMPUTE LOWER TRIANGULAR PART BY SYMMETRY
C....
      NL = NEL + NEL
      DO 330 I =2,NL
      DO 330 J = 1,I
330   S(I,J) = S(J,I)
      RETURN
4     L = D(2)
      IF(ISW.EQ.4) L = D(3)
      IF(L*L.NE.LINT) CALL PGAUSS(L,LINT,XI,ETA,WT)
      MATYPE = D(1)
C.... COMPUTE ELEMENT STRESSES, STRAINS, AND FORCES
      DO 600 L = 1,LINT
C.... COMPUTE ELEMENT SHAPE FUNCTIONS
        CALL SHAPE(XI(L),ETA(L),XL,SHP,DETJAC,NDM,NEL,IX,.FALSE.)
C.... COMPUTE STRAINS AND COORDINATES
        DO 410 I = 1,3
           EPS(I) = 0.0
410     CONTINUE
        XX = 0.0
        YY = 0.0
        DO 420 J = 1,NEL
          XX = XX + SHP(3,J)*XL(1,J)
          YY = YY + SHP(3,J)*XL(2,J)
          EPS(1) = EPS(1) + SHP(1,J)*UL(1,J)
          EPS(3) = EPS(3) + SHP(2,J)*UL(2,J)
          EPS(2) = EPS(2) + SHP(1,J)*UL(2,J) + SHP(2,J)*UL(1,J)
420     CONTINUE
C.... COMPUTE STRESSES
        IF (MATYPE.LE.2) THEN
          SIG(1) = D(5)*EPS(1) + D(6)*EPS(3)
          SIG(3) = D(6)*EPS(1) + D(7)*EPS(3)
          SIG(2) = D(8)*EPS(2)
        ELSE
          SIG(1) = D(5)*EPS(1) + D(6)*EPS(3) + D(7)*EPS(2)
          SIG(3) = D(6)*EPS(1) + D(8)*EPS(3) + D(9)*EPS(2)
```

```
          SIG(2) = D(7)*EPS(1) + D(9)*EPS(3) + D(10)*EPS(2)
        END IF
*       IF(ISW.EQ.6) GO TO 620
*       CALL PSTRES(SIG,SIG(4),SIG(5),SIG(6))
C.... OUTPUT STRESSES AND STRAINS
*       MCT = MCT - 2
*       IF(MCT.GT.0) GO TO 430
*       WRITE(6,2001) O,HEAD
*       MCT = 50
*430    WRITE(6,2002) N,MA,XX,YY,SIG,EPS
*       WRITE (25,2010) N,XX,YY,EPS(1),EPS(3),EPS(2)
*600    CONTINUE
*       RETURN
C.... COMPUTE INTERNAL FORCES
*620    DV = DETJAC*WT(L)
*       J1 = 1
*       DO 610 J = 1,NEL
*       P(J1) = P(J1) - (SHP(1,J)*SIG(1) + SHP(2,J)*SIG(2))*DV
*       P(J1+1) = P(J1+1) - (SHP(1,J)*SIG(2) + SHP(2,J)*SIG(3))*DV
*610    J1 = J1 + NDF
*       GO TO 600
C**C**C**C**C**C**C**C**C**C**C**C**C**C**C**C**C**C**C**C**C**C**C**C**C**C**C**
        IF (ISW.EQ.6) THEN
          DV = DETJAC*WT(L)
          J1 = 1
          DO 510 J = 1,NEL
            P(J1) = P(J1) - (SHP(1,J)*SIG(1) + SHP(2,J)*SIG(2))*DV
            P(J1+1) = P(J1+1) - (SHP(1,J)*SIG(2) + SHP(2,J)*SIG(3))*DV
            J1 = J1 + NDF
510       CONTINUE
C         RETURN
          GO TO 600
        ELSE
          CALL PSTRES(SIG,SIG(4),SIG(5),SIG(6))
C.... OUTPUT STRESSES AND STRAINS
          MCT = MCT - 2
          IF(MCT.LE.0) THEN
            WRITE(6,2001) O,HEAD
            MCT = 50
          END IF
          WRITE(6,2002) N,MA,XX,YY,SIG,EPS
          WRITE (25,2010) N,XX,YY,EPS(1),EPS(3),EPS(2)
        END IF
600   CONTINUE
*     WRITE (6,*) 'THIS IS AT THE END OF SUBROUTINE ELMT01.'
      RETURN
C**C**C**C**C**C**C**C**C**C**C**C**C**C**C**C**C**C**C**C**C**C**C**C**C**C**C**
C.... COMPUTE CONSISTENT MASS MATRIX
5     WRITE (6,990)
990   FORMAT (10X,'**** MASS MATRIX FORMULATION FOR THIS ELEMENT ',
     1 'IS NOT AVAILABLE AT THIS TIME ****')
      STOP
C.... FORMATS FOR INPUT-OUTPUT
2001  FORMAT(A1,20A4//5X,16HELEMENT STRESSES//,5X,20H  ELEMENT  MATERIAL
     1    ,7H1-COORD,6X,7H2-COORD,4X,9H11-STRESS,4X,9H12-STRESS,4X,
     2  9H22-STRESS,5X,8H1-STRESS,5X,8H2-STRESS,3X,5HANGLE/50X,
     3  9H11-STRAIN,4X,9H12-STRAIN,4X,9H22-STRAIN)
2002  FORMAT(2I10,2F13.4,5E13.4,F8.2/46X,3E13.4)
2010  FORMAT(I3,5E15.5)
      END
C*********************************************************************
C                                                                    *
C                            ELMT02                                  *
C                                                                    *
C*********************************************************************
      SUBROUTINE ELMT02(D,UL,XL,IX,TL,S,P,NDF,NDM,NST,ISW)
C
```

```
C.... ORTHOTROPIC NOTCH ROOT ELEMENT ROUTINE
C
      IMPLICIT COMPLEX*16 (Z)
      IMPLICIT DOUBLE PRECISION (A-H,O-Y)
      LOGICAL AFAC,SYMX,SYMY
*     REAL   DUMMY,T1,T2,T3,URTIMF
      COMMON /CDATA  / O,HEAD(20),NUMNP,NUMEL,NUMMAT,NEN,NEQ,IPR
      COMMON /ELDATA / DM,N,MA,MCT,IEL,NEL
      COMMON /ROOTS  / ZS(2),ZB,ZC
      COMMON /DISPC  / ZP(2),ZQ(2)
      COMMON /ELPMAP / ZC1(2),ZC2(2),ZK(2)
      COMMON /SYMTRY / SYMX,SYMY
      DIMENSION D(*),UL(NDF,*),XL(NDM,*),IX(*),TL(*),S(NST,NST),P(NST)
     1  ,SHP1(4),XI(40),WT(40),SIG(6),EPS(3)
      DIMENSION ZETA(2),ZOMEGA(2)
      DIMENSION R(2,40),U(2,40),STR(3,40),HCOL(820)
      DIMENSION KDIAG(40),BETA(40),URBP(2,40),URBQ(2,40)
      DATA PI/3.14159265358979238D00/
      PLMAX = 0.0D0
      SIGMAX = 0.0D0
C.... GO TO CORRECT ARRAY PROCESSOR.
      AFAC = .TRUE.
      SYMX = .FALSE.
      SYMY = .FALSE.
      GO TO (1,2,3,3,5,6), ISW
C.... INPUT MATERIAL PROPERTIES.
1     CALL ELPROP(D)
      LINT1 = 0
      RETURN
2     RETURN
C.... STIFFNESS COMPUTATION
3     MATYPE = D(1)
      L1     = D(2)
*     IF (ISW.EQ.3)  T1 = URTIMF(DUMMY)
      IF (ISW.EQ.4)  L1 = D(3)
      IF (L1*L1.NE.LINT1)  CALL GAUSS1(L1,LINT1,XI,WT)
      CALL  CLPXCT(D,MATYPE,IEL)
      XI0 = PI/180.0D00*(90.0 - (D(19) + D(18))/2.0D00)
C.... RECOVER INTEGER CONSTANTS RELATING TO THE NUMBER OF NODES
C.... (NUMNOD),NUMBER OF SIDES (NUMSID),NUMBER OF NODES/SIDE
C.... (NODSID), AND INITIAL (L0) AND FINAL (LF) SERIES SUMMATION TERMS
      NUMNOD = D(11)
      NODSID = D(12)
      NUMSID = D(13)
      L0     = D(14)
      LF     = D(15)
      NCOLU  = (LF - L0)*2
      ISYM   = D(23)
      NODEP  = D(26)
      NODEQ  = D(27)
      IF (ISYM.EQ.-1)  THEN
         NCOLU = LF - L0
         SYMY  = .TRUE.
      ELSE IF (ISYM.EQ.1)  THEN
         NCOLU = LF - L0
         SYMX  = .TRUE.
      ELSE IF (ISYM.EQ.2)  THEN
         NCOLU = (LF - L0)/2 + 1
         SYMX  = .TRUE.
         SYMY  = .TRUE.
      END IF
      IDIMS  = NEL*2
C.... TEST FOR CORRECT DIMENSIONING
      IF (NEL.NE.NUMNOD.OR.NCOLU.GT.NST.OR.NCOLU.GT.40.OR.
     1       IDIMS.GT.NST)   THEN
         WRITE (6,3910) NEL,NUMNOD,NCOLU,NST,IDIMS
*        WRITE (6,*) 'ELMT02 DIAGNOSTIC: 6TH LINE BEFORE LABEL 3000.'
```

```
         STOP
      END IF
C.... SET UP KDIAG FOR INVERSION OF [H] AND ZERO ARRAYS HCOL AND BETA
      DO 3000 I = 1,NCOLU
      KDIAG(I) = I*(I + 1)/2
3000  BETA(I) = 0.0
      DO 3001 I = 1,KDIAG(NCOLU)
3001  HCOL(I) = 0.0
      IF (ISYM.NE.2)  THEN
         XP   = XL(1,NODEP)
         YP   = XL(2,NODEP)
         YQ   = XL(2,NODEQ)
         YQMP = YQ - YP
            IF (DABS(YQMP).LT.1.0D-05)  THEN
               WRITE (6,99999) YQMP
*              WRITE (6,*) 'ELMT02 DIAGNOS.: 8TH LINE AFTER LABEL 3001.'
               STOP
            END IF
         YQMP = 1.0/YQMP
         XR   = XP - D(20)
         YR   = YP - D(21)
         CALL MAP(XR,YR,XI0,IEL,ZETA,ZOMEGA)
         CALL UMAT(ZETA,L0,LF,IEL,URBP)
         XR   = XL(1,NODEQ) - D(20)
         YR   = YQ - D(21)
         CALL MAP(XR,YR,XI0,IEL,ZETA,ZOMEGA)
         CALL UMAT(ZETA,L0,LF,IEL,URBQ)
      END IF
C....
C.... INTEGRATE OVER THE SIDES OF THE ELEMENT
C....
      IS     = 1
      NUMINT = D(24)
         DO 300 ISIDE = 1,NUMSID
         IE = IS + NODSID - 1
         KK = IE
         IF (KK.GT.NUMNOD)  KK = 1
         XSTART = XL(1,IS)
         YSTART = XL(2,IS)
C....    COMPUTE DIRECTION COSINES AND LENGTH OF SIDE
         XDIS   = (XL(1,KK) - XSTART)/D(24)
         YDIS   = (XL(2,KK) - YSTART)/D(24)
         DIS    =  DSQRT(XDIS**2 + YDIS**2)
         DRCOSX =  YDIS/DIS
         DRCOSY = -XDIS/DIS
C....
C....     INTEGRATE OVER EACH INTERVAL
          DO 305 MMM = 1,NUMINT
          XMMM = MMM
          DUM1 = XMMM - 1.0
C....
C....       COMPUTE CONTRIBUTION FROM EACH GAUSS POINT
C....
            DO 310 IP = 1,L1
            SL  = (XI(IP) + 1.0)/2.0
            XPT = XSTART + (SL + DUM1)*XDIS
            YPT = YSTART + (SL + DUM1)*YDIS
            XR  = XPT - D(20)
            YR  = YPT - D(21)
            CALL MAP(XR,YR,XI0,IEL,ZETA,ZOMEGA)
            CALL UMAT(ZETA,L0,LF,IEL,U)
            CALL RMAT(ZETA,ZOMEGA,L0,LF,IEL,DRCOSX,DRCOSY,STR,R)
            IF (ISYM.NE.2)  THEN
               DO 311 J = 1,NCOLU
               U(1,J) = U(1,J) + YQMP*((YPT - YQ)*URBP(1,J) -
     1                                 (YPT - YP)*URBQ(1,J))
               U(2,J) = U(2,J) - URBP(2,J) + (XPT - XP)*YQMP*
```

```
     1                                        (URBQ(1,J) - URBP(1,J))
311            CONTINUE
               END IF
C....
C....          COMPUTE CONTRIBUTION TO H(I,J) AT THIS GAUSS POINT
C....
               WTGP = WT(IP)*DIS/4.0D00
               KK = 1
                  DO 312 J = 1,NCOLU
                  DO 312 I = 1,J
                  HCOL(KK) = HCOL(KK) +  (U(1,I)*R(1,J) + U(2,I)*R(2,J) +
     1                                    R(1,I)*U(1,J) + R(2,I)*U(2,J))*WTGP
                  KK = KK + 1
312               CONTINUE
C....
C....          COMPUTE CONTRIBUTION TO G(I,J) AT THIS GAUSS POINT
C....          STORE IN S(I,J) WHICH HAS BEEN ZEROED IN SUBROUTINE ELMLIB
C....
               XILOC = 2.0*(SL + DUM1)/D(24) - 1.0
               CALL SHAP1D(XILOC,NODSID,SHP1)
               ISHAPE = 1
                  DO 314 JDUM = IS,IE
                  FACTOR = SHP1(ISHAPE)*WT(IP)*DIS/2.0D00
                  J = 2*JDUM - 1
                  IF (JDUM.GT.NUMNOD)  J = 1
                     DO 316 I = 1,NCOLU
                     S(I,J)   = S(I,J)   + R(1,I)*FACTOR
                     S(I,J+1) = S(I,J+1) + R(2,I)*FACTOR
316                  CONTINUE
                  ISHAPE = ISHAPE + 1
314               CONTINUE
               IF (ISYM.EQ.2)  GO TO 310
               JP = 2*NODEP - 1
               JQ = 2*NODEQ - 1
               WTGP = WTGP*YQMP
                  DO 320 I = 1,NCOLU
                  S(I,JP)   = S(I,JP)   - (-(YPT - YQ)*R(1,I) +
     1                                     (XPT - XP)*R(2,I))*WTGP
                  S(I,JQ)   = S(I,JQ)   - ( (YPT - YP)*R(1,I) -
     1                                     (XPT - XP)*R(2,I))*WTGP
                  S(I,JP+1) = S(I,JP+1) - (YQ - YP)*R(2,I)*WTGP
320               CONTINUE
310            CONTINUE
305         CONTINUE
            IS = IE
300         CONTINUE
C....
C.... COMPUTE [H]-INV * [G]
         ICOUNT = 1
         DO 350 JCOL = 1,IDIMS
            DO 351 IROW = 1,NCOLU
351         P(IROW) = S(IROW,JCOL)
         CALL ACTCOL(HCOL,P,KDIAG,NCOLU,AFAC,.TRUE.)
         IF (JCOL.EQ.1)  AFAC = .FALSE.
C.... COMPUTE S(I,JCOL) OR BETA(I)
            IF (ISW.EQ.3)   THEN
               DO 360 I = JCOL,IDIMS
               DUM = 0.0
                  DO 361 K = 1,NCOLU
361               DUM = DUM + S(K,I)*P(K)
360            S(I,JCOL) = DUM
            ELSE
               IF (ICOUNT.EQ.1)  NODE = (JCOL + 1)/2
               UDIS = UL(ICOUNT,NODE)
                  DO 370 K = 1,NCOLU
370               BETA(K) = BETA(K) + P(K)*UDIS
               ICOUNT = ICOUNT + 1
```

```
            IF (ICOUNT.EQ.3) ICOUNT = 1
         END IF
350   CONTINUE
*     WRITE (6,*) 'ELMT02 DIAGNOSTIC: 1ST LINE AFTER LABEL 350.'
      IF (ISW.EQ.4)  GO TO 4
C.... FILL S BY SYMMETRY
      DO 390 I = 1,IDIMS
      DO 390 J = I,IDIMS
390   S(I,J) = S(J,I)
*     T2 = URTIMF(DUMMY)
*     T3 = T2 - T1
*     WRITE (6,55555)  T1,T2,T3
*     WRITE (6,*) 'ELMT02 DIAGNOSTIC: 4TH LINE AFTER LABEL 390.'
      RETURN
C.... COMPUTE ANALYTIC STRESSES,STRAINS, AND DISPLACEMENTS
4     THETA  = D(18)*PI/180.0D00
*     WRITE (6,*) 'ELMT02 DIAGNOSTIC: 1ST LINE AFTER LABEL 4.'
      NSTRPT = D(25)
      NUMOUT = D(30)
      ANGINC = (PI/180.0D00)*(D(19) - D(18))/(NSTRPT - 1)
      WRITE (6,2020)  (BETA(I),I=1,NCOLU)
      WRITE (27,41000)  NCOLU
      WRITE (27,41001)  (BETA(I),I=1,NCOLU)
C...     COMPUTE OUTPUT FOR SPECIFIED NUMBER OF INTERVALS (NUMOUT)
         DO 500 IOUT = 0,NUMOUT
         IF (IOUT.NE.0)  THEN
            IDUM = 4*IOUT + 27
            XO   = D(IDUM)
            YO   = D(IDUM + 1)
            XINC = (D(IDUM + 2) - XO)/(NSTRPT - 1)
            YINC = (D(IDUM + 3) - YO)/(NSTRPT - 1)
         END IF
C....
C....       DETERMINE OUTPUT FOR NSTRPT POINTS ON THE INTERVAL
            DO 600 IPT = 1,NSTRPT
C....          ZERO NECESSARY VARIABLES
               DO 410 I = 1,3
410            SIG(I) = 0.0
               UAN    = 0.0
               VAN    = 0.0
C....       DETERMINE THE POINT (XPT,YPT) TO EVALUATE QUANTITIES
            IF (IOUT.EQ.0)  THEN
               XPT = D(16)*DCOS(THETA) + D(20)
               YPT = D(17)*DSIN(THETA) + D(21)
            ELSE
               XPT = XO + (IPT - 1)*XINC
               YPT = YO + (IPT - 1)*YINC
            END IF
            XR = XPT - D(20)
            YR = YPT - D(21)
            CALL MAP(XR,YR,XIO,IEL,ZETA,ZOMEGA)
            CALL UMAT(ZETA,LO,LF,IEL,U)
            CALL RMAT(ZETA,ZOMEGA,LO,LF,IEL,0.0D00,0.0D00,STR,R)
            IF (ISYM.NE.2)  THEN
               DO 411 J = 1,NCOLU
               U(1,J) = U(1,J) + YQMP*((YPT - YQ)*URBP(1,J) -
     1                                 (YPT - YP)*URBQ(1,J))
               U(2,J) = U(2,J) - URBP(2,J) + (XPT - XP)*YQMP*
     1                                 (URBQ(1,J) - URBP(1,J))
411            CONTINUE
            END IF
C....       COMPUTE STRESSES AND DISPLACEMENTS AT (XPT,YPT)
               DO 420 K = 1,NCOLU
               SIG(3) = SIG(3) + STR(1,K)*BETA(K)
               SIG(2) = SIG(2) + STR(2,K)*BETA(K)
               SIG(1) = SIG(1) + STR(3,K)*BETA(K)
               UAN    = UAN + U(1,K)*BETA(K)
```

```
                  VAN    = VAN + U(2,K)*BETA(K)
420               CONTINUE
                  UAN = UAN + (-(YPT - YQ)*UL(1,NODEP) +
     1                        (YPT - YP)*UL(1,NODEQ))*YQMP
                  VAN = VAN + UL(2,NODEP) + (XPT - XP)*(UL(1,NODEP) -
     1                        UL(1,NODEQ))*YQMP
C....             COMPUTE STRAINS AT (XPT,YPT)
                  IF (MATYPE.LE.2) THEN
                     EPS(1) = D(5)*SIG(1) + D(6)*SIG(3)
                     EPS(3) = D(6)*SIG(1) + D(7)*SIG(3)
                     EPS(2) = D(8)*SIG(2)
                  ELSE
                     EPS(1) = D(5)*SIG(1) + D(6)*SIG(3) + D(7)*SIG(2)
                     EPS(3) = D(6)*SIG(1) + D(8)*SIG(3) + D(9)*SIG(2)
                     EPS(2) = D(7)*SIG(1) + D(9)*SIG(3) + D(10)*SIG(2)
                  END IF
                  CALL PSTRES(SIG,SIG(4),SIG(5),SIG(6))
C....             OUTPUT STRESSES AND STRAINS
                  MCT = MCT - 2
                  IF(MCT.GT.0) GO TO 430
                  WRITE(6,2001) O,HEAD
                  MCT = 50
430               WRITE(6,2002) N,MA,XPT,YPT,SIG,EPS
                  WRITE (26,2010) XPT,YPT,UAN,VAN,EPS(1),EPS(3),EPS(2),SIG(1),
     1                                    SIG(3),SIG(2)
                  IF (IOUT.EQ.0)  THEN
                     IF (SIG(4).LT.1.0D-05)  SIG(4) = SIG(5)
                     PLTANG = THETA*180.0D00/PI
                     WRITE (28,41010) PLTANG,SIG(4)
                     IF (SIG(4).GT.SIGMAX) THEN
                        SIGMAX = SIG(4)
                        PLMAX = PLTANG
                     END IF
                     THETA = THETA + ANGINC
                  END IF
600            CONTINUE
               WRITE (28,610) 'MAX. FILLET HOOP STRESS', 'FILLET ANGLE'
610            FORMAT (A23, 3X, A12)
               WRITE (28,620) SIGMAX, PLMAX
620            FORMAT (5X, F12.4, 12X, F8.2)
500         CONTINUE
            RETURN
C....       COMPUTE CONSISTENT MASS MATRIX
5           WRITE (6,990)
990         FORMAT (10X,'**** MASS MATRIX FORMULATION FOR THIS ELEMENT ',
           1 'IS NOT AVAILABLE AT THIS TIME ****')
6           RETURN
C....       FORMATS FOR INPUT-OUTPUT
2001        FORMAT(A1,20A4//5X,16HELEMENT STRESSES//,5X,20H  ELEMENT  MATERIAL
           1    ,7H1-COORD,6X,7H2-COORD,4X,9H11-STRESS,4X,9H12-STRESS,4X,
           2  9H22-STRESS,5X,8H1-STRESS,5X,8H2-STRESS,3X,5HANGLE/50X,
           3  9H11-STRAIN,4X,9H12-STRAIN,4X,9H22-STRAIN)
2002        FORMAT(2I10,2F13.4,5E13.5,F8.2/46X,3E13.5)
2010        FORMAT (4E12.4/5X,6E12.4)
2020        FORMAT (//,20X,'BETAS',/,20(/,30X,D30.15))
3910        FORMAT (30X,'********** ERROR ***** DIMENSION MISTAKE IN ELMT02 **
           1        *********',/,40X,'NEL    = ',I3,/,40X,'NUMNOD = ',I3,/,40X,
           2       'NCOLU  = ',I3,/,40X,'NST    = ',I3,/,40X,'IDIMS = ',I3)
41000 FORMAT (I2)
41001 FORMAT (D20.10)
41010 FORMAT (2D20.10)
55555 FORMAT (//,15X,'STIFFNESS MATRIX COMPILATION TIME FOR HYBRID',
           1     'ELEMENT',/,25X,'T1      = ',E20.5,/,25X,'T2      = ',
           2     E20.5,/,25X,'T2 - T1 = ',E20.5,//)
99999 FORMAT (5X,'*** FATAL ERROR IN SUPPRESSING RIGID BODY MODES ***',
           1        /,20X,'YQ - YP = ',D30.15)
```

```
      END
C*********************************************************************
C                                                                     *
C                              SHAP3                                  *
C                                                                     *
C*********************************************************************
      SUBROUTINE SHAP3(XI,ETA,SHP,IX)
C
C.... ADD CUBIC FUNCTIONS AS NECESSARY
C
      IMPLICIT DOUBLE PRECISION (A-H,O-Z)
      DIMENSION IX(*),SHP(3,*)
      S2 = (1. - XI*XI)/2.
      T2 = (1. - ETA*ETA)/2.
      C0 = 27./16.
      ONETHD = 1./3.
      CXISQ = C0*S2
      CETASQ = C0*T2
      C1XI = XI - ONETHD
      C2XI = XI + ONETHD
      C1ETA = ETA - ONETHD
      C2ETA = ETA + ONETHD
      D1XI = CXISQ - C0*XI*C1XI
      D2XI = CXISQ - C0*XI*C2XI
      D1ETA = CETASQ - C0*ETA*C1ETA
      D2ETA = CETASQ - C0*ETA*C2ETA
      C1MXI = 1. - XI
      C1PXI = 1. + XI
      C1META = 1. - ETA
      C1PETA = 1. + ETA
C.... IF MIDSIDE NODE II IS NOT SPECIFIED THEN SHP(J,II) = 0
C.... THUS, THE CORNER NODES ON THIS EDGE WILL RETAIN ONLY
C.... QUADRATIC OR LINEAR TERMS
      DO 100 I = 5,12
      DO 100 J = 1,3
100   SHP(J,I) = 0.0
C.... MIDSIDE NODES (SERENDIPITY)
      IF (IX(5).EQ.0.AND.IX(9).EQ.0) GO TO 101
         IF (IX(5).NE.0.AND.IX(9).NE.0) THEN
            SHP(1,5) = -C1META*D1XI
            SHP(2,5) = C1XI*CXISQ
            SHP(3,5) = -C1META*SHP(2,5)
            SHP(1,9) = C1META*D2XI
            SHP(2,9) = -C2XI*CXISQ
            SHP(3,9) = -C1META*SHP(2,9)
         ELSE
            SHP(1,5) = -XI*C1META
            SHP(2,5) = -S2
            SHP(3,5) = S2*C1META
         END IF
101   IF (IX(6).EQ.0.AND.IX(10).EQ.0) GO TO 102
         IF (IX(6).NE.0.AND.IX(10).NE.0) THEN
            SHP(1,6) = -C1ETA*CETASQ
            SHP(2,6) = -C1PXI*D1ETA
            SHP(3,6) = C1PXI*SHP(1,6)
            SHP(1,10) = C2ETA*CETASQ
            SHP(2,10) = C1PXI*D2ETA
            SHP(3,10) = C1PXI*SHP(1,10)
         ELSE
            SHP(1,6) = T2
            SHP(2,6) = -ETA*C1PXI
            SHP(3,6) = T2*C1PXI
         END IF
102   IF (IX(7).EQ.0.AND.IX(11).EQ.0) GO TO 103
         IF (IX(7).NE.0.AND.IX(11).NE.0) THEN
            SHP(1,7) = C1PETA*D2XI
            SHP(2,7) = C2XI*CXISQ
```

```
            SHP(3,7) = C1PETA*SHP(2,7)
            SHP(1,11) = -C1PETA*D1XI
            SHP(2,11) = -C1XI*CXISQ
            SHP(3,11) = C1PETA*SHP(2,11)
         ELSE
            SHP(1,7) = -XI*C1PETA
            SHP(2,7) = S2
            SHP(3,7) = S2*C1PETA
         END IF
103   IF (IX(8).EQ.0.AND.IX(12).EQ.0) GO TO 104
         IF (IX(8).NE.0.AND.IX(12).NE.0) THEN
            SHP(1,8) = -C2ETA*CETASQ
            SHP(2,8) = C1MXI*D2ETA
            SHP(3,8) = -C1MXI*SHP(1,8)
            SHP(1,12) = C1ETA*CETASQ
            SHP(2,12) = -C1MXI*D1ETA
            SHP(3,12) = -C1MXI*SHP(1,12)
         ELSE
            SHP(1,8) = -T2
            SHP(2,8) = -ETA*C1MXI
            SHP(3,8) = T2*C1MXI
         END IF
C.... CORRECT CORNER NODES FOR PRESENCE OF MIDSIDE NODES
104   K = 8
      KK = 12
      DO 109 I = 1,4
      L = I + 4
      LL = I + 8
C.... ADJUST CORNER SHAPE FUNCTION FOR NODES ON THE CW SIDE
         IF(IX(KK).NE.0.AND.IX(K).NE.0)  THEN
            DO 111 J=1,3
111         SHP(J,I) = SHP(J,I) - ONETHD*(2.0*SHP(J,KK) + SHP(J,K))
         ELSE
            DO 121 J=1,3
121         SHP(J,I) = SHP(J,I) - 0.5*SHP(J,K)
         END IF
C.... ADJUST CORNER SHAPE FUNCTION FOR NODES ON THE CCW SIDE
         IF(IX(LL).NE.0.AND.IX(L).NE.0)  THEN
            DO 112 J=1,3
112         SHP(J,I) = SHP(J,I) - ONETHD*(2.0*SHP(J,L) + SHP(J,LL))
         ELSE
            DO 122 J=1,3
122         SHP(J,I) = SHP(J,I) - 0.5*SHP(J,L)
         END IF
      K = L
109   KK = LL
      RETURN
      END
C*********************************************************************
C                                                                    *
C                              SHAP2                                 *
C                                                                    *
C*********************************************************************
      SUBROUTINE SHAP2(XI,ETA,SHP,IX,NEL)
C
C.... ADD QUADRATIC FUNCTIONS AS NECESSARY
C
      IMPLICIT DOUBLE PRECISION (A-H,O-Z)
      DIMENSION IX(*),SHP(3,*)
      S2 = (1.-XI*XI)/2.
      T2 = (1.-ETA*ETA)/2.
C.... IF MIDSIDE NODE II IS NOT SPECIFIED THEN SHP(J,II) = 0
C.... THUS, THE CORNER NODES ON THIS EDGE WILL RETAIN ONLY
C.... THE LINEAR TERMS
      DO 100 I = 5,8
```

```
      DO 100 J = 1,3
100   SHP(J,I) = 0.0
C.... MIDSIDE NODES (SERENDIPITY)
      IF(IX(5).EQ.0) GO TO 101
      SHP(1,5) = -XI*(1.-ETA)
      SHP(2,5) = -S2
      SHP(3,5) = S2*(1.-ETA)
101   IF(NEL.LT.6) GO TO 107
      IF(IX(6).EQ.0) GO TO 102
      SHP(1,6) = T2
      SHP(2,6) = -ETA*(1.+XI)
      SHP(3,6) = T2*(1.+XI)
102   IF(NEL.LT.7) GO TO 107
      IF(IX(7).EQ.0) GO TO 103
      SHP(1,7) = -XI*(1.+ETA)
      SHP(2,7) = S2
      SHP(3,7) = S2*(1.+ETA)
103   IF(NEL.LT.8.OR.IX(8).EQ.0) GO TO 107
      SHP(1,8) = -T2
      SHP(2,8) = -ETA*(1.-XI)
      SHP(3,8) = T2*(1.-XI)
C.... CORRECT CORNER NODES FOR PRESENCE OF MIDSIDE NODES
107   K = 8
      DO 109 I = 1,4
      L = I + 4
      DO 108 J = 1,3
108   SHP(J,I) = SHP(J,I) - 0.5*(SHP(J,K)+SHP(J,L))
109   K = L
      RETURN
      END
C*********************************************************************
C                                                                    *
C                              SHAPE                                 *
C                                                                    *
C*********************************************************************
      SUBROUTINE SHAPE(XI,ETA,XL,SHP,DETJAC,NDM,NEL,IX,FLG)
C
C.... SHAPE FUNCTION ROUTINE FOR TWO DIMENSIONAL ELEMENTS
C
      IMPLICIT DOUBLE PRECISION (A-H,O-Z)
      DOUBLE PRECISION JAC(2,2),JACINV(2,2)
      LOGICAL FLG
      DIMENSION SHP(3,*),XL(NDM,*),S(4),T(4),IX(*)
      DATA S/-0.5,0.5,0.5,-0.5/,T/-0.5,-0.5,0.5,0.5/
C.... SHP(3,I) = SHAPE FUNCTION FOR NODE I - N(I)
C.... SHP(1,I) = PARTIAL N(I) PARTIAL XI
C.... SHP(2,I) = PARTAIL N(I) PARTIAL ETA
C.... FORM 4-NODE QUADRILATERAL SHAPE FUNCTIONS
      DO 100 I = 1,4
      SHP(3,I) = (0.5+S(I)*XI)*(0.5+T(I)*ETA)
      SHP(1,I) = S(I)*(0.5+T(I)*ETA)
100   SHP(2,I) = T(I)*(0.5+S(I)*XI)
      IF(NEL.GE.4) GO TO 120
C.... FORM TRIANGLE BY ADDING THIRD AND FOURTH TOGETHER
      DO 110 I = 1,3
110   SHP(I,3) = SHP(I,3)+SHP(I,4)
C.... ADD QUADRATIC TERMS IF NECESSARY
120   IF(NEL.GT.4.AND.NEL.LE.8) CALL SHAP2(XI,ETA,SHP,IX,NEL)
      IF(NEL.GT.8) CALL SHAP3(XI,ETA,SHP,IX)
C.... CONSTRUCT JACOBIAN AND ITS INVERSE
      DO 130 K = 1,NDM
      DO 130 J = 1,2
      JAC(K,J) = 0.0
      DO 130 I = 1,NEL
130   JAC(K,J) = JAC(K,J) + SHP(K,I)*XL(J,I)
      DETJAC = JAC(1,1)*JAC(2,2)-JAC(1,2)*JAC(2,1)
C.... IF FLAG = .TRUE. THE GLOBAL DERIVATIVES ARE NOT DETERMINED
```

```
      IF(FLG) RETURN
      JACINV(1,1) = JAC(2,2)/DETJAC
      JACINV(2,2) = JAC(1,1)/DETJAC
      JACINV(1,2) =-JAC(1,2)/DETJAC
      JACINV(2,1) =-JAC(2,1)/DETJAC
C.... FORM GLOBAL DERIVATIVES
C.... NOW SHP(1,I) = PARTIAL N(I) PARTIAL X
C.... AND SHP(2,I) = PARTIAL N(I) PARTIAL Y
      DO 140 I = 1,NEL
      TP        = JACINV(1,1)*SHP(1,I) + JACINV(1,2)*SHP(2,I)
      SHP(2,I)  = JACINV(2,1)*SHP(1,I) + JACINV(2,2)*SHP(2,I)
140   SHP(1,I)  = TP
      RETURN
      END
C*******************************************************************************
C                                                                              *
C                          FUNCTION DOT                                        *
C                                                                              *
C*******************************************************************************
      FUNCTION  DOT (A,B,N)
C
C.... VECTOR DOT PRODUCT
C
      IMPLICIT DOUBLE PRECISION (A-H,O-Z)
      DIMENSION A(*),B(*)
      DOT = 0.0
      DO 100 I=1,N
100   DOT = DOT + A(I)*B(I)
      RETURN
      END
C*******************************************************************************
C                                                                              *
C                              UACTCL                                          *
C                                                                              *
C*******************************************************************************
      SUBROUTINE UACTCL (A,C,B,JDIAG,NEQ,AFAC,BACK)
      IMPLICIT DOUBLE PRECISION (A-H,O-Z)
      DIMENSION A(1),B(1),JDIAG(1),C(1)
      WRITE (6,99)
99    FORMAT(10X,'**** SUBROUTINE UACTCL HAS NOT BEEN DEBUGED YET')
      STOP
      END
C*******************************************************************************
C                                                                              *
C                              EUPDAT                                          *
C                                                                              *
C*******************************************************************************
      SUBROUTINE EUPDAT (DR,U,V,A,XM,DT,NEQ)
      IMPLICIT DOUBLE PRECISION (A-H,O-Z)
      DIMENSION U(1),V(1),A(1),DR(1),XM(1)
      WRITE (6,98)
98    FORMAT(10X,'**** SUBROUTINE EUPDAT HAS NOT BEEN DEBUGED YET')
      STOP
      END
C*******************************************************************************
C                                                                              *
C                              PEIGS                                           *
C                                                                              *
C*******************************************************************************
      SUBROUTINE PEIGS(A,B,F,X,Y,Z,ID,IX,JDIAG,NDF,NDM,NEN1,DFL)
      IMPLICIT DOUBLE PRECISION (A-H,O-Z)
      DIMENSION A(1),B(1),F(1),X(1),Y(1),Z(1),ID(1),IX(1),JDIAG(1)
      WRITE (6,97)
97    FORMAT(10X,'**** SUBROUTINE PEIGS HAS NOT BEEN DEBUGED YET')
      STOP
      END
C*******************************************************************************
```

```
C                                                                       *
C                              OUTMSH                                   *
C                                                                       *
C***********************************************************************
      SUBROUTINE OUTMSH(X,IX,NDM,NEN1)
      IMPLICIT DOUBLE PRECISION (A-H,O-Z)
      COMMON /CDATA/ O,HEAD(20),NUMNP,NUMEL,NUMMAT,NEN,NEQ,IPR
      DIMENSION X(NDM,*),IX(NEN1,*)
      WRITE (24,90) NUMNP,NUMEL,NDM,NEN
      WRITE (24,90) ((IX(I,J),I=1,NEN),J=1,NUMEL)
      WRITE (24,91) ((X(I,J),I=1,NDM),J=1,NUMNP)
      END FILE 24
      RETURN
90    FORMAT (2014)
91    FORMAT (8D10.4)
      END
C***********************************************************************
C                                                                       *
C                              SHAP1D                                   *
C                                                                       *
C***********************************************************************
      SUBROUTINE SHAP1D(XI,NODSID,SHP1)
      IMPLICIT DOUBLE PRECISION (A-H,O-Z)
      DIMENSION SHP1(*)
      DATA  CONS/1.6875D00/,ONETHD/0.33333333333333333333D00/
      SHP1(1) = (1.0D00 - XI)/2.0D00
      DUM1    = (1.0D00 + XI)/2.0D00
      IF (NODSID.EQ.2)  THEN
         SHP1(2) = DUM1
         RETURN
      ELSE IF (NODSID.EQ.3)  THEN
         SHP1(2) = 1.0D00 - XI**2
         SHP1(1) = SHP1(1) - 0.5D00*SHP1(2)
         SHP1(3) = DUM1    - 0.5D00*SHP1(2)
         RETURN
      ELSE
         SHP1(2) = -CONS*(XI - ONETHD)*(1.0D00 - XI**2)
         SHP1(3) =  CONS*(XI + ONETHD)*(1.0D00 - XI**2)
         SHP1(1) = SHP1(1) - 2.0D00*ONETHD*SHP1(2) - ONETHD*SHP1(3)
         SHP1(4) = DUM1    - 2.0D00*ONETHD*SHP1(3) - ONETHD*SHP1(2)
         RETURN
      END IF
      END
C***********************************************************************
C                                                                       *
C                                UMAT                                   *
C                                                                       *
C***********************************************************************
      SUBROUTINE UMAT(ZETA,M,N,IEL,U)
C.... THIS SUBROUTINE COMPUTES THE 2 BY 2N MATRIX U AT THE
C.... (X,Y) POINT CORRESPONDING TO ZETA(1) AND ZETA(2)
      IMPLICIT COMPLEX*16 (Z)
      IMPLICIT DOUBLE PRECISION (A-H,O-Y)
      LOGICAL SYMX,SYMY
      DIMENSION ZETA(2),U(2,*)
      COMMON /ROOTS  / ZS(2),ZB,ZC
      COMMON /DISPC  / ZP(2),ZQ(2)
      COMMON /SYMTRY / SYMX,SYMY
      ICOUNT = 0
      KKK = 1
         DO 10 J = M,N
         ICOUNT = ICOUNT + 1
         IF (SYMY.AND.ICOUNT.EQ.2)  THEN
            ICOUNT = 0
            GO TO 10
         END IF
         IF (J.EQ.0)  GO TO 10
```

```
          L = J
          IF (IEL.EQ.2)  L = -J
          Z1J = (ZETA(1))**J
          Z2J = (ZETA(2))**J
          Z2L = (ZETA(2))**L
          ZDUM1 = ZB*Z2L + ZC*Z2J
          ZDUM2 = ZB*Z2L - ZC*Z2J
          U(1,KKK) = 2.0*DREAL(ZP(1)*Z1J + ZP(2)*ZDUM1)
          U(2,KKK) = 2.0*DREAL(ZQ(1)*Z1J + ZQ(2)*ZDUM1)
          KKK = KKK + 1
          IF (SYMX)  GO TO 10
          U(1,KKK) = 2.0*DIMAG(-ZP(1)*Z1J + ZP(2)*ZDUM2)
          U(2,KKK) = 2.0*DIMAG(-ZQ(1)*Z1J + ZQ(2)*ZDUM2)
          KKK = KKK + 1
10        CONTINUE
        RETURN
        END
C*************************************************************************
C                                                                        *
C                                  RMAT                                  *
C                                                                        *
C*************************************************************************
        SUBROUTINE RMAT (ZETA,ZOMEGA,M,N,IEL,DRCOSX,DRCOSY,STR,R)
C.... THIS SUBROUTINE DETERMINES THE 3 BY 2N MATRIX STR AND
C.... THE 2 BY 2N MATRIX R
        IMPLICIT COMPLEX*16 (Z)
        IMPLICIT DOUBLE PRECISION (A-H,O-Y)
        LOGICAL SYMX,SYMY
        DIMENSION ZETA(2),ZOMEGA(2),ZF(2,3)
        DIMENSION STR(3,*),R(2,*)
        COMMON /ROOTS  / ZS(2),ZB,ZC
        COMMON /SYMTRY / SYMX,SYMY
        ICOUNT = 0
        KKK = 1
        SIGN = 1.0
        IF (IEL.EQ.2)  SIGN = -1.0
        DO 1 I = 1,2
        DO 1 K = 1,3
1       ZF(I,K) = ZS(I)**(K - 1)/ZOMEGA(I)
           DO 10 J = M,N
           ICOUNT = ICOUNT + 1
           IF (SYMY.AND.ICOUNT.EQ.2)  THEN
              ICOUNT = 0
              GO TO 10
           END IF
           IF (J.EQ.0)  GO TO 10
           KP1 = KKK + 1
           L = J
           IF (IEL.EQ.2)  L = -J
           Z1JM1 = (ZETA(1))**(J - 1)
           Z2JM1 = (ZETA(2))**(J - 1)
           Z2LM1 = (ZETA(2))**(L - 1)
           ZDUM3 = SIGN*ZB*Z2LM1 + ZC*Z2JM1
           ZDUM4 = SIGN*ZB*Z2LM1 - ZC*Z2JM1
           DUM1 =  -2.0*J
              DO 2 I = 1,3
              DUM1 = -DUM1
              ZZ1 =  ZF(1,I)*Z1JM1 + ZF(2,I)*ZDUM3
              ZZ2 = -ZF(1,I)*Z1JM1 + ZF(2,I)*ZDUM4
              STR(I,KKK) = DUM1*DREAL(ZZ1)
              IF (SYMX)  GO TO 2
              STR(I,KP1) = DUM1*DIMAG(ZZ2)
2             CONTINUE
           KDUM = KKK
              DO 3 I = 1,2
              R(1,KDUM) = DRCOSY*STR(2,KDUM) + DRCOSX*STR(3,KDUM)
              R(2,KDUM) = DRCOSY*STR(1,KDUM) + DRCOSX*STR(2,KDUM)
```

```
            IF (SYMX)  THEN
               KKK = KKK + 1
               GO TO 10
            END IF
            KDUM = KP1
3           CONTINUE
         KKK = KKK + 2
10       CONTINUE
      RETURN
      END
C*********************************************************************
C                                                                    *
C                              GAUSS1                                *
C                                                                    *
C*********************************************************************
      SUBROUTINE GAUSS1(L,LINT,XI,WT)
C
C.... GAUSS POINTS AND WEIGHTS FOR ONE DIMENSION
C
      IMPLICIT DOUBLE PRECISION (A-H,O-Z)
      DIMENSION XI(*),WT(*)
      IF (L.EQ.24)  GO TO 24
      IF (L.EQ.32)  GO TO 32
      IF (L.EQ.40)  GO TO 40
      GO TO (1,2,3,4,5,6,7,8,9,10,99,12,99,99,99,16,99,99,99,20),L
C.... 1 PT INTEGRATION
1     XI(1) = 0.
      WT(1) = 2.
      LINT  = 1.
      RETURN
C.... 2 PT INTEGRATION
2     XI(2) = 1.0D00/DSQRT(3.0D00)
      WT(2) = 1.0
      GO TO 200
C.... 3 PT INTEGRATION
3     XI(3) = DSQRT(0.6D00)
      XI(2) = 0.0
      WT(3) = 0.555555555555556D00
      WT(2) = 0.888888888888889D00
      GO TO 100
C.... 4 PT INTEGRATION
4     XI(4) = 0.861136311594053D00
      XI(3) = 0.339981043584856D00
      WT(4) = 0.347854845137454D00
      WT(3) = 0.652145154862546D00
      GO TO 200
C.... 5 PT INTEGRATION
5     XI(5) = 0.906179845938664D00
      XI(4) = 0.538469310105683D00
      XI(3) = 0.0
      WT(5) = 0.236926885056189D00
      WT(4) = 0.478628670499366D00
      WT(3) = 0.568888888888889D00
      GO TO 100
C.... 6 PT INTEGRATION
6     XI(6) = 0.932469514203152D00
      XI(5) = 0.661209386466265D00
      XI(4) = 0.238619186083197D00
      WT(6) = 0.171324492379170D00
      WT(5) = 0.360761573048139D00
      WT(4) = 0.467913934572691D00
      GO TO 200
C.... 7 PT INTEGRATION
7     XI(7) = 0.949107912342759D00
      XI(6) = 0.741531185599394D00
      XI(5) = 0.405845151377397D00
      XI(4) = 0.0
```

```
      WT(7) = 0.129484966168870D00
      WT(6) = 0.279705391489277D00
      WT(5) = 0.381830050505119D00
      WT(4) = 0.417959183673469D00
      GO TO 100
C.... 8 PT INTEGRATION
8     XI(8) = 0.960289856497536D00
      XI(7) = 0.796666477413627D00
      XI(6) = 0.525532409916329D00
      XI(5) = 0.183434642495650D00
      WT(8) = 0.101228536290376D00
      WT(7) = 0.222381034453374D00
      WT(6) = 0.313706645877887D00
      WT(5) = 0.362683783378362D00
      GO TO 200
C.... 9 PT INTEGRATION
9     XI(9) = 0.968160239507626D00
      XI(8) = 0.836031107326636D00
      XI(7) = 0.613371432700590D00
      XI(6) = 0.324253423403809D00
      XI(5) = 0.0D00
      WT(9) = 0.081274388361574D00
      WT(8) = 0.180648160694857D00
      WT(7) = 0.260610696402935D00
      WT(6) = 0.312347077040003D00
      WT(5) = 0.330239355001260D00
      GO TO 100
C.... 10 PT INTEGRATION
10    XI(10) = 0.973906528517172D00
      XI(9)  = 0.865063366688985D00
      XI(8)  = 0.679409568299024D00
      XI(7)  = 0.433395394129247D00
      XI(6)  = 0.148874338981631D00
      WT(10) = 0.066671344308688D00
      WT(9)  = 0.149451349150581D00
      WT(8)  = 0.219086362515982D00
      WT(7)  = 0.269266719309996D00
      WT(6)  = 0.295524224714753D00
      GO TO 200
C.... 12 PT INTEGRATION
12    XI(12) = 0.981560634246719D00
      XI(11) = 0.904117256370475D00
      XI(10) = 0.769902674194305D00
      XI(9)  = 0.587317954286617D00
      XI(8)  = 0.367831498998180D00
      XI(7)  = 0.125233408511469D00
      WT(12) = 0.047175336386512D00
      WT(11) = 0.106939325995318D00
      WT(10) = 0.160078328543346D00
      WT(9)  = 0.203167426723066D00
      WT(8)  = 0.233492536538355D00
      WT(7)  = 0.249147045813403D00
      GO TO 200
C.... 16 PT INTEGRATION
16    XI(16) = 0.98940093499164993259 6D00
      XI(15) = 0.94457502307323257607 8D00
      XI(14) = 0.86563120238783174388 0D00
      XI(13) = 0.75540440835500303389 5D00
      XI(12) = 0.61787624440264374844 7D00
      XI(11) = 0.45801677765722738634 2D00
      XI(10) = 0.28160355077925891323 0D00
      XI(9)  = 0.09501250983763744018 5D00
      WT(16) = 0.02715245941175409485 2D00
      WT(15) = 0.06225352393864789286 3D00
      WT(14) = 0.09515851168249278481 0D00
      WT(13) = 0.12462897125553387205 2D00
      WT(12) = 0.14959598881657673208 1D00
```

```
      WT(11) = 0.16915651939500253818 9D00
      WT(10) = 0.18260341504492358886 7D00
      WT(9)  = 0.18945061045506849628 5D00
      GO TO 200
C.... 20 PT INTEGRATION
20    XI(20) = 0.99312859918509492478 6D00
      XI(19) = 0.96397192727791379126 8D00
      XI(18) = 0.91223442825132590586 8D00
      XI(17) = 0.83911697182221882339 5D00
      XI(16) = 0.74633190646015079261 4D00
      XI(15) = 0.63605368072651502545 3D00
      XI(14) = 0.51086700195082709800 4D00
      XI(13) = 0.37370608871541956067 3D00
      XI(12) = 0.22778585114164507808 0D00
      XI(11) = 0.07652652113349733375 5D00
      WT(20) = 0.01761400713915211831 2D00
      WT(19) = 0.04060142980038694133 1D00
      WT(18) = 0.06267204833410906357 0D00
      WT(17) = 0.08327674157670474872 5D00
      WT(16) = 0.10193011981724043503 7D00
      WT(15) = 0.11819453196151841731 2D00
      WT(14) = 0.13168863844917662689 8D00
      WT(13) = 0.14209610931838205132 9D00
      WT(12) = 0.14917298647260374678 8D00
      WT(11) = 0.15275338713072585069 8D00
      GO TO 200
C.... 24 PT INTEGRATION
24    XI(24) = 0.99518721999702136018 0D00
      XI(23) = 0.97472855597130949819 8D00
      XI(22) = 0.93827455200273275852 4D00
      XI(21) = 0.88641552700440103421 3D00
      XI(20) = 0.82000198597390292195 4D00
      XI(19) = 0.74012419157855436424 4D00
      XI(18) = 0.64809365193697556925 2D00
      XI(17) = 0.54542147138883953565 8D00
      XI(16) = 0.43379350762604513848 7D00
      XI(15) = 0.31504267969616337438 7D00
      XI(14) = 0.19111886747361630915 9D00
      XI(13) = 0.06405689286260562608 5D00
      WT(24) = 0.01234122979998719954 7D00
      WT(23) = 0.02853138862893366318 1D00
      WT(22) = 0.04427743881741980616 9D00
      WT(21) = 0.05929858491543678074 6D00
      WT(20) = 0.07334648141108030573 4D00
      WT(19) = 0.08619016153195327591 7D00
      WT(18) = 0.09761865210411388827 0D00
      WT(17) = 0.10744427011596563478 3D00
      WT(16) = 0.11550566805372560135 3D00
      WT(15) = 0.12167047292780339120 4D00
      WT(14) = 0.12583745634682829612 1D00
      WT(13) = 0.12793819534675215697 4D00
      GO TO 200
C.... 32 PT INTEGRATION
32    XI(32) = 0.99726386184948156354 5D00
      XI(31) = 0.98561151154526833540 0D00
      XI(30) = 0.96476225558750643077 4D00
      XI(29) = 0.93490607593773968917 1D00
      XI(28) = 0.89632115576605212396 5D00
      XI(27) = 0.84936761373256997013 4D00
      XI(26) = 0.79448379596794240696 3D00
      XI(25) = 0.73218211874028968038 7D00
      XI(24) = 0.66304426693021520097 5D00
      XI(23) = 0.58771575724076232904 1D00
      XI(22) = 0.50689908932229390024 0D00
      XI(21) = 0.42135127613063534536 4D00
      XI(20) = 0.33186860228212764978 0D00
      XI(19) = 0.23928736225213707454 5D00
```

```
      XI(18) = 0.14447196158279649348 5D00
      XI(17) = 0.04830766568773831623 5D00
      WT(32) = 0.00701861000947009660 0D00
      WT(31) = 0.01627439473090567060 5D00
      WT(30) = 0.02539206530926205945 6D00
      WT(29) = 0.03427386291302143310 3D00
      WT(28) = 0.04283589802222668065 7D00
      WT(27) = 0.05099805926237617619 6D00
      WT(26) = 0.05868409347853554714 5D00
      WT(25) = 0.06582222277636184683 8D00
      WT(24) = 0.07234579410884850622 5D00
      WT(23) = 0.07819389578707030647 2D00
      WT(22) = 0.08331192422694675522 2D00
      WT(21) = 0.08765209300440381114 3D00
      WT(20) = 0.09117387869576388471 3D00
      WT(19) = 0.09384439908080456563 9D00
      WT(18) = 0.09563872007927485941 9D00
      WT(17) = 0.09654008851472780056 7D00
      GO TO 200
C.... 40 PT INTEGRATION
40    XI(40) = 0.99823770971055920035 0D00
      XI(39) = 0.99072623869945700645 3D00
      XI(38) = 0.97725994998377426266 3D00
      XI(37) = 0.95791681921379165580 5D00
      XI(36) = 0.93281280827867653336 1D00
      XI(35) = 0.90209880696887429672 8D00
      XI(34) = 0.86595950321225950382 1D00
      XI(33) = 0.82461223083331166319 6D00
      XI(32) = 0.77830565142651938769 5D00
      XI(31) = 0.72731825518992710328 1D00
      XI(30) = 0.67195668461417954837 9D00
      XI(29) = 0.61255388966798023795 3D00
      XI(28) = 0.54946712509512820207 6D00
      XI(27) = 0.48307580168617871290 9D00
      XI(26) = 0.41377920437160500152 5D00
      XI(25) = 0.34199409082575847300 7D00
      XI(24) = 0.26815218500725368114 1D00
      XI(23) = 0.19269758070137109971 6D00
      XI(22) = 0.11608407067525520848 3D00
      XI(21) = 0.03877241750605082193 3D00
      WT(40) = 0.00452127709853319125 8D00
      WT(39) = 0.01049828453115281361 5D00
      WT(38) = 0.01642105838190788871 3D00
      WT(37) = 0.02224584919416695726 2D00
      WT(36) = 0.02793700698002340109 8D00
      WT(35) = 0.03346019528254784739 3D00
      WT(34) = 0.03878216797447201764 0D00
      WT(33) = 0.04387090818567327199 2D00
      WT(32) = 0.04869580763507223206 1D00
      WT(31) = 0.05322784698393682435 5D00
      WT(30) = 0.05743976909939155136 7D00
      WT(29) = 0.06130624249292893916 7D00
      WT(28) = 0.06480401345660103807 5D00
      WT(27) = 0.06791204581523390382 6D00
      WT(26) = 0.07061164739128677969 5D00
      WT(25) = 0.07288658239580405906 1D00
      WT(24) = 0.07472316905796826420 0D00
      WT(23) = 0.07611036190062624237 2D00
      WT(22) = 0.07703981816424796558 8D00
      WT(21) = 0.07750594797842481126 4D00
      GO TO 200
100   LOV2 = (L - 1)/2
      GO TO 300
200   LOV2 = L/2
300   DO 400 II = 1,LOV2
      KK = L - II + 1
      XI(II) = -XI(KK)
```

```
      WT(II) =  WT(KK)
400   CONTINUE
      LINT = L*L
      RETURN
99    WRITE (6,99999) L
      RETURN
99999 FORMAT (10X,'******* ABSCISSAS AND WEIGHT FACTORS NOT AVAILABLE FO
     1R ',I2,' ORDER INTEGRATION *******')
      END
C*********************************************************************
C                                                                    *
C                              MAP                                   *
C                                                                    *
C*********************************************************************
      SUBROUTINE MAP(X,Y,XIO,IEL,ZETA,ZOMEGA)
      IMPLICIT COMPLEX*16 (Z)
      IMPLICIT DOUBLE PRECISION (A-H,O-Y)
      DIMENSION ZETA(2),ZOMEGA(2)
      COMMON /ROOTS  / ZS(2),ZB,ZC
      COMMON /ELPMAP / ZC1(2),ZC2(2),ZK(2)
      DATA  TEST/ .999999999999D00/
C....
C.... THIS SUBROUTINE COMPUTES ZETA(I) AND ZOMEGA(I) (I=1,2)
C.... FOR THE ELLIPTICAL (IEL = 2) AND FILLET (IEL = 3) MAPPING
C.... FUNCTIONS AT THE POINT (X,Y)
C....
      ZDUM = DCMPLX(0.0D00,1.0D00)
      IF (IEL.EQ.2)  ZDUM = DCMPLX(1.0D00,0.0D00)
      DO 100 I = 1,2
         ZI  = X + ZS(I)*Y
         ZRT = ZI**2 - ZK(I)
         ZQR = CDSQRT(ZRT)
C....
C.... DETERMINE THE PROPER BRANCH FOR THE SQUARE ROOT
C....
         IF (X.GT.0.0)  THEN
            IF (DREAL(ZQR).GT.0.0)  ZQR = -ZQR
         ELSE IF (X.LT.0.0)  THEN
            IF (DREAL(ZQR).LT.0.0)  ZQR = -ZQR
         ELSE
            IF (Y.GT.0.0.AND.DIMAG(ZQR).GT.0.0)  ZQR = -ZQR
            IF (Y.LT.0.0.AND.DIMAG(ZQR).LT.0.0)  ZQR = -ZQR
         END IF
C....
C.... COMPUTE ZETA(I) AND THE DERIVATIVE OF OMEGA(I)
C....
         ZETA(I)   = (ZI - ZQR)/(ZC1(I)*ZDUM)
C....
C.... CHECK TO SEE IF THE CORRECT VALUE FOR ZETA(I) HAS BEEN OBTAINED
C.... THE CORRECT VALUE WILL BE OUTSIDE THE UNIT CIRCLE
         AZETA = CDABS(ZETA(I))
         IF (AZETA.LT.TEST)   THEN
            WRITE (6,299)  X,Y,AZETA
            ZETA(I)   = (ZI + ZQR)/(ZC1(I)*ZDUM)
            AZETA = CDABS(ZETA(I))
            IF (AZETA.LT.TEST)   STOP
         END IF
C....
         IF (IEL.EQ.2)  THEN
            ZOMEGA(I) = 0.5D00*(ZC1(I) - ZC2(I)/(ZETA(I)**2))
         ELSE
            ZOMEGA(I) = 0.5D00*(ZC1(I)*ZETA(I) + ZC2(I)/ZETA(I))
            ZETA(I)   = ZDUM*CDLOG(ZETA(I)) - DCMPLX(XIO,0.0D00)
         END IF
100   CONTINUE
      RETURN
299   FORMAT (5X,'*** WARNING - IMPROPER MAPPING INVERSION ***',
```

```
     1        2D15.5,D30.15)
      END
C*********************************************************************
C                                                                     *
C                              CLPXCT                                 *
C                                                                     *
C*********************************************************************
      SUBROUTINE CLPXCT(D,MATYPE,IEL)
      IMPLICIT COMPLEX*16 (Z)
      IMPLICIT DOUBLE PRECISION (A-H,O-Y)
      COMMON /ROOTS  / ZS(2),ZB,ZC
      COMMON /DISPC  / ZP(2),ZQ(2)
      COMMON /ELPMAP / ZC1(2),ZC2(2),ZK(2)
      COMMON /CHECKR / Z0(2)
      DIMENSION D(*),ZROOT(4)
C.... THIS SUBROUTINE COMPUTES THE ROOTS OF THE CHARACTERISTIC
C.... EQ AND OTHER COMPLEX CONSTANTS REQUIRED IN THE ANALYSIS
C....
C.... COMPUTE THE ROOTS FOR ORTHOTROPIC MATERIAL
      IF (MATYPE.EQ.2)  THEN
         C1 = 2.0D00*D(6) + D(8)
         C2 = C1**2 - 4.0D00*D(5)*D(7)
         IF (C2.LE.0.0D00)  THEN
            WRITE (6,99999)
            STOP
         ELSE
            C2    = DSQRT(C2)
            C3    = (C1 - C2)/(2.0D00*D(5))
            C4    = (C1 + C2)/(2.0D00*D(5))
            ZS(1) = DCMPLX(0.0D00,DSQRT(C3))
            ZS(2) = DCMPLX(0.0D00,DSQRT(C4))
            DO 1 J = 1,2
               ZP(J) = D(5)*ZS(J)**2 + D(6)
               ZQ(J) = D(6)*ZS(J) + D(7)/ZS(J)
               Z0(J) = D(5)*ZS(J)**4 + (2.0*D(6) + D(8))*ZS(J)**2 + D(7)
1           CONTINUE
         END IF
C.... DETERMINE ROOTS FOR ANISOTROPIC MATERIAL
      ELSE
         AR = -2.0*D(7)/D(5)
         BR = (2.0*D(6) + D(10))/D(5)
         CR = -2.0*D(9)/D(5)
         DR =  D(8)/D(5)
         P  = -BR
         Q  = AR*CR - 4.0*DR
         R  = 4.0*BR*DR - CR*CR -AR*AR*DR
         A0 = (3.0*Q - P*P)/3.0
         B0 = (2.0*P**3 - 9.0*P*Q + 27.0*R)/27.0
         ZR = CDSQRT(DCMPLX(B0*B0/4.0 + A0**3/27.0,0.0D00))
*        ZY = CDCBRT(-B0/2.0 + ZR) + CDCBRT(-B0/2.0 - ZR) - P/3.0
         ZY = (-B0/2.0 + ZR)**(1.0D0/3.0D0)
     $         + (-B0/2.0 - ZR)**(1.0D0/3.0D0) - P/3.0
         ZR = CDSQRT(AR*AR/4.0 - BR + ZY)
         IF (CDABS(ZR).GT.1.0D-05) THEN
            Z1 = (4.0*AR*BR - 8.0*CR - AR**3)/(4.0*ZR)
            Z2 = 3.0*AR*AR/4.0 - ZR*ZR - 2.0*BR
            ZD = CDSQRT(Z2 + Z1)
            ZE = CDSQRT(Z2 - Z1)
         ELSE
            Z1 = 2.0D00*CDSQRT(ZY*ZY - 4.0D00*DR)
            ZD = CDSQRT(0.75D00*AR*AR - 2.0D00*BR + Z1)
            ZE = CDSQRT(0.75D00*AR*AR - 2.0D00*BR - Z1)
            ZR = DCMPLX(0.0D00,0.0D00)
         END IF
         ZROOT(1) = -AR/4.0D00 + ZR/2.0D00 + ZD/2.0D00
         ZROOT(2) = -AR/4.0D00 + ZR/2.0D00 - ZD/2.0D00
         ZROOT(3) = -AR/4.0D00 - ZR/2.0D00 + ZE/2.0D00
```

```
          ZROOT(4) = -AR/4.0D00 - ZR/2.0D00 - ZE/2.0D00
          I = 0
             DO 2 J = 1,4
                IF (DIMAG(ZROOT(J)).LE.0.0)  GO TO 2
                I = I + 1
                IF (I.GE.3)  GO TO 3
                ZS(I) = ZROOT(J)
2            CONTINUE
             IF (DIMAG(ZS(2)).LT.DIMAG(ZS(1)))  THEN
                ZDUM  = ZS(1)
                ZS(1) = ZS(2)
                ZS(2) = ZDUM
             END IF
             DO 22 I = 1,2
                ZP(I) = D(5)*ZS(I)**2 - D(7)*ZS(I) + D(6)
                ZQ(I) = D(6)*ZS(I) - D(9) + D(8)/ZS(I)
                ZO(I) = D(5)*ZS(I)**4 - 2.0D00*D(7)*ZS(I)**3
     1             + (2.0D00*D(6) + D(10))*ZS(I)**2 - 2.0D00*D(9)*ZS(I)
     2             + D(8)
22           CONTINUE
          END IF
C....
C.... DETERMINE CONSTANTS B AND C . USE ZC1(1) FOR STORAGE
          ZC1(1) = ZS(2) - DCONJG(ZS(2))
          IF (DIMAG(ZC1(1)).GT.0.0D00)  THEN
             ZB = (DCONJG(ZS(2) - ZS(1)))/ZC1(1)
             ZC = (DCONJG(ZS(2)) - ZS(1))/ZC1(1)
          ELSE
             WRITE (6,99997)
             STOP
          END IF
C.... DETERMINE CONSTANTS NEEDED FOR INVERSION OF MAPPING FUNCTION
          IF (IEL.EQ.3)  D(17) = D(16)
             DO 10 I = 1,2
             ZC1(I) = D(16) - D(17)*DCMPLX(0.0D00,1.0D00)*ZS(I)
             ZC2(I) = 2.0D00*D(16) - ZC1(I)
             ZK(I)  = D(16)**2 + (D(17)*ZS(I))**2
10           CONTINUE
          RETURN
3            WRITE (6,99998)
             STOP
99997 FORMAT (10X,'*** ERROR - ZS(2) HAS NEGATIVE IMAGINARY PART ***')
99998 FORMAT (10X,'***ERROR - MORE THAN 2 ROOTS WITH POSITIVE REAL',
     1        ' PARTS FOUND')
99999 FORMAT (10X,'***** ERROR - REAL ROOT COMPUTED FOR S(I) *****')
          END
```

Appendix 2

User's Guide: Two-Dimensional Plane Stress/Plane Strain Finite Element Analysis Program with Circular Fillet and Elliptical Void Elements (FPLHYB)

The finite element analysis program FPLHYB was written by Dr. Terry D. Gerhardt while working at the USDA Forest Products Lab. in Madison, WI. It is an extension of the program of R.L. Taylor described in pages 677-757 of The Finite Element Method, 2nd Ed., by O.C. Zienkiewicz, which includes the linear (4-node) and quadratic (8-node) quadrilateral isoparametric elements. The cubic (12-node) quadrilateral isoparametric element is described by Dr. Gerhardt in USDA FPL Gen. Tech. Rpt. FPL 35, "Plane Stress Analysis of Wood Members Using Isoparametric Finite Elements" (March 1983). He explains the fillet and void elements in "A hybrid/finite element approach for stress analysis of notched anisotropic materials," ASME J. Appl. Mechanics 51:804-810 (Dec. 1984). Details on the usage of the program have been provided by Dr. Gerhardt.

Input Data File Instructions

Except for the macro instruction FEAP and the associated line of numeric data, the input instructions may appear in any order. (Note that the input instructions must precede the

macro control instructions, e.g., LOOP, TANG, NOPR, described later.) The data associated with each instruction must directly follow that instruction. All lines of the input data file begin in column 1 and are a maximum of 80 characters long. Entries typed in all-capital letters are to be included exactly as shown. Lower-case, italic, or Greek entries are to be replaced by the user with the appropriate data. Names of variables used in the program are given in italics or Greek letters. The FORTRAN format for each input line is given in brackets at the end of that line, e.g. [7F10.3]. Commas are included here for readability; no commas belong in the data file (except as desired in alphanumeric comments.) The term "unit" refers to the output device specified in the FORTRAN WRITE statement, e.g., WRITE(6,*) sends free-form output to unit 6. Blank lines may be included in the data file for clarity, but are unnecessary except as noted.

Input instruction FEAP (general mesh data):

FEAP alphanumeric comments regarding the data file [20A4]

numnp, numel, nummat, ndm, ndf, nen, nad [7I5]

where:

numnp = no. of nodes in the mesh

numel = no. of elements in the mesh

nummat = no. of material types. A different material type is needed for each type of element (e.g. cubic

isoparametric vs. hybrid fillet), and for each individual hybrid element, whether or not the elastic properties are the same. Similarly, separate material types would be needed for elements of the same type having different elastic properties or orientations (e.g. grain directions for wood).

ndm = no. of spatial dimensions, 1-3. For the element types currently implemented in this program, *ndm*=2.

ndf = no. of nodal degrees of freedom, i.e. no. of unknowns at each node. For typical plane stress mechanical problems, *ndf*=2 (i.e., x and y displacements).

nen = maximum no. of nodes per element. In a mesh containing both the 12-node cubic isoparametric element and a 13-node hybrid element, for example, *nen*=13.

nad = amount of additional space reserved for element matrices, above (*ndf***nen*). This may be omitted in most cases. See Zienkiewicz, pp. 690-691. *nad*>0 will be required if extra series expansion terms are used in the hybrid element definitions (see definitions of L_0 and L_F in "Macro Instruction MATE" below.)

Example:

```
FEAP   CENTER-NOTCHED RED OAK BEAM, PHI=.3, DELTA=.6
  235   37    2    2    2   13
```

(Note that *nad*=0 is implicit.)

Input Instruction MATE (material property and element type data):

(4 to 8 lines of data for each material/element type):

MATE [A4]

ma, *iel*, alphanumeric comments [I5,4X,I1,17A4]
matype, *i*, *l*, *k*, θ_g [4I5,F10.0]
Material Properties [8F10.0] :
(for *matype*=1) ρ, E, ν
(for *matype*=2) ρ, E_x, ν_{xy}, E_y, G_{xy}, (E_z, ν_{xz}, ν_{yz})
(for *matype*=3) ρ, E_1, ν_{12}, E_2, G_{12}, (E_3, ν_{13}, ν_{23})
(for *matype*=4) ρ, D_{11},D_{12},D_{13},D_{22},D_{23},D_{33}
{end of MATE data for isoparametric elements, *iel*=1}
for hybrid elements, *iel*=2 or 3:
numnod, *nodsid*, *numsid*, L_0, L_F, *isym*, *nstrpt*, *igint*,
numout, $ifix_2$, $ifix_1$ [16I5]
a, *b*, θ_s, θ_f, X_0, Y_0 [6F10.0]
for hybrid elements (*iel*=2 or 3), when numout> 0:
X_1, Y_1, (X_2, Y_2, X_3, Y_3, X_4, Y_4) [8F10.0; can be 2 lines]
where:

ma = material set number (consecutive integers)
iel = element type number. *iel*=1 for plane stress/ plane strain isoparametric elements; *iel*=2 for the hybrid elliptical void element; *iel*=3 for the hybrid circular fillet element

.....

matype = 1 for isotropic materials (not available for the hybrid elements);
2 for materials orthotropic in the global x-y plane;
3 for materials orthotropic in a local 1-2 plane, where θ_g is the angle (measured counter-clockwise) from the global x to the local 1 axis;
4 for anisotropic materials

i = 0 for plane strain loading;
any other integer for plane stress loading

l = order of Gauss quadrature for stiffness matrix determination (same recommendations as for k below)

k = order of Gauss quadrature for stress determination: recommended values are 3 for cubic, 2 for quadratic and 1 for linear isoparametric elements. For the hybrid elements, l and k can have the values 1-10, 12, 16, 20, 24, 32 or 40. Higher-order integration can be performed by using multiple integration intervals per hybrid element side, using *igint* > 1 (see below).

θ_g = as described above for *matype*=3. It is not needed otherwise.

.....

ρ = density (optional; used only in dynamic problems)

E, ν = elastic modulus and Poisson's ratio for isotropic material

E_x, E_y, E_z=elastic moduli in the principal directions of a material orthotropic in the global x-y plane

ν_{xy}, ν_{xz}, ν_{yz} G_{xy} = Poisson's ratios and shear modulus for a material orthotropic in the global x-y plane

E_1, ν_{12}, E_2, G_{12}, E_3, ν_{13}, ν_{23} =
elastic parameters for a material orthotropic in a local 1-2 plane oriented at θ_g degrees counterclockwise from the global x-y axes

D_{ij} = material stiffness matrix coefficients for an anisotropic material (see S.G. Lekhnitskii, Theory of Elasticity of an Anisotropic Body, Mir Publ., 1981.)

numnod = number of nodes per hybrid element

nodsid = number of nodes per side of the hybrid element (determines the polynomial order of the displacement vector {u})

numsid = number of hybrid element sides that contain nodes, i.e., over which integration is done

L_0, L_F = initial and final terms of the Laurent or Taylor series expansion to be assumed for the stress function in the hybrid element. If *iel*=2 (elliptical void element), the Laurent series expansion is performed. This calls for equal numbers of positive and negative series terms; use $L_0=-L_F$. (There is no "zeroth" term.) For *iel*=3 (circular fillet element), the Taylor series expansion is used, calling for positive terms only; use $L_0=1$. The number of Taylor series coefficients = $2(1+L_F-L_0)=2L_F$ when $L_0=1$. The number of Laurent series coefficients = $4L_F$ (assuming $L_0=-L_F$). The minimum number of series expansion coefficients needed to obtain a non-singular stiffness matrix is equal to the element degrees of freedom (DOF). For plane problems, element DOF=(*ndf***nen*)-3, since there are 3 rigid-body modes which are suppressed. Gerhardt found, and I concur, that results were changed insignificantly by the use of more than the theoretical minimum number of series terms. Thus, for a 13-node hybrid fillet element:

ndf=2, *nen*=13, ∴ element DOF = (2*13)-3=23.

no. of series coefficients ≥ 23

$L_0=1$, $L_F \geq 23/2$, ∴ minimum $L_F = 12$.

If you choose to use more series expansion terms

than are theoretically needed, you should specify *nad*>0 in the FEAP macro instruction. Add 2 to *nad* for each addition of one to L_F in excess of the number suggested above.

isym = variable to impose symmetry (for elliptical void element, *iel*=2, only)
isym = 0: no symmetry;
isym = 2: symmetry about x and y axes;
isym = 1: symmetry about x axis;
isym = -1: symmetry about y axis.
(The last 2 have not been thoroughly tested.)

nstrpt = number of points along the elliptical or circular free surface at which stresses and strains are to be evaluated. The displacements, strains and stresses at these points will be written to unit 26. The angle and principal non-zero stress at each of these points will be written to unit 28.

igint = number of integration intervals per hybrid element side. This is typically 1, but can be >1, e.g., to allow orders of integration greater than 40.

numout = number of lines within the hybrid element along which displacements, stresses and strains are to be calculated. $0 \leq$ *numout* ≤ 4. The starting and ending points of each such line are defined below. The quantities will be evaluated at *nstrpt* points equally spaced along each line, and written to unit 26.

$ifix_2$ = local node number on the hybrid element at which u and v nodal displacements are tied to the analytic displacement field. Not needed if *isym* = 2.

$ifix_1$ = local node number on the hybrid element at which the u nodal displacement is tied to the analytic displacement field. Not needed if *isym* = 2. $ifix_1$ and $ifix_2$ may be any two nodes on the hybrid element which have different x and y coordinates. A good choice for the fillet element is the pair of nodes defining the ends of the fillet. Note that the hybrid elements are numbered consecutively, counterclockwise around the element.

.....

a = length of the elliptical axis in the x direction (for *iel*=2); fillet radius (for *iel*=3).

b = length of the elliptical axis in the y direction (for *iel*=2); fillet radius (for *iel*=3).

θ_s = angle from the x-axis counterclockwise to the beginning of the elliptical or circular surface

θ_f = angle from the x-axis counterclockwise to the end of the elliptical or circular surface

X_0, Y_0 = coordinates of the center of the elliptical or circular cutout

.....

X_i, Y_i = coordinates of beginning and ending points for the *numout* lines along which stresses, etc. are calculated and output. Subscript i = 1,3,5... for starting points; i = 2,4,6... for ending points.

Input Instruction COOR (nodal coordinate data):

COOR [A4]

n, *ng*, X_n, Y_n [multiple lines, each 2I5,2F10.0]

(A blank line must follow the last data line.)

where:

n = node number

ng = generation increment for automatic generation of equally-spaced nodes along a straight line. For example, if such nodes are numbered 18,31,44,... then *ng* = 13. Only the first and last node in such a sequence need be specified with separate data lines here; *ng* for the last node in each sequence must be 0. For use with an external automatic mesh generator, *ng*=0 for all nodes, since each node is explicitly specified in the input file.

X_n, Y_n = coordinates of node *n*.

Input Instruction Command ELEM (element definition data):

ELEM [A4]

l, *ma*, ln_1, ln_2, ln_3, ln_4, ... ln_{nen}, *ng* [multiple lines, each 16I5]

(A blank line must follow the last data line.)

where:

l = element number (consecutive integers; elements must be defined in order)

ma = material set number (see MATE above)

ln_1 ... ln_{nen} =
global node numbers of the local nodes 1 through *nen* (see FEAP above). For the hybrid elements, nodes are numbered from the right end of the curved surface counterclockwise (CCL) around the element. For the cubic element, nodes are numbered CCL starting with the 4 corners, then the 4 nodes immediately CCL of the corners, then the remaining 4 nodes (see Figure A1). Note: In meshes containing element types having different numbers of nodes, use node numbers = 0 for the non-existent nodes in an element. That is, each line of the ELEM data must contain the same number of integer entries.

ng = generation increment for automatic generation of consecutive similar elements. For use with an external automatic mesh generator, set *ng* = 0 (or simply omit it.) Otherwise, *ng* is the integer difference in global node numbers of the same local node in adjacent elements. EX.: For a single row of 12-node cubic elements with global node numbering from lower left upward and then rightward, *nen* = 8. That is, local node 1 of element 1 is global #1, and ln_1 of el. 2 is global #9. For automatic element generation, specify the node numbers and *nen* for the first element in the repeated string, and specify the node numbers and *nen* = 0 for the

last element in the string. Example B illustrates this feature.

Input Instruction BOUN (boundary condition data):

BOUN [4I5]

n, ng, bc_1, bc_2, ..., bc_{ndf} [multiple lines, each 16I5]

(A blank line must follow the last data line.)

where:

n = global number of restrained node

ng = generation increment for automatic generation of identical boundary conditions (b.c.'s) for a series of nodes. ng is the integer difference between node numbers of adjacent nodes having the same b.c.'s. Use ng=0 for nodes with non-repeating b.c.'s.

$bc_1 \ldots bc_{ndf}$ =

boundary condition code for each nodal degree of freedom of node n. bc=0 for each unrestrained degree of freedom; bc<0 the first in a series of nodes with identical restraints; bc>0 specifies a restrained d.o.f. which is not part of a repeating series.

EXAMPLE:

```
BOUN
    1     1    -1     0
    7     0     1     0
  183     0     0     1
```

This describes one-half of a symmetrical beam with 2 d.o.f. per node (x and y displacements). The b.c.'s are a vertical

shear release along the centerline (nodes 1-7) and a simple support (free in x and restrained in y) at node 183.

Input Instruction FORC (forces applied at nodes):

FORC [A4]

n, ng, f_1, f_2,..., f_{ndf} [multiple lines, each 2I5, 7F10.0]

where:

n = global node number

ng = generation increment (as for BOUN above)

f_1, ..., f_{ndf} =
force applied at node n in the specified degree of freedom

EX: for the 2-DOF beam of the previous example:

```
FORC
    7     0          0.      -50.0
```

This specifies a downward (negative y) force applied at node 7.

Note: To specify a uniformly distributed load along a given line, the loads to be applied to the individual nodes will not be directly proportional to the "tributary area" of each node, except when using linear elements. The proportioning of loads among the nodes is governed by the polynomial interpolation function used (see Zienkiewicz, p. 222). For cubic elements, the loads are divided 1:3:3:1 among the 4 nodes along a side of a given element. This is shown in Examples A and B.

Macro Control Instructions:

The following instructions are included in the input stream to control the flow of job execution and the performance of auxiliary functions such as input echo (restatement of input

data in the output file to facilitate debugging). The order in which these commands appear corresponds to the order in which they will be executed. All macro control instructions occupy the first 4 columns of a line (A4 format) which contains no other characters or numeric data, except as noted below. All of these instructions (except LNZD, OTMH, and STOP) are described by R.L. Taylor in Zienkiewicz, pp. 693, 695-703. Macro instructions needed for solving problems other than static plane elasticity (e.g. thermal, dynamic and eigenvalue) are also described in that reference. In the following descriptions, "mesh data" refers to the data and instructions described earlier in this document (e.g. nodal coordinate and element data).

These descriptions are in an order in which the instructions might appear for a typical static linear elasticity problem. The MESH and END instructions are important in defining multiple loading cases to be solved for the given structure. LOOP and NEXT are used for iterative solutions, e.g. for nonlinear problems.

NOPR - Suppress input echo for subsequent portions of the input data. If placed between the end of the COOR data and the ELEM statement, for example, the output file would contain all of the user-input data up to and including the nodal coordinates, but not the element data and any subsequent data.

PRIN - Reactivate the (default) input echo feature.

END - End mesh data input.

MACR - Begin processing macro control instructions.

OTMH - optional instruction which writes a separate output file (sent to unit 24) containing the mesh data for subsequent plotting. (See "Output Files" below.)

LNZD - "linear, no non-zero displacements". This optional instruction is used in linear problems with no non-zero imposed nodal displacements to delete the unnecessary computational step of modifying the load vector.

TANG - compute symmetric tangent stiffness matrix of the f.e. structure.

FORM - Form the right-hand side of the system equations after imposing displacement boundary conditions.

SOLV - Solve the system of equations for the nodal unknowns.

DISP - Write the nodal displacements to the main output file (unit 6).

STRE - Calculate the stresses and strains at the Gauss points within each element, and write them to the main output file (unit 6).

MESH - Accept new mesh data, e.g. for a second loading case. The MESH instruction is followed by other macro instructions specifying subsequent program execution, then by an END instruction, followed by the new mesh data lines, and finally another END command. Multiple END instructions are used to specify multiple load cases; boundary conditions cannot be changed within a single FE run.

LOOP - Begin a repeated set of macro instructions. The loop will execute N times, where N is the integer in columns 11-15 of the line containing LOOP.

NEXT - end the LOOP construct

Example Data Files:

Example data files A and B include multiple load cases, with annotations indicating the lines which would be omitted for a single case. A drawing of each mesh is included.

Output Files:

Each finite element analysis using FPLHYB results in from one to six output files. Depending on the user's definition of input/output units on the given computer system, these files may be sent to a disk (or other storage system), the terminal, or an attached printer. A useful option is to route all output files to a disk for subsequent inspection, editing and optional printing. The files are described below with reference to the FORTRAN unit number to which they are sent.

Unit	Description
6	Main output file (120 columns wide): contains echo of input data except when NOPR is in effect; includes nodal displacements if DISP was invoked, and stresses and strains if STRE was invoked. It includes a record of all macro instructions which were executed, and all error and warning messages from the program. Each quantity in this file is labeled for ease of interpretation.
24	mesh output file, for diagnostic plotting (80 columns wide): The first line contains the number of nodes in the mesh, number of elements, number of spatial dimensions (2 for the cases discussed here) and maximum

number of nodes per element. The next group of lines (one line per element) gives the global node numbers of the nodes in each element, in order of their local node numbers. The last group of lines gives the nodal coordinates of each node in the structure (one line per node.) This file results from the macro instruction OTMH.

25 strains in isoparametric cubic elements (78 columns wide): each line gives the strains calculated at a particular Gauss point within a given element, in the format:
element number; x and y coordinates; strains ε_x; ε_y; γ_{xy}

26 quantities evaluated within hybrid element(s) (120 columns wide): The number of lines in this file depends on the values of *nstrpt* and *numout* set in the MATE data (see "Input Instruction MATE" above.) Each line gives the following values for a specified point within a given hybrid element:
coordinates x, y; displacements u, v; strains ε_x, ε_y, γ_{xy}; and stresses σ_x, σ_y, τ_{xy}.
The file will contain (*numout* + 1) sets of *nstrpt* lines. The first set gives the results for the specified points along the elliptical void or fillet surface (from angle θ_s to angle θ_f). Subsequent sets give the results for each line within the element specified for output with *numout*, X_i and Y_i (see pp. 4-5 above).

27 diagnostic file for hybrid elements (20 columns wide):
Line 1: number of coefficients in the series expansion.
Following lines: value of each series expansion coefficient . This format is repeated for each hybrid element in the mesh.

28 hoop stresses along elliptical or circular void surface (40 columns wide): one set of *nstrpt* lines for each hybrid element. Each line gives an angle, in degrees, between θ_s and θ_f, and the principal non-zero stress (i.e., the hoop stress) at that angle along the free surface. Angles are measured counterclockwise from the horizontal.

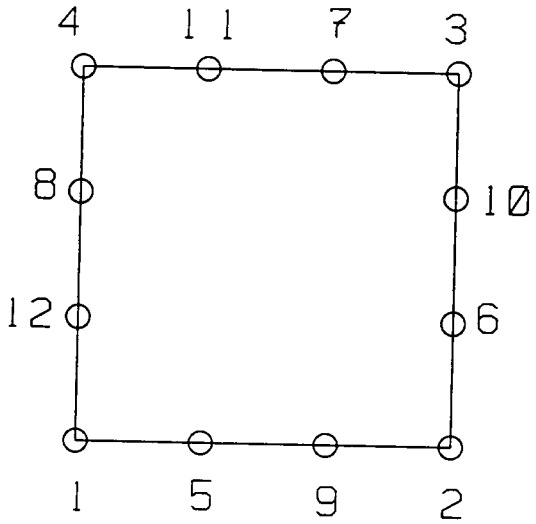

A. isoparametric cubic element

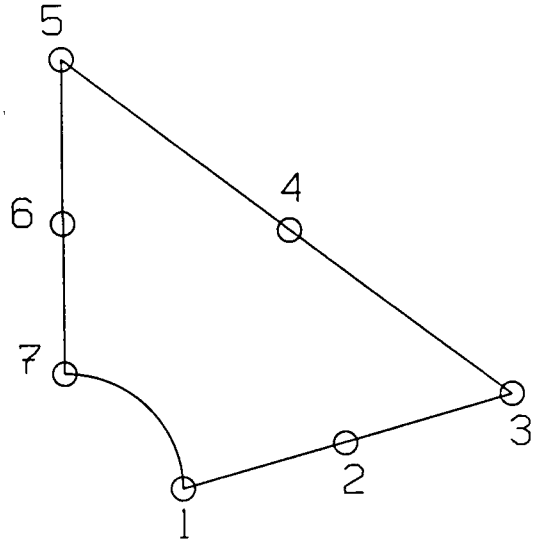

B. quadratic fillet element

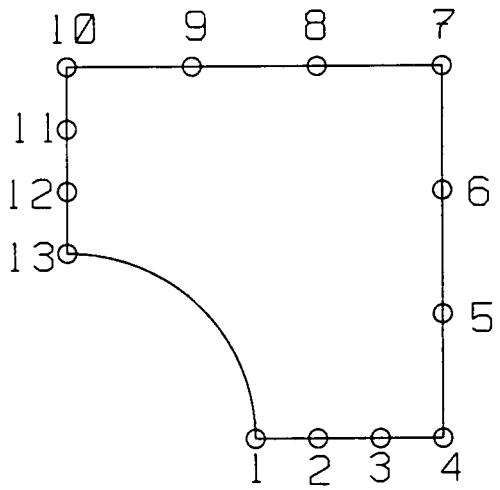

C. cubic fillet element

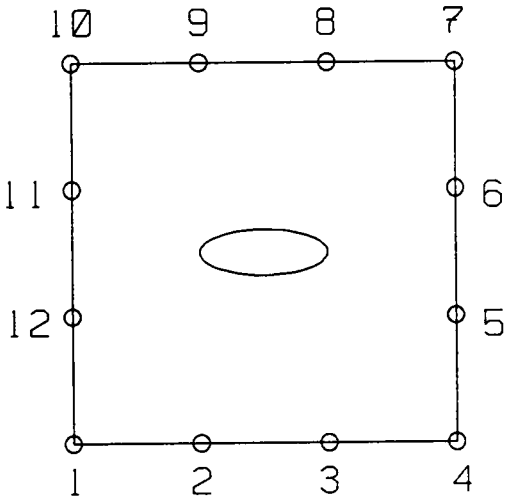

D. cubic elliptical void element

Figure A1. Local node numbering for the isoparametric cubic quadrilateral element (A); a 3-sided quadratic hybrid fillet element (B); a 4-sided cubic hybrid fillet element (C); and a 4-sided cubic hybrid elliptical void element (D). Note: The number of element sides and the order of the element are independent parameters.

Example A: Input Data File for Notched Beam

Notes: Comments enclosed in brackets {} are not part of the input data and must not be included in an actual data file. Two load cases are included: 1) center-notched beam with quarter-point load (only the right half of the symmetric beam is analyzed); and 2) stepped bar under axial tension. The mesh is shown in Figure A2.

```
FEAP
   94   13    2    2    2   13   {nad=0 is implicit.}
MATE
    1    1   ISOPARAMETRIC CUBIC ELEMENT   EX/EY = EX/GXY = 12
    2    1    3    3
             1200000      .4000    100000    100000
    2    3   HYBRID FILLET ELEMENT 1  EX/EY = EX/GXY = 12
    2    1   12   12
             1200000      .4000    100000    100000
   13    4    4    1   12    0   91    1    0   13    1
 1.155000  1.155000       0.0      90.0  0.621923  0.945000

NOPR  {This suppresses echo of the coordinate and element data.}

COOR
    1    0  0.000000  2.100000
    2    0  0.000000  2.566667
    3    0  0.000000  3.033333
    4    0  0.000000  3.500000
    5    0  0.207308  2.100000
    6    0  0.207308  3.500000
    7    0  0.414615  2.100000
    8    0  0.414615  3.500000
    9    0  0.621923  2.100000
   10    0  0.621923  2.566667
   11    0  0.621923  3.033333
   12    0  0.621923  3.500000
   13    0  1.473590  3.500000
   14    0  1.776923  0.000000
   15    0  1.776923  0.315000
   16    0  1.776923  0.630000
   17    0  1.776923  0.945000
   18    0  2.243590  0.000000
   19    0  2.243590  0.945000
   20    0  2.325256  3.500000
   21    0  2.710256  0.000000
   22    0  2.710256  0.945000
   23    0  3.176923  0.000000
```

24	0	3.176923	0.315000
25	0	3.176923	0.630000
26	0	3.176923	0.945000
27	0	3.176923	1.796667
28	0	3.176923	2.648333
29	0	3.176923	3.500000
30	0	3.806923	0.000000
31	0	3.806923	0.945000
32	0	3.806923	3.500000
33	0	4.436923	0.000000
34	0	4.436923	0.945000
35	0	4.436923	3.500000
36	13	5.066923	0.000000
75	0	22.000000	0.000000
37	13	5.066923	0.315000
76	0	22.000000	0.315000
38	13	5.066923	0.630000
77	0	22.000000	0.630000
39	13	5.066923	0.945000
78	0	22.000000	0.945000
40	13	5.066923	1.796667
79	0	22.000000	1.796667
41	13	5.066923	2.648333
80	0	22.000000	2.648333
42	13	5.066923	3.500000
81	0	22.000000	3.500000
43	13	6.948376	0.000000
69	0	18.237094	0.000000
44	13	6.948376	0.945000
70	0	18.237094	0.945000
45	13	6.948376	3.500000
71	0	18.237094	3.500000
46	13	8.829829	0.000000
72	0	20.118547	0.000000
47	13	8.829829	0.945000
73	0	20.118547	0.945000
48	13	8.829829	3.500000
74	0	20.118547	3.500000
82	0	22.666667	0.000000
83	0	22.666667	0.945000
84	0	22.666667	3.500000
85	0	23.333333	0.000000
86	0	23.333333	0.945000
87	0	23.333333	3.500000
88	1	24.000000	0.000000
91	1	24.000000	0.945000
94	0	24.000000	3.500000

```
 ELEM   {ng=0 is implicit, i.e., the rightmost column is omitted}
     1    1    1    9   12    4    5   10    8    3    7   11    6    2    0
     2    1   14   23   26   17   18   24   22   16   21   25   19   15    0
     3    2   17   19   22   26   27   28   29   20   13   12   11   10    9
     4    1   23   36   39   26   30   37   34   25   33   38   31   24    0
     5    1   26   39   42   29   31   40   35   28   34   41   32   27    0
     6    1   36   49   52   39   43   50   47   38   46   51   44   37    0
     7    1   39   52   55   42   44   53   48   41   47   54   45   40    0
     8    1   49   62   65   52   56   63   60   51   59   64   57   50    0
     9    1   52   65   68   55   57   66   61   54   60   67   58   53    0
    10    1   62   75   78   65   69   76   73   64   72   77   70   63    0
    11    1   65   78   81   68   70   79   74   67   73   80   71   66    0
    12    1   75   88   91   78   82   89   86   77   85   90   83   76    0
    13    1   78   91   94   81   83   92   87   80   86   93   84   79    0

 PRIN   {This reactivates input echo, to allow examination of the loads
          and boundary conditions within the output file.}
 BOUN   {boundary conditions for simply-supported center-notched beam}
     1    1   -1    0
     4    0    1    0
    75    0    0    1

 END
 MACR
 LNZD
 TANG
 LOOP          2
 MESH
 FORM
 SOLV
 DISP
 STRE
 NEXT
 END
 FORC     {single downward load at quarter-span}
    55    0          0 -0.180859

 END
 FORC     {loads applied to right-end nodes, scaled for uniform tension}
    88    0     .04725        0.
    89    0     .14175        0.
    90    0     .14175        0.
    91    0     .17500        0.
    92    0     .38325        0.
    93    0     .38325        0.
    94    0     .12775        0.

 END
 STOP
```

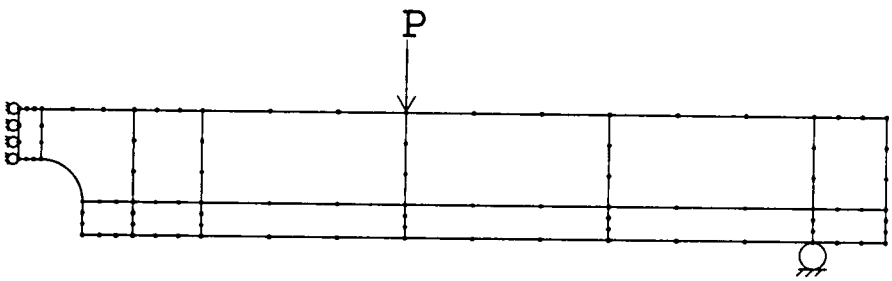

Figure A2. Finite element mesh, example A. R=1.155in., X_0=0.622in., Y_0=0.945in., h=3.5in., right support at x=22in.

Example B: Input Data File for Member with Elliptical Void

Notes: Comments enclosed in brackets {} are not part of the input data and must not be included in an actual data file. The mesh is shown in Figure A3.

```
FEAP
   76    9    2    2    2   12   {nad=0 is implicit.}
MATE
    1    1   ISOPARAMETRIC CUBIC ELEMENT   EX/EY = EX/GXY = 12
    2    1    3    3
             1200000      .4000    100000    100000
    2    2   HYBRID VOID ELEMENT  EX/EY = EX/GXY = 12
    2    1   12   12
             1200000      .4000    100000    100000
   12    4    4   -6    6    2  100    1    2  {ifix2, ifix1 unneeded}
       2.0       1.0       0.0     360.0      14.0       1.5
      12.0       1.5      13.0       1.5  {line from left edge of void}
      14.0       0.0      14.0       1.0  {line from bottom edge of void}

NOPR  {This suppresses echo of the coordinate and element data.}

COOR
    1    8       0.0       0.0
   33    0      12.0       0.0
    2    8       0.0       1.0
   34    0      12.0       1.0
    3    8       0.0       2.0
   35    0      12.0       2.0
    4    8       0.0       3.0
   36    0      12.0       3.0
    5    8       1.0       0.0
   29    0      10.0       0.0
    6    8       1.0       3.0
   30    0      10.0       3.0
    7    8       2.0       0.0
   31    0      11.0       0.0
    8    8       2.0       3.0
   32    0      11.0       3.0
   37    0 13.333333       0.0
   38    0 13.333333       3.0
   39    0 14.666667       0.0
   40    0 14.666667       3.0
   41    8      16.0       0.0
   73    0      28.0       0.0
   42    8      16.0       1.0
   74    0      28.0       1.0
   43    8      16.0       2.0
   75    0      28.0       2.0
   44    8      16.0       3.0
```

```
   76    0       28.0        3.0
   45    8       17.0        0.0
   69    0       26.0        0.0
   46    8       17.0        3.0
   70    0       26.0        3.0
   47    8       18.0        0.0
   71    0       27.0        0.0
   48    8       18.0        3.0
   72    0       27.0        3.0

ELEM
    1    1    1    9   12    4    5   10    8    3    7   11    6    2    8
    4    1   25   33   36   28   29   34   32   27   31   35   30   26    0
    5    2   33   37   39   41   42   43   44   40   38   36   35   34    0
    6    1   41   49   52   44   45   50   48   43   47   51   46   42    8
    9    1   65   73   76   68   69   74   72   67   71   75   70   66    0

PRIN   {This reactivates input echo, to allow examination of the loads
            and boundary conditions within the output file.}
BOUN
    1    1   -1    0
    4    0    1    1

FORC     {loads applied to right-end nodes, scaled for uniform tension}
   73    0       10.0        0.
   74    0       30.0        0.
   75    0       30.0        0.
   76    0       10.0        0.

END
MACR
LNZD
TANG
FORM
SOLV
DISP
STRE
END
STOP
```

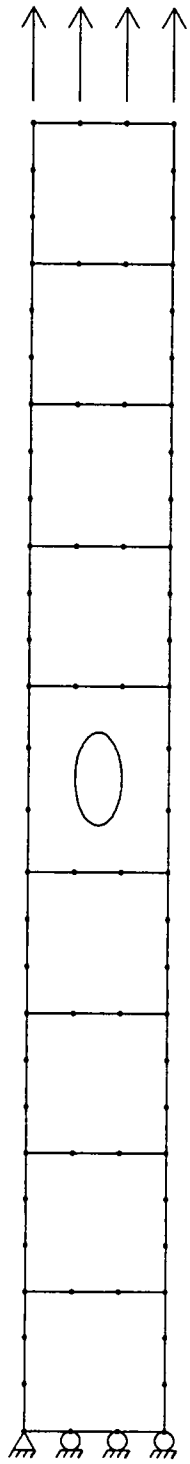

Figure A3. Finite element mesh, example B. a=2.0in., b=1.0in., X_0=14.0in.,. Y_0=1.5in., h=3.0in., length=28in.

Appendix 3: APL FE Mesh Generator for Interior-Notched Beams. Program Design and Listing

The overall structure of the mesh generator is given on this page. Each APL function begins on the page number shown in brackets {}. Indentation is used to indicate the level of the (sub)function, i.e., the name of a calling function is indented less than the names of its subfunction(s).

```
MESHDIM {297}
     MESH {298}
          NODE1 {302}
               EXTEND {284}
                    EXTDOWN {282}
                    EXTUP {289}
                    EXTRIGHT {287}
                    EXTLEFT {285}
                         OCNLEFT {304}
                    BTWFIL {274}
          INSRECT {293}
               REORD {303}
               NEWY {302}
               NEWX {301}
          ELEM1 {278}
               ELEM1S1 {279}
                    ELEM1S2 {280}
               ADD1 {271}
                    LEFTFIL {294}
          MATEDATA {295}
          COORDATA {276}
          ELEMDATA {277}
          BOUNFORC {272}
               BOUNFORCS1 {273}
                    BOUNFORCS2 {274}
          NEWBOUNFORC {299}
               FORCcp {291}
               FORCqp {292}
               FORCud {293}
```

```
    ∇ RES←ADD1;P
[1]  ⍝   This fn. catenates element side definition vectors counterclockwise
[2]  ⍝   around each element to form to 13-col.-wide elmt. definition array
[3]  ⍝   RES.  Each row contains the node no's. defining a given element.
[4]  ⍝   The side definition arrays AR, L, B and T are formed in ELEM1, which
[5]  ⍝   invokes ADD1.
[6]  ⍝.....................................................................
[7]  ⍝   Add right side nodes to bottom nodes:
[8]   P←AR[;1]⍳B[;4] ⍝                points to 1st occurrence of the bottom side
[9]  ⍝                                 ... end nodes among the R side bottom nodes
[10]  AR←AR,[1] 1 4 ⍴0 ⍝              add row of 0's to bottom of AR
[11]  RES←B,[2]AR[P; 2 3 4] ⍝         catenate approp. R side nodes onto B
[12] ⍝.....................................................................
[13] ⍝   Add top nodes to bottom + right side nodes:
[14]  P←T[;1]⍳RES[;7] ⍝               points to the 1st occurrence of right side
[15] ⍝                                 ... top nodes among the top side right nodes
[16]  T←T,[1] 1 4 ⍴0 ⍝                add row of 0's to bottom of T
[17]  RES←RES,[2]T[P; 2 3 4] ⍝        catenate approp. top nodes onto RES
[18] ⍝.....................................................................
[19] ⍝   Add left side nodes to bottom + right + top side nodes.
[20] ⍝   If node 13 ≡ node 1, then node 13 is set to 0 (i.e. for 12-node
[21] ⍝      isoparametric elements.)
[22]  P←L[;1]⍳RES[;10] ⍝              points to 1st occurrence of the top side...
[23] ⍝                                 ...left nodes among the left side top nodes
[24]  L←L,[1] 1 4 ⍴0 ⍝                add row of 0's to bottom of L
[25]  RES←RES,[2]L[P; 2 3 4] ⍝        catenate approp. L side nodes onto BRT
[26]  RES[;13]←RES[;13]×RES[;13]≠RES[;1] ⍝   replace 13-nodes w/ 0's as needed
[27]  ⍎(XCD>0)/'RES←LEFTFIL RES' ⍝            invoke LEFTFIL to define left f.e.
    ∇
```

```
    ∇ BOUNFORC;B1;B2;I;MIN;P;T;TEMP;X;Y
[1]   ⍝   This fn. writes the BOUN, FORC and macro control card lines to the
[2]   ⍝   DOS data file tied to file no. ¯999 for use with FORTRAN finite
[3]   ⍝   element analysis program FPLHYB.  Quarter-point loading is be used
[4]   ⍝   for V/M=0 (i.e., XCD=0); otherwise, center-point loading is used.
[5]   ⍝   Nodal coordinate array XY, and geometric parameters BL, OH, H and D
[6]   ⍝   must be in the active WS.        Latest update 26 November 1988.
[7]    X←XY[;1] ◇ Y←XY[;2]
[8]    T←⎕TCNL,⎕TCLF ⍝                     newline, linefeed characters
[9]   ⍝   for offcenter notches:
[10]   ⍎(XCD>0)/'TEMP←BOUNFORCS1 XY ◇ →L10'
[11] ⍝.....................................................................
[12] ⍝   for center notches:
[13]   MIN←⌊X-(BL-OH)÷2 ⍝                  x-distance of ea. node from 1/4 point
[14]   I←((MIN=⌊/MIN)∧Y=H)/⍳⍴X ⍝           node no. at which load will be placed
[15]   P←(H*2)÷6×BL-OH+X[I] ⍝              force for unit gross section stress
[16]   B1←¯1+(X>0)⍳1 ⍝                     highest x-constrained node (at x=0)
[17]   B2←(X=BL-OH)⍳1 ⍝                          y-constrained node (roller)
[18]   TEMP←T,'BOUN',T ⍝                         write top line (BOUN)
[19]   TEMP←TEMP,'    1    1   -1    0',T ⍝     1st constraint line
[20]   TEMP←TEMP,(,'4I5' ⎕FMT B1, 0 1 0),T ⍝     2nd constraint line
[21]   TEMP←TEMP,(,'4I5' ⎕FMT B2, 0 0 1),T,T ⍝   last constraint line
[22]   TEMP←TEMP,'FORC',T ⍝                     write top FORC line
[23]   TEMP←TEMP,(5 0 ⍕I),'    0          0 -',,'F8.6' ⎕FMT P
[24] ⍝.....................................................................
[25] L10:TEMP←TEMP,T,T
[26] ⍝   The next 2 lines append the macro control lines to the file :
[27]   TEMP←TEMP,'END',T,'MACRO',T,'LNZD',T,'TANG',T,'FORM',T,'SOLV',T
[28]   TEMP←TEMP,'OTMH',T,'DISP',T,'STRE',T,'END',T,'STOP',T
[29]   TEMP ⎕NAPPEND ¯999 ⍝                 append TEMP to DOS file, tie #¯999
[30]   ⎕NUNTIE ¯999 ⍝                       untie file ¯999
    ∇
```

```
    ∇ RES←BOUNFORCS1 XY;C;N1;N2;NN;P;RES;T;TN
[1]  ⍝   This fn. is invoked by BOUNFORC to define the lines of boundary
[2]  ⍝   restraint (BOUN) and nodal applied force (FORC) data to be written
[3]  ⍝   to the F.E. data files for offcenter-notched beams.  Nodal coordinate
[4]  ⍝   vectors X and Y are global from BOUNFORC.  RES is a character array
[5]  ⍝   to be written to the data file.
[6]  ⍝   Written 26 June 1988.
[7]   T←⎕TCNL,⎕TCLF ⍝                                  newline, linefeed characters
[8]  ⍝   ctr.-pt. load for unit gross section          stress :
[9]   RES←T,'BOUN',T ⍝                                 blank line, 'BOUN'
[10]  NN←⍴X ⍝                                          node numbers
[11]  N1←((X=OH)∧Y=0)/NN ⍝                             no. of left support node
[12]  N2←((X=BL+BL-OH)∧Y=0)/NN ⍝                       no. of right support node
[13]  RES←RES, 5 0 ⍕N1,0,1,1 ⍝                        node N1 fixed in x and y
[14]  RES←RES,T, 5 0 ⍕N2,0,0,1 ⍝                      node N2 fixed in y, free in x
[15]  RES←RES,(4⍴T),'FORC' ⍝                          add blank line, 'FORC'
[16]  TN←(Y=H)/X ⍝                                     x coord's. of top nodes
[17]  ⍎(XCD≤1E¯6)/'RES←BOUNFORCS2 RES ◇ →0' ⍝          for whole C-N beams, exit
[18]  C←|TN-BL ⍝                                       distance of top nodes from ctr.
[19]  C←1↑(C=⌊/C)/TN ⍝                                 x of top node closest to ctr.
[20] ⍝   Compute point load at x=C, y=H to give unit gross section stress at
[21] ⍝   the top of the critical fillet, assuming beam thickness = 1 :
[22]  P←(H*2)×(BL-OH)÷3×(C-OH)×BL+HL-XCD+R+OH ⍝        see MESH for H,BL,OH,XCD,R
[23]  C←((X=C)∧Y=H)/NN ⍝                               no. of top node closest to ctr.
[24] ⍝   ctr. node no., generation increment (0), x-force (0), y-force :
[25]  RES←RES,T,(5 0 ⍕C),'    0       0.0 -',,'F8.6' ⎕FMT P
    ∇
```

```
    ∇ RES←BOUNFORCS2 RES;NQ;P;Q;XQ
[1]  ⍝   This fn., invoked by BOUNFORCS1, writes the FORC lines appropriate
[2]  ⍝   for a center-notched beam (V/M = 0) using the whole-beam model.
[3]  ⍝   RES is the character string to be appended to the DOS disk file.
[4]  ⍝   Global, from BOUNFORCS1:
[5]  ⍝      TN ≡ x coord's. of top nodes;
[6]  ⍝      T  ≡ ⎕TCNL, ⎕TCLF (character vector, length 2);
[7]  ⍝      NN ≡ vector of node numbers;
[8]  ⍝   from WHOLEMESH :
[9]  ⍝      XY ≡ nodal coord. array;
[10] ⍝      BL, OH ≡ beam half-length and overhang past support.
[11] ⍝      H  ≡ beam height
[12] ⍝   Written 28 Oct. 1988.
[13]  Q←(BL-OH)÷2 ⍝                          dist. from center to quarter pt.
[14]  XQ←BL+Q,-Q ⍝                           x coord's. of L and R qtr. pts.
[15]  XQ←|TN∘.-XQ ⍝                          distances btw. top pts. & qtr. pts.
[16] ⍝      x coord's. of nodes nearest quarter points :
[17]  XQ←+⌿(XQ=(⍴XQ)⍴⌊⌿XQ)×TN,[1.5]TN
[18]  NQ←((XY[;1]∈XQ)∧XY[;2]=H)/NN ⍝         node numbers for applied forces
[19]  P←(H*2)÷6×(⌊/XQ)-OH ⍝                  load for (6M/th*2) = 1
[20]  RES←RES,T,(5 0 ⍕NQ[1]),'    0       0.0 -',,'F8.6' ⎕FMT P
[21]  RES←RES,T,(5 0 ⍕NQ[2]),'    0       0.0 -',,'F8.6' ⎕FMT P
    ∇
    ∇ RES←BTWFIL XY;AR1;AR2;CY;DX;DY;HTS;N;X;Y
[1]  ⍝   This function, invoked by EXTEND, adds nodes as needed between
[2]  ⍝   the 2 fillets in an offcenter notch.
[3]  ⍝.....................................................................
[4]   CY←(XY[;1]=XY[2;1])/XY[;2] ⍝                y-coord's. of nodes above notch
[5]   CY←CY[⍋CY] ⍝                               order from low to high
[6]   HTS←(1↓CY)-¯1↓CY ⍝                         hts. of elmts. above notch
[7]   DX←2×HL-R ⍝                                dist. btw. existing elements
[8]   AR1←(⌈/HTS)÷DX ⍝                           highest aspect ratio
[9]   AR2←(⌊/HTS)÷DX ⍝                           lowest aspect ratio
[10] ⍝   Branch based on aspect ratios :
[11] ⍝→(L10,L20,L30,L40,L50)[1+(AR1≤6)×(AR2≥÷ 2 4 100)⍳1]
```

```
[12]  →(L10,L20,L30,L40,L50)[1+(AR1≤6)×(AR2≥÷ 1 2 100)ι1]
[13] L10:'The mesh generator cannot handle a notch this short for the given'
[14]  '   fillet radius.  Increase zeta to 1 (semicircular notch) or increase'
[15]  '   notch length by decreasing zeta or increasing delta.  Execution '
[16]  '   has been terminated.' ◇ →
[17] L20: ⍝   for notches requiring only 1 element between fillets :
[18]  RES←XY ◇ →0
[19] L30: ⍝   for notches requiring 2 elmts. btw. fillets :
[20]  RES←XY,[1]⍪(2,ρCY)ρ((ρCY)ρBL+XCD),CY ⍝    add nodes at ctr. of notch
[21]  →0
[22] L40: ⍝   for notches requiring >2 elmts. btw. fillets :
[23]  X←XY[;1] ◇ Y←XY[;2] ⍝                    define X, Y coord. vectors
[24]  DY←Y[4]-Y[2] ⍝                           ht. of fillet elmt. above notch
[25]  X←X,(ρCY)ρX[2]-DY ⍝                      col. of nodes to L of rt. fillet
[26]  Y←Y,CY ⍝                                 y for these new nodes
[27]  X←X,(ρCY)ρX[7]+DY ⍝                      col. of nodes to rt. of L fillet
[28]  Y←Y,CY
[29]  DX←DX-2×DY ⍝                             updated distance btw. elmts.
[30]  N←⌈DX÷3×DY ⍝                             no. of new elmt. col's. needed
[31]  X←X,(¯1↑X)+(ρCY)/(ιN-1)×DX÷N ⍝           x for N-1 col's. of new nodes
[32]  Y←Y,((N-1)×ρCY)ρCY ⍝                     y coord's. of new nodes
[33]  RES←X,[1.5]Y
[34]  →0
[35] L50:'The notch is too long.  Increase zeta.  Execution halted.' ◇ →
    ∇
```

```
    ∇ COORDATA AR;I;N;NN;NR;RN;T;TEMP;Z
[1]  ⍝   This fn., invoked by MESH, appends nodal coordinate
[2]  ⍝   input data for the Taylor/Gerhardt FE program to the DOS file
[3]  ⍝   opened by function MATEDATA.  AR is the nodal coordinate array.
[4]  ⍝   EL (element def'n. array) must be present in the active workspace.
[5]  ⍝   Last revision 25 June 1988.
[6]   T←⎕TCNL,⎕TCLF
[7]   N←1↑⍴AR ⍝                                  N= no. of rows in AR
[8]   →(N<2000)/L20 ⍝                            unless AR is very large, →L20
[9]  ⍝.....................................................................
[10]  NN←⌊N÷1000 ⍝                               no. of thousands of rows in AR
[11]  Z← 1000 1 ⍴0 ⍝                             column of zeroes
[12]  I←1
[13] L1:→(I>NN)/L10 ⍝                            →L10 when I>NN
[14]  RN← 1000 1 ⍴(1000×I-1)+⍳1000 ⍝             the Ith thousand row numbers
[15]  TEMP←AR[,RN;] ⍝                            the Ith thousand rows of AR
[16]  TEMP←'2I5,2F10.6' ⎕FMT(RN;Z;TEMP) ⍝        format as needed for FE program
[17]  TEMP←TEMP,[2](1000,2)⍴T ⍝                  add newline, linefeed to each row
[18]  TEMP ⎕NAPPEND ¯999 ⍝                       store the data in name.DAT
[19]  I←I+1
[20]  →L1
[21] L10:NR←N-NN×1000 ⍝                    no. of rows remaining to be added
[22]  RN←(NR,1)⍴(NN×1000)+⍳NR
[23]  Z←(NR,1)⍴0
[24]  TEMP←AR[,RN;]
[25]  TEMP←'2I5,2F10.6' ⎕FMT(RN;Z;TEMP) ⍝        format as needed for FE program
[26]  TEMP←TEMP,[2](NR,2)⍴T ⍝                    add newline, linefeed to each row
[27]  TEMP ⎕NAPPEND ¯999 ⍝                       store the data in name.DAT
[28]  →0 ⍝                                       exit COORDATA
[29] ⍝.....................................................................
[30] ⍝   insert col. of node no's., col. of zeros to L of x,y values :
[31] L20:Z←(N,1)⍴0 ⋄ RN←(N,1)⍴⍳N
[32]  AR←'2I5,2F10.6' ⎕FMT(RN;Z;AR) ⍝            format as needed for FE program
[33]  AR←AR,[2](N,2)⍴T ⍝                         add newline, linefeed to each row
[34]  AR ⎕NAPPEND ¯999 ⍝                         store the data in name.DAT
    ∇
```

```
    ∇ ELEMDATA AR;I;MATYPE;N;T;TEMP
[1]  ⍝   This fn. is invoked by MESH to generate FE meshes for notched beams.
[2]  ⍝   It appends nodal connectivity input data, for the Taylor/Gerhardt
[3]  ⍝   FE program, to the DOS file already containing material
[4]  ⍝   and nodal coordinate data for the mesh.  AR is the element definition
[5]  ⍝   array.                                  Last update 26 June 1988.
[6]   I←1 ◇ N←1↑⍴AR ⍝                            N= no. of rows in AR
[7]   T←⎕TCNL,⎕TCLF ⍝                            newline, linefeed characters
[8]   (T,'ELEM',T)⎕NAPPEND ¯999 ⍝                write blank line, 'ELEM'
[9]   AR←(N⍴1),[2]AR ⍝                           append a col. of 1s to front of AR
[10]  AR←(⍳N),[2]AR ⍝                            append col. of node #s. to "  "  "
[11]  MATYPE←AR[;NPE+2]>0 ⍝                      points to hybrid elements (13-node >0)
[12] ⍝   differentiates btw. 2 hyb. elmts. for offctr. notches (XCD>0) :
[13]  ⍎(XCD>0)/'MATYPE←MATYPE+AR[;15]=1↑¯2↑AR[⍋AR[;15];15]'
[14] ⍝  AR[;2] = 1 for non-hybrid elements, =2 for rt. f.e., =3 for left f.e.:
[15]  AR[;2]←AR[;2]+MATYPE
[16]  AR←'15I5' ⎕FMT AR ⍝                        format as needed for FE program
[17] ⍝      add newline, linefeed characters to the end of each row :
[18]  AR←AR,[2](N,2)⍴T
[19]  AR ⎕NAPPEND ¯999 ⍝                         append AR to end of name.DAT file
    ∇
```

```
    ∇ AR←ELEM1 XY;B;HORIZ;I;L;NC;T;VERT;XMAX
[1]  ⍝   This fn. is to generate the nodal connectivity array AR, i.e. the
[2]  ⍝   element definitions, from the nodal coordinate array XY.  It is for
[3]  ⍝   use ONLY with simple rectangular meshes such as those used by T.D.
[4]  ⍝   Gerhardt and those generated by fn. NODE1 (with midside nodes as
[5]  ⍝   defined by fn. INSRECT, i.e. cubic elements).  f.e.= fillet element.
[6]  ⍝   No diagonal sides are allowed.  All elements are assumed to have 13
[7]  ⍝   nodes.  The last node # in each elmt. except the f.e. will be 0.
[8]  ⍝   Global from NODE1: XCD ≡ distance from notch center to beam center;
[9]  ⍝                       HL ≡ half-length of notch
[10] ⍝                       BL ≡ length of half-beam
[11] ⍝                        H ≡ height of beam
[12] ⍝                        D ≡ depth of notch
[13] ⍝   Latest revision: 20 June 1988.
[14] ⍝.....................................................................
[15]  VERT←1 ELEM1S1 XY ⍝                          form 4-col. array of vert. sides
[16]  HORIZ←2 ELEM1S1 XY ⍝                         form 4-col. array of hor. sides
[17]  ⍎((XCD>0)∧XCD≤1E¯6)/'NC←BL ◇ XMAX←2×BL ◇ →L10'
[18]  NC←XCD+BL×XCD>0 ⍝                            x-coord. of Notch Center
[19]  XMAX←BL×1+XCD>0 ⍝                            x-coord. of right end of model
[20] ⍝   Remove inappropriate sides from VERT to make AR the 4-col. array of
[21] ⍝      node #s in right elmt. sides, and L the array of left elmt. sides:
[22] L10:AR←((XY[VERT[;1];1]>0)∧XY[VERT[;1];1]≠NC+HL)⌿VERT
[23]  L←⍉((XY[VERT[;1];1]<XMAX)∧XY[VERT[;1];1]≠NC-HL)⌿VERT
[24] ⍝   Remove inappropriate sides from HORIZ to make B the 4-col. array of
[25] ⍝      node #s in bottom elmt. sides, and T the array of top elmt. sides:
[26]  B←(XY[HORIZ[;1];2]<H)⌿HORIZ
[27]  T←⍉((XY[HORIZ[;1];2]>0)∧XY[HORIZ[;1];2]≠D)⌿HORIZ
[28] ⍝.....................................................................
[29] ⍝    Invoke ADD1 (niladic function) to catenate sides together:
[30]  AR←ADD1
[31] ⍝   Reorder the nodes to correspond to TDG's numbering schemes for
[32] ⍝      isoparametric (12-node) and hybrid (13-node) elements:
[33]  I←(AR[;13]=0)/⍳1↑⍴AR ⍝          I points to 12-node elements
```

```
[34]  AR[I;]←AR[I; 1 4 7 10 2 5 8 11 3 6 9 12 13]
[35] ⍝   Reorder the elements from lower left to upper right, based on
[36] ⍝   the highest node number in each element:
[37]  AR←AR[⍋⌈/AR;]
    ∇


    ∇ RES←I ELEM1S1 XY;NE;NN;TN;X;Y;YMAX
[1]  ⍝   This function, invoked by ELEM1, takes the nodal coord. mesh
[2]  ⍝   array XY and creates a 4-column array, RES, of node numbers.  If
[3]  ⍝   I=1, then RES corresponds to nodes involved in vertical element
[4]  ⍝   sides.  If I=2, then RES is for horizontal elmt. sides.  Each row of
[5]  ⍝   RES contains the node #s for the 4 nodes in a given side of a given
[6]  ⍝   element.  Global from the active WS:
[7]  ⍝      D ≡ notch depth; R ≡ fillet radius; HL ≡ notch half-length;
[8]  ⍝      BL ≡ beam half-length; XCD ≡ distance, notch center to beam ctr.
[9]  ⍝   Written 22 June 1988.
[10]  X←XY[;I] ⍝                              Note: X ≡ y when I=2.
[11]  Y←XY[;1+I=1] ⍝                          Note: Y ≡ x when I=2.
[12]  YMAX←⌈/Y ⍝                              Note: YMAX ≡ max. x when I=2.
[13]  NN←⍳⍴X ⍝                                node numbers
[14]  TN←(Y=YMAX)/NN ⍝                        nodes at top (or right) of beam
[15]  TN←TN[¯2+3×⍳⌈(⍴TN)÷3] ⍝                 elmt. corner nodes at top (or right)
[16] ⍝   NE ≡ coord's. of Notch End nodes needed to form elmt. sides.
[17] ⍝      for vertical elmt. sides :
[18]  ⍎((I=1)∧(XCD>0)∧XCD≤1E¯6)/'NE←(D>R)/(HL+BL-0,2×HL) ◇ →L10'
[19]  ⍎(I=1)/'NE←(D>R)/(HL+(XCD>0)×BL+XCD+HL×¯2 0) ◇ →L10'
[20] ⍝      for horizontal elmt. sides :
[21]  ⍎(I=2)/'NE←(HL>R)/D'
[22] L10:RES←((X∈X[TN])∨X∈NE)/NN ⍝             node #s involved in given sides
[23]  RES←ELEM1S2 RES ⍝                       convert vector to 4-col. array
    ∇
```

```
    ∇ RES←ELEM1S2 NN;CV;IN;NC;NPC;NREP;SV;TA;UX;UY;X;XMAX
[1]  ⍝   This fn., invoked by ELEM1S1, takes the vector (NN) of node
[2]  ⍝   numbers involved in vertical (or horizontal) element sides and
[3]  ⍝   converts it into the appropriate 4-column array of element side
[4]  ⍝   definitions (RES).  NPC = no. of nodes per column (row) of the
[5]  ⍝   mesh.  XY ≡ nodal coord. array, from ELEM1.  Global from ELEM1S1:
[6]  ⍝      I=1: vertical element sides; I=2: horizontal sides.
[7]  ⍝   The mnemonics and comments are for I=1; for I=2, just switch
[8]  ⍝   "vertical" with "horizontal", "y" with "x", and "row" for "column".
[9]  ⍝   Last update 9 Nov. 1988.          OCN ≡ off-center notch
[10] ⍝.....................................................................
[11]  X←XY[NN;I] ⍝                          x coord's. of nodes in vert. sides
[12]  XMAX←BL+BL×XCD>0 ⍝                    x coord. of right end of model
[13]  ⍎(I=2)/'X←X[⍋X]' ⍝                    if X ≡ y, then sort
[14]  CV←X≠1⌽X ⍝                            marks ends of columns
[15]  UX←CV/X ⍝                             unique values of x
[16]  CV←+\CV ⍝                             replace 1's w/ consec. integers
[17]  NPC←CV⍳(⍳⍴UX) ⍝                       cumulative nodes per column
[18]  NPC←NPC-0,¯1↓NPC ⍝                    nodes per column
[19]  →(XCD>0)/L0 ⍝                         skip selection process if OCN
[20]  SV←NPC∈1+3×⍳100 ⍝                     select col's. w/ 4, 7, 10... nodes
[21]  NPC←SV/NPC ⋄ UX←SV/UX ⍝               delete other columns
[22] L0:→(1<⍴,NPC)/L1 ⍝                     trap for insufficient node col's.
[23]  'ELEM1S2 crashed due to ≤ 1 col. of nodes. Execution halted.' ⋄ →
[24] ⍝.....................................................................
[25] L1:→(I=2)/L5 ⍝                         →L2 for horiz. sides
[26]  NREP←⌈/¯1+(NPC-1)÷3 ⍝                 max. # of repeat nodes in a col.
[27] ⍝   IN ≡ index array: position in NN of possible repeated nodes :
[28]  IN←(+\NPC)∘.-3×⍳NREP
[29]  IN←(IN>0)×IN ⍝                        replace negative values w/ 0's
[30]  IN←IN+IN=0 ⍝                          replace 0's w/ 1's
[31] ⍝   TA will be an array of node #s to be repeated in each column :
[32]  NN←(XY[NN;1]∈UX)/NN ⍝                 update NN, removing excluded nodes
```

```
[33]  TA←NN[IN]×NPC∘.>1+3×⍳NREP
[34]  0 0 ρ⎕ERASE 'IN' ⍝                          discard IN to prevent full WS
[35]  RES←(1+NN∈TA)/NN ⍝                          repeat each node # that is in TA
[36]  →L10
[37] ⍝.....................................................................
[38] L5:NN←NN[⍋XY[NN;2]] ⍝                       reorder NN by Y
[39]  NN←(XY[NN;I]∈UX)/NN ⍝                      take node #s selected above
[40]  RES←(NN∈VERT[; 1 4])/NN ⍝                  element-corner nodes
[41]  X←XY[RES;1] ⍝                              x coord's. of corner nodes
[42]  RES←((X>0)∧X<XMAX)/RES ⍝                   delete nodes at beam ends
[43]  X←XY[RES;1] ⍝                              update x
[44]  NC←XCD+BL×XCD>0 ⍝                          x-coord. of Notch Center
[45] ⍝  The 2 lines commented out below are replaced by versions to allow
[46] ⍝  treatment of center notches with fictitious XCD < 1E¯6 to give
[47] ⍝  a full beam mesh (not just a symmetric half-beam.)
[48]  RES←(~(1E¯6≥|X-NC+HL)∨1E¯6≥|X-NC-HL)/RES
[49] ⍝                                           delete nodes at fillet edges
[50] ⍝      delete node(s) at theta=90 degrees along fillet:
[51]  X←XY[RES;1] ⋄ Y←XY[RES;2] ⍝                update x, y
[52]  RES←(~(Y=D)∧(1E¯6≥|X-NC+HL-R)∨1E¯6≥X-NC+R-HL)/RES
[53]  RES←(1+NN∈RES)/NN ⍝                        repeat each node # that is in RES
[54]  RES←RES[⍋XY[RES;2]] ⍝                      order on y from low to high
[55] ⍝.....................................................................
[56] L10:
[57]  RES←(((ρRES)÷4),4)ρRES ⍝                   convert RES into 4-column array
    ∇
```

```
    ∇ RES←C EXTDOWN XY;N;YL
[1]  ⍝   This fn. is invoked by EXTEND, which is invoked by NODE1 for simple
[2]  ⍝   1-fillet-element meshes, adds nodes as needed below the hybrid
[3]  ⍝   fillet element.  C is an integer scalar used to choose the proper
[4]  ⍝   number of new elmts. below the fillet elmt..  XY is the orig. nodal
[5]  ⍝   coord. array, and RES is the revised nodal coord. array.
[6]  ⍝   X, Y are the coord's. of the 5 nodes in the f.e. (global from NODE1).
[7]  ⍝   Last update 3 May 1988.
[8]   →(L1,L10,L20,L30,L40,L50,L60)[(C≤⍳6)⍳1] ⍝   select proper mesh option
[9]  ⍝.....................................................................
[10] L1: ⍝ The fillet elmt. touches the bottom.  No new elmts. needed.
[11]  RES←XY
[12]  →L100
[13] ⍝.....................................................................
[14] L10:'The notch is too shallow with this large fillet radius.  It may '
[15]  '   be done if you reduce the length of the fillet element specified'
[16]  '   in function NODE1.  Execution has halted in fn. EXTDOWN.' ◇ →
[17] ⍝.....................................................................
[18] L20: ⍝                                    a single below-fillet elmt.
[19]  RES←XY,[1]⍉ 2 2 ⍴X[1 3],0,0 ⍝            add 2 nodes on beam bottom
[20]  →L100
[21] ⍝.....................................................................
[22] L30: ⍝                                    two equal-height below-fillet elmts.
[23]  RES←XY,[1]⍉ 2 2 ⍴X[1 3],0,0 ⍝            add 2 nodes on beam bottom
[24]  RES←RES,[1]⍉ 2 2 ⍴X[1 3],Y[1 3]÷2 ⍝ add 2 nodes 1/2way btw. y=0 and Y[1]
[25]  →L100
[26] ⍝.....................................................................
[27] L40: ⍝                                  two unequal-height below-fillet elmts.
[28]  RES←XY,[1]⍉ 2 2 ⍴X[1 3],0,0 ⍝                add 2 nodes on beam bottom
[29]  RES←RES,[1]⍉ 2 2 ⍴X[1 3],Y[1 3]-R ⍝          add 2 nodes at y= Y[1]-R
[30]  →L100
[31] ⍝.....................................................................
[32] L50: ⍝                                      >2 but ≤7 below-fillet elmts.
```

```
[33]  RES←XY,[1]⍪ 2 2 ρX[1 3],0,0 ⍝          add 2 nodes on beam bottom
[34]  RES←RES,[1]⍪ 2 2 ρX[1 3],Y[1 3]-R ⍝    add 2 nodes at y= Y[1]-R
[35]  YL←¯1↑RES[;2] ⍝                        lowest nonzero y thus far
[36]  N←⌈YL÷3×R ⍝                            no. of addl. elmts. needed below
[37] ⍝   divide remaining space below fillet into N-1 equal parts:
[38]  RES←RES,[1]⍪(2,2×N-1)ρ((N-1)/X[1 3]),(2×N-1)ρYL×(⍳N-1)÷N
[39]  →L100
[40] ⍝.....................................................................
[41] L60:'The notch is too deep for this small fillet radius.  The resulting'
[42]  '   mesh would be >7 elements high below the fillet.  Execution has '
[43]  '   halted in fn. EXTDOWN.' ◇ →
[44] ⍝.....................................................................
[45] L100: ⍝   The End
     ∇
```

```
    ∇ OUT←EXTEND XY;AR;BO;LH;LHL;LHR;TA;TD;XMAX
[1]  ⍝   This fn., invoked by NODE1, extends the mesh definition from the
[2]  ⍝   hybrid fillet element (f.e.) to the edges and ends of the beam.
[3]  ⍝   XY and OUT are x-y coord. arrays, before and after the addition of
[4]  ⍝   the new nodes.  Global, from NODE1: R = fillet radius; X, Y =
[5]  ⍝      coord's. of the 5 or 10 fillet elmt. nodes.
[6]  ⍝   Last update 17 Nov. 1988.  "CN" = center-notch
[7]  ⍝   The next 4 lines define TD as a 4-vector of test distances.
[8]   TD←Y[1] ⍝                      distance below fillet element
[9]   XMAX←BL×1+XCD>0 ⍝              max. x, CN vs. offctr-notch beam
[10]  TD←TD,XMAX-OH+X[3] ⍝           distance from right f.e. to right support
[11]  TD←TD,H-Y[4] ⍝                 distance from f.e. to beam top
[12] ⍝   Distance from L edge of leftmost f.e. to L end of model:
[13]  TD←TD,⌊/X ⍝                    Note: left end of CN model is centerline
[14]  LH←(X=⌊/X)/Y ⍝                 y coord's. at L edge of leftmost f.e.
[15]  LH←LH[⍋LH],(H>⌈/LH)/H ⍝        append H if needed to L edge node vector
[16]  LH←⌊/(1↓LH)-¯1↓LH ⍝            hts. of elmts. on left edge
[17] ⍝   LHR ≡ least height of elmts. to right of f.e. :
[18] ⍝ LHR←TD[1 3],2×R ◇ LHR←(LHR>0)/LHR ◇ LHR←⌊/LHR
[19]  LHR←2×R ⍝                      hardwire for testing, 16 Nov. 1988
[20] ⍝   LHL ≡ least height of elmts. to left of f.e. (16 June '88 version):
[21]  LHL←((TD[3],LH)[1+(TD[3]>LH)∨TD[3]=0],LHR)[1+XCD>0]
[22] ⍝   Aspect ratios (4): test distances ÷ shortest adjacent side lengths.
[23]  AR←TD÷(X[3]-X[1]),LHR,(X[5]-X[4]),LHL
[24] ⍝   TA = test array, used to select correct option for mesh extension
[25]  TA←(AR∘.≤0,0.333333,1.5,2,7,37)× 4 6 ⍴⌊6 ⍝     3rd version, 16 Nov. 1988
[26]  BO←⌊/TA+7×TA=0 ⍝              branch option vector: gives the correct option
[27] ⍝                               ...for each of the 4 directions (down,R,up,L)
[28]  OUT←BO[1]⍎'EXTDOWN XY' ⍝       extend mesh to bottom of beam
[29]  OUT←BO[3]⍎'EXTUP OUT' ⍝        extend mesh to top of beam
[30]  OUT←BO[2]⍎'EXTRIGHT OUT' ⍝     extend mesh to right end of beam
[31]  OUT←BO[4]⍎'EXTLEFT OUT' ⍝      extend mesh to centerline of beam
[32] ⍝   add nodes if needed btw. f.e.'s :
[33]  ⍎((XCD>0)∧HL>R)/'OUT←BTWFIL OUT' ⍝     HL ≡ notch half-length (global)
    ∇
```

```
    ∇ RES←C EXTLEFT XY;ERR;HTS;LHY;MH;N;XL
[1]  ⍝   This fn. is invoked by EXTEND, which is invoked by NODE1 for simple
[2]  ⍝   1-fillet-element meshes.  It adds nodes as needed to the left of
[3]  ⍝   the hybrid fillet element, extending to the centerline of the beam.
[4]  ⍝   C is an integer scalar used to choose the appropriate number
[5]  ⍝   of new elmts. left of the fillet elmt. (f.e.).  XY is the original
[6]  ⍝   nodal coord. array, and RES is the revised nodal coord. array.
[7]  ⍝   Global var's. from NODE1: R=fillet radius; XCD=distance from notch
[8]  ⍝     center to beam ctr.; X, Y=coord's. of fillet elmt. nodes (1-5).
[9]  ⍝   Global var's. from EXTEND: LHL=least ht. of elmts. to left of f.e.
[10]  LHY←(XY[;1]=⌊/XY[;1])/XY[;2] ⍝              y coord's. of leftmost nodes
[11]  LHY←LHY[⍋LHY] ⍝                            order, low to high
[12]  HTS←(1↓LHY)-¯1↓LHY ⍝                       elmt. heights
[13]  MH←⍴LHY ⍝                                  mesh height (no. of elmts.)
[14]  ⍎(XCD>0)/'RES←OCNLEFT XY ◇ →L100' ⍝        for offcenter notches
[15]  →(L1,L10,L20,L30,L40,L50,L60)[(C≤⍳6)⍳1] ⍝   select proper mesh option
[16] ⍝.....................................................................
[17] L1: ⍝The notch abuts the centerline.  No addl. elmts. needed to the left.
[18]  RES←XY ◇ →L100
[19] ⍝.....................................................................
[20] L10:'The fillet is too close to the centerline.  It may be treated by'
[21]  '   reducing the length or height of the fillet element specified in'
[22]  '   fn. NODE1.  Execution has halted in fn. EXTLEFT.' ◇ →
[23] ⍝.....................................................................
[24] L20: ⍝   add a single elmt. column btw. fillet elmt. and centerline:
[25]  RES←XY,[1]⍉(2,MH)⍴(MH/XCD),LHY ⍝              add nodes at x=XCD
[26]  →L100
[27] ⍝.....................................................................
[28] L30: ⍝   add two col's. of equal-length elmts. btw. f.e. and centerline
[29]  RES←XY,[1]⍉(2,MH)⍴(MH/XCD),LHY ⍝              add nodes at x=XCD
[30]  RES←RES,[1]⍉(2,MH)⍴(MH/0.5×XCD+X[2]),LHY ⍝    add halfway nodes
[31]  →L100
[32] ⍝.....................................................................
```

```
[33] L40: ⍝   add 2 cols. of unequal-length elmts. btw. f.e. and centerline
[34]  RES←XY,[1]⍉(2,MH)⍴(MH/XCD),LHY ⍝                add nodes at x=XCD
[35] ⍝                  new version, 3 May 1988:
[36] ⍝ RES←RES,[1]⍉(2,MH)⍴(MH/X[2]-2×LHL),LHY ⍝       add nodes at x=X[2]-2LHL
[37]  RES←RES,[1]⍉(2,MH)⍴(MH/X[2]-LHL),LHY ⍝        add nodes at x=X[2]-LHL
[38]  →L100
[39] ⍝.....................................................................
[40] L50: ⍝   add >2 but ≤7 cols. of elmts. btw. fillet elmt. and centerline
[41] ⍝                  new version, 3 May 1988:
[42] ⍝ RES←XY,[1]⍉(2,MH)⍴(MH/X[2]-2×LHL),LHY ⍝       add nodes at x=X[2]-2LHL
[43]  RES←XY,[1]⍉(2,MH)⍴(MH/X[2]-LHL),LHY ⍝          add nodes at x=X[2]-LHL
[44]  XL←¯1↑RES[;1] ⍝                                lowest x thus far
[45] ⍝N←⌈XL÷6×⍳/HTS ⍝                                rows of nodes needed to L
[46]  N←⌈XL÷3×⍳/HTS ⍝                                rows of nodes needed to L
[47] ⍝   Add N rows of MH nodes each to left of existing mesh:
[48]  RES←RES,[1]⍉(2,MH×N)⍴((MH×N)⍴XL×(¯1+⍳N)÷N),N/LHY
[49]  →L100
[50] ⍝.....................................................................
[51] L60:'The notch is too long, requiring >7 elmts. L of the fillet. '
[52]  '   Execution has halted in EXTLEFT.' ◇ →
[53] ⍝.....................................................................
[54] L100:
    ∇
```

```
    ∇ RES←C EXTRIGHT XY;MH;N;RHY;XMAX;XR
[1]  ⍝   This fn. is invoked by EXTEND, which is invoked by NODE1 for simple
[2]  ⍝   1-fillet-element meshes.  It adds nodes as needed to the right of
[3]  ⍝   the hybrid fillet element, extending to the right end of the beam.
[4]  ⍝   C is an integer scalar (from 1 to 7) used to choose the appropriate
[5]  ⍝   number of new elmts. above the fillet elmt..  XY is the orig. nodal
[6]  ⍝   coord. array, and RES is the revised nodal coord. array.
[7]  ⍝   Global Vars., from NODE1: BL=beam half-length; OH= overhang; X, Y;
[8]  ⍝     "     "    from EXTEND: LHR=least height of elmts. to right of f.e.
[9]  ⍝     are coord's. of the 5 fillet element (f.e.) nodes.
[10] ⍝   Last update 3 May 1988.
[11]  XMAX←BL×1+XCD>0 ⍝                          rt. endpt., ctr. vs. offctr. notch
[12]  RHY←(XY[;1]=⌈/XY[;1])/XY[;2] ⍝             vector of y's of rtmost nodes
[13]  MH←⍴RHY ⍝                                  mesh ht. (no. of nodes,bot.→top)
[14]  →(L1,L10,L20,L30,L40,L50,L50)[C] ⍝         select proper mesh option
[15] ⍝.....................................................................
[16] L1: ⍝                                       fillet elmt. touches the support
[17]  RES←XY,[1]⍉(2,MH)⍴(MH/XMAX),RHY ⍝          add nodes at x=XMAX, y=RHY
[18]  →L100
[19] ⍝.....................................................................
[20] L10: ⍝    f.e. very close to support.  Extend it to touch support :
[21]  XY[;1]←(XY[;1]×XY[;1]≠XY[3;1])+(XMAX-OH)×XY[;1]=XY[3;1]
[22]  →L1
[23] ⍝'The notch is too close to the support.  It may be treated by'
[24] ⍝ '   reducing the length or height of the fillet element specified in'
[25] ⍝ '   fn. NODE1.  Execution has halted in fn. EXTRIGHT.' ◇ →
[26] ⍝.....................................................................
[27] L20: ⍝        need a single elmt. col. btw. fillet elmt. and support
[28]  RES←XY,[1]⍉(2,MH)⍴(MH/XMAX-OH),RHY ⍝        add nodes above support
[29]  RES←RES,[1]⍉(2,MH)⍴(MH/XMAX),RHY ⍝         add nodes at x=XMAX, y=RHY
[30]  →L100
[31] ⍝.....................................................................
[32] L30: ⍝        need 2 cols. of equal-length elmts. btw. f.e. and support
```

```
[33]  RES←XY,[1]⍪(2,MH)⍴(MH/XMAX-OH),RHY ⍝          add nodes above support
[34] ⍝   add column of nodes btw. f.e. and support:
[35]  RES←RES,[1]⍪(2,MH)⍴(MH/0.5×X[3]+¯1↑RES[;1]),RHY
[36]  RES←RES,[1]⍪(2,MH)⍴(MH/XMAX),RHY ⍝          add nodes at x=XMAX, y=RHY
[37]  →L100
[38] ⍝.....................................................................
[39] L40: ⍝        need 2 cols. of unequal-length elmts. btw. f.e. and support
[40] ⍝    add nodes 2×LHR from right edge of f.e.:
[41] ⍝ RES←XY,[1]⍪(2,MH)⍴(MH/X[3]+2×LHR),RHY
[42]  RES←XY,[1]⍪(2,MH)⍴(MH/X[3]+LHR),RHY ⍝       new version, 16 Nov. 1988
[43]  RES←RES,[1]⍪(2,MH)⍴(MH/XMAX-OH),RHY ⍝       add nodes above support
[44]  RES←RES,[1]⍪(2,MH)⍴(MH/XMAX),RHY ⍝          add nodes at x=XMAX, y=RHY
[45]  →L100
[46] ⍝.....................................................................
[47] L50: ⍝        need >2 col's. of elmts.btw. fillet elmt. and support
[48] ⍝    add nodes 2×LHR from right edge of f.e.:
[49] ⍝ RES←XY,[1]⍪(2,MH)⍴(MH/X[3]+2×LHR),RHY
[50]  RES←XY,[1]⍪(2,MH)⍴(MH/X[3]+LHR),RHY ⍝     new 16 Nov. 1988
[51]  XR←XMAX-OH+¯1↑RES[;1] ⍝                    x distance remaining to support
[52] ⍝N←⌈XR÷6×LHR ⍝                              # of elmt. col's. needed to ...
[53]  N←⌈XR÷3×LHR ⍝                              # of elmt. col's. needed to ...
[54] ⍝                                           ...get to the support
[55]  RES←RES,[1]⍪(2,N×MH)⍴((N×MH)⍴(¯1↑RES[;1])+XR×(⍳N)÷N),N/RHY
[56] ⍝                  add N cols. of nodes btw. rtmost. prev. node and support
[57]  RES←RES,[1]⍪(2,MH)⍴(MH/XMAX),RHY ⍝         add nodes at x=XMAX, y=RHY
[58] ⍝.....................................................................
[59] L100:
    ∇
```

```
    ∇ RES←C EXTUP XY;N;YH
[1]  ⍝   This fn. is invoked by EXTEND, which is invoked by NODE1 for simple
[2]  ⍝   1-fillet-element meshes.  It adds nodes as needed above the hybrid
[3]  ⍝   fillet element.  C is an integer scalar used to choose the proper
[4]  ⍝   number of new elmts. above the fillet elmt..  XY is the orig. nodal
[5]  ⍝   coord. array, and RES is the revised nodal coord. array.
[6]  ⍝   Global var's., from NODE1: H=beam ht.; X, Y = coords. of fillet elmt.
[7]  ⍝   nodes (nodes 1-5).
[8]  ⍝   Latest revision: 3 May 1988.
[9]   →(L1,L10,L20,L30,L40,L50,L60)[(C≤⍳6)⍳1] ⍝   select proper mesh option
[10] ⍝.....................................................................
[11] L1: ⍝'The fillet elmt. reaches the beam top.  No new elmts. needed.'
[12]  RES←XY ◇ →L100
[13] ⍝.....................................................................
[14] L10:'The notch is too deep with this large fillet radius.  It may be '
[15]  '   treated if you reduce the length or height of the fillet element'
[16]  '   specified in fn. NODE1.  Execution has halted in fn. EXTUP.' ◇ →
[17] ⍝.....................................................................
[18] L20: ⍝                                   a single above-fillet elmt.
[19]  RES←XY,[1]⍉ 2 2 ⍴X[2 3],H,H ⍝           add 2 nodes at beam top
[20]  →L100
[21] ⍝.....................................................................
[22] L30: ⍝                                   two equal-height above-fillet elmts.
[23]  RES←XY,[1]⍉ 2 2 ⍴X[2 3],H,H ⍝           add 2 nodes at beam top
[24] ⍝   add 2 nodes midway btw. top of fillet elmt. and top of beam:
[25]  RES←RES,[1]⍉ 2 2 ⍴X[2 3],2⍴(H+Y[4])÷2
[26]  →L100
[27] ⍝.....................................................................
[28] L40: ⍝                                     2 unequal-ht. above-fillet elmts.
[29]  RES←XY,[1]⍉ 2 2 ⍴X[2 3],H,H ⍝             add 2 nodes at beam top
[30] ⍝ RES←RES,[1]⍉ 2 2 ⍴X[2 3],2⍴Y[4]+4×R ⍝    new version, 3 May 1988
[31]  RES←RES,[1]⍉ 2 2 ⍴X[2 3],2⍴Y[4]+2×R ⍝    new version, 16 Nov. 1988
[32]  →L100
```

```
[33] A.....................................................................
[34] L50: A                                              >2 but ≤7 above-fillet elmts.
[35] A   add 2 nodes at y=Y[4]+3×X[5]-X[4], noting that X[5]- X[4]=2R :
[36] A RES←XY,[1]⍪ 2 2 ρX[2 3],2ρY[4]+4×R A      new version, 3 May 1988
[37]  RES←XY,[1]⍪ 2 2 ρX[2 3],2ρY[4]+2×R A      new version, 16 Nov. 1988
[38]  YH←¯1↑RES[;2] A                           highest non-H y thus far
[39] AN←⌈(H-YH)÷12×R A                          # of addl. elmts. needed above
[40]  N←⌈(H-YH)÷6×R A                          # of addl. elmts. needed above
[41] A   add N x-y pairs above current mesh, up to y=H :
[42]  RES←RES,[1]⍪(2,2×N)ρ((2×N)ρX[2 3]),2/YH+(H-YH)×(⍳N)÷N
[43]  →L100
[44] A.....................................................................
[45] L60:'The notch is too shallow for this small fillet radius.  The '
[46]  '   mesh would be >7 elements high above the fillet.  Execution has '
[47]  '   halted in fn. EXTUP.' ◇ →
[48] A.....................................................................
[49] L100: A The End
    ∇
```

```
    ∇ RES←FORCcp XY;NN;P;RES;TN
[1]  ⍝   This fn. is invoked by NEWBOUNFORC to define the lines of boundary
[2]  ⍝   restraint (BOUN) and nodal applied force (FORC) data to be written
[3]  ⍝   to the F.E. data files for offcenter-notched beams.
[4]  ⍝   Global from NEWBOUNFORC :
[5]  ⍝      X, Y : nodal coord. vectors; T←⎕TCNL,⎕TCLF (newline, linefeed).
[6]  ⍝   RES is a character array to be written to the data file.
[7]  ⍝   Latest revision 30 Nov. 1988.
[8]   RES←'FORC',T
[9]   TN←(Y=H)/X ⍝                                    x coord's. of top nodes
[10]  NN←⍳1↑⍴XY ⍝                                     node #s
[11] ⍝   if CN, place laod @ x=0, →L10 :
[12] ⍝   P is only 1/2 of the total cp load, since only 1/2-beam is modeled.
[13]  ⍎(XCD=0)/'C←0 ◇ P←(H*2)÷6×BL+R-OH+HL ◇ →L10'
[14]  C←|TN-BL ⍝                                      distance of top nodes from ctr.
[15]  C←1↑(C=⌊/C)/TN ⍝                                x of top node closest to ctr.
[16] ⍝   C is left global for use in FORCqp, but is local within NEWBOUNFORC.
[17] ⍝   Compute point load at x=C, y=H to give unit gross section stress at
[18] ⍝   the top of the critical fillet, assuming beam thickness = 1 :
[19]  P←(H*2)×(BL-OH)÷3×(C-OH)×BL+HL-XCD+R+OH ⍝     see MESH for H,BL,OH,XCD,R
[20] L10:C←((X=C)∧Y=H)/NN ⍝                          no. of top node closest to ctr.
[21] ⍝   ctr. node no., generation increment (0), x-force (0), y-force :
[22]  RES←RES,(5 0 ⍕C),'     0       0.0 -',,'F8.6' ⎕FMT P
[23]  RES←RES,T,T,'END',T ⍝                           end of this group of loads
    ∇
```

```
    ∇ TEMP←FORCqp XY;DEL;DENOM;I;P
[1]  ⍝   This fn., invoked by NEWBOUNFORC, calculates symmetric offcenter
[2]  ⍝   loads for notched beam models.  For offcenter notched (OCN) beams,
[3]  ⍝   loads are placed above the notch center and at the corresponding
[4]  ⍝   point on the unnotched end of the beam.  Note that the loads for
[5]  ⍝   OCN beams will, in general, not be perfectly symmetric, due to the
[6]  ⍝   granularity of the FE discretization.  For center notched (CN)
[7]  ⍝   beams, the load is placed at the quarter point of the half-beam.
[8]  ⍝   Global, from NODE1: XCD, BL, OH, H (beam dimensions).
[9]  ⍝   Global, from NEWBOUNFORC:
[10] ⍝      X, Y (nodal coord's.); TOP ≡ node #s along top sfc. of beam.
[11] ⍝   Written 25-26 Nov. 1988.          See derivations dated 25-26 Nov. '88.
[12]  →(XCD>0)/L10 ⍝                       for OCN, →L10
[13]  DEL←|X[TOP]-(BL-OH)÷2 ⍝              distance of top nodes from 1/4 point
[14]  I←(DEL=⌊/DEL)/TOP ⍝                  node # at which load will be placed
[15]  P←(H*2)÷6×BL-OH+X[I] ⍝               force for unit gross section stress
[16]  →L20
[17] ⍝.....................................................................
[18] L10: ⍝   for OCN (whole beam model):
[19]  DEL←|X[TOP]-BL+XCD ⍝                 dist. from top nodes to notch ctr.
[20]  I←1↑(DEL=⌊/DEL)/TOP ⍝                node # for right load
[21] ⍝   find node most nearly opposite beam ctr. from X[I] :
[22]  DEL←|X[TOP]-(⌽1↑X)-X[I]
[23]  I←I,(DEL=⌊/DEL)/TOP ⍝                I[2] ≡ node # for left load
[24] ⍝   The next 2 lines calculate the force for unit gross section stress
[25] ⍝      at section w/ critical fillet.  See 28 Nov. '88 notes.
[26]  DENOM←6×((X[I[2]]-OH)×BL+HL-OH+XCD+R)+(BL+XCD+R-HL+OH)×(2×BL)-OH+X[I[1]]
[27]  P←(H*2)×(2×BL-OH)÷DENOM
[28] L20:TEMP←'FORC',T ⍝                   write top FORC line
[29]  TEMP←TEMP,(5 0 ⍕C,0), 10 0 ⍕0,0 ⍝    set to 0 the old ctrpt. load
[30]  TEMP←TEMP,T,(5 0 ⍕1↑I),'     0        0 -',,'F8.6' ⎕FMT P
[31]  →(XCD=0)/L30 ⍝                       if CN, →L30
[32]  TEMP←TEMP,T,(5 0 ⍕I[2]),'     0        0 -',,'F8.6' ⎕FMT P
[33] L30:TEMP←TEMP,T,T,'END',T ⍝          write blank line, END
    ∇
```

```
    ∇ cv←FORCud XY;CA;FA
[1]  ⍝   This fn., invoked by NEWBOUNFORC, composes the FORC data lines for
[2]  ⍝   a uniformly distributed load between the supports along the top beam
[3]  ⍝   surface.  Global, from NEWBOUNFORC: T ≡ ⎕TCNL, ⎕TCLF (newline,
[4]  ⍝   linefeed characters.)
[5]  ⍝   Written 26 Nov. 1988.
[6]   cv←'FORC',T ⍝                              1st line of udl FORC data
[7]   FA←UDL XY ⍝                                find node #s, nodal loads
[8]  ⍝   Add 2 col's. of 0's (generation increment and x-load) :
[9]   FA←FA,[2](⍴FA)⍴0 ⋄ FA←FA[; 1 3 4 2]
[10]  CA← 5 0 5 0 10 5 ⍕FA[;⍳3] ⍝                char. array: 1st 3 cols. of FA
[11]  CA←CA,[2]((1↑⍴CA),2)⍴' -' ⍝                add space, '-' at end of rows
[12]  CA←CA,[2]((1↑⍴CA),8)⍴(8 7 ⍕FA[;4])
[13]  CA←CA,[2]((1↑⍴CA),2)⍴T ⍝                   append newline, linefeed chars.
[14]  cv←cv,(,CA),T,'END',T ⍝                    ravel CA and append to result
    ∇

    ∇ AI←INSRECT AR;A;B;IV;T;TD;X;Y
[1]  ⍝   This is a new version of INSERT to apply to meshes with one hybrid
[2]  ⍝   element per fillet (like Dr. Gerhardt's meshes in FPL 452.)
[3]  ⍝   THIS FN. INSERTS ELEMENT-SIDE NODES BETWEEN EXISTING CORNER NODES,
[4]  ⍝   e.g., THE OUTPUT ARRAY FROM FUNCTION 'NODES'.  AR HAS DIMENSIONS
[5]  ⍝   n×2.  AI IS THE ARRAY, WITH DIMENSIONS (n+?)×2, WHICH INCLUDES THE
[6]  ⍝   NEW NODES IN BETWEEN THE CORNER NODES.
[7]   X←AR[;1] ⋄ Y←AR[;2]
[8]   A←REORD AR ⍝                    reorder AR, using x-precedence
[9]   B←A[⍋A[;2];] ⍝                  reorder A, using y-precedence
[10]  A←NEWY A ⍝                      NEWY defines midside nodes at new y coord's.
[11]  B←NEWX B ⍝                      NEWX defines midside nodes at new x coord's.
[12]  AI←REORD AR,[1]A,[1]B ⍝         original nodes w/ additions, reordered from
[13] ⍝                                ...lower L to upper R w/ x-precedence
    ∇
```

```
    ∇ RES←LEFTFIL IN;LFS
[1]  ⍝   This fn., invoked by ADD1 within ELEM1, defines the left fillet
[2]  ⍝   element in an offcenter-notched beam mesh.  Whereas all other
[3]  ⍝   elmts. are defined counterclockwise from the lower left, this one
[4]  ⍝   is best handled ccl from lower right, i.e. the top corner of the
[5]  ⍝   fillet.  AR, T, L, and B are the 4-column arrays of nodes numbers
[6]  ⍝   for right, top, left and bottom elmt. sides, respectively.  They
[7]  ⍝   are global, from ELEM1.  'f.e.' ≡ fillet element.
[8]  ⍝   Written 21 June 1988
[9]  ⍝   The lower right node of the left f.e., i.e. the leftmost node on the
[10] ⍝   notch top, is the only node in a right elmt. side which doesn't
[11] ⍝   belong also to a bottom elmt. side.
[12]  LFS←(~AR[;1]∈B[;4])/AR[;1] ⍝          Left Fillet Starting node no.
[13]  LFS←(LFS>0)/LFS ⍝                     remove any 0s
[14]  RES←,(AR[;1]=LFS)⌿AR ⍝                rt. side of left f.e.
[15]  RES←RES,1↓,(T[;1]=RES[4])⌿T ⍝         find connecting top elmt. side
[16]  RES←RES,1↓,(L[;1]=RES[7])⌿L ⍝            "      "       left side
[17]  RES←RES,1↓,(B[;1]=RES[10])⌿B ⍝           "      "       bottom side
[18]  RES←IN,[1]RES
[19] ⍝   Remove the old row(s) with zero(s) in any of nodes 1-12 :
[20]  RES←(∧/RES[;⍳12]>0)⌿RES
    ∇
```

```
    ∇ name MATEDATA V;CN;I;LINE;T;TEMP;X0;Y0;name
[1]  ⍝   This is the 1st fn. invoked by MESH to generate the input data file
[2]  ⍝   for T.D. Gerhardt's finite element program FPLHYB.  After the obli-
[3]  ⍝   gatory 1st few lines, it writes the MATE data for the isoparametric
[4]  ⍝   cubic 12-node element and for 1 or 2 4-sided, 13-node hybrid fillet
[5]  ⍝   elements, depending on whether the beam is center- or offcenter-
[6]  ⍝   notched.  End-notched beams are treated as center-notched.
[7]  ⍝   V is the vector of Ex, Gxy, Ey and NUxy.  Global, from MESH :
[8]  ⍝      XY ≡ nodal coordinate array; EL ≡ element definition array.
[9]  ⍝   Latest revision 17 Mar. 1989.
[10]  name←name,'.DAT' ⍝                          append extension .DAT
[11]  name ⎕NCREATE ¯999 ⍝                        tie name.DAT to tie no. ¯999
[12]  T←⎕TCNL,⎕TCLF ⍝                             newline, linefeed characters
[13] ⍝   first line of data file:
[14]  TEMP←'FEAP ',T
[15]  TEMP ⎕NAPPEND ¯999 ⍝                        write 1st line of name.DAT
[16]  CN←XCD=0 ⍝                                  indicates center-notched beam
[17] ⍝  no. of nodes, elements, mat'l. sets (2), spatial dimensions (2),
[18] ⍝  ...unknowns per element (2), and max. nodes per element (NPE):
[19]  TEMP←,'I5' ⎕FMT(1↑⍴XY),(1↑⍴EL),(2+~CN),2,2,NPE
[20] ⍝   for center-notches, define fillet center of curvature :
[21]  ⍎CN/'X0←HL-R ◇ Y0←D-R ◇ →L10'
[22] ⍝   for OCN beams, define center of curvature for each of the 2 fillets :
[23]  X0←BL+XCD+(HL-R)× 1 ¯1 ◇ Y0←2/D-R
[24] L10:TEMP←TEMP,T,'MATE',T
[25]  LINE←'EX/EY = ',(4 1 ⍕÷/V[1 3]),' , EX/GXY = ', 4 1 ⍕÷/V[1 4]
[26]  →(NPE=13)/L13 ⍝                                  →L13 if using cubic elmts.
[27]  TEMP←TEMP,'    1    1   ISOPARAMETRIC LINEAR ELEMENT   ',LINE,T
[28]  TEMP←TEMP,'    2    1    1    1',T
[29]  →L16
[30] L13:TEMP←TEMP,'    1    1   ISOPARAMETRIC CUBIC ELEMENT   ',LINE,T
[31]  TEMP←TEMP,'    2    1    3    3',T
[32] L16:TEMP←TEMP,(10⍴' '), 10 0 10 4 10 0 10 0 ⍕V
```

```
[33]  I←1
[34] L20: ⍝     write mat'l. set no., elmt. type (3), comment :
[35]  TEMP←TEMP,T,(5 0 ⍕I+1),'    3   HYBRID FILLET ELEMENT #',(⍕I),' ',LINE,T
[36] ⍝   write: 2 for orthotropic in global x-y; 1 for plane stress; and order
[37] ⍝... of Gauss quadrature for stiffness and stress determinations :
[38]  TEMP←TEMP,,'4I5' ⎕FMT 2 1 40 40
[39]  TEMP←TEMP,T,(10⍴' '), 10 0 10 4 10 0 10 0 ⍕V
[40] ⍝   4th and 5th entries in this line are L0 and LF, the beginning and
[41] ⍝ ... ending terms of the Taylor series expansion :
[42]  →(NPE=13)/L30 ⍝                          if cubic elmts., →L30
[43]  TEMP←TEMP,T,,'11I5' ⎕FMT 5 2 4 1 12 0 91 1 0 5 1
[44]  →L40
[45] L30:TEMP←TEMP,T,,'11I5' ⎕FMT 13 4 4 1 12 0 91 1 0 13 1
[46] L40:
[47]  TEMP←TEMP,T,,'2F10.6,2F10.1,2F10.6' ⎕FMT 1 6 ⍴R,R,((0 90)+90×I>1),(1↑X0),1
      ↑Y0
[48]  I←I+1
[49]  X0←⌽X0 ⍝                                 rotate so 1↑X0 is 2nd fillet ctr.
[50]  →((I≤2)∧XCD>0)/L20 ⍝                     repeat as needed for 2nd f.e.
[51]  TEMP←TEMP,(4⍴T),'NOPR' ⍝                 turn off input echo after MATE data
[52]  TEMP←TEMP,(4⍴T),'COOR',T ⍝               COOR data will be appended next
[53]  TEMP ⎕NAPPEND ¯999 ⍝                     append to file ¯999
    ∇
```

```
    ∇ V MESHDIM PARS;NEWPARS
[1]  ⍝   This function invokes the function MESH to generate a finite element
[2]  ⍝   mesh data file for use with FORTRAN program FPLHYB.  In this fn.,
[3]  ⍝   PARS is input as a 7-vector of notch and beam geometry parameters
[4]  ⍝   in units of inches (except for V/M, in [1/inch]).  The 7 parameters
[5]  ⍝   are:
[6]  ⍝      notch depth, fillet radius, notch length, beam depth, V/M, beam
[7]  ⍝      half-length, and overhang beyond the support.
[8]  ⍝   This fn. transforms them into the parameters needed by MESH (NEWPARS:
[9]  ⍝   phi, delta, zeta, h, XCD, BL, OH).  V is a 4-vector of elastic
[10] ⍝   parameters: Ex, NUxy, Ey, Gxy.      Latest update 4 Sept. 1988.
[11]  NEWPARS←PARS
[12]  NEWPARS[1]←÷/PARS[1 4] ⍝               phi=D/d
[13]  NEWPARS[2]←÷/PARS[2 1] ⍝               delta=R/D
[14]  NEWPARS[3]←2×÷/PARS[2 3] ⍝             zeta=2R/L
[15]  NEWPARS←xcd NEWPARS ⍝                  fn. xcd converts V/M into XCD
[16]  V MESH NEWPARS ⍝                       invoke MESH to generate data file
    ∇
```

```
    ∇ V MESH PARS;EL;I;NPE;P;VOM;XY;name
[1]  ⍝   This function generates a finite element mesh data file for use
[2]  ⍝   with FORTRAN program FPLHYB.  PARS is a 7-vector of notch and
[3]  ⍝   beam geometry parameters (phi, delta, zeta, h, XCD, BL, OH)
[4]  ⍝   as described and used in NODE1.  V is a 4-vector of elastic
[5]  ⍝   parameters: Ex, NUxy, Ey, Gxy.   Last update August, 1988.
[6]  ⍝
[7]   'Begin at ',⍕(⎕TS)[4 5 6]
[8]   NPE←13 ⍝                                  cubic mesh
[9]   XY←INSRECT NODE1 PARS ⍝                   generate nodal coordinate array
[10]  EL←ELEM1 XY ⍝                             generate element connectivity array
[11]  ⍎(XCD=0)/'VOM←0 ◇ →L10' ⍝                 set VOM=0 if XCD=0
[12]  VOM←÷(BL+((×/PARS[1 2 4])×(¯1+÷PARS[3]))-XCD+OH)
[13]  ⍎(PARS[4]=3.5)/'P←(VOM≤ 0 0.05 1)⍳1 ◇ →L10'
[14] ⍝⍎(PARS[4]≠3.5)/'P←3+(((2×-/PARS[6 7])÷PARS[4])≤6.5 7 9 10 12 13 16 20)⍳1'
[15]  ⍎(PARS[4]≠3.5)/'P←3+(PARS[4]≤3.5 5.5 7 9 12 16 20)⍳1'
[16] ⍝ If h=3.5" - 'C' (Center notch) or 'N' (Near center) or 'F' (Far from
[17] ⍝    center) and 1st 2 signif. digits of phi :
[18] ⍝ If h≠3.5" - Q,R,S,T,U,V,W,X distinguish between increasing levels of
[19] ⍝    beam depth; then, add 1st 2 signif. digits of phi :
[20] L10:name←'CNFQRSTUVWX'[P],¯2↑ 4 2 ⍕PARS[1]
[21]  name←name,¯2↑ 4 2 ⍕PARS[2] ⍝              1st 2 signif. digits of delta
[22]  name←name,¯2↑ 4 2 ⍕PARS[3] ⍝              1st 2 signif. digits of zeta
[23] ⍝   append A,B,C,D, or E to filename denoting Ex/Gxy ≤ 8,12,17,22 or 32:
[24]  name←name,'ABCDE'[((V[1]÷V[4])≤ 8 12 17 22 32)⍳1]
[25]  'Filename:          ',name
[26]  'No. of Nodes:      ',⍕1↑⍴XY
[27]  'No. of Elements:   ',⍕1↑⍴EL
[28]  name MATEDATA V ⍝                         open file, write mat'l. data
[29]  COORDATA XY ⍝                             write nodal coord. data
[30]  ELEMDATA EL ⍝                             write element connectivity data
[31]  'Type S for single load case, M for multiple (cp + qp + udl).'
[32]  I←⎕INKEY
```

```
[33] ⍝   write BOUN, FORC and macro lines :
[34]  ⍎(I='S')/'BOUNFORC ◇ →0' ⍝                for single loading case
[35]  NEWBOUNFORC ⍝                             multiple cases, as noted above
[36]  'End at ',⍕(⎕TS)[4 5 6]
      ∇

      ∇ NEWBOUNFORC;B1;B2;C;NN;N1;N2;T;TEMP;TOP;X;XMAX;Y
[1]   ⍝   This fn. writes the BOUN, FORC and macro control card lines to the
[2]   ⍝   DOS data file tied to file no. ¯999 for use with FORTRAN finite
[3]   ⍝   element analysis program FPLHYB.  Quarter-point,center-point and
[4]   ⍝   uniformly distributed loads are applied for all beam geometries.
[5]   ⍝   Nodal coordinate array XY, and geometric parameters BL, OH, H and D
[6]   ⍝   must be in the active WS.  CN ≡ center notch; OCN ≡ offctr. notch.
[7]   ⍝   Written 25 November 1988
[8]    X←XY[;1] ◇ Y←XY[;2]
[9]    T←⎕TCNL,⎕TCLF ⍝                                  newline, linefeed characters
[10] ⍝.....................................................................
[11]   TEMP←T,'BOUN',T ⍝                               begin constraint data
[12]   →(XCD>0)/L10 ⍝                                  for OCN, →L10
[13]   B1←¯1+(X>0)⍳1 ⍝                                 top x-constrained node (at x=0)
[14]   B2←(X=BL-OH)⍳1 ⍝                                y-constrained node (roller)
[15]   TEMP←TEMP,'    1    1   -1    0',T ⍝           CN: bottom of shear release
[16]   TEMP←TEMP,(,'4I5' ⎕FMT B1, 0 1 0),T ⍝           top of shear release
[17]   TEMP←TEMP,(,'4I5' ⎕FMT B2, 0 0 1),T,T ⍝         right support node
[18]   →L20
[19] ⍝.....................................................................
[20] L10: ⍝ constraint data for OCN (whole beam model):
[21]   NN←⍳⍴X ⍝                                        node numbers
[22]   N1←((X=OH)∧Y=0)/NN ⍝                            no. of left support node
[23]   N2←((X=BL+BL-OH)∧Y=0)/NN ⍝                      no. of right support node
[24]   TEMP←TEMP, 5 0 ⍕N1,0,1,1 ⍝                      node N1 fixed in x and y
[25]   TEMP←TEMP,T,(5 0 ⍕N2,0,0,1),T,T ⍝              node N2 fixed in y, free in x
[26] ⍝.....................................................................
[27] ⍝   The next 2 lines append the macro control lines to the file :
```

```
[28] L20:TEMP←TEMP,'END',T,'MACRO',T,'LNZD',T,'TANG',T,'LOOP          3',T
[29]  TEMP←TEMP,'MESH',T,'FORM',T,'SOLV',T,'DISP',T,'STRE',T,'NEXT',T
[30]  TEMP←TEMP,'OTMH',T,'END',T
[31] A.....................................................................
[32] A   TOP ≡ node #s along top sfc. between supports :
[33]  XMAX←BL×1+XCD>0 A                              right end of model
[34]  TOP←((XY[;2]=H)∧XY[;1]≤XMAX-OH)/⍳1↑⍴XY A used in fns. below
[35] A   Calculate center point load needed :
[36]  TEMP←TEMP,FORCcp XY
[37] A   Calculate offcenter loads :
[38]  TEMP←TEMP,FORCqp XY
[39] A   Calculate uniformly distributed loads :
[40]  TEMP←TEMP,FORCud XY
[41]  TEMP←TEMP,'STOP'
[42]  TEMP ⎕NAPPEND ¯999 A                  append TEMP to DOS file, tie #¯999
[43]  ⎕NUNTIE ¯999 A                        untie file ¯999
    ∇
```

```
    ∇ RES←NEWX B;ADD;BA;BB;D1;D2;LV;XHI;XLO
[1]  ⍝   B is the n×2 array of corner nodal coord's. with the fillet box
[2]  ⍝   interior nodes removed.  B must already be ordered from lower L to
[3]  ⍝   upper right w/ y-precedence.  This is assured if NEWX is invoked by
[4]  ⍝   INSRECT.  Global, from INSRECT: X, Y (coordinate vectors).
[5]  ⍝   Global, from NODE1: R ≡ fillet radius; D ≡ notch depth; HL ≡ notch
[6]  ⍝      half-length; XCD ≡ distance from notch center to beam center.
[7]  ⍝   Latest update 28 June 1988.
[8]   BA←(B[;2]>D)⌿B ⍝                                  pts. above the fillet
[9]   BB←(B[;2]≤D)⌿B ⍝                                  pts. below the fillet
[10]  D1←BA[1↓⍳1↑⍴BA;]-BA[¯1↓⍳1↑⍴BA;] ⍝                 DIFFERENCE ARRAY
[11]  LV←(D1[;1]>0)∧D1[;2]=0 ⍝                          LOGICAL SELECTION VECTOR
[12]  D1←LV⌿D1
[13] ⍝    BA ≡ nodes to whose right new nodes are to be inserted :
[14]  BA←(LV,0)⌿BA
[15]  D2←BB[1↓⍳1↑⍴BB;]-BB[¯1↓⍳1↑⍴BB;] ⍝                 DIFFERENCE ARRAY
[16]  LV←(D2[;1]>0)∧D2[;2]=0 ⍝                          logical selection vector
[17] ⍝    more pts. to whose R insertions will be made :
[18]  BB←(LV,0)⌿BB
[19]  D2←LV⌿D2
[20]  ADD←((⍴BA)+ 1 0 ×⍴BB)⍴0 ⍝                        DUMMY VALUES
[21] ⍝    Δx values to be added to corner node coord's. :
[22]  ADD[;1]←(D1[;1]÷3),D2[;1]÷3
[23]  B←BA,[1]BB
[24]  RES←(B+ADD),[2](B+2×ADD)
[25]  RES←((2×1↑⍴RES),2)⍴RES
[26]  XHI←XCD+HL+BL×XCD>0 ⍝                             L edge of right fillet elmt.
[27]  XLO←(XCD-HL)+BL×XCD>0 ⍝                           right edge of L fillet elmt.
[28] ⍝   Remove any spurious nodes within the notch :
[29]  RES←(~(RES[;1]<XHI)∧(RES[;1]>XLO)∧RES[;2]≤D-R)⌿RES
    ∇
```

```
     ∇ R←NEWY AR;D;LV;ADD
[1]   ⍝   AR IS A 2-D NODAL COORD. ARRAY, ORDERED FROM LOWER L TO UPPER R, WITH
[2]   ⍝   x-PRECEDENCE.  'NEWY' ADDS MIDSIDE NODES ALONG VERTICAL ELMT. SIDES.
[3]    D←AR[1↓⍳1↑⍴AR;]-AR[¯1↓⍳1↑⍴AR;] ⍝          DIFFERENCE ARRAY
[4]    LV←(D[;1]=0)∧D[;2]>0 ⍝                    LOGICAL SELECTION VECTOR
[5]   ⍝   nodes above which new nodes are to be inserted :
[6]    AR←(LV,0)⌿AR
[7]    D←LV⌿D
[8]   ⍝   ADD ≡ array of Δy values to be added to existing y coord's. :
[9]    ADD←(⍴AR)⍴0
[10]   ADD[;2]←D[;2]÷3
[11]   R←(AR+ADD),[2]AR+2×ADD ⍝                          additions to AR
[12]   R←((2×1↑⍴R),2)⍴R
     ∇
```

```
     ∇ RES←NODE1 PARS;X;XMAX;Y
[1]   ⍝   This fn. defines the nodal coordinate array for notched beams
[2]   ⍝   using a single 90-degree hybrid fillet element at each fillet.
[3]   ⍝   PARS is a 7-vector of geometric parameters:
[4]   ⍝      phi, delta, zeta, h, XCD, BL, OH.
[5]   ⍝   R is a 2-column array of nodal x-y coordinates.  The order of the
[6]   ⍝   rows of RES is important to the functions called by NODE1.  Vari-
[7]   ⍝   ables BL, D, H, HL, OH, R, XCD are left global for use by other fns..
[8]    →((∧/1≥PARS[⍳3])∧∧/0≤PARS)/START
[9]    'Input error in NODE1.  Execution halted.' ◇ →
[10]  START:ZET←PARS[3] ⍝          zeta, for global use in INSRECT
[11]   H←PARS[4] ⍝                 beam height (≡ depth)
[12]   D←PARS[1]×H ⍝               notch depth = phi × beam depth
[13]   R←PARS[2]×D ⍝               fillet radius = delta × notch depth
[14]   HL←R÷ZET ⍝                  notch half-length
[15]   XCD←PARS[5] ⍝               XCD ≡ distance, beam center to notch center
[16]   BL←PARS[6] ⍝                BL ≡ beam half-length
```

```
[17]  OH←PARS[7] ⍝                    OH ≡ overhang beyond right support
[18]  XMAX←BL×1+XCD>0 ⍝               maximum x in model (half vs. full beam)
[19]  X←HL+(XCD>0)×BL+XCD ⍝           x coord. of node 1
[20]  Y←D-R ⍝                         y coord. of node 1
[21]  X←X,X-R ◇ Y←Y,D ⍝               coord's.  "   "  2
[22]  X←X,X[1]+R ◇ Y←Y,Y[1] ⍝           "      "   "  3
[23]  X←X,X[2] ◇ Y←Y,Y[2]+R ⍝           "      "   "  4
[24]  X←X,X[3] ◇ Y←Y,Y[4] ⍝             "      "   "  5
[25] ⍝   Make sure no nodes have y > H; if needed, extend fillet box to top
[26] ⍝    of beam and adjust X[3] and X[5] to keep the fillet box "square":
[27]  ⍎((H-Y[4])<R)/'Y[4 5]←H ◇ X[3 5]←X[1]+H-Y[2]'
[28] ⍝   Abort if f.e. extends beyond support :
[29]  →(X[3]≤XMAX-OH)/L10 ⍝           →L10 under normal circumstances
[30]  'The fillet element extends beyond the right support.  Reduce XCD or '
[31]  '   notch length.  Execution halted.' ◇ →
[32] L10:→(XCD=0)/L20 ⍝               →L20 if center notch
[33] ⍝   for offcenter notch, reflect fillet nodes about notch centerline :
[34] ⍝      if notch is semicircular (ZET=1), don't reflect nodes 2, 4:
[35]  ⍎(ZET=1)/'X←X,(2×BL+XCD)-X[1 3 5] ◇ Y←Y,Y[1 3 5]'
[36]  ⍎(ZET<1)/'X←X,(2×BL+XCD)-X ◇ Y←Y,Y'
[37] L20:RES←X,[1.5]Y ⍝               temporary definition of RES
[38]  RES←EXTEND RES ⍝                EXTEND extends the mesh outward from the...
[39] ⍝                                ...fillet elmt. to the beam edges and ends
    ∇
```

```
    ∇ R←REORD A;X;Y
[1]  ⍝   A IS AN n×2 ARRAY OF x-y NODAL COORDINATES.  THIS FN. REORDERS THE
[2]  ⍝   NODES (i.e., THE ROWS OF A) TO GO FROM LOWER LEFT TO UPPER RIGHT,
[3]  ⍝   GROUPING TOGETHER EACH SET OF NODES WITH x=constant.
[4]  ⍝
[5]   Y←A[;2] ⍝        DEFINE Y AS THE 2ND COLUMN OF THE INPUT COORD. ARRAY
[6]   R←A[⍋Y;] ⍝       REORDER ROWS OF A BY THE ORDER OF THE y-COORD'S.
[7]   X←⌈32000×R[;1]÷⌈/R[;1] ⍝   define x as the 1st col. of the reordered
[8]  ⍝                            coord. array, then convert to integers
[9]   R←R[⍋X;] ⍝       reorder rows of R by the order of X
    ∇
```

```
    ∇ RES←OCNLEFT XY;DL;HTS;IV;LHY;N;X;Y
[1]  ⍝   This fn., invoked by EXTLEFT, extends the nodal coordinate mesh
[2]  ⍝   to the left of an offcenter notch (V/M ≠ 0).  The mesh will cover
[3]  ⍝   the entire beam length (2×BL), not just the right half-beam.
[4]  ⍝   Global, from NODE1: XCD ≡ distance from notch center to beam center;
[5]  ⍝      BL ≡ half-length of beam; OH ≡ length of overhang beyond each
[6]  ⍝      support.
[7]  ⍝   Last revision 18 June 1988.
[8]   X←XY[;1] ◇ Y←XY[;2] ⍝                    define x, y coord. vectors
[9]   IV←(X∈X[1 3])∧~Y∈Y[1 4] ⍝                indexes pts. to be reflected
[10] ⍝     reflect pts. @ x=X[2] if X[2] is NOT the notch centerline :
[11]  IV←IV∨(HL>R)∧(X=X[2])∧~Y∈Y[1 2 4] ⍝      node 2 already reflected by NODE1
[12]  X←X,(2×BL+XCD)-IV/X ⍝                    x for new pts. immed. L of notch
[13]  Y←Y,IV/Y ⍝                               y for new pts. immed. L of notch
[14]  LHY←(X=⌊/X)/Y ⍝                          y coord's. of leftmost pts.
[15]  LHY←LHY[⍋LHY] ⍝                          order from low to high
[16]  HTS←(1↓LHY)-¯1↓LHY ⍝                     leftmost elmt.heights
[17]  X←X,(⍴LHY)⍴(⌊/X)-2×⌊/HTS ⍝               col. of nodes to L of L f.e.
[18]  Y←Y,LHY ⍝                                y coord's. of these nodes
[19] ⍝     distance from L support to L edge of existing mesh :
[20]  DL←(⌊/X)-OH
[21]  N←⌈DL÷6×⌊/HTS ⍝                          # of new elmt. cols. needed to L
[22]  X←X,(⍴LHY)/0,OH+(¯1+⍳N)×DL÷N ⍝           x coord's. of new nodes
[23]  Y←Y,((N+1)×⍴LHY)⍴LHY ⍝                   y coord's. of new nodes
[24]  RES←X,[1.5]Y ⍝                           reconstituted 2-D coord. array
    ∇
```

Appendix 4: APL FE Mesh Generator for End-Notched Beams. Program Design and Listing

'Part 1: For Tension Face Notches

The overall structure of the mesh generator is given on this page. Each APL function begins on the page number shown in brackets {}. Indentation is used to indicate the level of the (sub)function, i.e., the name of a calling function is indented less than the names of its subfunction(s).

```
ENDMESHT {310}
     ENDNODE {311}
          LEFTEND {312}
               LEFTENDS1 {313}
          ENDEXTEND {307}
               EXTDOWN {282}
               ENDEXTRT {308}
     INSRECT {293}
          REORD {303}
          NEWY {302}
          NEWX {301}
     ELEM1 {278}
          ELEM1S1 {279}
               ELEM1S2 {280}
          ADD1 {271}
               LEFTFIL {294}
     MATEDATA {295}
     COORDATA {276}
     ELEMDATA {277}
     ENDBOUNFORC {306}
```

```
    ∇ ENDBOUNFORC;B1;B2;I;MIN;P;T;TEMP;X;Y
[1]  ⍝   This fn. writes the BOUN, FORC and macro control card lines to the
[2]  ⍝   DOS data file tied to file no. ¯999 for use with FORTRAN finite
[3]  ⍝   element analysis program FPLHYB.  This is for the case of double-end-
[4]  ⍝   notched beams (modeling only the left 1/2.)  Center-point loading is
[5]  ⍝   used.  Nodal coordinate array XY, and geometric parameters BL, OH, H
[6]  ⍝   and D must be in the active WS.     Written 11 Nov. 1988.
[7]   X←XY[;1] ◇ Y←XY[;2]
[8]   T←⎕TCNL,⎕TCLF ⍝                          newline, linefeed characters
[9]   I←((X=BL)∧Y=H)/⍳⍴X ⍝                     node no. at which load will be placed
[10]  P←H÷6 ⍝                                  force for unit gross section stress
[11]  B1←(X=OH)⍳1 ⍝                            y-constrained node (x=OH, y=0)
[12]  B2←(X=BL)⍳1 ⍝                            lowest x-constrained node (at x=BL)
[13]  TEMP←T,'BOUN',T ⍝                              write top line (BOUN)
[14]  TEMP←TEMP,(5 0 ⍕B1, 0 0 1),T ⍝                 1st constraint line
[15]  TEMP←TEMP,(5 0 ⍕B2,1),'    -1    0' ⍝       2nd   "          "
[16]  TEMP←TEMP,T,(5 0 ⍕I,0,1,0),T,T ⍝              last  "          "
[17]  TEMP←TEMP,'FORC',T ⍝                           write top FORC line
[18]  TEMP←TEMP,(5 0 ⍕I),'     0         0 -',,'F8.6' ⎕FMT P
[19] ⍝.....................................................................
[20] L10:TEMP←TEMP,T,T
[21] ⍝   The next 2 lines append the macro control lines to the file :
[22]  TEMP←TEMP,'END',T,'MACRO',T,'LNZD',T,'TANG',T,'FORM',T,'SOLV',T
[23]  TEMP←TEMP,'OTMH',T,'DISP',T,'STRE',T,'END',T,'STOP',T
[24]  TEMP ⎕NAPPEND ¯999 ⍝                     append TEMP to DOS file, tie #¯999
[25]  ⎕NUNTIE ¯999 ⍝                           untie file ¯999
    ∇
```

```
    ∇ OUT←ENDEXTEND XY;AR;BO;LHR;TA;TD
[1]  ⍝   This fn., invoked by ENDNODE, extends the mesh definition from the
[2]  ⍝   hybrid fillet element (f.e.) to the edges and right end of the beam.
[3]  ⍝   This fn. is for double-end-notched beams only.
[4]  ⍝   XY and OUT are x-y coord. arrays, before and after the addition of
[5]  ⍝   the new nodes.  Global, from ENDNODE: R = fillet radius; X, Y =
[6]  ⍝      coord's. of the nodes in, above and left of the fillet element
[7]  ⍝      (f.e.).
[8]  ⍝   Written 9 Nov. 1988.
[9]  ⍝   The next 4 lines define TD as a 2-vector of test distances.
[10]  TD←Y[1] ⍝                    distance below f.e.
[11]  TD←TD,BL-X[3] ⍝              distance from f.e. to right end
[12] ⍝   LHR ≡ least height of elmts. to right of f.e. :
[13]  LHR←TD[1],2×R ◇ LHR←(LHR>0)/LHR ◇ LHR←⌊/LHR
[14] ⍝   Aspect ratios (2): test distances ÷ shortest adjacent side lengths.
[15]  AR←TD÷(X[3]-X[1]),LHR
[16] ⍝   TA = test array, used to select correct option for mesh extension
[17]  TA←(AR∘.≤0,0.333333,2,4,8,38)× 2 6 ⍴⌊6 ⍝     new version, 3 May 1988
[18]  BO←⌊/TA+6×TA=0 ⍝           branch option vector: gives the correct option
[19] ⍝                            ...for each of the 4 directions (down,R,up,L)
[20]  OUT←BO[1]EXTDOWN XY ⍝      extend mesh to bottom of beam
[21]  OUT←BO[2]ENDEXTRT OUT ⍝    extend mesh to right end of beam
    ∇
```

```
    ∇ RES←C ENDEXTRT XY;MH;N;RHY;XMAX;XR
[1]  ⍝   This fn. is invoked by ENDEXTEND, which is invoked by ENDNODE for
[2]  ⍝   single end notch meshes.  It adds nodes as needed to the right of
[3]  ⍝   the hybrid fillet element, extending to the right end of the model,
[4]  ⍝   i.e., the centerline of the beam.
[5]  ⍝   C is an integer scalar (from 1 to 7) used to choose the appropriate
[6]  ⍝   number of new elmts. above the fillet elmt..  XY is the orig. nodal
[7]  ⍝   coord. array, and RES is the revised nodal coord. array.
[8]  ⍝   Global Vars., from ENDNODE: BL=beam half-length; OH= overhang; X, Y;
[9]  ⍝     are coord's. of the 5 fillet element (f.e.) nodes.
[10] ⍝   Global, from ENDEXTEND: LHR=least height of elmts. to rt. of f.e.
[11] ⍝   Written 17 Mar. 1989 from EXTRIGHT.
[12]  XMAX←BL×1+XCD>0 ⍝                          rt. endpt., ctr. vs. offctr. notch
[13]  RHY←(XY[;1]=⌈/XY[;1])/XY[;2] ⍝             vector of y's of rtmost nodes
[14]  MH←⍴RHY ⍝                                  mesh ht. (no. of nodes, bot.→top)
[15]  →(L1,L10,L20,L30,L40,L50,L50)[C] ⍝         select proper mesh option
[16] ⍝.....................................................................
[17] L1: ⍝                                       fillet elmt. touches the beam end
[18]  RES←XY,[1]⍉(2,MH)⍴(MH/XMAX),RHY ⍝          add nodes at x=XMAX, y=RHY
[19]  →L100
[20] ⍝.....................................................................
[21] L10: ⍝    f.e. very close to beam end.  Extend it to touch beam end :
[22]  XY[;1]←(XY[;1]×XY[;1]≠XY[3;1])+XMAX×XY[;1]=XY[3;1]
[23]  →L1
[24] ⍝'The notch is too close to the beam end.  It may be treated by'
[25] ⍝ '   reducing the length or height of the fillet element specified in'
[26] ⍝ '   fn. ENDNODE.  Execution has halted in fn. ENDEXTRT.' ◇ →
[27] ⍝.....................................................................
[28] L20: ⍝        need a single elmt. col. btw. fillet elmt. and beam end
[29]  RES←XY,[1]⍉(2,MH)⍴(MH/XMAX),RHY ⍝          add nodes at x=XMAX, y=RHY
[30]  →L100
[31] ⍝.....................................................................
[32] L30: ⍝        need 2 cols. of equal-length elmts. btw. f.e. and beam end
```

```
[33]  RES←XY,[1]⍉(2,MH)⍴(MH/XMAX),RHY ⍝          add nodes at beam end
[34] ⍝   add column of nodes btw. f.e. and beam end:
[35]  RES←RES,[1]⍉(2,MH)⍴(MH/0.5×X[3]+XMAX),RHY
[36]  →L100
[37] ⍝.....................................................................
[38] L40: ⍝      need 2 cols. of unequal-length elmts. btw. f.e. and beam end
[39] ⍝    add nodes 2×LHR from right edge of f.e.:
[40]  RES←XY,[1]⍉(2,MH)⍴(MH/X[3]+LHR),RHY ⍝      new version, 16 Nov. 1988
[41]  RES←RES,[1]⍉(2,MH)⍴(MH/XMAX),RHY ⍝         add nodes at x=XMAX, y=RHY
[42]  →L100
[43] ⍝.....................................................................
[44] L50: ⍝        need >2 col's. of elmts.btw. fillet elmt. and beam end
[45] ⍝    add nodes LHR from right edge of f.e.:
[46]  RES←XY,[1]⍉(2,MH)⍴(MH/X[3]+LHR),RHY ⍝    new 16 Nov. 1988
[47]  XR←XMAX-¯1↑RES[;1] ⍝                     distance remaining to beam end
[48]  N←⌈XR÷3×LHR ⍝                            # of elmt. col's. needed to ...
[49] ⍝                                         ...get to the beam end
[50] ⍝   add N cols. of nodes btw. rtmost. prev. node and beam end :
[51]  RES←RES,[1]⍉(2,N×MH)⍴((N×MH)⍴(¯1↑RES[;1])+XR×(⍳N)÷N),N/RHY
[52] ⍝ RES←RES,[1]⍉(2,MH)⍴(MH/XMAX),RHY ⍝       add nodes at x=XMAX, y=RHY
[53] ⍝.....................................................................
[54] L100:
     ∇
```

```
    ∇ V ENDMESHT PARS;BL;D;EL;H;HL;L;NPE;OH;R;XCD;XY;name
[1]  ⍝   This function generates a finite element mesh data file for use
[2]  ⍝   with FORTRAN program FPLHYB.  PARS is a 6-vector of notch and
[3]  ⍝   beam geometry parameters (D, R, L, h, BL, OH) as described and
[4]  ⍝   used in ENDNODE.  V is a 4-vector of elastic parameters:
[5]  ⍝   Ex, NUxy, Ey, Gxy.                    Latest update 17 Mar. 1989.
[6]  ⍝
[7]   'Begin at ',⍕(⎕TS)[4 5 6]
[8]   NPE←13 ⍝                                 max. # of nodes per cubic elmt.
[9]   XY←INSRECT ENDNODE PARS ⍝                generate nodal coordinate array
[10]  EL←ELEM1 XY ⍝                            generate element connectivity array
[11] ⍝    'E' (End notch) and 1st 2 signif. digits of phi ≡ D/h :
[12] L10:name←'E',¯2↑ 4 2 ⍕÷/PARS[1 4]
[13]  name←name,¯2↑ 4 2 ⍕÷/PARS[2 4] ⍝     1st 2 signif. digits of rho ≡ R/h
[14]  name←name,¯2↑ 4 2 ⍕0.1×÷/PARS[3 4] ⍝ 1st 2 signif. digits of .1×L/h
[15] ⍝   append A, B, C, D, E or F to filename denoting elastic properties :
[16]  name←name,'BADECF'[((V[1]÷V[4])≤ 8 10 14 17 22 32)⍳1]
[17]  'Filename:         ',name
[18]  'No. of Nodes:     ',⍕1↑⍴XY
[19]  'No. of Elements: ',⍕1↑⍴EL
[20]  name MATEDATA V ⍝                        open file, write mat'l. data
[21]  COORDATA XY ⍝                            write nodal coord. data
[22]  ELEMDATA EL ⍝                            write element connectivity data
[23]  ENDBOUNFORC ⍝                            write BOUN, FORC and macro lines
[24]  'End at ',⍕(⎕TS)[4 5 6]
    ∇
```

```
    ∇ XY←ENDNODE PARS;L;X;Y
[1]   ⍝   This fn. generates the element-corner nodes for a finite element
[2]   ⍝   mesh of the left 1/2 of a symmetric double-end-notched beam.  PARS
[3]   ⍝   is a 6-vector of beam and notch dimensions, all in the same units.
[4]   ⍝   XY is a 2-column array of nodal x-y coordinates.
[5]   ⍝   Written 3 Nov. 1988.
[6]    D←PARS[1] ⍝                          notch depth
[7]    R←PARS[2] ⍝                          fillet radius
[8]    L←PARS[3] ⍝                          distance, support to fillet ctr.
[9]    H←PARS[4] ⍝                          beam depth
[10]   BL←PARS[5] ⍝                         beam half-length
[11]   OH←PARS[6] ⍝                         overhang beyond support
[12]   X←L+OH+R ◇ Y←D-R ⍝                   coord's. of node 1
[13]   X←X,L+OH ◇ Y←Y,D ⍝                   coord's.  "   "  2
[14]   X←X,X[1]+R ◇ Y←Y,Y[1] ⍝               "      "   "  3
[15]   X←X,X[2] ◇ Y←Y,Y[2]+R ⍝               "      "   "  4
[16]   X←X,X[3] ◇ Y←Y,Y[4] ⍝                 "      "   "  5
[17]  ⍝   Make sure no nodes have y > H; if needed, extend fillet box to top
[18]  ⍝     of beam and adjust X[3] and X[5] to keep the fillet box "square":
[19]   ⍎((H-Y[4])<R)/'Y[4 5]←H ◇ X[3 5]←X[1]+H-Y[2]'
[20]   XY←X,[1.5]Y
[21]   XY←LEFTEND XY ⍝                      add nodes from fillet to L end
[22]   XCD←0 ⍝                              dummy value for use in other fns.
[23]  ⍝  Extend the mesh to the beam edges and ends :
[24]   HL←L+OH+R ⍝                          dummy value for use in EXTEND
[25]   XY←ENDEXTEND XY
[26]  ⍝  Order nodes from lower L to upper R w/ x-precedence :
[27]   XY←XY[⍋XY[; 1 2];]
    ∇
```

```
    ∇ XY←LEFTEND XY;HA;LY;NA;X;Y
[1]  ⍝   This fn., invoked by ENDNODE, adds element-corner nodes from the
[2]  ⍝   fillet element (f.e.) to the left end of the beam.  XY is the
[3]  ⍝   2-column nodal x-y coordinate array.  "f.e" ≡ fillet element.
[4]  ⍝   Global, from ENDNODE :
[5]  ⍝      D, R, L :  notch depth, fillet radius, length (from center of
[6]  ⍝                 fillet radius to support);
[7]  ⍝      OH ≡ overhang, i.e. distance from L end to support;
[8]  ⍝      H, BL ≡ beam depth and half-length.
[9]  ⍝   Written 7 November 1988; latest revision 17 Mar. 1989.
[10]  X←XY[;1] ⋄ Y←XY[;2]
[11] ⍝   Select branch depending on ht. remaining above f.e. :
[12]  HA←H-Y[4] ⍝                              height remaining above f.e.
[13]  →(L40,L10,L20,L30)[((HA÷R)≤ 0 3 60 1000000)⍳1]
[14] L10: ⍝   one element above f.e. :
[15]  X←X,X[4 5] ⋄ Y←Y,2/H ⍝                   2 nodes at top of beam
[16]  →L40
[17] L20: ⍝  2 or more elmts. above f.e.
[18]  NA←1+⌈(¯1+HA÷2×R)÷3+3×NPE=13 ⍝           # of elmts. above f.e.
[19]  X←X,(2×NA)⍴X[4 5] ⍝                      x for nodes above f.e.
[20]  Y←Y,2/Y[4]+(2×R) ⍝                       y for 1st pair of new nodes
[21]  HA←HA-2×R ⋄ NA←NA-1 ⍝                    revise HA, NA
[22]  Y←Y,2/(¯1↑Y)+(⍳NA)×HA÷NA ⍝               y for new nodes to beam top
[23]  →L40
[24] L30: ⍝  too much space above f.e.; crash w/ msg.
[25]  'This beam is very high for this small fillet radius, and would lead '
[26]  '    to a mesh with very many nodes and elements.  Execution has been'
[27]  '    terminated in LEFTEND.' ⋄ →
[28] L40: ⍝  no more space above f.e.
[29]  XY←LEFTENDS1 XY←X,[1.5]Y ⍝               extend mesh to left end
    ∇
```

```
    ∇ RES←LEFTENDS1 XY;CD;HTS;LHY;NC;NR;X;Y
[1]  ⍝   This fn., invoked by LEFTEND, takes the 2-col. array XY of corner
[2]  ⍝   nodal coordinates at and above the fillet element (f.e.) and
[3]  ⍝   extends it leftward to the end of the beam.  This is specifically
[4]  ⍝   for double-end-notched beams.   Global from ENDNODE :
[5]  ⍝      R ≡ fillet radius;  L ≡ distance from support to center of fillet
[6]  ⍝      curvature; OH ≡ overhang beyond left support
[7]  ⍝   Latest update 17 Mar. 1989.
[8]   X←XY[;1] ⋄ Y←XY[;2]
[9]   LHY←(X=⌊/X)/Y ⋄ LHY←LHY[⍋LHY] ⍝          y coord's. of nodes L of f.e.
[10]  HTS←1↓LHY-¯1⌽LHY ⍝                      heights of elmts. L of f.e.
[11]  NR←⍴LHY ⍝                               # of rows of nodes L of f.e.
[12]  X←X,NR/X[2]-R ⍝                         1st col. of nodes L of f.e.
[13]  Y←Y,LHY
[14]  CD←(⌊/HTS)×3+3×NPE=13 ⍝                 comparison distance
[15]  NC←⌈(L-R)÷CD ⍝                          # of col's. of nodes L to support
[16]  →(NC=0)/L1 ⍝                            →L1 if no nodes needed
[17]  X←X,NR/OH+(¯1+⍳NC)×(L-R)÷NC ⍝           x of nodes L to support
[18]  Y←Y,(NR×NC)⍴LHY ⍝                       y of nodes L to support
[19] L1:NC←⌈OH÷CD ⍝                           # node col's. from supt. to L end
[20]  X←X,NR/(¯1+⍳NC)×OH÷NC ⍝                 x of nodes L from support to end
[21]  Y←Y,(NR×NC)⍴LHY ⍝                       y of  "    "   "     "     "  "
[22]  RES←X,[1.5]Y
    ∇
```

Part 2: For Compression Face Notches

```
ENDMESHC {316}
     ENDNODE {311}
          LEFTEND {312}
               LEFTENDS1 {313}
          ENDEXTEND {307}
               EXTDOWN {282}
               ENDEXTRT {308}
     INSRECT {293}
          REORD {303}
          NEWY {302}
          NEWX {301}
     ELEM1 {278}
          ELEM1S1 {279}
               ELEM1S2 {280}
          ADD1 {271}
               LEFTFIL {294}
     MATEDATA {295}
     COORDATA {276}
     ELEMDATA {277}
     ENDBOUNFORCK {315}
```

```
    ∇ ENDBOUNFORCK;B1;B2;I;MIN;P;T;TEMP;X;Y
[1]  ⍝   This is the version of ENDBOUNFORC for compression side notches.
[2]  ⍝   This fn. writes the BOUN, FORC and macro control card lines to the
[3]  ⍝   DOS data file tied to file no. ¯999 for use with FORTRAN finite
[4]  ⍝   element analysis program FPLHYB.  This is for the case of double-end-
[5]  ⍝   notched beams (modeling only the left 1/2.)  Center-point loading is
[6]  ⍝   used.  Nodal coordinate array XY, and geometric parameters BL, OH, H
[7]  ⍝   and D must be in the active WS.
[8]  ⍝   Written 13 Feb. 1989 from ENDBOUNFORC of 11 Nov. 1988.
[9]   X←XY[;1] ◇ Y←XY[;2]
[10]  T←⎕TCNL,⎕TCLF ⍝                        newline, linefeed characters
[11]  I←((X=BL)∧Y=0)/⍳⍴X ⍝                   node no. at which load will be placed
[12]  P←H÷6 ⍝                                force for unit gross section stress
[13]  B1←((X=OH)∧Y=H)/⍳⍴X ⍝                  y-constrained node (x=OH, y=H)
[14]  B2←((X=BL)∧Y=H)/⍳⍴X ⍝                  highest x-constrained node (at x=BL)
[15]  TEMP←T,'BOUN',T ⍝                           write top line (BOUN)
[16]  TEMP←TEMP,(5 0 ⍕B1, 0 0 1),T ⍝              1st constraint line
[17]  TEMP←TEMP,(5 0 ⍕I,1),'   -1    0' ⍝      2nd   "          "
[18]  TEMP←TEMP,T,(5 0 ⍕B2,0,1,0),T,T ⍝          last  "          "
[19]  TEMP←TEMP,'FORC',T ⍝                        write top FORC line
[20]  TEMP←TEMP,(5 0 ⍕I),'    0         0  ',,'F8.6' ⎕FMT P
[21] ⍝.....................................................................
[22] L10:TEMP←TEMP,T,T
[23] ⍝   The next 2 lines append the macro control lines to the file :
[24]  TEMP←TEMP,'END',T,'MACRO',T,'LNZD',T,'TANG',T,'FORM',T,'SOLV',T
[25]  TEMP←TEMP,'OTMH',T,'DISP',T,'STRE',T,'END',T,'STOP',T
[26]  TEMP ⎕NAPPEND ¯999 ⍝                   append TEMP to DOS file, tie #¯999
[27]  ⎕NUNTIE ¯999 ⍝                         untie file ¯999
    ∇
```

```
    ∇ V ENDMESHC PARS;BL;D;EL;H;HL;L;OH;R;XCD;XY;name
[1]   ⍝   This function generates a finite element mesh data file for use
[2]   ⍝   with FORTRAN program FPLHYB.  PARS is a 6-vector of notch and
[3]   ⍝   beam geometry parameters (D, R, L, h, BL, OH) as described and
[4]   ⍝   used in ENDNODE.  V is a 4-vector of elastic parameters:
[5]   ⍝   Ex, NUxy, Ey, Gxy.  ENDMESHC is for compression side notches.
[6]   ⍝   Written 13 Feb. 1989 from ENDMESH of 11 Nov. 1988.
[7]   ⍝
[8]    'Begin at ',⍕(⎕TS)[4 5 6]
[9]    NPE←13 ⍝                                    cubic elements
[10]  XY←INSRECT ENDNODE PARS ⍝                    generate nodal coordinate array
[11]  EL←ELEM1 XY ⍝                                generate element connectivity array
[12] ⍝     'K' (compression notch) and 1st 2 signif. digits of phi ≡ D/h :
[13] L10:name←'K',¯2↑ 4 2 ⍕÷/PARS[1 4]
[14]  name←name,¯2↑ 4 2 ⍕÷/PARS[2 4] ⍝             1st 2 signif. digits of rho ≡ R/h
[15]  name←name,¯2↑ 4 2 ⍕0.1×÷/PARS[3 4] ⍝ 1st 2 signif. digits of .1×L/h
[16] ⍝   append A, B, C, D, E or F to filename denoting elastic properties :
[17]  name←name,'BADECF'[((V[1]÷V[4])≤ 8 10 14 17 22 32)⍳1]
[18]  'Filename:          ',name
[19]  'No. of Nodes:      ',⍕1↑⍴XY
[20]  'No. of Elements:   ',⍕1↑⍴EL
[21]  name MATEDATA V ⍝                            open file, write mat'l. data
[22]  COORDATA XY ⍝                                write nodal coord. data
[23]  ELEMDATA EL ⍝                                write element connectivity data
[24]  ENDBOUNFORCK ⍝                               write BOUN, FORC and macro lines
[25]  'End at ',⍕(⎕TS)[4 5 6]
    ∇
```

Appendix 5: Numerical Results

Tabulated values are FE-calculated MCF results. The V/M values corresponding to these loading conditions and notch locations are given later in this appendix (see Section 3.1.3.1). The geometry numbers refer to the sequence of notch geometries shown in Table 3, page 59. Loading codes: CP=center-point QP=quarter-point UD=uniformly distributed

G8-E12:

	Center Notch			Near-Center			Far Offcenter		
Geom.	CP	QP	UD	CP	QP	UD	CP	QP	UD
1	3.57	3.66	3.64	3.81	3.70	3.69	3.94	3.73	3.87
2	5.36	5.62	5.54	5.88	5.64	5.66	6.13	5.65	5.98
3	5.42	5.58	5.56	5.85	5.65	5.62	6.11	5.69	5.96
4	4.52	4.71	4.65	4.89	4.73	4.74	5.12	4.75	5.00
5	4.56	4.68	4.67	4.87	4.73	4.72	5.11	4.75	4.99
6	9.49	9.86	9.77	10.25	9.89	9.92	10.69	9.93	10.44
7	7.73	8.08	7.96	8.41	8.08	8.12	8.70	8.09	8.51
8	7.81	8.09	8.02	8.40	8.10	8.12	8.70	8.14	8.51
9	8.13	8.38	8.37	8.68	8.39	8.42	8.96	8.39	8.78
10	6.93	7.15	7.10	7.42	7.18	7.19	7.68	7.19	7.52
11	15.59	16.07	15.93	16.57	16.07	16.14	16.95	16.06	16.69
12	15.70	16.02	15.98	16.52	16.07	16.07	16.91	16.15	16.64
13	13.13	13.47	13.38	13.86	13.48	13.53	14.15	13.47	13.95
14	13.17	13.38	13.36	13.77	13.46	13.43	14.09	13.55	13.88
15	25.30	25.69	25.62	26.13	25.64	25.71	26.50	25.66	26.24

G12-E12:

	Center Notch			Near-Center			Far Offcenter		
Geom.	CP	QP	UD	CP	QP	UD	CP	QP	UD
1	3.77	3.89	3.87	4.08	3.92	3.92	4.21	3.96	4.13
2	5.61	5.92	5.82	6.23	5.93	5.96	6.52	5.95	6.35
3	5.76	5.95	5.92	6.25	6.01	5.99	6.54	6.07	6.36
4	4.75	4.98	4.91	5.20	4.99	5.02	5.46	5.02	5.32
5	4.89	5.01	5.00	5.23	5.08	5.05	5.48	5.11	5.35
6	9.90	10.34	10.24	10.79	10.37	10.41	11.30	10.41	11.01
7	8.11	8.52	8.38	8.88	8.51	8.57	9.24	8.53	9.02
8	8.20	8.53	8.46	8.88	8.54	8.57	9.24	8.58	9.02
9	8.86	9.13	9.12	9.44	9.15	9.19	9.74	9.15	9.55
10	7.31	7.57	7.52	7.88	7.60	7.62	8.19	7.61	8.00
11	16.35	16.90	16.75	17.45	16.91	16.99	17.93	16.90	17.62
12	16.54	16.91	16.86	17.43	16.95	16.96	17.91	17.03	17.60
13	13.86	14.26	14.16	14.68	14.27	14.33	15.04	14.26	14.80
14	13.97	14.23	14.20	14.65	14.31	14.29	15.01	14.41	14.78
15	26.78	27.22	27.14	27.69	27.16	27.24	28.12	27.17	27.84

MCF Results, continued

G17-E17:

	Center Notch			Near-Center			Far Offcenter		
Geom.	CP	QP	UD	CP	QP	UD	CP	QP	UD
1	4.12	4.26	4.24	4.50	4.30	4.30	4.67	4.34	4.57
2	6.08	6.48	6.36	6.86	6.50	6.54	7.26	6.52	7.03
3	6.35	6.56	6.53	6.92	6.63	6.61	7.30	6.72	7.08
4	5.15	5.44	5.36	5.71	5.47	5.50	6.06	5.50	5.89
5	5.40	5.54	5.52	5.79	5.62	5.58	6.12	5.67	5.95
6	10.75	11.32	11.19	11.88	11.37	11.42	12.57	11.42	12.19
7	8.80	9.32	9.14	9.76	9.32	9.38	10.26	9.33	9.98
8	8.93	9.34	9.25	9.76	9.35	9.39	10.26	9.40	9.98
9	9.91	10.28	10.27	10.62	10.28	10.34	10.99	10.26	10.77
10	7.95	8.29	8.22	8.66	8.32	8.35	9.08	8.33	8.84
11	17.78	18.48	18.28	19.16	18.49	18.59	19.81	18.48	19.41
12	18.08	18.53	18.47	19.17	18.58	18.60	19.81	18.69	19.42
13	15.07	15.58	15.45	16.10	15.60	15.67	16.59	15.59	16.28
14	15.24	15.61	15.57	16.11	15.71	15.68	16.59	15.82	16.29
15	29.17	29.75	29.65	30.34	29.67	29.77	30.90	29.70	30.55

G22-E22:

	Center Notch			Near-Center			Far Offcenter		
Geom.	CP	QP	UD	CP	QP	UD	CP	QP	UD
1	4.42	4.58	4.56	4.87	4.62	4.62	5.07	4.67	4.95
2	6.49	6.97	6.82	7.42	7.00	7.05	7.92	7.03	7.65
3	6.86	7.10	7.06	7.52	7.19	7.16	7.98	7.31	7.72
4	5.49	5.85	5.74	6.16	5.87	5.90	6.59	5.92	6.38
5	5.84	5.99	5.97	6.27	6.08	6.04	6.67	6.15	6.47
6	11.50	12.18	12.02	12.84	12.25	12.31	13.70	12.32	13.24
7	9.38	10.02	9.80	10.52	10.01	10.09	11.15	10.03	10.80
8	9.55	10.06	9.95	10.52	10.06	10.10	11.15	10.12	10.81
9	10.79	11.29	11.27	11.63	11.25	11.33	12.11	11.21	11.84
10	8.47	8.92	8.83	9.36	8.94	8.98	9.87	8.95	9.58
11	19.01	19.86	19.62	20.68	19.90	20.01	21.49	19.89	21.01
12	19.43	19.99	19.91	20.73	20.05	20.07	21.53	20.19	21.05
13	16.07	16.72	16.55	17.40	16.78	16.87	18.01	16.77	17.64
14	16.33	16.80	16.76	17.46	16.96	16.94	18.06	17.09	17.69
15	31.15	31.91	31.77	32.60	31.78	31.90	33.34	31.81	32.89

MCF Results, concluded

G32-E12:

Geom.	Center Notch			Near-Center			Far Offcenter		
	CP	QP	UD	CP	QP	UD	CP	QP	UD
1	4.73	4.95	4.93	5.31	4.94	4.97	5.48	4.98	5.36
2	6.78	7.37	7.21	7.94	7.40	7.48	8.51	7.41	8.20
3	7.37	7.66	7.61	8.13	7.72	7.72	8.62	7.86	8.34
4	5.77	6.22	6.11	6.66	6.26	6.33	7.15	6.30	6.91
5	6.36	6.52	6.50	6.88	6.65	6.60	7.29	6.76	7.07
6	11.99	12.82	12.64	13.60	12.88	12.99	14.62	12.95	14.08
7	9.86	10.62	10.37	11.22	10.63	10.74	12.03	10.66	11.61
8	10.10	10.73	10.60	11.25	10.70	10.78	12.04	10.75	11.62
9	12.10	12.59	12.54	12.92	12.56	12.65	13.44	12.55	13.14
10	9.12	9.69	9.58	10.08	9.58	9.65	10.72	9.60	10.37
11	20.01	21.02	20.74	21.90	21.04	21.19	22.95	21.04	22.38
12	20.59	21.30	21.21	22.09	21.33	21.42	23.08	21.47	22.53
13	17.06	17.85	17.65	18.58	17.89	18.00	19.39	17.87	18.94
14	17.59	18.18	18.12	18.82	18.27	18.29	19.57	18.37	19.14
15	33.18	34.16	34.00	34.94	34.01	34.17	35.92	34.04	35.37

Loading Parameter, V/M

Tabulated values are 100×(V/M) for the given notch geometry, notch location, and loading condition. See Section 3.1.3.1.

Geom.	Center Notch			Near-Center			Far Offcenter		
	CP	QP	UD	CP	QP	UD	CP	QP	UD
1	-5.04	.00	-.90	5.00	.59	.83	10.00	-.03	7.06
2	-5.38	.00	-1.45	5.00	.68	.83	10.00	-.07	7.06
3	-4.77	.00	-.44	5.00	.51	.83	10.00	-.01	7.06
4	-5.33	.00	-1.37	5.00	.66	.83	10.00	.07	7.06
5	-4.73	.00	-.36	5.00	.47	.83	10.00	-.08	7.06
6	-5.08	.00	-.96	5.00	.61	.83	10.00	.03	7.06
7	-5.60	.00	-1.78	5.00	.73	.83	10.00	.10	7.06
8	-5.04	.00	-.90	5.00	.59	.83	10.00	.09	7.06
9	-4.58	.00	-.06	5.00	.42	.83	10.00	.07	7.06
10	-5.00	.00	-.83	5.00	.58	.83	10.00	-.07	7.06
11	-5.38	.00	-1.45	5.00	.68	.83	10.00	-.07	7.06
12	-4.77	.00	-.44	5.00	.51	.83	10.00	-.01	7.06
13	-5.33	.00	-1.37	5.00	.66	.83	10.00	-.11	7.06
14	-4.73	.00	-.36	5.00	.47	.83	10.00	-.04	7.06
15	-5.04	.00	-.90	5.00	.59	.83	10.00	.09	7.06

Best-fit values of f1 from Eq. (5.2), over 9 V/M ratios.

Geom.	G8-E12	G12-E12	G17-E17	G22-E22	G32-E12
1	3.91	4.29	4.62	3.69	4.97
2	5.92	6.48	6.98	5.62	7.38
3	5.99	6.61	7.17	5.62	7.72
4	4.98	5.45	5.85	4.72	6.24
5	5.05	5.59	6.05	4.71	6.61
6	10.35	11.34	12.20	9.87	12.84
7	8.51	9.31	9.99	8.07	10.61
8	8.53	9.34	10.05	8.09	10.70
9	9.13	10.26	11.23	8.38	12.54
10	7.58	8.30	8.92	7.16	9.61
11	16.90	18.47	19.87	16.06	21.01
12	16.94	18.58	20.04	16.06	21.33
13	14.26	15.58	16.74	13.47	17.85
14	14.28	15.66	16.89	13.44	18.22
15	27.19	29.71	31.84	25.67	34.07

Best-fit values of f2 from Eq. (5.2), over 9 V/M ratios.

Geom.	G8-E12	G12-E12	G17-E17	G22-E22	G32-E12
1	.866	1.081	1.296	.731	1.540
2	1.714	2.198	2.663	1.427	3.238
3	1.518	1.869	2.190	1.358	2.481
4	1.337	1.700	2.041	1.114	2.595
5	1.166	1.404	1.618	1.072	1.828
6	2.659	3.420	4.141	2.284	4.948
7	2.088	2.682	3.223	1.794	3.940
8	1.991	2.542	3.023	1.705	3.651
9	1.721	2.086	2.490	1.654	2.500
10	1.687	2.166	2.651	1.449	3.008
11	2.953	3.794	4.628	2.577	5.449
12	2.700	3.414	4.090	2.392	4.809
13	2.220	2.850	3.641	1.948	4.339
14	2.041	2.599	3.318	1.817	3.763
15	2.609	3.357	4.204	2.336	5.178

FE Results, G32-E12 substudy with variable beam depth and span (see Section 3.1.3.2). The geometry numbers refer to the sequence of notch and beam geometries shown in Table 5, Chapter 3. Table 5 also gives the V/M ratios for each geometry and loading condition. Loading codes: cp=center-point qp=quarter-point ud=uniformly distributed

Geom.	MCFcp	MCFqp	MCFud	f1	f2
1	25.88	21.19	25.00	21.21	5.42
2	25.85	21.26	24.65	21.21	5.36
3	20.64	17.92	20.18	17.94	4.86
4	20.64	17.95	20.00	17.93	4.84
5	26.16	22.65	25.30	22.61	4.00
6	26.12	22.64	24.97	22.59	3.93
7	20.82	18.68	20.38	18.66	3.81
8	20.82	18.67	20.20	18.65	3.78
9	29.71	24.18	28.64	24.13	6.46
10	29.68	24.20	28.22	24.13	6.39
11	23.49	20.29	22.94	20.27	5.76
12	23.49	20.30	22.72	20.27	5.75
13	29.96	25.47	28.92	25.43	5.15
14	29.93	25.49	28.51	25.41	5.08
15	23.65	20.97	23.11	20.95	4.77
16	23.64	20.97	22.90	20.94	4.75
17	14.77	11.62	14.14	11.63	3.62
18	14.78	11.70	13.92	11.68	3.55
19	11.45	9.52	11.12	9.53	3.43
20	11.45	9.55	10.99	9.53	3.42
21	14.93	12.66	14.32	12.64	2.56
22	14.95	12.69	14.12	12.65	2.53
23	11.57	10.16	11.25	10.14	2.48
24	11.57	10.16	11.13	10.14	2.47
25	16.93	13.28	16.19	13.25	4.25
26	16.96	13.32	15.93	13.27	4.22
27	13.06	10.82	12.66	10.81	4.02
28	13.06	10.83	12.51	10.81	4.01
29	17.08	13.99	16.35	13.95	3.54
30	17.11	14.03	16.11	13.97	3.52
31	13.16	11.39	12.78	11.37	3.15
32	13.17	11.40	12.64	11.37	3.13
33	9.42	8.01	9.16	8.02	2.00
34	44.12	39.38	43.21	39.38	6.72
35	22.55	18.38	21.58	18.38	5.80
36	16.06	13.55	15.44	13.53	3.49
37	19.30	17.42	18.65	17.39	2.52
38	18.23	14.61	17.48	14.62	5.08
39	12.79	11.45	12.53	11.45	3.80
40	23.59	18.50	22.23	18.47	4.66
41	18.20	15.10	17.06	15.03	4.38
42	18.26	15.04	17.73	15.04	4.51
43	18.26	15.05	17.52	15.04	4.49

FE Results, G8-E12 substudy with variable beam depth (see Section 3.1.3.2). The geometry numbers refer to the sequence of notch and beam geometries shown in Table 6, Chapter 3. Table 6 also gives the V/M ratios for each geometry and loading condition. Loading codes:
cp=center-point qp=quarter-point ud=uniformly distributed

Geom.	MCFcp	MCFqp	MCFud	f1	f2
1	8.69	7.76	8.34	7.54	2.19
2	11.88	9.64	10.87	9.09	3.10
3	8.70	7.74	8.35	7.52	2.25
4	11.84	9.73	10.83	9.20	2.90
5	7.40	6.65	7.10	6.47	1.74
6	10.04	8.31	9.21	7.87	2.39
7	7.40	6.65	7.11	6.47	1.75
8	9.99	8.21	9.15	7.76	2.46
9	18.19	16.79	17.67	16.47	3.26
10	23.77	20.58	22.45	19.81	4.45
11	18.23	16.70	17.72	16.36	3.60
12	23.79	20.55	22.48	19.77	4.53
13	15.45	14.40	15.05	14.15	2.46
14	19.98	17.52	18.95	16.91	3.44
15	15.49	14.33	15.10	14.07	2.74
16	19.99	17.53	18.97	16.92	3.44
17	6.63	5.75	6.26	5.54	1.52
18	32.43	30.12	31.63	29.59	4.07
19	16.22	14.02	15.30	13.49	3.82
20	11.31	9.95	10.74	9.62	2.37
21	13.30	11.73	12.65	11.35	2.73
22	12.97	11.28	12.30	10.88	2.96
23	9.26	8.66	9.06	8.53	2.11
24	16.72	13.51	15.19	12.70	3.69
25	12.96	11.28	12.29	10.88	2.93

The vita has been removed from the scanned document